Mechanism of chondrocyte death in osteoarthritis.

Nabila Yasmin Intekhab Alam

School of Life Sciences

MECHANISM OF CHONDROCYTE DEATH IN OSTEOARTHRITIS

NABILA YASMIN INTEKHAB ALAM

A thesis submitted in partial fulfilment of the requirements of the University of Westminster for the degree of Doctor of Philosophy

August 2006

DEDICATION

For my Mum and Dad, Intekhab, Ami and Abu, Sundus and Ihab, our daughters

Zenab and Bakhtawar, you have been my strength,

when I needed most,

with all my love

ABSTRACT

Osteoarthritis (OA) is the most common rheumatic disease and is predominantly a disease of the elderly and middle aged characterized by a loss of joint mobility and pain. OA is manifested by a loss of articular cartilage (AC) which is thought to occur as a result of the apoptotic death of the chondrocytes which normally maintain the cartilage matrix. Certain stimuli such as NO and TNF-α have been shown *in vivo* to contribute to accelerated damage of articular tissue and to amplify the inflammatory process. This study focuses on the effects of these stimuli on chondrocyte death and endogenous mechanisms which exist to protect against that death.

C-20/A4 cells treated with SNAP (NO donor) and TNF-α demonstrated an increased level of apoptosis when analysed by TUNEL and Annexin V/PI staining and necrosis analysed by LDH release. One of these stimuli, SNAP was shown to induce the production of UCN, a CRH-like cytoprotective peptide implicated in the prevention of cell death in many systems. TNF-α did not induce UCN production. UCN depletion and the addition of α helical CRH resulted in increased cell death suggesting a role for UCN in chondrocytes as an autocrine/paracrine endogenous cytoprotective agent. This was further supported by the observation that exogenous UCN administration at a concentration of 10^{-8}M protected chondrocytes further against pro-apoptotic stimuli and was observed to be more protective against SNAP than TNF-α.

The data presented here would indicate that UCN cytoprotection may be mediated via the PI3K, P38 MAPK and P42/P44 MAPK pathways as determined using the selective inhibitors LY294002 (PI3K), SB202190 (P38 MAPK) and PD98059 (P42/P44 MAPK), but P42/P44 MAPK would appear to be the most important. This was further confirmed by Western blotting which showed that in the presence of UCN, P42/P44 MAPK activation increased significantly. Caspase 3 cleavage was observed in SNAP treated cells but was reduced in cells treated with SNAP+UCN. Caspase 8 and 9 failed to show consistant results.

This research is the first to report the existence of endogenous UCN in human chondrocytes and also suggests a chondroprotective role for UCN. This, along with the identification of other possible areas of intervention, such as the PI3K and MAPK pathways implicated in UCN activity may indicate potential future therapeutic avenues in OA.

ACKNOWLEDGEMENTS

I've come a long, long way for this and boy has it been a journey! Firstly, and most importantly, I would like to thank my supervisory team, Dr. Ian C. Locke, Prof. Chas Chowdrey and Dr. Richard Knight, for their excellent scientific input and advice during the course of this PhD.

Sincere thanks goes to my director of studies Dr. Ian C. Locke for his patience, dedication, excellent supervision and continuous encouragement throughout the duration of this PhD and for being a friend.

Many thanks to the University of Westminster for the Quintin Hogg scholarship.

Many thanks to the technical staff and stores staff, Alan, Thakor, Vanita, Jean-Pierre, Louisa, Trevor, Sue, Allrick, Sylvia and Roger, that have been very resourceful and extremely helpful.

This PhD would not have been possible if it was not for my parents and Intekhab, for their unconditional love, support and encouragement they have given me throughout the duration of this PhD, especially my parents for looking after our daughters. Many thanks to all members of our family, in Preston, Manchester, London, Oxford, France, America, Canada and Pakistan, for their immeasureable support and constant encouragement, especially to bayjee, Drs Sündüs and Ihab Tewfik, Asjed, Mona, Majed, Munira, Mobina, Umar Bhai, Rani, Bhabhi and Bhaijaan Javaid and nephews and nieces Ammaar, Arva, Kanwal, Jamshed, Jahanzheb, Junaid and Nawal.

To my friends, thank you for your love and support, a special mention goes to Sandra, Rehana, Supriya, Arva, Corinne, Babak, Jane, Chirag, and Anna, Drs. Mohammad, and especially Drs. Gopal and Anjali for their encouragement and support and my best friends Neeta and Priti.

I would also like to remember my dadijaan and dada abu, abba, late uncles Tayajaan Fazal Karim and Mamujaan Nazir Ahmed and aunty Pupijaan Asha Bhi who are not with us today and will always be remembered.

CONTENTS

LIST OF FIGURES

LIST OF TABLES

ABBREVIATIONS

A	Adenine
AA	Arachidonic acid
AC	Articular cartilage
ACTH	Adrenocorticotropic hormone
ADAMTS	Disintegrin and metalloproteinase with thrombospondin motifs
AGE	Agarose gel electrophoresis
AIF	Apoptosis inducing factor
ANOVA	Analysis of variance
AP	Alkaline phosphatase
AP-1	Activating protein - 1
APAF-1	Apoptotic protease activity factor 1
ATP	Adenosinetriphosphate
AUC	Area under curve
β-actin	Beta-actin
Bcl-2	B cell leukaemia/lymphoma-2
BH	Bcl-2 homology
BLAST	The Basic Local Alignment Search Tool
bp	Base pairs
BPB	Bromophenol blue
BSA	Bovine serum albumin
C	Cytosine
C-20/A4	Human chondrocyte cell line
$CaCl_2$	Calcium chloride
cAMP	cyclic adenosine monophosphate
CARDs	Caspase activation and recruitment domains
CASPases	Cytosolic aspartate-specific proteases
cDNA	Complementary DNA
Ced -3	Cell death 3
C. elegans	Caenorhabditis elegans
c-FLIP	Cellular flice inhibitory protein
cGMP	cyclic guanylate monophosphate
CNS	Central nervous system
CNTL	Control

CRH-BP	Corticotropin releasing hormone-binding protein
CRH/F	Corticotropin releasing hormone/factor
CRH-R1	Corticotropin releasing hormone-receptor 1
CRH-R2	Corticotropin releasing hormone-receptor 2
ct	cycle threshold
DD	death domain
DED	Death effector domain
DEPC	Diethyl pyrocarbonate
DISC	Death inducing signaling complex
DMEM	Dulbeccos modified Eagles medium
DMSO	Dimethyl sulphoxide
DNA	Deoxyribonucleic acid
dNTPs	deoxynucleotide triphosphates
DPBS	Dulbecco's phosphate buffered saline
EC_{50}	The concentration of a compound where 50% of its effect is observed
ECL	Enhanced Chemiluminescence
ECM	Extracellular matrix
EDTA	Ethylenediaminetetraacetic acid
ELISA	Enzyme-Linked Immuno Sorbent Assay
eNOS	endothelium nitric oxide synthase
ER	Endoplasmic reticulum
ERK	Extracellular signal regulated kinases
EtBr	Ethidium bromide
FACS	Fluorescent activated cell sorter
FADD	Fas associated death domain
Fas	CD95
Fas L	Fas ligand (CD95L)
FCS	Fetal calf serum
FITC	Fluorescein isothiocyanate
FLIP	Flice inhibitory protein
$FLIP_L$	Flice inhibitory protein long
$FLIP_S$	Flice inhibitory protein short
G	Guanine
GAGs	Glycosaminoglycans

GAPDH	Glyceraldehyde-3-phosphate dehydrogenase
GPCR	G protein-coupled receptors
G_S	Stimulatory G protein
GTP	Guanylate triphosphate
GSNO	*S*-nitrosoglutathione
HEPES	(N-[2-hydroxyethyl]piperazine-N'-[4-butanesulfonic acid]
HPA Axis	Hypothalamic-pituitary adrenal axis
HRP	Horseradish peroxidase
hrs	Hours
HSP90	Heat shock protein 90
IAPs	Inhibitory of apoptosis proteins
ICAD	Inhibitor of caspase-activated deoxyribonuclease
IFN- γ	Interferon-γ
Ig	Immunoglobulin
IgA	Immunoglobulin A
IgG	Immunoglobulin G
IgM	Immunoglobulin M
K_{ATP}	Potassium adenosinetriphosphate
KCL	Potassium chloride
IC_{50}	The half maximal inhibitory concentration
IL-6	Interleukin-6
IL-17	Interleukin-17
IL-1α	Interleukin-1alpha
IL-1β	Interleukin-1beta
IL-1R	Interleukin-1 receptor
IMM	Inner mitochondrial membrane
iNOS	Inducible nitric oxide synthase (NOS II)
$iPLA_2$	Calcium insensitive phospholipase A_2
I/R	Ischeamic reperfusion
Kb	Kilobase
kDa	kilodalton
IκB	Inhibitory kappa B
IKK	Inhibitory κB kinase
L-glu	L-glutamine
LIF	Leukemia inhibitory factor

L-NMMA	N^G-monomethyl-L-arginine
LPC	Lysophosphatidylcholine
LY294002	PI3K inhibitor
LPS	Lipopolysaccharide
MAPK	Mitogen activated protein kinase
MAPK Kinase	Mitogen activated protein kinase kinase
MAPKK/MEK1/2	MAPK kinase kinase
Mg^{2+}	Magnesium
$MgCl_2$	Magnesium chloride
mins	minutes
MLCK	Myosin light chain kinases
mM	millimolar
M-MLV	Murine moloney leukaemia virus
MMP	Metalloproteinases
mRNA	messenger ribonucleic acid
MTT	3-[4,5-dimethylthiazol-2yl] 2,5-diphenyl tetrazolium bromide assay
3-NT	3-nitrotyrosine
NaCl	Sodium chloride
NaOH	Sodium hydroxide
NCBI	National centre for biotechnology Information
NF-κB	Nuclear factor-kappa B
NGF	Nerve growth factor
NH_4^-	Ammonium
NIK	NF-κB-inducing kinase
nM	nanomolar
NMDA	*N*-methyl-*D*-asparate
NO	Nitric oxide
NOS	Nitric oxide synthase
NR	Neutral Red
$O_2^{-\cdot}$	Superoxide
OA	Osteoarthritis
oCRH	Ovine CRH
OD	Optical density
Oligo-dT	Oligo-deoxythymidine

$ONOO^-$	Peroxynitrite
OMM	Outer mitochondrial membrane
P38 MAPK	P38 mitogen activated protein kinases
P42/P44 MAPK	P42/P44 mitogen activated protein kinases
PAGE	Polyacylamide gel electrophoresis
PARP	Poly (ADP-ribosyl) polymerase
PBS	Phosphate buffered saline
PC	Preconditioned control media
PC12	Pheochromocytoma 12
PCR	Polymerase chain reaction
PD98059	P42/P44 MAPK inhibitor
PDK1/2	Phosphoinositide dependent kinases 1 and 2
PEN/STREP	Penicillamine and streptomycin solution
PI	Propidium iodide
PIP2	Phosphorylate inositol phospholipids
PI3K	phosphatidylinositol 3 kinase
PKA	Protein kinase A
PKC	Protein kinase C
PKCε	Protein kinase C epsilon
pM	Picomolar
POD	Peroxidase
PS	Phosphatidylserine
PS	Preconditioned SNAP media
PT	Preconditioned TNF-α media
PTK	Protein tyrosine kinase
PVN	Paraventricular nucleus
RA	Rheumatoid arthritis
RAIDD	RIP associated protein with death domain
RIP-1	Receptor interacting protein-1
RNA	Ribonucleic acid
RNasin	RNase inhibitor
ROS	Reactive oxygen species
RT	Room temperature
RT-PCR	Reverse transcriptase – polymerase chain reaction
SAPKs/JNKs	Stress activated protein kinases/c-jun N- terminus kinases

SB202190	P38 MAPK inhibitor
SCP	Stresscopin (UCN III)
SD	Standard Deviation
SDS	Sodium dodecyl sulphate
SDS-PAGE	Sodium dodecyl sulphate polyacrylamide gel electrophoresis
SIN-1	3-morpholinosyndonimine
Smac/Diablo	Second mitochondrial-derived activator of caspase/direct IAP binding protein with low pI
SNAP	*S*-Nitroso-*N*-acetyl-*D*-*L*-penicillamine
SNP	Sodium nitroprusside
SOD	Superoxide dismutase
SPNT	Supernatant
SRP	Stresscopin related peptide (UCN II)
STAT-1	Signal transducer and activator of transcription
SVG	Sauvagine
T	Thymine
TAE	Tris-acetate-EDTA
Taq Polymerase	Thermophilus aquaticus polymerase
tBid	truncated BID
TdT	Terminal deoxynucleotidyl transferase
TEMED	Tetramethylethylenediamine
TGF-β	Tumour growth factor-beta
TIMPs	Tissue inhibitor of metalloproteinases
TNF	Tumour necrosis factor
TNF-α	Tumour necrosis factor – alpha
TNF–β	Tumour necrosis factor – beta
TNF–R	Tumour necrosis factor receptor
TNF–R1	Tumour necrosis factor receptor 1 (TNF-R55)
TRADD	TNF receptor associated death domain
TRAF-2	TNF-receptor-associated factor-2
TRAIL–R1/DR4	TNF–related apoptosis-inducing ligand receptors
TUNEL	Terminal deoxy nucleotidyltransferase (TdT)- mediated deoxyuridine triphosphate (dUTP) nick end labeling
μM	Micromolar
UCN	Urocortin

UHQ	Ultra high quality
URO	Urotensin-1
UV	Ultra violet
XCFF	Xylene cyanole FF

CHAPTER 1

INTRODUCTION

1.1 The skeletal system

The skeletal system is composed of a large number of bones of various shapes and sizes linked together by a variety of joints also known as articulations or arthroses, where they meet. Joints are classified either as synarthroses (immovable joints), amphiarthroses (slightly movable joints) or diarthroses (freely movable joints), also known as synovial joints.

Whilst all diarthroidal joints generally have a related structure, the shapes of the articulating surfaces differ. Synovial joints are therefore divided in 6 subtypes: Gliding (or planar) joints, where articulating surfaces are flat and allow movement from side to side and back and fourth, (e.g. intercarpal joints); Hinge joints where the convex oval surface of one bone fits into the concave surface of another bone, (e.g. knee joints); Pivot joints, where the rounded surface of one bone articulates within a ring made partly by another bone, (e.g. condyloid joints); Ellipsoidal joints where the convex oval shaped projection of one bone fits into the oval shaped hollow of another bone (e.g. wrists); saddle joints where the articular surface of one bone is 'saddle' shaped and the articular surface of the other bone fits into the "saddle" (e.g. carpometacarpal joint); ball and socket joint where a ball-like surface of one bone fits into a cuplike hollow of another bone (e.g. hip joints) (Rosen, 2000).

The main focus of this thesis is the mechanisms involved in the pathogenesis of osteoarthritis (OA), a degenerative joint disease which can affect virtually all the joints of the skeletal system but is predominantly found in the larger synovial joints.

1.2 Joint composition, chondrocyte function and the extra cellular matrix

Diarthroidal joints consist of bone, articular cartilage (comprising chondrocytes and extracellular matrix) and other associated connective tissues. Articular cartilage is a thin layer of tissue that covers the articulating ends of the bones comprising the diarthrodial joint and acts as a shock absorber and wear resistant surface within the joint (Archer *et al*, 1994). Cartilage tissue does not contain components of the nervous, lymphatic or vascular systems and possesses only one cell type, the chondrocytes, which are related to fibroblasts and occupy small chambers called lacunae within the extracellular matrix

(ECM). Chondrocytes account for only 2-3% of the total tissue volume and are completely enclosed by their ECM hence they do not form cell-to-cell contacts (Buckwalter and Mankin, 1998). Chondrocytes from articular cartilage live in a largely anoxic environment and utilize anaerobic metabolic pathways. Cartilage can be divided into four zones. From the surface inward, these zones are the superficial, middle and deep zones and the calcified zone (Blanco *et al*, 2004) and the chondrocytes in each zone vary in morphology, metabolic and biochemical activity (Mobasheri *et al*, 1998; Aydelotte *et al*, 1996). Chondrocytes are responsible for the biosynthesis, maintenance and repair of the articular cartilage and contain abundant endoplasmic reticulum & Golgi apparatus needed for the production of ECM components and the enzymes that degrade or build the matrix (Buckwalter and Mankin, 1998).

Maintenance of the articular cartilage requires continual replacement of degraded matrix components and may need changes in the macromolecular framework of the matrix in response to joint usage. In order for this to occur, the chondrocyte must recognize changes in matrix composition that takes place as a result of macromolecule degradation including changes induced by the day-to-day strain placed on the articular surface. The cells must then respond by synthesizing appropriate types and amounts of macromolecules (Buckwalter and Mankin, 1998).

The ECM of articular cartilage is composed mainly of water (60-70% of the tissue wet weight) and matrix macromolecules which interact with the water to determine the mechanical properties of the tissue. The matrix macromolecules include proteoglycans, collagen fibres and a complex network of link proteins, which help organize and stabilize the macromolecular framework of the matrix (Dharmavaram *et al*, 1993; Rucklidge *et al*, 1996). Proteoglycans are highly hydrophilic and swell to expand the collagen network contributing to the hydrodynamic properties of cartilage giving the tissue its typical elasticity, strength and ability to resist mechanical stress (Archer *et al*, 1994).

Normal articular cartilage contains six of the 27 known types of collagen, types II, V, VI, IX, X, and XI, with type II collagen being the most abundant constituting 90-95% of the proteins in adult cartilage (Rucklidge *et al*, 1996). Type II collagen forms the primary component of the cross-banded fibrils with smaller amounts of collagen IX and XI. Type IX collagen molecules covalently bind to the superficial layers of the cross

banded fibrils and project into the matrix, where they also bind covalently to other type IX collagen molecules, whilst type XI collagen acts to control processing of type II collagen and fibrillogenesis (Upholt and Olsten, 1991). Both type IX and XI collagens also help to stabilize the collagen fibrils (Buckwalter and Mankin, 1998).

The matrix surrounds the chondrocytes and protects them from mechanical injury during normal joint movement, helping in the maintenance of their phenotype. The delivery of nutrients, substrates for the synthesis of matrix molecules and newly synthesized molecules, occurs via diffusion through the ECM (Blanco *et al*, 2004). Similarly, degraded matrix molecules and metabolic waste products diffuse out of the matrix (Buckwalter and Mankin, 1998). Other molecules that help to regulate cell function, such as cytokines and growth factors also move to and from the cells by diffusion through the ECM (Blanco *et al*, 2004).

Cartilage remodeling is triggered by endogenous cytokines (e.g. tumour necrosis factor-alpha and interleukin-1beta) produced by activated synoviocytes (cells in the synovial membrane), or articular chondrocytes themselves (Fernandes *et al*, 2002) and locally produced growth factors (e.g. IGF-I, BMP, NGF and TGFβ) (Poiraudeaud *et al*, 1996), which influence chondrocyte function by inducing two main functional programs: the catabolic and the anabolic processes. The up-regulation of catabolic processes is induced by pro-inflammatory stimuli and distinguished by the secretion of proteases, suppression of matrix synthesis, and inhibition of chondrocyte proliferation. The anabolic program seems to be a reaction to structural requirements of the matrix and/or stimuli such as local growth factors and mechanical loading of the tissue and includes the synthesis of protease inhibitors, production of extracellular matrix and cell replication (Blanco, 1999).

Several stimuli may be involved in the regulation of the anabolic/catabolic processes. It has been suggested that chondrocytes may react to the existence of fragmented matrix molecules, enhancing their synthetic activity in order to replace the degraded components of the ECM (Burrage *et al*, 2006). Another factor which may be involved in the manipulation of the equilibrium between synthetic and degradative activity is the frequency and intensity of joint loading. A decrease in joint loading alters chondrocyte activity such that degradation exceeds synthesis of at least the proteoglycan content matrix and it seems likely that the opposite also occurs (Buckwalter and Lane, 1996).

Dysregulation of cartilage maintenance can result in irreversible joint damage and the associated clinical symptoms of osteoarthritis.

1.3 Osteoarthritis

The arthritides are a group of the most common and best known of all joint disorders characterized by joint inflammation. The three most common classes of arthritis are (i) arthritis associated with metabolic & endocrine diseases, gouty arthritis (ii) diffuse connective tissue diseases, rheumatoid arthritis (RA) and (iii) degenerative joint disease, osteoarthritis (OA). Gouty arthritis (gout) occurs when there is an increase of uric acid in the blood resulting in sodium urate crystals being deposited in the soft tissues and joints (Tortora and Grabowski, 2000). Rheumatoid Arthritis (RA) is an autoimmune disease distinguished by synovial inflammation resulting in the destruction of the cartilage and bone (Kim *et al*, 2005). Osteoarthritis is a result of joint 'wear and tear' and as such is more common in older or more active individuals where the joints have experienced more accumulated damage. Loading can also be affected by obesity and joint injury, both of which can increase the likelihood of developing OA (Hunter and Felson, 2006).

Osteoarthritis (OA) is the most common rheumatic disease and affects 190 million people worldwide, and its occurrence is expected to climb as the age of the population increases (Tortorella and Malfait, 2003). OA is predominantly a disease of the elderly and middle aged, characterized by a loss of joint mobility and pain (Buckwalter and Mankin, 1998). OA can occur in any synovial joint in the body, but is most common in the knees, hips, hands and vertebrae (Hunter and Felson, 2006). OA affects females more than it does males (ratio of 10:1), especially OA of the hand and knee, where, after the age of fifty, the prevalence and incidence of disease in these joints is significantly greater in women than in men. Hip OA however, occurs at the same rate in both genders, although progression tends to be more rapid in females (Arden and Nevitt, 2006). The cause of OA is most likely multi-factorial, although, a hereditary factor appears to play an important role. Currently, there is no complete cure for OA, although early detection followed by efficient therapy can slow its detrimental effects (Ishihara *et al*, 2005). One of the main clinical observations of OA is that it predominantly affects the larger joints. OA can also affect small joints such as at the fingers but this generally occurs later in the disease process resulting in the formation of hard bony enlargements,

known as Heberden's nodes, which significantly limit the movement of the fingers (Dharmavaram *et al*, 1993).

OA manifests as morphological, molecular, and biochemical changes of both chondrocytes and matrix. In a healthy individual, articular cartilage covers the opposing surfaces within synovial joints where it forms a smooth shock-absorbing surface essential for normal function of the joint and also absorbs energy from the shock of physical movement (Dharmavaram *et al*, 1993). In OA the surface layer of cartilage breaks down and wears away. This allows bones under the cartilage to rub together, causing pain, swelling, and loss of motion of the joint and over time, the joint loses its normal shape (Micane and Huether, 1994). Figure 1.1 illustrates the structural differences between normal and OA joints.

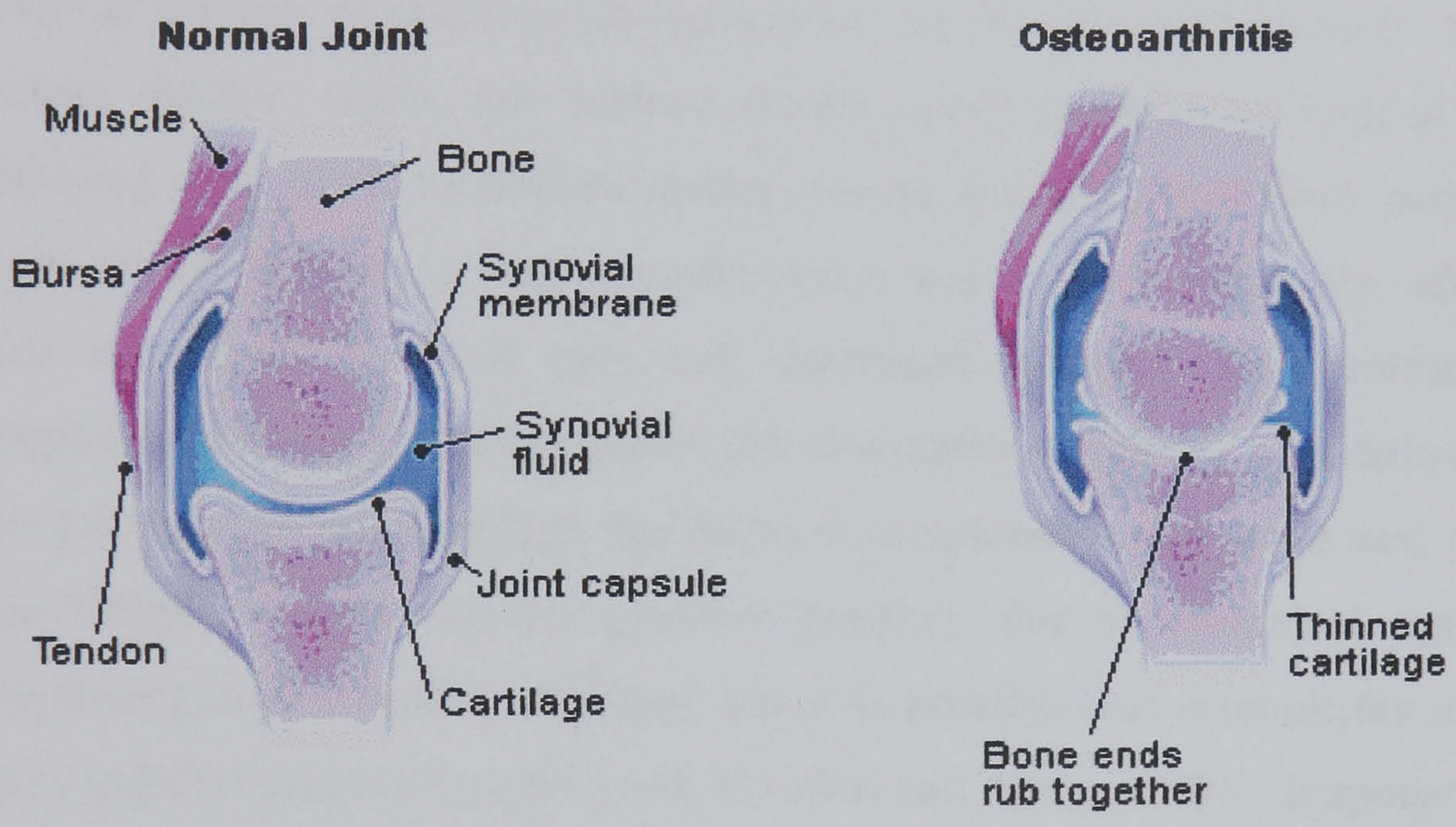

Figure 1.1: Structural Differences between normal and osteoarthritic joints.
(www.medicinenet.com/osteoarthritis/page2.htm)

OA affects not only the cartilage, but also the entire joint structure, including the synovial membrane, bone, ligaments and periarticular muscles (Abramson and Yazici, 2006). The onset of OA occurs with trauma or irregular pressure to the joint. As cartilage is damaged, it becomes thinner and proteoglycan synthesis declines. The chondrocytes release lysosomal proteases, leading to cartilage loss and exposure of the underlying bone (McCarberg and Herr, 2001). This results in the two opposing bones rubbing over one another and they become smooth (eburnation). As the disease progresses, crimped cartilage (cartilage containing hydroxyapatite crystals) is released into the synovial fluid (fluid that lubricates the joint) of the joint causing more pain and damage. Although the exact etiology of OA is unknown, the onset of this disease is

generally divided into three stages: Stage I is the proteolytic breakdown of the cartilage. Stage II is when cartilage swells and gross surface defects, known as fibrillation and erosion occur on the cartilage surface which is followed by a release of breakdown products into the synovial fluid. During the third and final stage, synovial inflammation becomes apparent which is largely a result of the ingestion of cartilage breakdown products by phagocytes resulting in the production of proteases and pro-inflammatory cytokines (Blanco *et al*, 2004). Synovitis is also common in advanced OA, with infiltration of activated B and T lymphocytes (Goldring and Goldring, 2004).

The breakdown of the cartilage matrix in OA results in the eventual thinning of the cartilage with a loss of shock absorption. In early OA the cartilage can actually become thicker as a result of chondrocyte replication. As OA develops however, the cartilage becomes thinner, softer and surface breaks occur resulting in vertical clefts. The underlying bone starts to thicken in response to the increasing stress and bone spurs known as osteophytes or osteochondrophytes are formed within the affected joint, which results in increased pain and decreased mobility. The presence of such osteophytes in the joints differentiates OA from other arthritides. Osteophyte formation is an example of new cartilage and bone development in the joints and occurs from tissue linked with the chondro-synovial junction. The physiological significance of osteophyte growth remains uncertain, but it is possible that osteophytes may actually help to stabilize joints affected by OA (Sandell and Aigner, 2001). It appears likely that both mechanical and humoral factors are involved in stimulating the production of osteophytes.

Martin and Buckwalter (2003) reported that chondrocytes (in both genders) begin to lose their capability to carry on restoring articular cartilage well before they reach replicative senescence. Research has shown that chondrocyte proliferation is unusual in normal adult cartilage and a reduction in the number of active chondrocytes occurs with age (Vignon *et al*, 1976; Horton *et al*, 1998; Hashimoto *et al*,1998b) along with a reduction in their response to anabolic cytokines (Guerne *et al*, 1995). Increasing age is also linked with changes in ECM proteoglycans, collagens and deterioration of the mechanical properties of articular cartilage. The standard size of the proteoglycan aggregates decreases in mature cartilage, as does the water content, and there are increased amounts of proteolytically cleaved link proteins, the biglycans and hyaluronans present are of shorter chain length. Age related decline in the number of

chondrocytes present to synthesize normal matrix proteins, muscle strength, and joint movement may also affect mechanical stresses in aging joints (Blanco *et al*, 2004). It is believed that such an increase in chondrocyte cell death may be involved in the pathogenesis of OA and when chondrocytes are lost due to cell death they are unlikely to be replaced (Loeser and Shakoor, 2003).

As well as chondrocyte loss, changes in chondrocyte phenotype may also be partly responsible for the cartilage damage observed in OA. In particular, changes have been noted in the expression of various catabolic enzymes in osteoarthritic cartilage especially the matrix metalloproteinase (MMP) family of enzymes. Increased expression of several MMPs, especially, MMP-1, MMP-2, MMP-3, MMP-9, MMP-13 and MMP-14 has been demonstrated in OA cartilage (Bramono *et al*, 2004). MMP-1 and MMP-13 mainly cleaves type II collagen, and MMP-3 (stromelysin-1), breaks down proteoglycan and activates other proenzymes. These MMPs are produced by chondrocytes and synoviocytes (cells in the synovial membrane) especially when stimulated by both isoforms of IL-1 (α and β) (Nakamura *et al*, 2006). Imbalance between MMPs and tissue inhibitors of MMPs occurs and may be mainly responsible for cartilage matrix degradation (Blanco, 1999). The activity of MMPs is normally controlled by endogenous MMP inhibitors, known as tissue inhibitor of metalloproteinases (TIMPs) (Smith, 1999). Human joint tissue contains TIMP-1, TIMP-2, and TIMP-3 and the expression of these metalloproteinases (TIMP-1 especially) is differentially down regulated by tumour necrosis factor-α in OA (Hui *et al*, 2001). Breakdown of these proteoglycans by the aggrecanases, ADAMTS (a disintegrin and metalloproteinase with thrombospondin motifs) 4 and 5 is thought to be an early step in the loss of cartilage in OA (Bonfanti *et al*, 1998). These enzymes appear to be responsible for aggrecan degradation without MMP participation (Malfait *et al*, 2002).

1.4 Cell death

There are several different types of cell death pathways (13 in total) (for review, see Melino *et al*, 2005) but in general cell death occurs in two distinct forms, necrosis and apoptosis, which are characterised by different morphological, molecular and biochemical features (Los *et al*, 2002). As well as differences in their characteristics these two types of cell death occur in different circumstances in different tissues throughout the body.

1.4.1 Necrosis

Necrotic cell death is a pathological cell death mechanism usually associated with an insult or injury of some nature. Necrosis occurs with an impairment of the cells ability to maintain homeostasis, leading to an influx of water and extracellular ions. Necrotic cell death is characterized by cell swelling, deterioration of organelles (most notably the mitochondria) and disruption of the cell membrane (Ward *et al*, 1999; Los *et al*, 2002). This process results in the release of cytoplasmic content, including lysosomal enzymes into the extracellular fluid (Fiers *et al*, 1999) and such degradative enzymes may subsequently damage adjacent cells. Therefore, *in vivo* necrotic cell death is often linked with extensive tissue damage, which triggers an inflammatory response resulting from the release of the cellular materials (Bonventure, 1993).

1.4.2 Apoptosis

The definitive description of apoptosis or programmed cell death is credited to Kerr, Wyllie and Currie (Kerr *et al*, 1972) who recognised that cells can die via two different mechanisms, necrosis and apoptosis. The concept of apoptosis began however, in 1858 and was originally defined by Rudolph Virchow who called the process 'necrobiosis', in order to distinguish it from necrosis (Virchow, 1989; for review, see Conti *et al,* 2005). Apoptosis is morphologically, biochemically and molecularly distinct from necrosis, the main differences between the two are shown in Table 1.1. Apoptosis occurs naturally in all tissues and plays an important physiological role in tissue remodeling during development, cell transformation and inflammation (Stockwell, 1991). Unlike necrosis, apoptosis represents a controlled, energy dependent, mechanism of cell death where components are removed without damage to neighbouring cells. Apoptosis is a

physiological process for maintaining homeostasis in both embryogenic and adult tissue, but abnormalities in apoptosis i.e. insufficient apoptosis triggers the onset of cancer (Thompson, 1995) whilst high levels of apoptosis triggers neuro-degenerative and ischaemic diseases which may also have a role in various disease states including those involving articular cartilage degeneration, such as OA (Kouri *et al*, 1996).

In eukaryotic multi-cellular organisms, apoptosis eliminates unwanted cells through a program of changes within the targeted cell (Weil *et al*, 1996). Apoptosis can occur when a cell is damaged beyond repair, infected with a virus or simply no longer required e.g. during development. The apoptotic stimulus can arise from the cell itself, from neighbouring cells in the tissues or from a cell that is part of the immune system. Physiological/pathological stress and/or damage to the cell's DNA from toxicity or exposure to ultraviolet or X-rays may also initiate the apoptotic process. During apoptosis, a cell activates an intrinsic 'suicide' mechanism where the chromatin in the nucleus condenses (called pyknosis). The DNA is then degraded into oligonucleosome-sized fragments (multiples of approx. 200 base pairs, a result of specific cleavage between nucleosomes) a process known as karyorrhexis. This is effected by activation of a calcium dependent endogenous endonuclease, e.g. caspase-activated deoxyribonuclease (CAD), (Wyllie *et al*, 1986) which is discussed later, that leads to shrinkage of the cytoplasm and condensation of the nucleus resulting in the break up of the cell into discreet membrane bound blebs called apoptotic bodies. These apoptotic bodies are normally taken up by neighbouring phagocytic cells or cells of the immune system without any inflammatory reaction (Verschure *et al*, 1994; Lotz *et al*, 1995).

Once started, apoptosis proceeds quickly and cells may completely disappear in minutes to hours. If apoptotic bodies are not phagocytosed however, they will eventually swell and lyse (known as secondary necrosis). If this occurs *in vivo*, damage to neighbouring cells may result from the release of their contents.

Table 1.1: Principal features of apoptosis and necrosis (Hetts, 1998; Vermes *et al,* 2000)

Features	**Necrosis**	**Apoptosis**
Cellular role	Abnormal, accidental	Usually normal
Energy requirement	Passive, results from lack of ATP	ATP-dependent
Stimuli	Sudden transfer of energy, specific toxins, and major ATP depletion	Physiological and pathological conditions minor ATP depletion
Histology	Cellular swelling, disruption of organelles, death of patches of tissue	Chromatin condensation apoptotic bodies, death of single isolated cells
DNA breakdown pattern	Random DNA cleavage	Ladder of fragments in internucleosomal multiples of 185 base pairs.
Plasma membrane	Loss of integrity, with spilling of cell constituents	Integrity preserved, blebbing of intact plasma membrane
Phagocytosis of dead cells	Local phagocytes	Neighbouring cells and local phagocytes
Tissue reaction	Inflammation	No inflammation
Nuclear Changes	Pattern conserved	Condensation, DNA fragmentation, segmentation.
Metabolic/Synthetic Changes	Disordered structure	Active changes in gene expression (e.g. Bcl-2, Bax); active protein synthesis; protease activation.

Chondrocyte death by apoptosis has been implicated as one of the possible mechanisms involved in the pathogenesis of OA. A decreased number of active chondrocytes will result in decreased maintenance of the articular cartilage ECM and, eventually cartilage destruction (Blanco *et al*, 2004). The duration of chondrocyte apoptosis in cartilage is unknown. If clearance of apoptotic bodies in cartilage is slow, secondary necrosis may occur resulting in damage to other chondrocytes and the matrix itself leading to increased extracellular matrix degradation. Such mechanisms may therefore account for the damage seen in OA with a lack of chondrocyte activity resulting in a lack of repair of the damaged matrix and the release of the contents of apoptotic bodies following secondary necrosis having the potential for further active destruction.

It has been established that articular chondrocyte apoptosis increases with age in both humans and rodents (Adams and Horton, 1998; Caswell *et al*, 1987). *In situ* studies on normal and osteoarthritic human cartilage have demonstrated increased chondrocyte apoptosis in OA tissue lending support to this hypothesis (Kim *et al*, 2000) and this apoptosis is linked with the breakdown of the matrix and accumulation of apoptotic bodies in chondrocyte lacunae. Apoptotic bodies most probably remain at these sites because articular cartilage does not usually contain phagocytic cells. This increased rate of chondrocyte apoptosis may also explain abnormal calcium crystal deposition in the articular cartilage of OA patients. Hashimoto *et al*, (1998a) showed that chondrocyte-derived apoptotic bodies contribute to the pathological calcification of OA cartilage observed in humans and other mammalian species. A link between chondrocyte apoptosis and calcification has been observed in menisci from human OA joints where apoptotic cells were co-localized with strong expression of enzymes that mediate calcium pyrophosphate dehydrate deposition (Johnson *et al*, 2001).

Studies have shown that human chondrocyte apoptosis is greater in OA cartilage than in normal cartilage (Blanco *et al*, 1998) and a linkage between the rate of chondrocyte apoptosis and the severity of cartilage damage has also been reported (Hashimoto *et al*, 1998a). Chondrocyte apoptosis can be induced *in vitro* by a variety of agents, such as nitric oxide (NO), oxygen free radicals (Blanco *et al*, 1995), tumour necrosis factor α or β (TNF-α or TNF-β) (Rath and Aggrawal, 1999), and interleukin-1β (IL-1β) (Stadler *et al*, 1991), and the existence of all of these factors has been reported in OA synovium.

There is some debate concerning the exact nature of chondrocyte apoptotic death, and recently, Roach *et al*, (2004) proposed the term 'chondroptosis' to reflect the fact that these cells are enduring apoptosis in a non-classical way which appears to be characteristic of programmed chondrocyte death *in vivo*. They suggested that unlike normal apoptosis, chondroptosis shows increases in the endoplasmic reticulum (ER) and Golgi apparatus, which enhances protein synthesis. These elevated ER membranes then section the cytoplasm and form the compartments where the cytoplasm and organelles are digested. This leads to destruction within autophagic vacuoles and cell remnants are blebbed into the lacunae. Simultaneously these developments lead to total self destruction of the chondrocyte as evidenced by the presence of empty lacunae.

Regardless of the cell type involved, the process of apoptotic cell death from early events such as phosphatidylserine (PS) exposure, through to later events such as nucleic acid fragmentation, is a complex one. Many families of regulatory proteins (e.g. the Bcl-2 family) and active enzymes (e.g. the caspases) are involved and the mechanism will be discussed further in the next section.

1.5 Mechanisms of apoptosis

1.5.1 The Caspases

The genetics and molecular mechanisms of apoptosis were initially established in the late 1980s and early 1990s in studies of the nematode worm *Caenorhabditis elegans (C. elegans)* (Yuan *et al*, 1993; Reddien and Horvitz, 2004). Programmed cell death during *C. elegans* development is precise and predictable: from the 1090 somatic cells produced in the development of the adult worm, 131 go through apoptosis. Studies of the worm showed that apoptosis consists of 4 chronological steps:

- Commitment to death by extracellular or intracellular triggers
- Cell killing by activation of intracellular proteases
- Engulfment of the cell corpse by other cells
- Degradation of the cell corpse within the lysosomes of phagocytic and neighbouring cells

These stages, and the genes that control them (known as *ced* genes in *C. elegans*), are extremely well conserved during animal evolution, from worm to human. The mammalian genes involved in the apoptotic pathway have to a large extent been identified as homologues of the *C. elegans* genes originally associated with apoptotic control. In *C. elegans*, three proteins act early in the apoptotic pathway: *ced-3, ced-4* and *ced-9*. Whilst *ced-3* has an effector function in the destruction of target cells, the cytoplasmic protein *ced-4* was identified as an adapter protein which activated *ced-3*. The mitochondrial protein *ced-9* in turn controls the activation of *ced-4* (Seshagiri *et al*, 1998) by binding to pro-*ced-4* and preventing its activation and so that of pro-*ced-3*, possibly also anchoring *ced-4* away from cytoplasmic pro-*ced-3*. Consequently, *ced-3 and ced-4* cause apoptosis, and *ced-9* protects against apoptosis. *Ced-3* was the first member of this family to be discovered with mutations in the gene encoding *ced-3* preventing the death of the cells programmed to die during development. *ced-3* was subsequently found to be homologous to a mammalian protein named caspase 3.

The caspases (*cysteinyl aspartate-specific proteases*) are a family of protease enzymes involved in the process of apoptosis in mammals (Los *et al*, 2002). The binding of certain ligands to their appropriate receptors results in the biochemical activation of one or more of these caspases which exist as dormant zymogens/proenzymes in normal healthy cells. These pro-caspases are generally activated through proteolytic processing to form the active caspase (Thornberry and Lazebnik, 1998). Different members of the caspase family may be found confined to the nucleus, cytoplasm or mitochondrial intermembrane space and some may also be translocated to the plasma membrane receptors through adaptor proteins (Mancini *et al*, 1998).

Caspases cleave their target proteins at specific aspartate residues generally resulting in activation of that target protein. Caspases themselves are activated by proteolytic cleavage at cysteine residues in their active sites, usually by another caspase. Those caspases that are activated later in the processing cascade, termed effector caspases, (e.g. caspase 3) finally cleave many substrates (for review, see Fischer *et al*, 2003), resulting in biochemical and morphological changes that are features of apoptotic cells. Such features include cell membrane blebbing, external exposure of phosphatidylserine, cell shrinkage, nuclear condensation and DNA fragmentation (Lawen, 2003).

There are a total of 14 caspases recognized in mammalian cells which are partially structurally homologous to each other (Bonventure, 1993). These caspases are generally classified into initiators (2, 8, 9, 10) which cleave upstream of the apoptotic pathway and are activated in response to the initial pro-apoptotic signal. Effector caspases (3, 6, 7) which are normally activated by the initiator caspases and cleave downstream targets to effect the apoptotic process and form apoptotic bodies (Thornberry and Lazebnik, 1998) and caspases involved in cytokine maturation (1, 4, 5 and 13). The initiation of this cascade reaction is usually blocked by endogenous caspase inhibitors. Induction of apoptosis thus means overactivation of the initial caspases, overcoming the inhibition. Caspases 8, 9, and 3, are discussed later, as these are the major initiator (8 and 9) and final effector (3) caspases studied in this piece of work.

Caspase 8 (also known as FLICE, MACHα1, Mch5) is one of the two main initiator caspases and is associated with the induction of apoptosis by cell surface receptors where it is activated as part of a complex with the receptor and Fas associated death domain (FADD). The complex is formed when a cell surface receptor (e.g. TNF receptor) binds its ligand (e.g. TNF-α) and then recruits FADD (an adaptor protein) and pro-caspase 8. The inactive form of caspase 8 is cleaved to produce the 20kDa active peptide. Caspase 8 contains two N-terminal stretches homologous to the death effector domain (DED) of adapter proteins, (these are discussed later). The over activation of this protease induces apoptosis, but the co-activation of some of its isoforms blocks cell death (Chinnaiyan *et al*, 1995). There are 8 different isoforms (a-h), of caspase 8. Caspase 8a and 8b are the complete forms known to mediate apoptosis. However, the physiological role of other isoforms has yet to be clarified.

Caspase 9 (also known as ICE-LAP6, Mch6) is a member of the *ced-3* subfamily and has similarities to caspase 3, but they differ in the active-site pentapeptide. The inactive form of caspase 9 is cleaved to produce the 34kDa active peptide. The active site pentapeptide of caspase 9 is different from that of the other family members (being QACGG instead of QACRG). The key requirement for caspase 9 activation is its association with a dedicated protein cofactor, Apaf-1 (discussed in detail later in this thesis). Caspase 9 has a longer N terminal prodomain than other caspases with high similarity to the prodomains of *ced-3,* which contains caspase activation and recruitment domains (CARDs) (Duan *et al*, 1996). The proenzyme form is activated by caspase 3 *in vitro* (Li *et al*, 1997).

Caspase 3 (also known as CPP32, Yama, apopain), is one of the key effectors of apoptosis and is activated during the late stages of apoptosis. Caspase 3 belongs to the ICE subfamily of caspases. The inactive form of caspase 3 is first cleaved at Asp-175-Ser-176 to produce the 17 and 12kDa peptide. The active caspase 3 proteolytically cleaves significant targets in the cytoplasm (e.g. cytokeratin 18) and in the nucleus (e.g. poly (ADP-ribose) polymerase (PARP)). PARP is an enzyme involved in DNA repair and the regulation of several vital cellular processes such as differentiation and proliferation. This enzyme is largely located in the nucleus and is found in all eukaryotic cells except yeast. It is a polypeptide of about 118kD and when activated is cleaved into two fragments of 89kD and 24kD (Ruf *et al*, 1996). The effect of PARP cleavage by caspase 3 in apoptoisis is as yet unclear but there is evidence to suggest that, after an initial burst of PARP activity (Zaniolo *et al*, 2005) cleavage of the molecule results in de-activation, presumably interfering with DNA repair (Simbulan-Rosenthal *et al*, 1999).

Caspases are activated via controlled protein-protein interactions with upstream regulators. Caspase 8 contains a DED, while caspase 9 contains a CARD. These two domains share little sequence identity, but fold into almost identical 3D structures, comprising six antiparallel α-helices (Hoffman, 1999) which are also found in the death domain (DD), a third protein interaction module present in several upstream apoptotic regulators (e.g. CD95 and FADD). It appears likely that DD, DED and CARD are derived from a common ancestral domain (Hoffman, 1999). The death adaptor molecules normally trigger DD/DD, DED/DED and CARD/CARD interactions and structural analyses suggest that there is sufficient surface area on DDs, DEDs and CARDs to allow interaction with other proteins. Death adaptor proteins may act as integration platforms, binding to several proteins resulting in caspase activation (Hengartner, 2000).

Caspases are activated via two main pathways: the death receptor pathway (relying on the stimulus of cell surface receptors, e.g. TNF-α or Fas-L) and the mitochondrial pathway (relying on the stimulus of mitochondrial proteins, such as cytochrome c and smac/diablo due to cellular stress or DNA damage). The initiator caspases are generally activated by autoactivation, which occurs when several procaspase proteins are transported into close proximity.

1.5.2 Death receptor pathway

Death receptors are a family of cell surface receptors which instigate the process of apoptosis, but also promote proliferation and differentiation when activated by specific ligands. Induction of apoptosis through this mechanism is extremely rapid. Death receptors belong to the superfamily of tumour necrosis factor receptors (TNF-R), which include TNF-R1 (p55), TNF-R2 (p75) CD95 (also known as Apo-1 or Fas), decoy receptors (Dc1, Dc2 and Dc3), TRAIL-R1/DR4 (TNF-related apoptosis-inducing ligand receptors) and TRAIL-R2/DR5 as well as DR6 (Rudner *et al*, 2005).

TNF is produced by T_H cells ($CD4^+$) and activated macrophages in response to infection. Binding of TNF with TNF-R1 may have many effects and appears to proceed via two sequential signaling complexes. Complex I, the initial plasma membrane bound complex, consists of TNF-R1, TNF receptor associated death domain (TRADD), receptor interacting protein-1(RIP-1) and TRAF-2 and rapidly signals (in most cell systems) activation of nuclear factor-kappa B (NF-κB), a transcription factor that regulates the expression of a variety of anti-apoptotic proteins and usually therefore mediates cell survival signals (discussed later) and AP-1 (activating protein-1). The second step consists of TRADD and RIP-1 which are linked with FADD and caspase 8, forming a cytoplasmic complex, complex II. The activation of complex II results in cell death. In some cells however, TNF-α induces complex II-mediated apoptosis only and the complex I-initiated pro-survival pathway (i.e. NF-κB) fails to be activated (Micheau and Tschopp, 2003).

NF-κB has been documented as playing a key role in apoptosis. In dormant cells, NF-κB is stored in the cytoplasm in an inactive form via its interaction with numerous inhibitory proteins, e.g. IκB-α, IκB-β, IκB-ε, p105 and p100. NF-κB activation takes place via the formation of an intracellular complex (complex I) comprising several adaptor proteins, TRADD and RIP-1 (which interact with the DD of TNF-R1) and TRAF2. Following TNF-R1 activation, RIP-1 chiefly interacts with and activates the inhibitory κB kinase (IKK) signalosome (involving IKK1, IKK2 and IKKγ/NEMO). This sequentially results in phosphorylation, polyubiquitination and breakdown of the NF-κB inhibitor IκBα (Figure 1.2). This process allows translocation of the NF-κB p50–p65 heterodimer to the nucleus to bind DNA and induce anti-apoptotic gene expression. The anti-apoptotic pathway then activates c-$FLIP_L$ (cellular flice inhibitory

protein) which is a caspase-8 inhibitor, leading to the suppression of the cell death pathway (for review, see Chen *et al*, 2001).

FLIP (flice like inhibitory protein), is an enzymatically inactive homologue of caspase 8 and has recently been considered as a controller of cellular sensitivity to apoptotic cell death. FLIP was originally identified as a viral protein, which inhibited Fas mediated apoptosis when overexpressed in cells. Two isoforms were also identified $FLIP_L$ (long) and $FLIP_S$ (short). In particular, the $FLIP_L$ isoform appears to be a stronger inhibitor than the $FLIP_S$ isoform at similar expression levels (Irmler *et al*, 1997). $FLIP_L$ and $FLIP_S$ are catalytically inactive and possess the capacity to block procaspase 8 recruitment and activation at the complex called the death inducing signaling complex (DISC) when overexpressed *in vivo* (Scaffidi *et al*, 1999). Grassi *et al*, (2004) reported that immunoblotting of cultured chondrocytes treated with interferon-γ revealed an increased expression of cFLIP, at both the mRNA and protein levels.

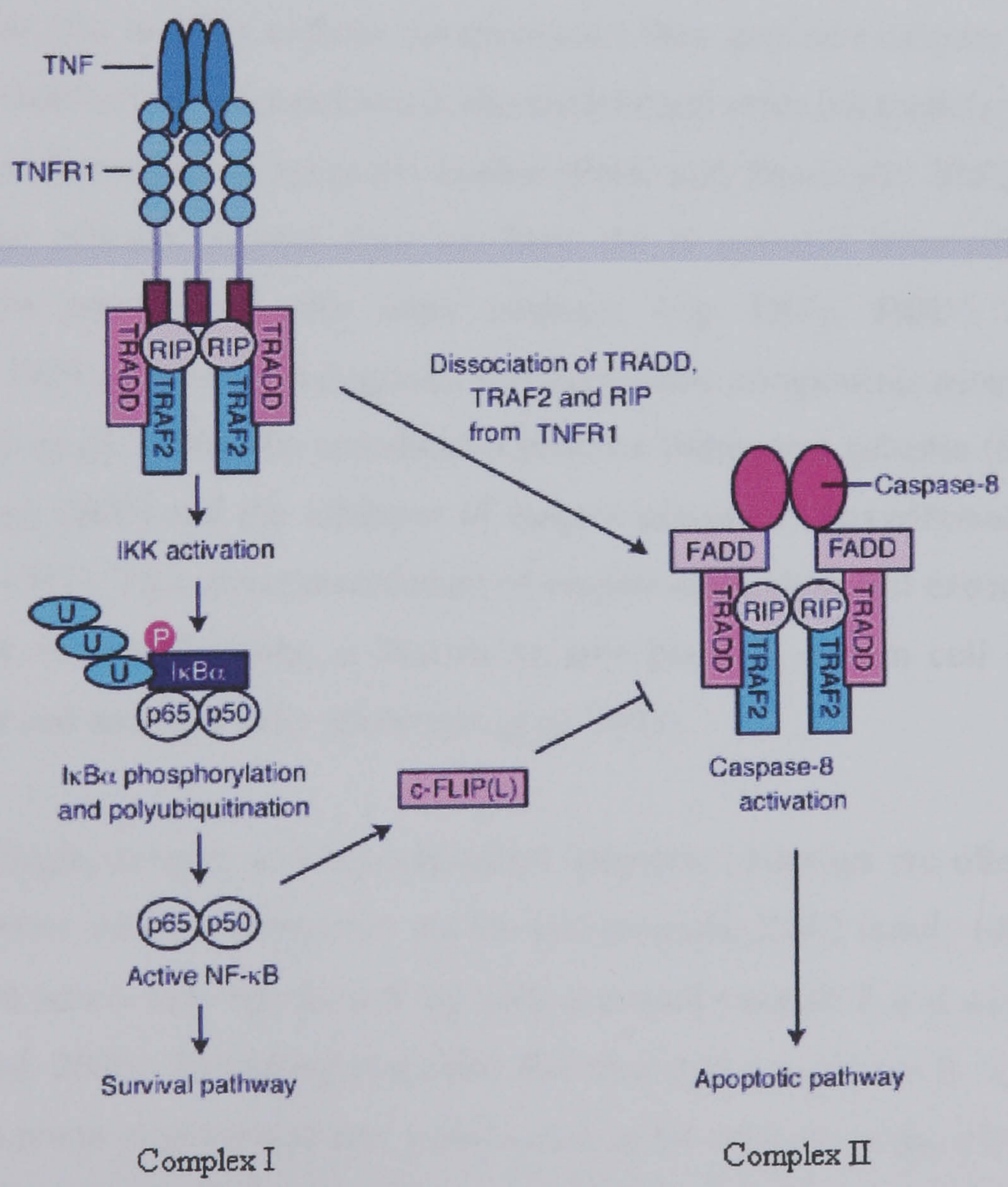

Figure 1.2: TNF-induced cell survival and cell death pathways

(Adapted from www-ermm.cbcu.cam.ac.uk/05009762h.htm, with slight modifications)

When NF-κB is not activated upon TNF-R1 mediated signaling, the lack of inhibition by c-FLIP$_L$ results in activation of the apoptotic pathway through caspase 8 (Figure 1.2). The death domain binds adapter proteins such as FADD, TRADD, and RIP-1 (Fraser and Evan, 1996). FADD possesses a DD that interacts either with the DD of death receptors, or indirectly through TRADD. TRADD can recruit several adaptor protein including FADD, TNF-receptor-associated factor (TRAF) and RIP1. RIP1 interacts with caspase 2 and RIP associated protein with death domain (RAIDD), to transduce death signals.

FADD contains a DED, which interacts with a comparable domain on the weakly active procaspase 8 (complex II), to form an intracellular multi-protein complex called the death inducing signaling complex (DISC) (Boatright *et al*, 2003). Once formed the DISC facilitates activation of caspase 8, which is further processed via an auto-proteolytic mechanism (Salvesen and Dixit, 1999). Active caspase 8, whether bound to the DISC or free in other cellular compartments then activates caspase 3 (an effector caspase), resulting in the breakdown of the nucleus and other intracellular structures and the eventual formation of apoptotic bodies (Peter and Krammer, 2003) (Figure 1.3). This smaller effector caspase does not have the N terminal homoaffinity domains, which allow interactions with other caspases (e.g. DD's, DED's and CARDS) (Hoffman, 1999), but rather it degrades various cellular components such as the nuclear lamins (Rao *et al*, 1996), the cytoskeletal proteins fodrin and gelsolin (for review, see Fischer *et al*, 2003) and the inhibitor of caspase-activated deoxyribonuclease (ICAD) (Liu *et al*, 1997). This direct mechanism of caspase-dependent cell execution, which is independent of mitochondria, is known to take place in certain cell types such as hepatocytes and neuronal cells (Boatright *et al*, 2003).

Whilst the death receptor and mitochondrial apoptotic pathways are often regarded as separate entities they are connected via the pro-apoptotic Bcl-2 family (discussed later) member Bid which may be cleaved by both activated caspase 8 and caspase 3 (Degli Esposti *et al*, 2003). Following cytosolic Bid cleavage by caspase 8, a p15 carboxy-terminal fragment is generated that translocates to the mitochondria, where it interacts with multidomain Bcl-2 family members to rapidly release cytochrome c from the mitochondria into the cytoplasm (Li *et al*, 1998; Liang *et al*, 2005), a central event in the mitochondrial mediated apoptotic pathway (Jiang and Wang, 2000). Figure 1.3

shows a diagram of the two main apoptotic pathways; the death receptor pathway and the mitochondrial pathway and the role of Bid in connecting the two pathways.

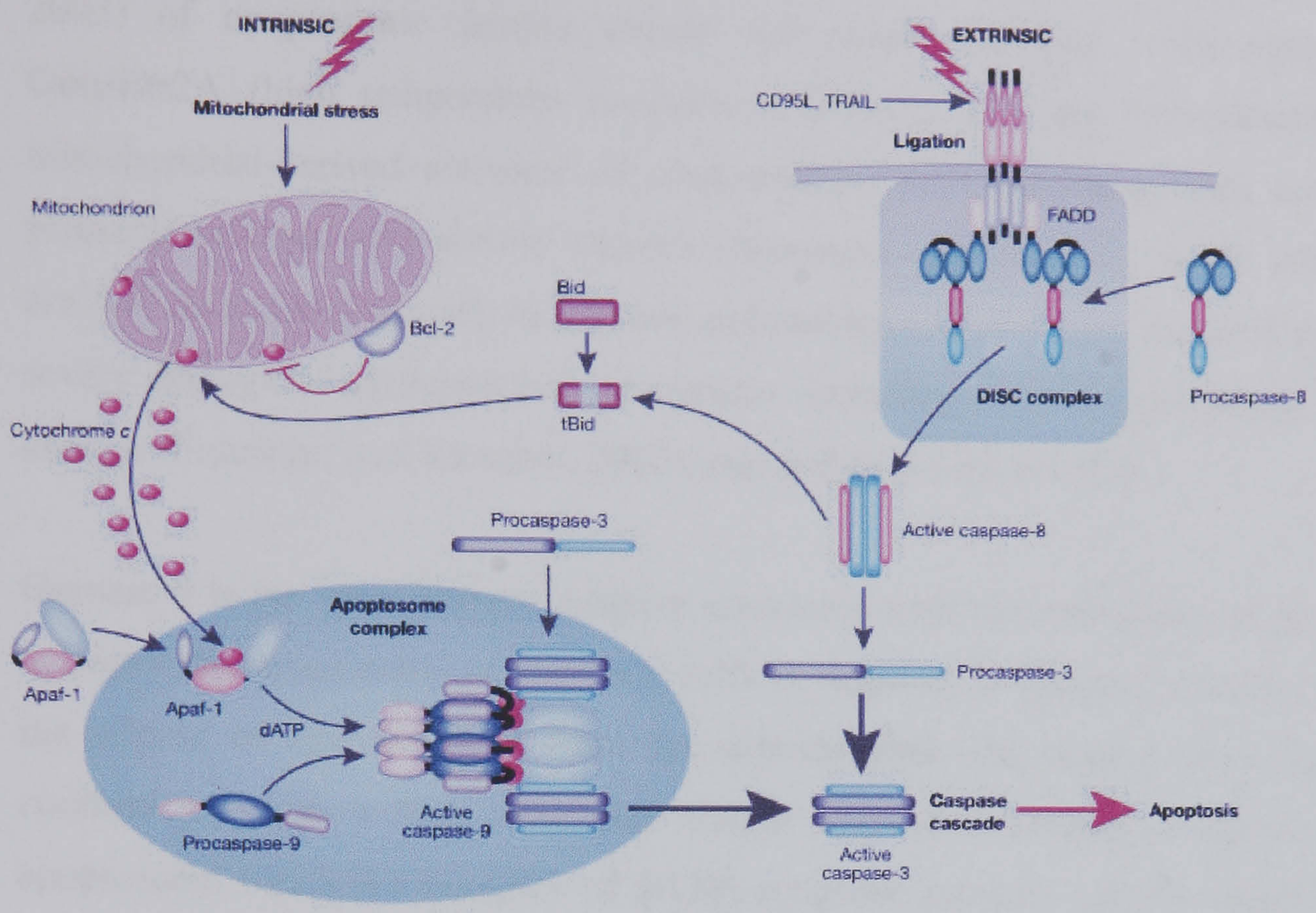

Figure 1.3: The intrinsic (mitochondrial) and extrinsic (death receptor) pathways to caspase activation (reviewed in Danial and Korsmeyer, 2004; and Macfarlan and Williams, 2004), with slight modifications.

1.5.3 Mitochondrial pathway

Mitochondria are now considered to be the central intracellular organelles which take part in mediating the majority of apoptotic pathways in mammalian cells (Reed, 2000). The mitochondrial pathway can be initiated by several stress stimuli including UV radiation, heat and DNA damage to name a few. These types of stress are perceived or translated by multiple cytosolic or intra-organellar molecules, which then transduce the signals to mitochondria resulting in changes in the outer mitochondrial membrane. This change leads to an increased permeability to proteins which are generally trapped between the outer and inner mitochondrial membrane, hence allowing these proteins to escape the mitochondria and diffuse into the cytosol (Saelens *et al*, 2004).

Amongst the proteins which are released from the mitochondria, some (e.g. cytochrome c) play a vital role in encouraging the caspase cascade of cell death, and are collectively

referred to as 'apoptogenic factors'. There seems to be a hierarchical release (Hill *et al*, 2003) of apoptogenic factors during cell death signaling, with cytochrome c, Omi/Htr2A (high temperature requirement protein A2) and Smac/Diablo (second mitochondrial-derived activator of caspase/direct IAP binding protein with low pI) primarily released with similar kinetics (Penninger and Kroemer, 2003). Also released are AIF (apoptosis inducing factor) and endonuclease G which are associated with more severe damage of mitochondrial membranes, including inner mitochondrial membrane change (Penninger and Kroemer, 2003), and will be discussed later.

Caspase 9 is the main initiator caspase associated with the mitochondrial pathway and activates the disassembly of apoptotic cells in response to agents or insults that trigger the release of cytochrome c from the mitochondria. Pro-caspase 9 is activated by combination with a high molecular weight caspase activating complex called the apoptosome which is a complex of dATP, apoptotic protease activity factor-1 (APAF-1), and extramitochondrial cytochrome c (Li *et al*, 1997). APAF-1 recognises and binds to cytosolic procaspase-9 through a CARD and induces processing and activation of this enzyme which activates the downstream caspase cascade. After activation, caspase 9/apoptosome complex is a stable and potent structure which stays intact during apoptosis and results in higher caspase enzymatic activity than the caspase alone (Jiang and Wang, 2000). The primary target of the caspase 9/apoptosome complex is procaspase 3. This complex is also known to allow caspase 3 entry into the nucleus which then cleaves the inhibitory subunit of ICAD resulting in CAD activation and DNA fragmentation, as for the death receptor pathway (Lorenzo *et al*, 1999)

The apoptosome does however require extra regulatory factors to completely activate the caspase cascade. These factors include Smac/Diablo which is released from the mitochondria alongside cytochrome c in response to apoptotic stimuli and binds to inhibitor of apoptosis proteins (IAPs) preventing inhibition of caspase 9 and 3 activation by these proteins (Baliga and Kumar, 2003). The IAPs are a family of anti-apoptotic proteins that are conserved across numerous species. Their main role is to bind and inhibit the activation and activity of specific caspases (Schimmer, 2004).

Bid is a member of a large family of proteins known as the Bcl-2 family which are involved in the control of apoptosis, chiefly via the mitochondrial pathway.

1.5.4 The Bcl-2 family of proteins

The B cell leukaemia/lymphoma proto-oncogene 2 (Bcl-2) family of proteins are vital regulators of apoptosis in mammalian cells. The Bcl-2 family consists of, both anti-apoptotic, and pro-apoptotic proteins, located mainly in the outer mitochondrial membrane, the endoplasmic reticulum and the outer nuclear envelope. At least 15 Bcl-2 family members have been identified in mammalian cells (Gross *et al*, 1999) and several others in viruses (Chao and Korsmeyer, 1998), which can indirectly control the activity of caspases by changing mitochondrial events during apoptosis. Pro-apoptotic members of the Bcl-2 family increase mitochondrial membrane permeability, whereas anti-apoptotic members of the family act to oppose this increase and prevent the release of pro-apoptotic mitochondrial proteins into the cytoplasm. Bcl-2 family proteins are classified into three subfamilies (for a recent detailed review, see Danial and Korsmeyer, 2004), which share some regions of homology known as Bcl-2 homology (BH) regions. The three families are:

- The Bcl-2 subfamily (including Bcl-2, Bcl-x_L, Bcl-w, Mcl-1, A1, ced-9), are anti-apoptotic, and promote cell survival. These proteins are present on several intracellular membranes and link both the inner and outer mitochondrial membranes. Their main action is to prevent increases in mitochondrial membrane potential by preserving the integrity of the membranes. Bcl-2 directly or indirectly inhibits the release from mitochondria of cytochrome c, which (along with ATP) could facilitate a change in APAF-1 structure permitting procaspase 9 recruitment and processing. They possess up to four conserved Bcl-2 homology (BH) domains designated BH1, BH2, BH3 and BH4, which correspond to α helical segments (Reed, 1997).

- The BH3-only subfamily (including Bad, Bmf, Bik, Bid and Bim_L), are pro-apoptotic and promote cell death. These are present in subcellular locations other than the mitochondria on which they function and require activation before they can translocate to the mitochondria where they interact with multi-domain Bcl-2 family members. For example, Bad forms heterodimers with Bcl-2 and Bcl-x_L (anti-apoptotic) preventing them from exerting their anti-apoptotic action. Bid, which is freely present in the cytosol of live cells, is cleaved by caspase 8 to

form a 15 kDa N-truncated derivative (tBid) which moves to the mitochondria and causes cytochrome c release by changing the conformation of Bax.

- The Bax subfamily (including Bax, Bak, and Bok) are also pro-apoptotic and promote cell death (Gross *et al*, 1999). The Bax subfamily is structurally similar to the Bcl-2 subfamily but without the functional BH4 domain. Bax and Bax-like proteins may mediate caspase-independent death via channel forming activity that may trigger the mitochondrial permeability transition by penetrating the outer mitochondrial membrane and allowing cytochrome c release.

The balance of pro-apoptotic and anti-apoptotic members of the Bcl-2 family of proteins in a cell partially determines the fate of that cell: cells with more pro- apoptotic proteins are prone to death; cells with a large amount of protective family members are generally resistant to death. For example, chondrocyte apoptosis is associated with downregulation of Bcl-2 expression (Feng *et al*, 1998) resulting in alterations in ECM proteins and cartilage degeneration (Kim *et al*, 2002).

1.6 Pro-apoptotic Stimuli

1.6.1 Nitric Oxide

Nitric oxide (NO) is a potent inducer of apoptosis and is the product of NO synthases (NOS) (NADPH-dependent cytosolic enzymes) (Blanco *et al*, 1995; Stadler *et al*, 1991) and as well as being a pro-apoptotic stimulus is involved as a regulator and effector molecule in diverse biological systems.

NO is a short lived (0.5-5s) inorganic free radical gas, that is labile and quickly metabolized to nitrate and nitrite in the presence of oxygen. NO behaves as an intercellular messenger at a low physiological level but is thought to have pathophysiological relevance when it is produced in large amounts by the inducible form of NOS (iNOS). NO is synthesized by the oxidation of the amino acid L-arginine to NO and L-citrulline via a complex reaction using the cofactor tetrahydrobioterin, and molecular oxygen as cofactors and catalysed by three isomeric forms of the synthetic enzyme NOS. Of these three isoforms, two are constitutive and one inducible. The two constitutive forms are calcium/calmodulin dependent and were originally named for the

tissues in which they were first isolated NOS-1/nNOS (neuronal) and NOS-III/eNOS (endothelial). The inducible form of NOS is calcium independent and known as NOS II/iNOS. The three NOS isoforms share approximately 60% homology and fall into the cytochrome P450 reductase-like family (Crane *et al*, 1997). In addition to these well established NOS isoforms, a distinct isoform has recently been described in mitochondria, named mtNOS (Giulivi *et al*, 1998). This isoform is calcium dependent, and appears to play an important role in the regulation of respiration, matrix pH and transmembrane potential in mitochondria (Ghafourifar and Richter, 1999).

The NO produced by neuronal, NOS-I and endothelial NOS III isoforms performs the biological roles of regulating the cardiovascular and nervous system (Amin and Abrahamson, 1998) and release NO for short time periods in response to receptor stimulation (Moncada *et al*, 1991). The Ca^{2+}/calmodulin dependence of NOS I and NOS III permits stimulation via first messengers or agents which enhance intracellular Ca^{2+} levels resulting in the increase of other Ca^{2+} dependent enzymes. NOS II (iNOS) is usually however only expressed in response to an immune challenge or cell/tissue damage (Gellar *et al*, 1993), and once expressed, this enzyme binds to calmodulin (at normal intracellular Ca^{2+} levels (30-70nM)) and constantly produces a considerably greater amount of NO than the constitutive isoforms.

NO, is a highly diffusible, highly reactive second messenger molecule which can readily diffuse through cell membranes to exert its biological actions through interaction with a variety of proteins (Beckman and Koppenol, 1996). These include:

- Haemproteins, leading to activation of guanylate cyclase (discussed later) interaction with hemoglobin and modulation of cyclooxygenases;
- Iron-sulphur enzymes, leading to inhibition of aconitase, ribonucleotide reductase and mitochondrial complexes following blockade of electron transport chains;
- Poly (ADP-ribosyl) polymerase (PARP), whose indirect activation leads to a dramatic fall in energy store resulting in cellular death.
- Nitrosoproteins and nitrosoglutathione interact through its high affinity for thiol functions resulting in prolonged cellular effects despite its short half life

NO is also known as an inhibitor of cell proliferation and many of the biological actions of NO are mediated when soluble guanylate cyclase is stimulated and acts on guanylate

triphosphate (GTP) to generate intracellular cyclic guanylate monophosphate (cGMP) (Mcdonald and Murad, 1995). Increased cGMP can then activate several kinases that subsequently lead to alterations in intracellular calcium content and protein de-phosphorylation by activating phosphatases (Koppal *et al*, 1999), thus linking the NO-induced increase in guanylate cyclase activity to other known second messenger system in a number of cells.

NO changes the biological action of many proteins by reacting directly with their iron centres and also by *S*-nitrosylating cysteine residues to form *S*-nitrosothiols. It was originally expected therefore that NO might block apoptosis through *S*-nitrosation of the active site cysteine residue in caspases. This does in fact occur and *S*-nitrosation and inactivation of processed caspases can take place *in vitro* (Bernassola *et al*, 2001), however the exogenous addition of NO generated from chemical NO donors (discussed later) has been shown to induce apoptosis in a variety of cells (Blanco *et al*, 1995). As NO is capable of influencing several biological activities, apoptosis induction by NO is dependant on both the type of cell and the cellular redox state, the concentration and release of NO are also important (Heigold *et al*, 2002). NO has a toxic effect and causes cell death (Sandau *et al*, 1997), it may play a role of intercellular messenger; when cell capacities to neutralize the NO with reactive oxygen species (like superoxides) are exhausted. Sandau and Bruene, (2000) later reported that the apoptosis inducing effect of NO was completely blocked by the simultaneous presence of superoxide anions. A more direct mechanism for NO-mediated apoptosis is reported by Nguen *et al*, (1992) who showed that NO may deaminate purine and pyrimidine bases in DNA and enhance DNA strand breaks.

NO is produced by both synoviocytes and chondrocytes and has been implicated in the pathophysiology of OA (Stefanovic-Racic *et al*, 1994; Castro *et al*, 2006). Farrell *et al*, (1992) and Hilliquin *et al*, (1997) have demonstrated increased levels of nitrite, nitrate and nitrosoproteins (used as a measurement of NO) in both serum and synovial fluid samples from OA patients. NO release stimulates chondrocyte apoptosis (Del Carlo and Loeser, 2002) and inhibits aggrecan synthesis, as well as activating MMPs (Taskiran *et al*, 1994), and therefore may be a factor in disease pathogenesis in a number of ways. Elevated production of NO by either synovial cells or chondrocytes in OA would also encourage increased vasodilation and permeability (Mayhan, 1992), and the possibility of TNF and IL-1 release by leukocytes (Leibovich *et al*, 1994). NO synthesis is

triggered by many cytokines which exist in OA joints, such as IL-1β, TNF-α and IL-17 and there is increased evidence that NO may be an important second mediator of IL-1β and TNF-α activity in the inhibition of chondrocyte proteoglycan synthesis. Conversely, McInnes *et al*, (1996) reported that synoviocytes and macrophage cell lines, cultured with the NO donor, s-nitrosoacetyl penicillamine, generated increased concentrations of TNF-α, indicating that NO may mediate pathology by the induction of TNF-α and vice versa. NO may also be produced in cartilage in response to various mechanical and chemical stresses (Buckwalter and Mankin, 1997). Normal cartilage however, does not produce NO or express NOS unless stimulated with cytokines like IL-1β, TNF-α or lipopolysaccharide (LPS). Van de Loo *et al*, (1998) showed that in mice, NO synthesis by iNOS plays a vital role in the inhibition of proteoglycan synthesis caused by IL-1β and experimental joint inflammation. The work of Amin *et al*, (1995) however studied chondrocytes isolated from patients with OA and proposed that the osteoarthritic NOS expressed in chondrocytes resembled nNOS rather than iNOS, both from its immuno-reactivity and from its apparent molecular mass. A correlation has also been reported, between the level of NO production and the prevalence of apoptotic cells in cartilage (Blanco *et al*, 1995).

Human articular chondrocytes can actively produce reactive oxygen species (ROS), including, superoxide anion, the hydroxyl radical, and hydrogen peroxide (Hiron *et al*, 1997). Many of the vital biological reactions involving NO appear to be those with oxygen, transition metal ions and free thiols (Stamler *et al*, 1992). Since NO can combine with superoxide ($O_2^{\cdot-}$), these two radicals undergo a rapid, diffusion-limited, reaction leading to the production of peroxynitrite ($ONOO^-$), a powerful oxidant with potent biological effects (Fukai *et al*, 2000), which can decompose into inactive compounds, or generate hydroxyl radicals or nitrate tyrosine residues in proteins to form 3-nitrotyrosine (3-NT). The presence of 3-NT, can act as a marker for oxidative damage and in a recent study 3-NT was detected in the articular cartilage of older nonarthritic monkeys and humans and in OA cartilage, but not in normal cartilage from young adults (Loeser *et al*, 2002). Peroxynitrite and related NO species encourage nitrosative and oxidative stress, and thus may be responsible for much NO-dependent cytotoxicity (Wink *et al*, 1996), possibly by changing the mitochondrial membrane potential (Li *et al*, 1999). The initiation of experimentally induced arthritis in animal models can be blocked by the NOS inhibitor N^G-monomethyl-L-arginine (L-NMMA) (Stefanovic-

Racic *et al*, 1994) and the addition of a NOS II inhibitor reduces cartilage damage and chondrocyte apoptosis (Pelletier *et al*, 1999).

NO also regulates chondrocyte function in various other ways including the inhibition of β1 integrin dependent adhesion to extracellular matrix, synthesis of cartilage-specific ECM molecules such as type II collagen and proteoglycan, and provoking dedifferentiation of chondrocytes (Cao *et al*, 1997). NO modulation of matrix metalloproteinases also occurs causing further degradation of the cartilage matrix (Sabatini *et al*, 2000).

1.6.1.1 NO donors

The growth of interest in the physiology of NO since the mid 1980s has led to the development of a range of chemicals known as NO donors which release NO when added into aqueous systems. There are a number of NO donor molecules with different chemical properties which are used to supply NO to cells for potential therapy and research purposes and, to evaluate the biological activity of exogenously produced NO. The biological effects of the different NO donors vary (Uehara *et al*, 1999) but they are generally toxic and produce changes in cell morphology consistant with the induction of apoptosis. The effects of NO donors appear to be largely dependent on the redox state of the NO related species released; NO, nitrosonium ions, or nitroxyl anions (Lipton *et al*, 1998). Common NO donors include sodium nitroprusside (SNP), *S*-Nitroso-*N*-acetyl-*D*-*L*-penicillamine (SNAP), NOC18, *S*-nitrosoglutathione (GSNO) and *3*-morpholinosyndonimine (SIN-1). However, the main two types of NO donors used are: the NONOates, which are allegedly 'pure' NO donors and the -*S*-nitrosothiols, which may liberate NO, as well as transfering the NO^+ group to a range of proteins which contain reduced thiol groups (a process referred to as transnitrosylation) (Feelisch *et al*, 1995). Most research on NO-induced apoptosis has been performed using nitrosothiols like SNAP and GSNO as NO donors (Hortelano *et al*, 1997; Balakirev *et al*, 1997; Jia *et al*, 1996; Shen *et al*, 1998). Whilst these reagents will certainly induce apoptosis the exact mechanism is not always clear as they can cause glutathione depletion and may transnitrosylate nearby thiols in many if not most proteins, resulting in changes in protein function (Ji *et al*, 1999).

It seems likely that the cartilage damage observed in OA may be a result of the combined effects of NO and other stimuli including the cytokines TNF-α and IL-1β. Murakami *et al*, (2000) showed that all three of these stimuli are present in human osteoarthritic cartilage but not in normal cartilage and have been shown to cause suppression of chondrocyte function and induction of apoptosis (Sakurai *et al*, 1995).

1.6.2 Cytokines

Cytokines are small multifunctional proteins with short half lives that act as intercellular signaling molecules. They are actively secreted by immune cells and other cell types in response to a variety of stimuli and generally exert their effects through either a paracrine, or autocrine mechanism (Goldring and Goldring, 2004). Cytokines act by binding to specific cell membrane receptors each of which triggers a distinct signal transduction cascade that eventually will lead to biochemical and phenotypical changes in the target cell.

In terms of chondrocyte function, it is feasible to categorize the cytokines which control cartilage changes as anabolic cytokines (that behave as growth and differentiation factors on chondrocytes to enhance synthetic activity) or as catabolic cytokines (which promote matrix degradation) (Goldring, 2000). Many of these biological mediators appear to be released by synoviocytes in the synovial membrane and diffuse into the cartilage where they activate the chondrocytes (Wang *et al*, 2001). The pro-inflammatory cytokines TNF-α, IL-1β, IL-6, IL-8, and IFN-γ are associated with inflammation in synovial joints and destructive mechanisms in the joint such as prostaglandin and metalloproteinase production and cartilage resorption (Kacena *et al*, 2001). IL-11 is known to be involved in preventing excessive ECM degeneration induced by synovial inflammation (Yao *et al*, 1995), whilst, IL-17 is known to increase the production of NO in chondrocyte cultures (Attur *et al*, 1997).

Tumour necrosis factor-alpha (TNF-α) and Interleukin-1beta (IL-1β) are two of the most prominent pro-inflammatory cytokines that initiate various biological responses involved in tissue damage and repair (Kobayashi *et al*, 2005) and have been implicated in many inflammatory disorders (Symons *et al*, 1992; Woolley and Tetlow, 2000; Marks and Donaldson, 2005). TNF-α and IL-1β have also been implicated as two of the main catabolic factors in osteoarthritic cartilage.

1.6.2.1 TNF-α

TNF-α (also referred to as cachectin or lymphotoxin), was first isolated by Carswell *et al,* (1975) as a soluble factor released by host cells that caused necrosis of a transplanted tumour 'sarcoma Meth A'. TNF-α is produced by a wide variety of cells including neutrophils, activated lymphocytes, macrophages, natural killer cells, astrocytes, endothelial cells, smooth muscle cells and some transformed cells (Aizawa *et al*, 2001). TNF-α occurs as both a secreted, soluble form (17kDa) and as a membrane-anchored form (26kDa), both of which are biologically active. The naturally occurring form of TNF-α is glycosylated, but non-glycosylated type II recombinant TNF-α has comparable biological activity, (Ah-Kim *et al*, 2000; Tartaglia and Goeddel, 1992).

TNF has been implicated in the pathogenesis of a variety of diseases including arthritis, infection and malignancy (Aggarwal and Natarajan, 1996). Both TNF-α and the closely related TNF-β mediate similar biological activities to each other and to that of IL-1, although TNF and IL-1 are not structurally related (Ah-Kim *et al*, 2000). Recent research suggests that both TNF-α and IL-1β may play a role in the cartilage loss seen in OA, and, in particular, in post traumatic OA where a more marked increase in TNF-α and IL-1β than their inhibitors has been demonstrated. This possible imbalance between cartilage damaging and cartilage-preserving factors may therefore lead to progressive cartilage loss over time (Marks and Donaldson, 2005). Other authors have however, reported low levels of TNF-α in OA articular tissue (Fernandes *et al*, 2002).

As mentioned earlier, TNF-α binds to two specific receptors present on the cell membrane of numerous cell types (Eger *et al*, 1999) but not erythrocytes (Tartaglia and Goeddel, 1992). The two TNF receptors have molecular masses of 55 to 60kD and 75 to 80kD and are often referred to according to their molecular weight TNF-R55 (TNF-RI) and TNF-R75 (TNF-RII). TNF receptors are members of a large family of homologous receptors (currently 30 different members) with cysteine rich extracellular motifs that also include Fas and CD40 (Gaur and Aggarwal, 2003). Both receptors have significant homologies but the cytoplasmic domains of TNF-R55 (414 amino acids) and TNF-R75 (461 amino acids) are distinct, indicating these receptors may use different signal transduction pathways to enhance a specific subset of TNF-α activities (Howard *et al*, 1993; Alsalameh, *et al*, 1998). In articular tissue cells, TNF-R55 appears to be the main

receptor responsible for mediating TNF-α activity and enhanced expression of TNF-R55 has been reported in OA chondrocytes and synovial fibroblasts (Alaaeddine *et al*, 1997). TNF-R55 initiates signals for cytotoxicity, fibroblast proliferation, cell adhesion and the induction of several other genes whereas TNF-R75 may regulate the amount of TNF-α binding to TNF-R55 (Tartaglia *et al*, 1993) and specifically takes part in the control of cell proliferation and cytokine secretion (Alsalameh *et al*, 1998). As well as a general increase in TNF-R expression in OA cartilage, focal loss of articular cartilage in OA joints is linked with local upregulation of the TNF-R55 (Webb *et al*, 1997). The expression of TNF-R on human articular chondrocytes is upregulated by OA synovial fluid and TNF-α itself (Webb *et al*, 1998).

Whilst TNF-α is produced by a variety of cells it is possible that the chondrocytes themselves are the most likely source of TNF-α in OA joints. OA chondrocytes and synoviocytes show high expression of this cytokine with increased messenger RNA levels of TNF and the TNF convertase enzyme as compared with those of normal cartilage (Melchiorri *et al*, 1998; Amin, 1999) resulting in an enhanced production of functional TNF-α. Treatment of primary OA cartilage explants with soluble TNF-α receptors (as specific inhibitors) inhibited the sudden release of IL-8 by chondrocytes further suggesting that OA cartilage generates functional TNF-α, and that this TNF-α plays a role in the regulation of cytokine production by osteoarthritic chondrocytes (van der Kraan and van den Berg, 2000).

TNF-α may mediate cartilage loss by two mechanisms. First, it induces the production of metalloproteases, free radicals, and other cytokines that directly destroy the cartilage matrix. Second, it prevents the chondrocyte from repairing the damaged articular matrix, and over time these two mechanisms result in cartilage loss. TNF-α inhibits collagen synthesis, induces prostaglandin synthesis and also stimulates the production of colony-stimulating factors by connective tissue cells. The TNF-α mediated increase in prostaglandin synthesis by synovial cells may be related to the clinical symptoms of OA such as pain and joint swelling (Ah-Kim *et al*, 2000). TNF-α involvement in arthritis is also supported by data from animal models where the potency of TNF-α in initiating inflammation in the collagen induced arthritis mouse model was clearly observed (Mukherjee *et al*, 2003). It has also been shown that a single intra-articular injection of TNF-α in rats triggered the onset of arthritis, but a combined injection of

TNF-α and IL-1β triggered a more serious inflammatory response than when the cytokines are given separately (Tonussi and Ferreira, 1999).

1.6.2.2 IL-1β

IL-1 is a member of the interleukin family of cytokines that are expressed by white blood cells and other cell types as a way of communication. IL-1 plays an important role in the inflammatory response but is also known to exert effects on bone formation and remodeling, insulin secretion, appetite regulation, fever induction and neuronal development (Goldring and Goldring, 2004). IL-1 exists in two forms, IL-1α and IL-1β which are 30% homologous to each other, bind to the same cell surface receptors and mediate the same biological activities (Martel-Pelletier *et al*, 1992). A role for IL-1β in OA is suggested by the demonstration of this active form of IL-1 in synovial membrane, synovial fluid and cartilage of OA joints (Pelletier *et al*, 1999).

IL-1 is primarily synthesized as a 31 kilodalton (kD) precursor and proteolytically cleaved by IL-1β converting enzyme (ICE/caspase 1) to yield the active form of IL-1β at 17.5kDa and the smaller cleaved product, IL-1α (Siders, *et al*, 1993). ICE was the first member of the mammalian caspase family to be described (Stellar, 1995). The biological activity of cells by IL-1 is mediated via association with two specific cell surface receptors (IL-1R), named type I and type II (Slack *et al*, 1993). Type I receptor binds IL-1β more than IL-1α and is mostly accountable for signal transduction as well as being expressed in almost all cell types (Martel-Pelletier *et al*, 1992). Type II IL-1R has a greater affinity for IL-1α than IL-1β and is expressed predominantly on B lymphocytes but, may be induced on other cell types. Its major function appears to be to act as a 'decoy' receptor and competitively inhibit IL-1β binding to the type I signaling receptor. Type I IL-1R is increased significantly in OA chondrocytes and synovial fibroblasts and may be responsible for the hypersensitivity of these cells to stimulation by IL-1 (Martel-Pelletier *et al*, 1992). Interleukin 1 receptor antagonist (IL-1ra) has also been established, and its known action is the competitive inhibition of the binding of interleukin 1 (IL-1) to its receptor.

IL-1β is known to play an important role in the inflammation and joint destruction which are typical features of both RA and OA (Ysuhara *et al*, 2005). IL-1β is produced

in significant quantites in OA joints, by OA chondrocytes, and induces an increased production of destructive proteases (Pelletier *et al*, 1995). The first description of IL-1 as a regulator of chondrocyte function comes from the studies of Fell *et al* (1977). In an *in vitro* model, Fell *et al* cultured normal, noninflamed porcine synovial tissue with cartilage fragments. They observed cartilage matrix breakdown by local chondrocytes and established that the synovial tissue was producing a soluble factor, catabolin that encouraged chondrocytes to breakdown their surrounding cartilage matrix. The two isoforms of catabolin detected were later identified as IL-1β and IL-1α (Saklatvala *et al*, 1984). IL-1β is also known to suppress cartilage-specific collagen (Goldring *et al*, 1988) and proteoglycan (Yaron *et al*, 1989) production in cartilage explants, primary chondrocyte cultures and immortalized human chondrocyte cultures (Goldring *et al*, 1994). Goldring *et al*, (1988) have also reported the up-regulation of the production of non-cartilage collagen types by chondrocytes subjected to IL-1β. This cytokine may also take part in normal development, as it has been demonstrated in the cartilage resorption zone during endochondral ossification of immature mouse bone (Takacs *et al*, 1988). IL-1β is considered to be the major cytokine inducing catabolic processes in cartilage and stimulates the expression of metalloproteinases (MMPs). It is also a potent inhibitor of chondrocyte proliferation (Knott *et al*, 1994).

1.6.3 Other Pro-apoptotic Stimuli

The Fas (CD95)/Fas ligand (CD95L) system is the other main initiator of apoptosis. Fas is a 48kDa transmembrane receptor glycoprotein, which belongs to the TNF-R superfamily and is present on many cell types including chondrocytes. Fas is activated by the binding of Fas ligand (FasL) which may be membrane bound or in a soluble form. Fas activation, in common with other TNF-R mechanisms, induces apoptosis via a caspase 8 mediated signaling pathway. Fas/FasL induction of chondrocyte apoptosis leads to defective cartilage homeostasis and joint destruction as described earlier (Hashimoto *et al*, 1997). Large quantities of Fas-L have been reported in the serum and synovial fluid of patients with OA and RA (Renoux *et al*, 1996). Moreover, Fas expression near OA cartilage lesions was discovered to be enhanced compared to areas also away from the lesion (Kim *et al*, 2000) and was also found to be in older cartilage (Todd Allen *et al*, 2004). Fas expression is mainly a feature of chondrocytes in the superficial and upper midzone of articular cartilage, but other groups have shown similar levels of Fas expression in OA cartilage as compared to normal joints. These

data would indicate that expression of Fas is not upregulated in OA and suggests that increases of Fas-L expression, or sensitization of Fas pathways, may be accountable for the increase in apoptosis noticed in OA (Hashimoto *et al*, 1997). The Fas/FasL system has been shown to be present in growth plate chondrocytes *in vivo* suggesting that it also plays a role in chondrocyte apoptosis during endochondral development. NO synthesis is not stimulated in Fas-L induced chondrocyte apoptosis suggesting there are several apoptotic pathways working in chondrocytes (Aizawa *et al*, 1997).

1.7 Urocortin and other related CRH family peptides

1.7.1 The CRH family of peptides

Corticotropin-releasing hormone or factor (CRH/CRF) is a 41 amino acid (aa) residue neuropeptide which effects various behavioural, neuroendocrine, and autonomic responses by inducing secretion of adrenocorticotrophic hormone (ACTH) from the hypothalamic-pituitary axis (HPA) (Porcher *et al*, 2006). The paraventricular nucleus (PVN) of the hypothalamus is the primary source for synthesizing CRH that controls stress-induced pituitary-adrenal activation in the brain (Konishi *et al*, 2003). Following its initial isolation in 1981, CRH was subsequently isolated in the placenta, and found to be identical to CRH in the hypothalamus (Shibasaki *et al*, 1982). It has since been reported in extrahypothalamic sites in the brain (Swanson *et al*, 1983) and other tissues in the periphery, such as the adrenal gland, testis, placenta, gut, spleen, thymus and skin. CRH is a highly conserved molecule with human and rat CRH identical to one another and ovine CRH differing only by seven amino acids. All are produced by proteolytic cleavage of the C terminus of the 196 aa precursor pre-pro CRH.

CRH is also known to stimulate IL-1β, TNF-α and IL-6 production by peripheral blood mononuclear cells (Kohno *et al*, 2001) and is found in peripheral inflammatory sites where, in comparison to its indirect systemic immunosuppressive effects, it actually acts as an autocrine or paracrine inflammatory peptide. Kohno *et al*, (2001) have reported the native production of immune CRH in various inflammatory sites including streptococcal cell wall and adjuvant induced arthritic joints in rats (Donaldson *et al*, 1996; Bamberger *et al*, 1998) and it has also been demonstrated in the joints of RA and OA patients (Bamberger *et al*, 1998).

In 1995, research guided by Vale (Vaughan *et al*, 1995) cloned and established a new mammalian member of the CRH related peptide family by probing a rat midbrain cDNA library Urotensin I (fish) which was named urocortin (UCN). Two further peptides closely related to UCN have been more recently isolated, urocortin II (Reyes *et al*, 2001), and urocortin III (Lewis *et al*, 2001). These three peptides are now considered to comprise the urocortin family of CRH like peptides.

1.7.1.1 Urocortin

Urocortin (UCN) shares 45% sequence homology with CRH (Vaughan *et al*, 1995) and is expressed in both the central nervous system and periphery (Poliak *et al*, 1997) and was the second member of the CRH family to be identified in humans. As well as CRH, it showed close homology to other members of the family discovered in non human species such as urotensin I (URO I) from fish, and sauvagine (SVG) from amphibia (Latchman, 2002).

Human UCN possesses only about 44-59% sequence identity with the URO I (41 aa) isolated from various fish species (Lovejoy and Balment, 1999) and the UCN mRNA shows a series of truncations relative to that in URO mRNA. Rat UCN possesses about 40% sequence similarity with the primary structure of sauvagine and about 50% with URO. Although SVG and URO were initially thought to be CRH homologs in fish and amphibians, the cloning of CRH from fish and frogs determined that many vertebrates possesses additional members of the CRH peptide family (Zhao *et al*, 1998).

Regardless of species, the UCN genes hold two exons (with all the coding information contained within the second exon) and a short intron (260 bp) with only subtle differences between the various mammalian genes (Zhao *et al*, 1998). The mRNA created from this gene translates into a protein with 122 amino acids containing an N-terminal methionine and signal peptide which is then processed by proteolytic cleavage to form the 40aa active peptide (Latchman, 2002).

UCN is expressed centrally in the Edinger-Westphal nucleus, the lateral superior olive, the lateral hypothalamus, and the supraoptic nucleus of rat brain (Vaughan *et al*, 1995) and has also been observed in many sites other than the CNS, such as peripheral blood lymphocytes, placenta, heart, GI tract, spleen, testis and kidney (Kageyama *et al*, 1999).

In keeping with its wide distribution, UCN has been reported to have many modes of action. UCN affects the cardiovascular system and when given systemically, those effects exceed those elicited by CRH i.e. UCN is more potent than CRH. It has been reported that UCN activates the immune system in both a corticosterone-dependent and independent manner, and the presence and function of UCN in peripheral inflammatory sites has been reported (Reyes *et al*, 2001). UCN has however been recognized in macrophages in the lamina propria of human colonic mucosa, where it may be taking part in the control of the inflammatory response (Muramatsu *et al*, 2000). Central administration of UCN to rats results in a reduction in feeding (Spina *et al*, 1996) and an increase in anxiety-like behaviour (Moreau *et al*, 1997).

The most interesting action of UCN with regard to this study is its cytoprotective properties first reported by Brar *et al*, (1999) who showed a protective effect of UCN against hypoxia mediated apoptosis in cardiomyocytes. It is therefore possible that UCN may perform a similar function in chondrocytes preventing or ameliorating the pathogenesis of OA. In the presence of a CRH antagonist, α helical CRH, it has been shown that cardiomyocytes cell death is increased when subjected to ischaemia indicating that an endogenous CRH family peptide, (specifically UCN), protects cells in an autocrine/paracrine fashion. This protective response of UCN is dependent upon its ability to activate the PI-3 kinase/Akt pathway and the P42/P44 MAPK pathway in cardiomyocytes as demonstrated by inhibition of these pathways with the chemical inhibitors LY294002 and PD98059 respectively (Brar *et al*, 2000; Brar *et al*, 2002a). These data are further supported by Parkes *et al*, (1997), who showed that UCN protected neonatal rat cardiomyocytes *in vitro* when given before hypoxia or at the point of reoxygenation and protecting the adult rat heart *ex vivo*, lowering the infarct size of a perfused intact rat heart exposed to local ischaemia. Many of the CRH peptides appear to be cytoprotective but relative potencies with which they protect cells from ischaemia induced necrotic and apoptotic death is UCN > URO I > CRH (Parkes *et al*, 1997). UCN was also shown to be protective against thermal injury and hypoxia (Okosi *et al*, 1998) with protective effects occurring through the cAMP dependent protein kinase A (PKA) pathway and the MAPK-dependent pathway (Ikeda *et al*, 1998). The Latchman group (Lawrence *et al*, 2002a) have analysed global changes in gene expression in cardiomyocytes after UCN treatment using gene chip technology. These experiments established that UCN specifically induces enhanced expression of the Kir6.1 cardiac potassium channel subunit, and showed that the cardioprotective effect of UCN, both in

isolated cardiac cells and in the intact heart, is specifically blocked by generalized and mitochondrial-specific K_{ATP} channel blockers (Lawrence *et al*, 2002b). The other main gene product modulated by UCN is the calcium-insensitive phospholipase A_2 ($iPLA_2$) enzyme, which was thought to be localized to cardiomyocyte mitochondria. In their latest study (Lawrence *et al*, 2005), they demonstrated that protein kinase C epsilon (PKCε) activation is important for cardioprotection against ischaemia and reperfusion injury and UCN cardioprotection is dependent on PKCε activation (Lawrence *et al*, 2005).

Since hypoxic damage is linked with excess intracellular calcium, these cardiovascular effects may imply that calcium channels could play some roles in UCN's cardioprotection. Tao *et al,* (2004) demonstrated that UCN exerted an inhibitory effect on the L-type calcium channels of adult rat ventricular myocytes, which was not reversed by a CRH antagonist implying that such effects are not mediated via CRH receptors. This inhibition of L-type calcium channels by UCN may be mediated by decreasing excess calcium influx through the voltage-gated calcium channels, a hypothesis further supported by Scarabelli *et al,* (2002) who verified that UCN protection of the cardiomyocytes against apoptosis, was linked with intracellular calcium overload.

The concept that UCN may be involved in inflammatory conditions is further supported by findings that the expression of UCN mRNA is increased in synovium of patients with RA and OA (Kohno *et al*, 2001; Uzuki *et al*, 2001), indicating that UCN may play an important role as an autocrine and/or paracrine regulator of synovial inflammation. However, the source of the UCN detected in these studies was not investigated.

Recently two new mammalian neuropeptides of the CRH peptide family, stresscopin related peptide (SRP/UCN II) (38 aa) and stresscopin (SCP/UCN III) (38 aa) have been identified which have N-terminally shortened sequences (38aa) compared to UCN (40aa) (Reyes *et al*, 2001; Lewis *et al*, 2001). UCN II mRNA has been found in the heart, hypothalamus, spinal cord, adrenal gland and peripheral blood cells (Hsu and Hsueh, 2001). UCN II has been shown to produce delayed decreases in feeding and drinking (Inoue *et al,* 2003), and mild motor suppressive and delayed anxiolytic like effects in rats (Valdez *et al*, 2002) suggesting that UCN II may play a role in behavioural and neuroendocrine responses (Reyes *et al*, 2001). UCN III mRNA is

significantly less abundant than UCN II mRNA, but increased quantites of UCN III mRNA expression have been found in the gastrointestinal tract, muscle, hypothalamus adrenal gland and skin (Lewis *et al*, 2001). Accordingly, UCN III stimulated cAMP production in cells expressing CRH-R2 but not in cells expressing CRH-R1 (Hsu and Hsueh, 2001). Recent studies have confirmed that UCN II and UCN III are selective for CRH-R2 (Martinez *et al*, 2002). Both UCN II and UCN III have also been reported to possess cytoprotective attributes and these appear to be mediated exclusively through CRH-R2 receptors. UCN however, can act on both CRH-R1 and CRH-R2 (Brar *et al*, 2004) or perhaps through non CRH receptor routes (Lawrence *et al*, 2002).

1.7.2 The CRH receptors

The CRH family of peptides including UCN exert their effects by binding to receptors which are coupled to the stimulatory class B subtype of G protein-coupled receptors (GPCR). These show significant homology to vasoactive intestinal polypeptide/calcitonin family of GPCR that are positively linked to adenylate cyclase and increased cAMP levels (Perrin *et al*, 1995). Prior to cloning of UCN in mammals, a variety of studies has helped to identify different CRH receptor subtypes. A comparison of the relative pharmacological potencies of ovine CRH (oCRH), sauvagine, and urotensin I on mesenteric vasodilation in the dog showed the existence of two distinct classes of high affinity binding sites (MacCannell *et al*, 1982). The two receptor subtypes were named CRH-R type 1 & 2 (which share 69% sequence homology) and have since been cloned and characterized from various species. The two receptors are identical except for a 29 amino acid insert present in the first intracellular loop of the type 1 receptor but have diverse anatomical distribution, pharmacology and affinities for the different CRH family peptides. Structurally, the CRH-R1 (415-420 aa polypeptide) and CRH-R2 (397-438 aa protein) are highly conserved, the majority of divergence occurring in the putative signal peptide and the extracellular N terminal, the second and third receptor domain, as well as in the N terminus juxtamembrane region which has been shown to be important in establishing ligand binding and receptor specificity (Klose *et al*, 2005; Brauns *et al*, 2002). In contrast, the intracellular and transmembrane domains are more homologous (80-85% aa identity) with the third intracellular loop being totally alike in all cloned CRH receptors (Ariai *et al*, 2001). As both CRH-R1 and CRH-R2 receptors signal through cAMP as a second messenger, the stimulatory G

protein (G_s) is most likely to link to this intracellular loop (Dautzenberg and Hauger, 2002).

Pharmacological studies have shown that UCN is a more potent activator than CRH of both types of CRH receptor, but in general the difference in potencies is greater for CRH-R2 (Hillhouse *et al*, 2002). Cells expressing mammalian CRH-R1 can be activated by CRH, sauvagine and UCN, to produce cAMP with similar half maximally effective concentrations (EC_{50}) (Dautzenberg *et al*, 1997). Cells expressing CRH-R2 generate cAMP especially in response to sauvagine and UCN, as indicated by low EC_{50} values and high affinity binding of these peptides (Brauns *et al*, 2002).

CRH-R1 and CRH-R2 are generated via distinct genes and possess many splice variants which are expressed in several central and peripheral tissues (Bale and Vale, 2004). Alternatively spliced forms or subtypes of the CRH-R1 (named a, b, c, d, e, f, g, h, v) are produced by differential splicing of exons 3-6 and 10-13, and have been detected in human and rodents. The CRH-R2 receptor exists as three known subtypes (named CRH-R2α, CRH-R2β and CRH-R2γ) which have been reported to be 70% identical in amino acid sequence (Hauger *et al*, 2003). These are produced by the use of alternate 5' exons and hence differ only at the N terminus that forms part of the first extracellular domain (Klose *et al*, 2005). CRH-R2α and CRH-R2β are detected in human and rodents (Lovenberg *et al*, 1995a), whereas CRH-R2γ has so far only been detected in humans, and is expressed in limbic regions of the CNS (Kostich *et al*, 1998). CRH-R2α is the dominant variant expressed both in the mammalian brain and in peripheral tissues of humans (Hauger *et al*, 2003).

UCN is known to bind to both CRH-R1 and CRH-R2 with high affinity (K_i = 0.2-1 nm) (Behan *et al*, 1996) and is thought to be an endogenous ligand for CRH-R2 (approximately 40 fold higher activity than CRH) (Latchman, 2002; Bruijnzeel and Gold, 2005). UCN II binds CRH-R2 selectively and with high affinity (1000 fold more UCN). UCN III also specifically binds and has high affinity for CRH-R2. Both peptides activate cAMP production only in cells containing this receptor (Brauns *et al*, 2002) and both peptides are much less active on the CRH-R1 receptor (Hoare *et al*, 2005). It is currently known that the CRH/UCN system is composed of four ligands, two receptors, and one binding protein, CRH-binding protein (CRH-BP) (Dautzenberg and Hauger, 2002). CRH-BP expressed in rodent, primate brain, pituitary (Potter *et al*, 1994) and in

humans is found in the liver and in the circulation. CRH-BP binds CRH and UCN (but not UCN II and UCN III), therefore inhibiting their ability to activate their receptors (Kemp *et al*, 1998), and preventing pituitary–adrenal stimulation when CRH plasma levels are high (Potter *et al*, 1991). Woods *et al*, (1997) measured plasma CRH-BP levels in arthritic patients using immunoassays directed against the N- and C terminals of the CRH-BP and demonstrated an elevated level of N terminally immunoreactive material, indicating heterogeneity and perhaps truncation of the CRH-BP. With its high affinity for CRH-BP, UCN may control CRH levels within the brain by displacing CRH from the binding protein (Kahl *et al*, 1998) but CRH-BP has also been detected in brain regions and periphery not linked with CRH activity, suggesting that it may also have CRH independent actions (Bale and Vale, 2004).

1.7.3 CRH receptor antagonists

Several CRH pharmacological receptor antagonists are available, some selective for the different isoforms and some not. Following the detection of these CRH family members, several small molecule CRH-R1 antagonists (e.g. Antalarmin, CP-154.526) and CRH-R2 antagonists (e.g. Astressin-2B, anti-sauvagine 30) have been produced in recent years along with some which bind to both CRH-R1 and CRH-R2 (e.g. Astressin, α-helical CRH) (Bale and Vale, 2004). Many of these novel antagonists were derived through deletion of N-terminal residues (Braun *et al*, 2002) resulting in small molecular weight molecules that can diffuse easily.

These peptide CRH antagonists have been used mainly to distinguish the physiological role and mode of action of the CRH family of peptides. The first CRH antagonist to be described (and one of the most available) was α-helical $CRH_{(9\text{-}41)}$. α-helical $CRH_{(9\text{-}41)}$, is a non specific CRH receptor antagonist binding to both CRH-RI and R2 but has been shown to have greater affinity for CRH-R2 and has been used throughout this study as it has been shown to inhibit the cardiac and vasorelaxant effects of UCN (Terui *et al*, 2001; Huang *et al*, 2004).

1.8 Intracellular signal transduction and the kinases

Signal transduction networks allow cells to receive external stimuli and respond to those signals in an appropriate manner. Eukaryotic cells have mitogen activated protein kinase (MAPK) signaling cascades which are activated as a result of growth factors, cytokines, stress stimuli (e.g. viral infection and ultraviolet irradiation), inflammatory responses, extracellular matrix components and both osmotic and heat shock (Cooray *et al*, 2005). MAPKs are specific protein kinases which regulate various cellular activities such as gene expression, mitosis, differentiation, and cell survival/apoptosis. MAPKs are generally activated by dual phosphorylation on tyrosine and threonine residues of the kinase sub-domain VII (sequence pTXpY), and are all proline directed serine/threonine kinases with numerous substrates. Dephosphorylation of either residue results in inactivation of the enzyme, indicating that both threonine and tyrosine phosphorylation are important for maximal activation (Khokhlatchev *et al*, 1997).

Extracellular stimuli lead to activation of a MAPK via a signaling cascade composed of MAPK, MAPK kinase (MAPKK or MEK1/2), and MAPKK kinase (MAPKKK or MEKK). A MAPKKK that is activated by extracellular stimuli phosphorylates a MAPKK on its serine and threonine residues, and this MAPKK in turn activates a MAPK via phosphorylation on its tyrosine and threonine residues. This MAPK signaling cascade has been evolutionarily well-conserved from yeasts through to mammals and is shown overleaf in figure 1.4.

In mammalian cells, three MAPK pathways are well studied, two of which, the P42/P44 MAPK (also known as ERK 1/2) and the P38 MAPK will be discussed in detail here. Another kinase pathway of relevance to this study is the phosphoinositide 3-kinase (PI3K)-Akt pathway which participates in phosphorylation of phosphatidylinositol lipids (Cooray *et al*, 2005) and will also be discussed.

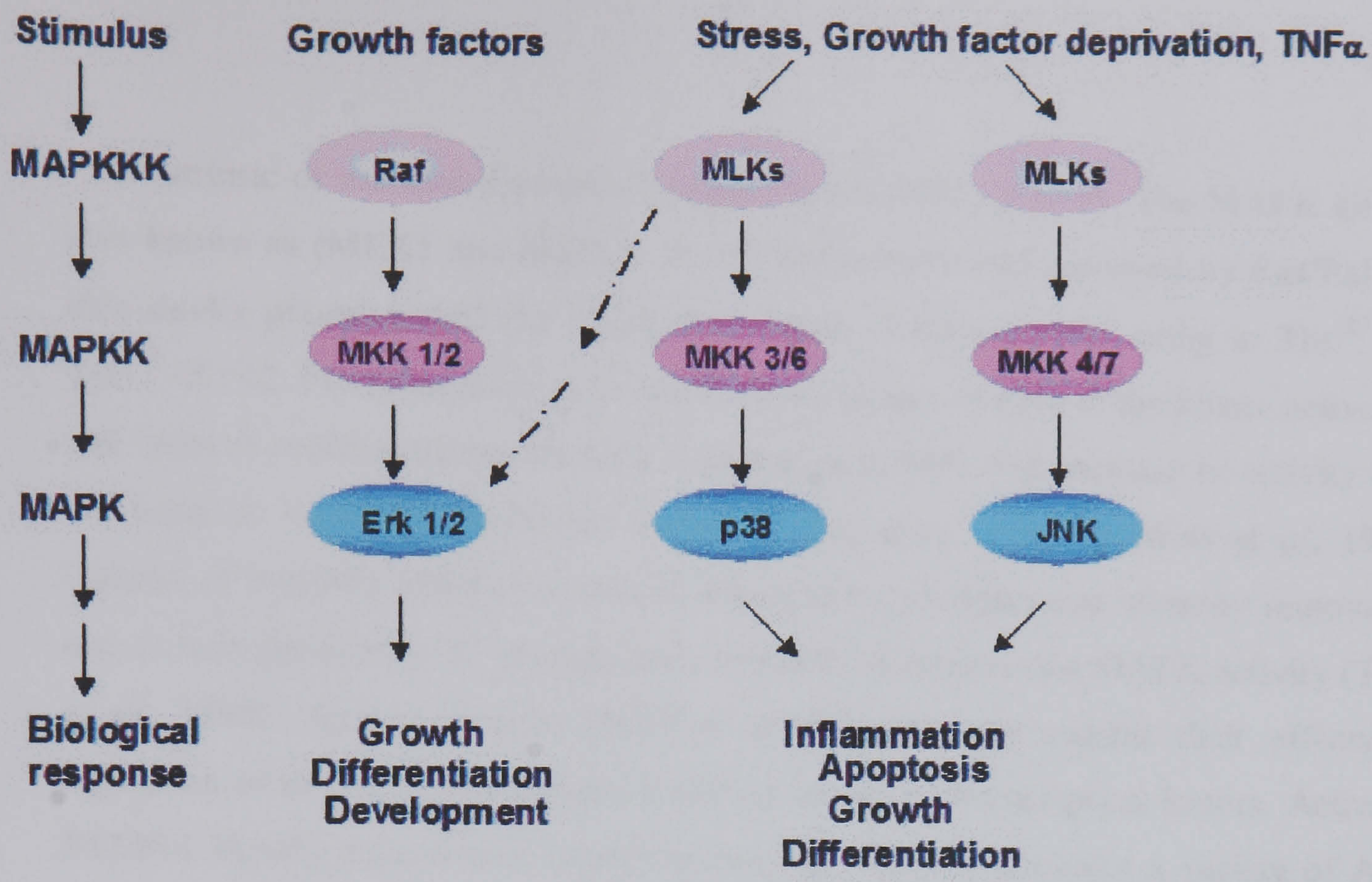

Figure 1.4: Activation of different MAPK signaling cascades by different extracellular stimuli.

(Adapted from focosi.altervista.org/mapkmap.html, with slight modifications)

The P42/P44 MAPK (above) signaling pathway is preferentially activated in response to growth factors and phorbol esters, and is involved in the regulation of cell proliferation and differentiation. The stress activated protein kinases/c-jun N-terminus kinases (SAPKs/JNKs) and P38 signaling pathways are responsive to stress stimuli, and involved in cell differentiation and apoptosis. MAPK activity is down regulated by a set of dual specificity phosphatases (known as MAPK phosphatases (MKPs) that remove phosphate from both threonine and tyrosine residues. MKP family members are triggered in response to growth factors and take part in the reduction of the constant activation phase of P42/P44 MAPKs (Sun *et al*, 1994).

The protein MAP-2 kinase was first reported by Sturgill and Ray, in 1986, as a 42-kDa protein kinase which became phosphorylated after insulin exposure, and in turn phosphorylated the cytoskeletal protein MAP-2. A further 44-kDa isoform of this enzyme, was reported by Boulton and Cobb in 1991 and named ERK 1 whilst, the 42 kDa protein was renamed ERK 2. Since the discovery of these proteins several growth factors and mitogens have been shown to activate these enzymes and the acronyms for these enzymes were consequently altered to P42/P44 MAPK (Dent *et al*, 2003). P42/P44 MAPK activation can be initiated via activation of transmembrane receptors

with intrinsic or associated protein tyrosine kinase (PTK) activity. The MAPK kinases also known as (MEK1 and MEK2), are phosphorylated and activated by Ras/Raf and then dually phosphorylate the P42/P44 enzymes at sites corresponding to Thr^{183} and Tyr^{185} of P42. Phosphorylation of these residues causes closure of the kinase active site and induces conformational changes resulting in a 1000 fold increase in activity over the basal or monophosphorylated forms (Zhang *et al*, 1995; Robbins *et al*, 1993). Control of P42/P44 MAPK activity is achieved by phosphatases whereby removal of one or both phosphates by phosphatases radically decreases this MAPK activity (Todd *et al*, 1999). Once activated, P42/P44 MAPK generally exhibit their effects by regulation of the activating protein 1 (AP-1) family of transcription factors. Activated P42/P44 MAPK translocates inside the nucleus where it activates a variety of AP-1 transcription factors such as *c-jun and Elk-1*, which bind to DNA and contribute to the control of cell cycle reactions (Pearson *et al*, 2001). Even though transcription factors are vital MAPK targets, only some of the active MAPK pool translocates to the nucleus and mostly stays in the cytoplasm and other subcellular compartments (Chen *et al*, 2000).

The P38/HOG (high osmolarity glycerol) MAPK pathway was originally described as a mammalian homologue of a yeast osmolarity sensing pathway (Han *et al*, 1994) and at least four isoforms of P38 MAPK exist; P38 MAPK α, β, γ, and δ (Kyriakis and Avruch, 2001). P38 MAPK belong to a family of stress kinases, and, when activated, phosphorylate transcriptional factors resulting in changes in gene expression in response to many extracellular stimuli such as cytokines (TNF-α and IL-1β), increased osmolarity (Han *et al*, 1994), nutrient defiency, increased mechanical loading, and decreased oxygen tension (Chang and Karin, 2001), all conditions which occur in OA cartilage.

P38 MAPK is activated by dual specificity MAP kinase kinases, including MKK3 (activator for P38 δ and α isoforms) and MKK6 (activator for all P38 isoforms) (Raingeaud *et al*, 1996). The P38 pathway has been implicated as playing a critical role in apoptosis (Xia *et al*, 1995) and is activated by several cytokines and other cell surface binding ligands. Signals are transmitted from cell membrane bound receptors via several small GTP-binding proteins (e.g. Ras, Raf) to the level of the MKK kinases (MKKK 1/2/3). An MKKK then activates MKK3/6, which in turn, activates the P38 MAPK, which phosphorylates transcription factors (e.g. ATF-2) (Conrad *et al*, 1999).

Whilst the activation of P38 has been correlated with the induction of apoptosis in many cell types MKK signaling may not be that simple. Huang *et al*, (1997) showed that expression of constitutively activated MKK3 or MKK6 (both are upstream P38 activators) was able to induce apoptosis in T lymphocyte Jurkat cells, but surprisingly, it was found that P38 was not activated, suggesting that MKK3 and MKK6 may induce apoptosis via activation of other unknown substrates (Huang *et al*, 1997). The role of P38 MAPK signaling in cellular responses is varied, depending on the cell type and stimulus. P38 MAPK signaling has been observed to both encourage cell death and increase cell growth and survival (Juretic *et al*, 2001). The capability of ionizing radiation to control P38 MAPK activity is shown to be extremely unpredictable with different groups reporting either no activation (Kim *et al*, 2002), weak activation (Taher *et al*, 2000) or strong activation (Lee *et al*, 2002). These reports suggest that the action of P38 in the apoptotic cascade depends on the cell type, method of stimulation, and the timing of injury.

Both the P42/P44 MAPK and P38 MAPK pathways have been shown to be important in chondrocyte survival and function. Kim *et al*, (2002) demonstrated that NO induced chondrocyte differentiation and apoptosis were mediated through both P42/P44 MAPK and P38 MAPK pathways, whilst Zhen *et al*, (2001) demonstrated that P38 MAPK is important in controlling apoptosis in growth plate chondrocytes during endochondral ossification (replacement of cartilage with bone tissue). P38 MAPK signaling has also been demonstrated to be important for the differentiation of mesenchymal precursor cells to chondroblasts during cartilage development (Lee *et al*, 2002). The role of P38 in the later stages of chondrocyte growth and proliferative differentiation, has not been studied significantly, nor has P38 signaling in mature chondrocytes. Stanton *et al*, (2004) have however established a requirement for P38 signaling in the hypertropic differentiation of chondrocytes and the work of Wei *et al*, (2006) indicates a strong link between P38 MAPK activity and cell death in human OA chondrocytes.

Alongside the MAPK signaling pathways, the phosphatidylinositol 3 kinase (PI3K) signaling pathway represents one of the other ubiquitous, multifunctional signaling pathways. PI3K is a vital intracellular signaling enzyme that takes part in phosphorylation of phosphatidylinositol lipids, thus influencing a variety of cell functions including growth, migration and survival (El-kholy *et al*, 2003). PI3K enzymes have two subunits, a catalytic P110 subunit and a regulatory and localizing

P85 subunit, (Vanhaesebroeck and Alessi, 2000). The major catalytic function of the PI3K is to phosphorylate membrane inositol phospholipids (PIP2: phosphatidyl inositol 4,5 bis-phosphate), at the 3' position within the inositol sugar ring. These 3' phosphoinositides recruit the proteins Akt and phosphoinositide dependent kinases 1 and 2 (PDK1/2) to the plasma binding membrane through their pleckstrin homology domains (Vanhaesebroeck *et al*, 2001), when PDK1/2 activates Akt via phosphorylation at Ser^{473} and Thr^{308} (Datta *et al*, 1999), activated Akt influences cell survival by phosphorylating and inhibiting a range of pro-apoptotic proteins including BAD, caspase 9, GSK-3β and Forkhead transcription factors (Cardone *et al*, 1998).

1.9 Aims

The aims of this project are to establish the cell death pathway and intracellular signalling cascades that operate in chondrocytes in response to agents already implicated in chondrocyte apoptosis in OA and to investigate a possible protective mechanism involving the CRH like peptide UCN.

Greater understanding of the mechanisms involved is a step towards the possible controlled pharmacological inhibition of key stages in this process with the recent discovery of a possible endogenous protective agent, UCN, and may reveal further potential therapeutic pathways to be explored.

The aims of the present study were to:

- Evaluate the relative roles of the pro-apoptotic stimuli, NO and TNF-α on C-20/A4 chondrocyte cell death
- establish if NO and TNF-α induce chondrocyte apoptosis or necrosis
- investigate the effect of CRH receptor antagonists on UCN mediated cytoprotection
- evaluate the chondroprotective efficacy of UCN in preventing chondrocyte apoptosis and
- the stimuli that result in UCN expression
- investigate the signal transduction pathway(s) involved in the chondroprotective effect of UCN.
- identify the initiator caspase involved in chondrocyte apoptosis following administration of TNF-α and NO donor SNAP

In the long term, it is hoped that data gathered in this study may help to suggest novel therapeutic strategies so that appropriate clinical studies may be formulated for the treatment and cure of OA.

CHAPTER 2

MATERIALS AND GENERAL METHODS

2.1 Materials

2.1.1 Cell culture

C-20/A4 human chondrocyte cell line (derived from Juvenile coastal chondrocytes immortalized with the origin-defective Simian virus 40 containing large T-antigen (SV40-Tag) vector) (Goldring *et al*, 1994). Dulbecco's Modified Eagles Medium (DMEM) with 1g/L glucose, without L-glutamine (Cambrex, Wokingham, UK), Dulbecco's phosphate buffered saline (DPBS) containing no Calcium or Magnesium (Cambrex). Heat inactivated fetal calf serum (FCS) (Biowest, Ringmer, UK), Penicillin (10,000U/ml) / Streptomycin (10,000μg/ml) solution (Cambrex), L-Glutamine Solution (200mM in 0.85%(w/v) NaCl) (Cambrex). Dimethyl Sulphoxide (DMSO), (Sigma, Poole, UK), liquid nitrogen (BOC Ltd Speciality gases, London, UK), tumour necrosis factor-α (TNF-α) and interleukin-1β (IL-1β) (R & D Systems, Abingdon, UK), SNAP (S-nitroso-N-acetyl-D-L-penicillamine) (Calbiochem, Lutterworth, UK), α helical $CRH_{(9-41)}$ (Sigma), Urocortin (UCN) (Sigma), PD98059 (P42/P44 MAP Kinase inhibitor) (Calbiochem, UK), SB202190 (P38 MAP Kinase inhibitor) (Calbiochem, UK), LY294002 (Phosphatidylinositol 3-kinase (PI3K) inhibitor) (Calbiochem, UK). Plastic tissue culture flasks, pipettes, 0.2μm filters, centrifugal tubes, (Triple Red, Thame, UK).

2.1.2 Analysis of cell death

Ethanol (Merck, Leicester, UK), chloroform (Merck), 4%(w/v) paraformaldehyde solution in PBS (Sigma), blocking solution - 0.3%(v/v) hydrogen peroxide (H_2O_2) (Sigma) in methanol (Merck), permeabilization solution - 0.1%(w/v) Sodium citrate + 0.1%(v/v) Triton x-100 (t-Octyl phenoxypolyethoxyethanol) (Sigma) in distilled water. *In situ* cell death detection, peroxidase kit (Roche diagnostics, Lewes, UK), polysine™ microscope slides (Merck). TACS™ Annexin V-FITC kit (R & D Systems, Abingdon, U.K), HEPES (Sigma), NaCl (Merck), KCl (Merck), $MgCl_2$ (Merck). TOX 7 *in vitro* Toxicology assay kit lactate dehydrogenase based (Sigma). 1M HCL, Neutral Red dye (Sigma), $CaCl_2$ (Merck), Formaldehyde (Merck) acetic acid (Merck), 96 well plates (Triple Red). AF1 glycerol/PBS mounting solution (Citifluor, London, U.K), improved Neubauer haemocytometer (Hawksley, Lancing, Sussex, U.K), 0.25% (w/v) trypan blue, in PBS (Sigma, U.K.). Anti-human urocortin antibody (Sigma, Dorset, U.K), anti-

human albumin antibody (Sigma), Sephadex nick columns (Amersham Pharmacia, Chalfont, U.K),

2.1.3 Molecular biology techniques

Tri–reagent™ (Sigma), Propan-2-ol (Merck), DEPC (diethyl pyrocarbonate) (0.01%v/v) (Sigma) treated UHQ water, ethanol (Merck), Oligo – dt $_{(18)}$ (Sigma Genosys, Gillingham, UK), Moloney-murine leukemia virus-reverse transcriptase (M-MLV-RT) (Promega, Southampton, UK), 5x RT buffer (Promega), RNasin® ribonuclease inhibitor (Promega), BIOTAQ polymerase (Bioline, London, UK), dNTP mixture (dATP, dTTP, dGTP, dCTP) (Bioline), magnesium chloride ($MgCl_2$) (Bioline), 10x ammonium buffer (NH_4^+) (Bioline), oligonucleotide primers (UCN, β-actin, GAPDH) (Sigma Genosys), mineral oil (Sigma). Agarose (Bioline), Tris acetate EDTA (TAE) 50x buffer (24.2%(w/v) glacial acetic acid (Merck), 5.7%(w/v) Trizma® base (Sigma), 0.0372%(w/v) sodium EDTA (Merck), distilled water, 0.01%(w/v) ethidium bromide (Sigma). Ready-Load 2 Kilobase (Kb) DNA ladder (Sigma), ready-Load 1 Kilobase (Kb) DNA ladder (Invitrogen Life Technologies, Paisley, UK), ready-Load 1 Kilobase (Kb) hyperladder IV (Invitrogen Life Technologies). Xylene cyanol FF dye (XCFF) (Sigma), bromophenol blue dye (BPB) (Sigma) and ficoll (Merck). Spin Prep™ PCR clean up kit (Calbiochem). TaqMan reverse transcription reagent kit®, assay-on-demand kits for UCN (Cat no. HS0017020-ml) and GAPDH (Cat no. HS99999905-ml), TaqMan universal PCR mastermix®, 96 well optical reaction plates, optical adhesive covers (all from Applied Biosystems, Warrington, U.K.).

2.1.4 Electrophoretic techniques and Western blotting

30%(w/v) (37:1) bis-acrylamide mix (Sigma), tris(hydroxymethyl)aminomethane base (Sigma), sodium dodecyl sulphate (SDS) (Merck), ammonium peroxodisulphate (persulphate) (Merck), 10x PBS (12.2%(w/v) sodium chloride (Merck), 26.8%(w/v) potassium chloride (Merck), 1.92%(w/v), disodium hydrogen orthophosphate-2-hydrate (Merck), TEMED (N, N, N', N' - tetramethylethylenediamine) (Sigma), 1x transfer buffer (w/v), (39mM glycine, 48mM tris base, 0.037%(w/v) SDS, 20%(v/v) Methanol), 5x SDS polyacrylamide gel electrophoresis (SDS PAGE) running buffer (25mM tris, 192mM glycine, 0.1%(v/v) SDS), SDS-PAGE gel loading buffer (10%(v/v) glycerol, 3%(v/v) SDS, 0.1%(w/v) 2-mercaptoethanol, 0.1%(w/v) bromophenol blue). Picric acid

coomassie blue stain – solution 1 (0.5%(w/v) coomassie brilliant blue R-250, 45%(v/v) methanol, 10%(v/v) glacial acetic acid), solution 2- (132g damp picric acid in 2L distilled water neutralized to pH 7 with 1M NaOH, until picrate was dissolved. Final staining solution was prepared from 750ml solution 1 with all of solution 2, and adjusted to 3L final volume with UHQ water), picric acid coomassie washing solution-(45%(v/v) methanol, 10%(v/v) glacial acetic acid in distilled water), picric acid coomassie destain-(10%(v/v) methanol, 7%(v/v) glacial acetic acid in water). Ponceau S staining solution-(2%(w/v) Ponceau S, 30%(w/v) trichloroacetic acid, 30%(w/v) sulfosalicyclic acid), Protease inhibitor cocktail (Sigma), CelLytic™-Mammalian cell lysis buffer (Sigma), Polyoxyethylenesorbitan monolaurate (Tween-20) (Sigma). Low-Range Rainbow Molecular Weight marker (Amersham, Little Chalfont, U.K.), Pre-stained protein marker, Broad Range (6-175kDa) (Biolabs, Hitchin, Hertfordshire), Hybond™ C nitrocellulose Transfer membrane (Amersham), anti-caspase 3 antibody (Cell signaling, Hitchin, Hertfordshire, U.K.), anti-caspase 8 antibody, anti-caspase 9 antibody, anti-p-ERK (E-4): sc-7383, p-ERK (Tyr 204): sc-7976 (all from Santa Cruz, supplied by Autogen, Calne, U.K), Polyclonal rabbit anti-mouse Ig HRP (Dako Cytomation, Ely, U.K), Polyclonal goat anti-rabbit Ig HRP (Dako), GAPDH, 4%(w/v) powdered milk.

2.2 General Methods

2.2.1 Cell Culture

Since its discovery in the 1940's and 1950's, several developments in cell culture have contributed to its greater feasibility and current widespread use. Some of the more notable advances include the development of antibiotics to avoid contamination problems, the use of trypsin (for the continuous culture of adherent cells) and the development of standardized, chemically defined culture media (Galbraith, 2004). Two basic culture systems are used for growing cells which depend on the nature of the cells being cultured. Some cell types grow attached to a glass or treated plastic substrate (Monolayer Culture Systems) (including the C-20/A4 cells used in this research) whilst others grow floating free in the culture medium (Suspension Culture Systems).

The main problem encountered in cell culture is contamination. Contamination is mainly of two types: chemical or biological. Chemical contamination is the most difficult to detect since it is caused by agents such as endotoxins, plasticizers, metal ions or traces of chemical disinfectants, which are invisible to the naked eye during cell culture. Biological contaminants in the form of fast growing yeast, bacteria and fungi usually have visible effects on the culture (changes in medium turbidity or pH) and are thus easier to detect, especially if antibiotics are absent from the culture (Lincoln and Gabridge, 1998). To ensure optimal cell growth, cultures should be examined daily, observing the cell morphology, the colour of the medium and the density of the cells. Important factors affecting cell growth include appropriate temperature (usually 37°C), a suitable substrate for attachment (glass or specially treated plastics) and the provision of the correct balance of essential gases (O_2 and CO_2). The selection of the culture medium is also critical in order to meet the basic nutritional requirement of the cells, to provide necessary growth factors (usually supplied by a 5-20% supplement of animal serum or serum free medium supplements) and to regulate pH and osmolality (MacLeod *et al*, 1999).

When cells grown in monolayer have covered all of the available culture substrate, they must be subcultured to give them room for continued growth. This is performed by releasing them as gently as possible from the substrate. Some cell types may be released from the culture flask simply by tapping the side of the flask, others require enzymatic

(e.g. trypsin) release. Once released, the cell suspension can then be subdivided and placed into new culture flasks.

2.2.1.1 Growth and maintenance of C-20/A4 cell line

In this work, *in vitro* experiments were performed on an adherent human chondrocyte cell line (C-20/A4), which displays morphological and biochemical characteristics of the chondrocyte phenotype. The C-20/A4 human chondrocyte cell line was derived from Juvenile costal chondrocytes immortalized using the origin defective Simian Virus 40 containing large T antigen (SV40 Tag) (Goldring *et al*, 1994) and were the kind gift of Professor Mary Goldring, Harvard Medical School, USA. This cell line has been routinely and extensively used as a reproducible *in vitro* model for the investigation of cartilage cell biology requiring large numbers of cells for health and disease by several groups (Goldring *et al*, 1994; Moulton *et al*, 1997; Finger *et al*, 2004).

C-20/A4 cells were cultured in Dulbecco's Modified Eagles Medium (DMEM), supplemented as detailed in table 2.1, and maintained in a Galaxy S humidified incubator (Wolf Laboratories, York, U.K.) at 37°C and 5% CO_2. All culture handling was performed in an Aura 2000 class II cabinet (Bioair Instruments, UK). Complete media was sterilized prior to use by passing through a 0.2μM syringe filter and pre-warmed to 37°C, in a water bath. When a fully confluent monolayer was achieved (usually 3-4 days), cells were passaged by treatment with sterile Ca^{2+} & Mg^{2+} free PBS pre-warmed to 37°C. A volume of 10ml of PBS was added to each 75cm^2 flask and the cells replaced in the incubator for 5 minutes. Cells were released by banging the side of the flask against the palm of the hand, then pelleted by centrifugation at 2500g at 20°C for 5 minutes. Pellets were then re-suspended in fresh medium and used as required. Chondrocytes were continuously cultured in order to ensure availability and cycled into, or out of, storage as appropriate. Experiments were undertaken on cells between passages 3 to 15.

Table 2.1: Composition of growth medium employed for culture of C-20/A4 human chondrocytes

Components	Concentration
DMEM	88.0% (v/v)
Foetal calf serum (FCS)	10% (v/v)
Penicillin-Streptomycin solution (10000 units ml^{-1} Penicillin G Sodium + 10000µg ml^{-1} Streptomycin Sulphate in 0.85% saline)	1.0% (v/v)
L-Glutamine 200mM (100x)	1.0% (v/v)

2.2.1.2 Storage and revival of the C-20/A4 cell line

C-20/A4 cells were routinely stored as frozen aliquots in liquid nitrogen (-196°C), which allows for long term storage with good viability. The process of freezing can however be detrimental to cell viability due to the effects of ice crystal formation, dehydration and changes in pH. In order to minimise these effects, cells destined for storage were centrifuged and the pellets re-suspended in a freezing medium composed of 10% (v/v) of the cryoprotective agent DMSO in the complete media. The cells were first slow frozen at -80°C overnight, at a rate of 1-3°C/minute in a 'Mr. Frosty' container (Merck, Leicester, U.K.) (filled with 200ml isopropranol). Following slow freezing, the vials were removed and transferred to liquid nitrogen storage (-196°C) for longer durations to stabilize the cells and minimize ice crystal growth, which is retarded below -130°C (Freshney, 1987). To maximise recovery of the cells when thawing, vials are warmed very quickly by hand and the thawed cell suspension diluted immediately into 20ml of pre-warmed complete medium and centrifuged at 2500g 20°C for 5 minutes. This procedure was repeated twice prior to transfer of cells into tissue culture flasks.

2.2.2 Analysis of cell death

The increasing interest in mechanisms of cell death has resulted in the development of a variety of different methods for its detection and characterisation. Several methods have been routinely used, including the characteristic 180bp DNA ladder banding pattern on agarose gels, the TUNEL (TdT mediated dUTP nick-end labeling) assay, Annexin V assay, DNA fragments ELISA, LDH release and vital dye staining. Assays for activity of the caspase family of cysteine proteases, common mediators of apoptotic cell death

pathways, have also been developed for characterising apoptosis. Apoptosis assay systems have been categorised as measuring 'early' or 'late' events in the overall process of apoptosis with some combined tests assessing both (Vermes *et al*, 2000). Necrotic cell death can be conveniently measured by the assessment of cytoplasmic enzyme activity (e.g. lactate dehydrogenase (LDH)) released into culture medium following cell lysis.

Apoptotic induction caused by insults such as TNF-α and NO, can be conducted both via receptor ligation and by the release of cytochrome c from the mitochondria leading to a breakdown of the mitochondrial membrane potential (ψ). Subsequent activation of caspases then leads to cleavage of apoptosis-related proteins such as PARP, which is implicated in DNA repair. The exact mechanisms involved are dependent on the nature of the insult and the cell or tissue type involved. An early event in this process is the exposure of phosphatidylserine from the inner leaflet of the cell membrane to the outer, leading to morphological changes resulting in cell shrinkage and blebbing. The final stages of the apoptotic process include DNA fragmentation before cell death and phagocytosis of its remains.

In this research, apoptosis has been assessed with a combination of Annexin V binding to exposed phosphatidylserine (early apoptosis) and terminal deoxynucleotidyl transferase biotin dUTP nick end labeling (TUNEL) (late apoptosis). Necrosis has been assessed by LDH release.

2.2.2.1 Preparation of cell slides

In order to assess cell morphology and death, cells were cytospun onto poly-L-lysine coated microscope slides. Using a cytospin 3 cytocentrifuge (Shandon, Manchester, U.K.), chondrocyte cell suspensions of approximately $3x10^4$ cells/ml were prepared in DPBS and cytocentrifugation was carried out at 500 rpm for 3 mins using 100μl (~3000 cells) per slide. Multiple slides were prepared for each experiment then used for TUNEL and Annexin analysis. The prepared slides were air dried after preparation and either used immediately or stored at –80°C (in aluminium foil) until required.

2.2.2.2 Annexin V assay

One of the earliest features in the apoptotic process is the externalisation of the lipid phosphatidyl serine (PS), from the inner to the outer leaflet of the plasma membrane, (Kuypers *et al*, 1996). Annexin V is a 35-36 kDa, Ca^{2+} dependent, phospholipid binding protein which specifically binds PS with a Kd of ~5 x 10^{-2} (Vermes *et al*, 1995). Fluorescent labeling of Annexin V enables the detection of externalisated PS, and hence apoptotic cells. Annexin V binding was first demonstrated in model membranes (Andree *et al*, 1990) and later in blood platelets, which expose PS at their surface under certain activating conditions (Thiagarajan and Tait, 1990; Dachary-Prigent *et al*, 1993), but is now in routine use for the detection of cellular apoptosis. Necrotic cells also expose PS, but tend to lose membrane integrity soon after cell injury (Koopman *et al*, 1994), whereas, in the initial stages of apoptosis, the cell membrane remains intact. Measurement of Annexin V binding to the cell surface is usually therefore performed in conjunction with a dye exclusion test (e.g. propidium iodide (PI) to establish integrity of the cell membrane, and distinguish between apoptosis and necrosis (Fadok *et al*, 1992)

Figure 2.1 shows the distribution of phosphatidylserine in normal and apoptotic cells, and the principles of the Annexin V/PI assay.

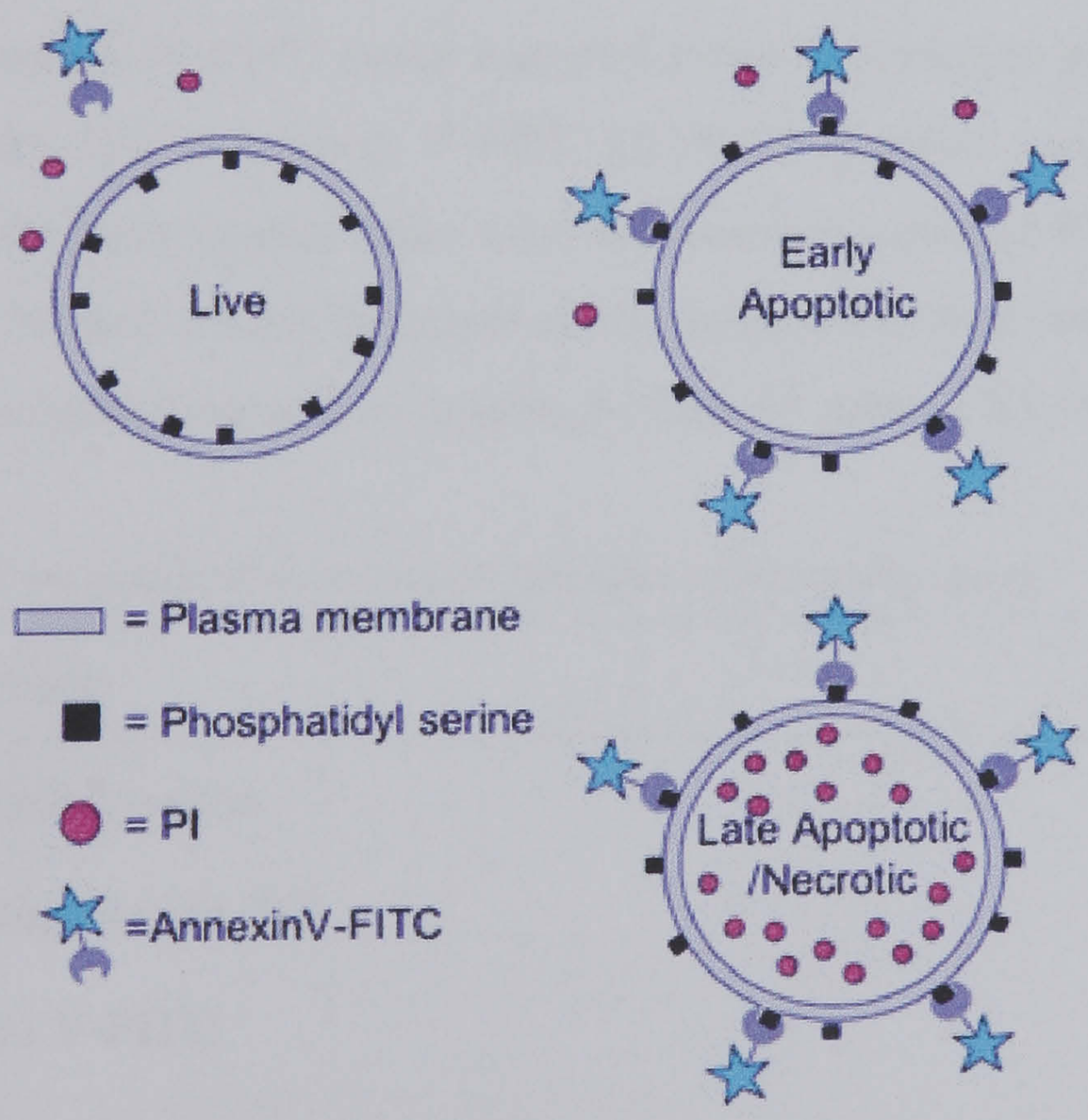

Figure 2.1: Annexin V-FITC/Propidium iodide assay principle.

(Adapted from www.dundee.ac.uk/lifesciences/ FACS/cell_death.htm,)

This combination of Annexin V and PI allows the investigator to distinguish between viable cells which are Annexin V and PI negative, early apoptotic cells (Annexin V positive; PI negative) and late apoptotic cells or necrotic cells (both Annexin V and PI positive). This assay does not however, differentiate between cells that have already undergone apoptotic death and those that have died due to a necrotic pathway because in either case, the dead cells will stain with both Annexin V and PI. Annexin V-FITC is detected as a green fluorescence and PI as a red fluorescence.

Whilst Annexin V binding is robust when used to assay cells growing in suspension (Koopman *et al*, 1994), there are difficulties when assessing apoptosis in adherent cells. The most common method used to detach adherent cells is trypsination with or without EDTA, both of which can affect the assay. Trypsinising can affect both membrane integrity and PS localisation and EDTA will remove calcium, which is essential for Annexin V binding. To avoid such problems, PBS was used to detach cells in this research, rather than trypsin-EDTA treatment.

2.2.2.2.1 Annexin V-FITC / Propidium Iodide methodology

The Annexin V-FITC assay was performed on cytospin preparations of C-20/A4 cells using the TACS-Annexin V FITC kit (R+D systems) according to the manufacturer's protocol. The prepared slides were incubated in a cold (2-8°C) 1x PBS wash for 10 mins gently blotted around the edges of the sample and then incubated with the Annexin V-FITC reagent (prepared as in table 2.2) for 15 mins at RT in a humidified chamber.

Table 2.2: Preparation of the Annexin V/ Propidium iodide working reagent

Component	Concentration
10x Binding buffer	10.0% (v/v)
Propidium Iodide (PI)	10.0% (v/v)
Annexin V-FITC	1.0% (v/v)
Distilled water	79.0% (v/v)

The cytospin slides were then washed twice for 2 mins each with 50ml 1x binding buffer (100mM HEPES pH 7.4, 1.5M NaCl, 50mM KCl, 10mM $MgCl_2$, 18mM $CaCl_2$),

mounted in AF1 fluorescent mounting medium and analyzed by fluorescence microscopy with an excitation wavelength between 450-500nm (blue) and detection between 515-565nm (green). Annexin V/PI positive cells are detected as a green fluorescence ring (Annexin V) with red, nuclear fluorescence (propidium iodide) as shown in Figure 2.2 (PI is not clearly detected in the picture). The total number of chondrocytes and the number of chondrocytes staining positively were quantified for 100 cells in three different microscopic fields which were randomly chosen. The final result was expressed as the percentage of positive cells. The mean and SD of readings for each condition were calculated.

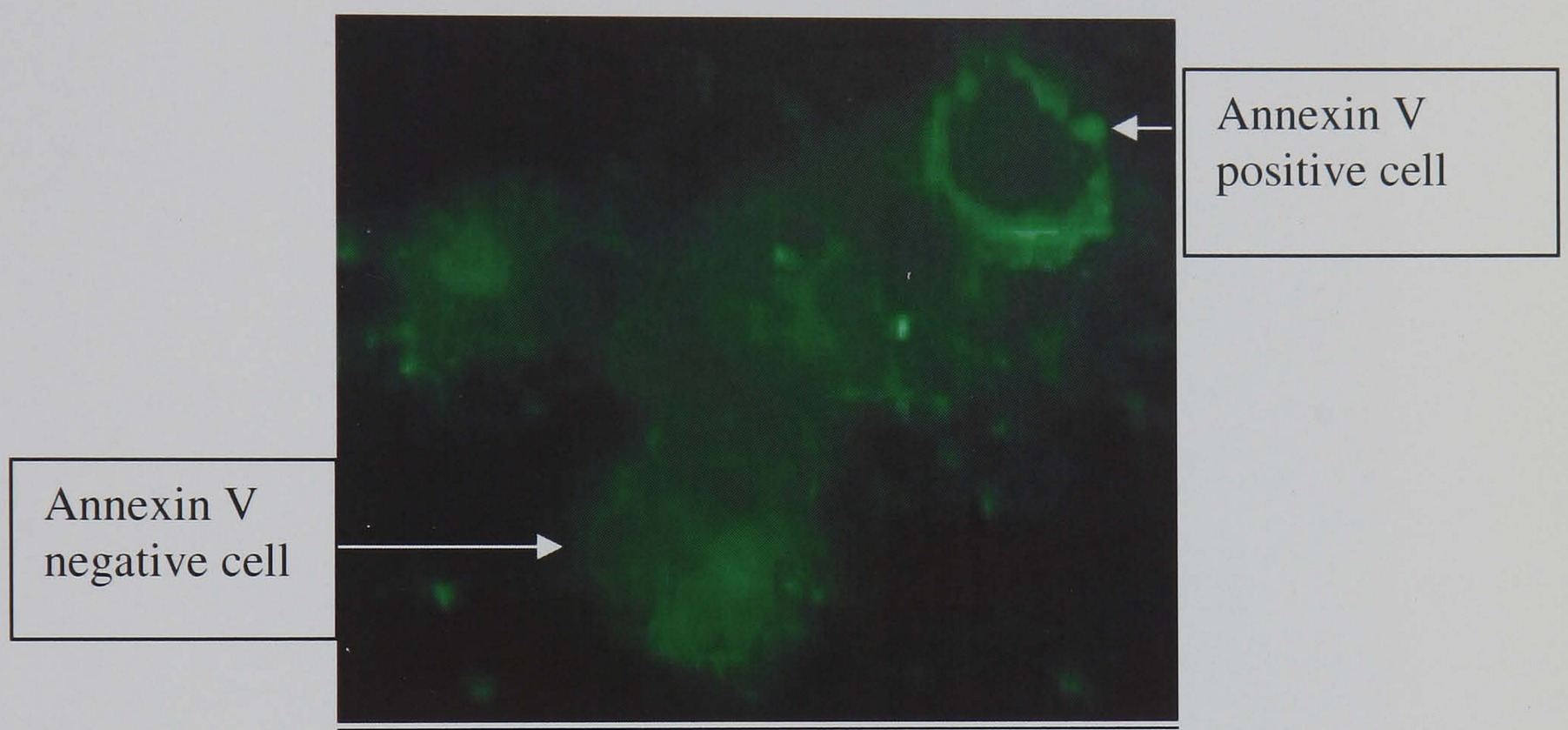

Figure 2.2: Microscopic appearance of Annexin V/PI positive apoptotic C-20/A4 cells after treatment with TNF-α (x 400 magnification).

2.2.2.3 TUNEL assay

As well as PS externalization, apoptosis is also characterized by a variety of other morphological and molecular changes, the most common of which is DNA fragmentation. DNA fragmentation takes place late in apoptosis and is easily detected by a variety of methods including TUNEL (terminal deoxynucleotidyl transferase biotin dUTP nick end labeling) (Enari *et al*, 1998).

The central principle of the TUNEL assay is the *in situ* labeling of the DNA strand breaks which occur during apoptosis. This is effected by the integration of labeled dUTP into these strand breaks by the enzyme terminal deoxynucleotidyl transferase (TdT). The assay used here is a commercial variant of the original assay developed by Sgonc *et al*, (1996), and relies on the incorporation of FITC labeled dUTP at the free 3'

OH ends of DNA fragments and single strand breaks ("nicks"). This may then be analysed by fluorescence microscopy or 'converted' to a peroxidase based detection method with the use of a supplied "POD Converter", (anti-fluorescein antibody fab fragments conjugated with horse-radish peroxidase (POD). Figure 2.3 shows the detection principle of the Roche TUNEL assay used in this research.

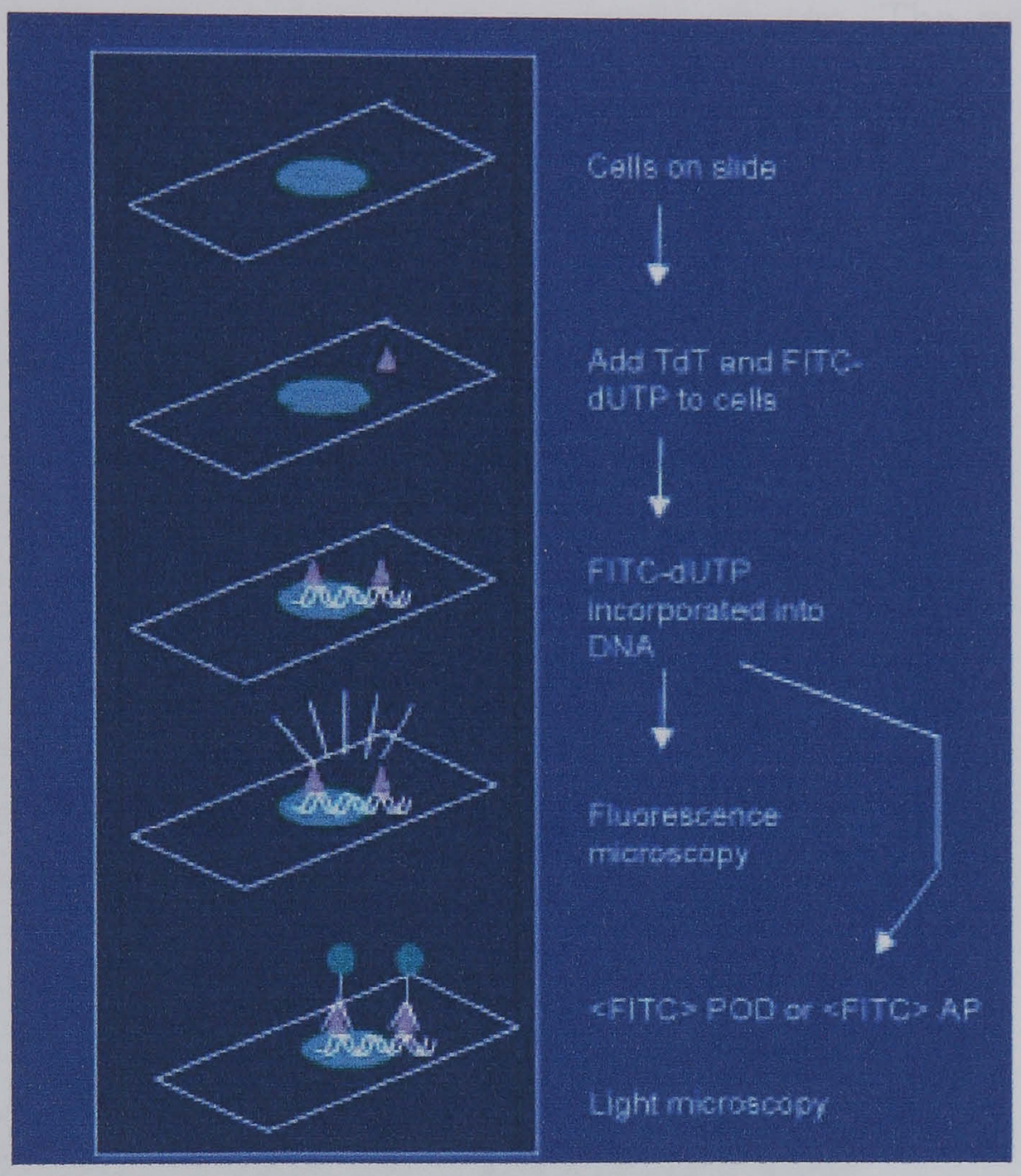

Figure 2.3: The TUNEL Assay Principle.

(Adapted from www.roche-applied-Science.com/fst/apoptosis.htm)

2.2.2.3.1 TUNEL Methodology

The TUNEL procedure was performed on cytospin preparations of C-20/A4 cells using the TUNEL assay *in situ* cell death detection Peroxidase (POD) kit (Roche diagnostics) according to the manufacturer's protocol. Cells were fixed with 4%(w/v) paraformaldehyde solution (prepared in PBS) for 1hr at RT, washed twice with PBS then, blocked with 30%(v/v) hydrogen peroxide in methanol for 10 mins at RT (to inhibit endogenous peroxidase). Following blocking, slides were washed twice with PBS then permeabilized with 0.1%(w/v) sodium citrate in 0.1%(v/v) triton x-100 solution for 2 mins on ice. Slides were again washed twice in PBS and incubated with 50µl of TUNEL reaction mixture (5µl terminal deoxynucleotide transferase (TdT) in 10x storage buffer and 45µl nucleotide mix in 1x reaction buffer) in a humidified

chamber at 37°C for 1hr. TUNEL assay slides were assessed by fluorescence microscopy, with an excitation wavelength between 450-500nm (blue) and a detection wavelength between 515-565nm (green) for FITC marked fragmented DNA of the apoptotic chondrocytes (TUNEL positive cells). TUNEL is detected as a bright green speckled nuclear fluorescence as shown in Figure 2.4. The total number of chondrocytes and the number of chondrocytes staining positively were quantified for 100 cells in three different microscopic fields which were randomly chosen. The percentage of normal cells against apoptotic cells was subsequently recorded and the mean and SD (standard deviation) of readings for each condition calculated.

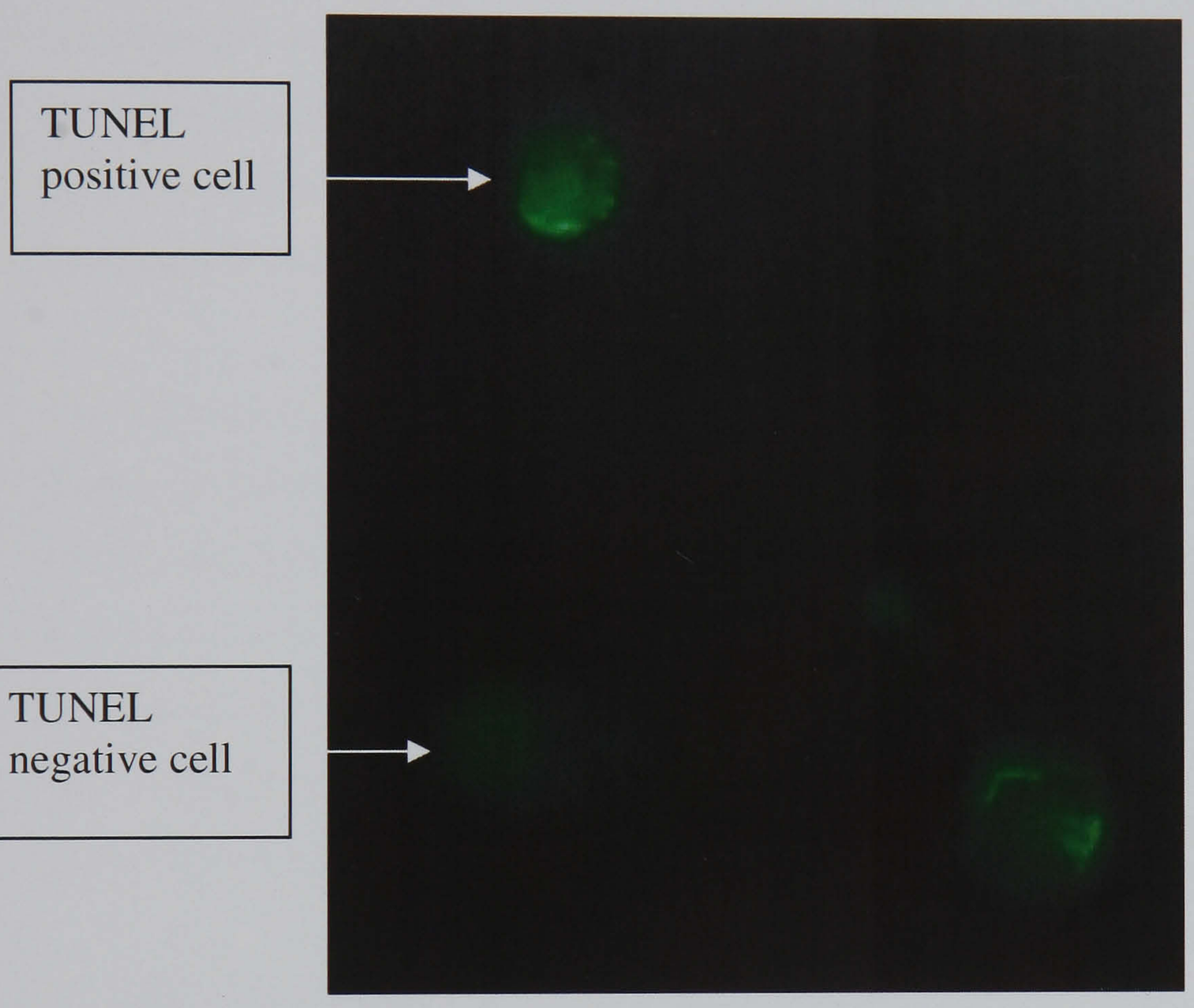

Figure 2.4: Microscopic appearance of TUNEL positive, apoptotic C-20/A4 cells after treatment with TNF-α (x 400 magnification).

2.2.2.4 Lactate Dehydrogenase Release Assay

During the course of cell viability research several methods have been developed to assess cell membrane integrity. Cell integrity may be assessed by pre-labelling with a radioisotope or fluorescing material that is released upon lysis of the cell, or may include the use of vital dyes and dye exclusion assays (Oldham *et al*, 1977). More recent methods involve the measurement of cytoplasmic enzymes released into culture supernatant following cell death, with enzyme activity in the supernatant being proportional to the level of cell death. Such methods are generally rapid and more economical, than procedures involving pre- or post-labeling of target cells (Decker and

Lohmann-Matthes, 1988). An assay of this type, measuring cytoplasmic lactate dehydrogenase (LDH) release, is used in this research.

Whilst many cytoplasmic enzymes could be used in theory, many exist in low amounts (e.g. alkaline and acid phosphatase) or are unstable (e.g. creatine kinase) (Korzeniewski and Callewaert, 1983). LDH however, is a stable, abundant cytoplasmic enzyme present within all mammalian cells and is rapidly released into cell culture supernatant when damage occurs to plasma membranes. The normal intact, plasma membrane is impermeable to LDH (Rae *et al*, 1977). *In vitro* release of LDH from cells therefore provides an accurate measure of cell membrane integrity and therefore cell viability and as a result, has proved to be a popular and reliable test for cytotoxicity (Decker and Lohmann-Matthes, 1988; Korzeniewski and Callewaert, 1983).

The kit used in this research to quantify necrotic cell death, the TOX 7 kit supplied by Sigma, is based on the LDH assays devised by Legrand *et al*, (1992) and Decker *et al*, (1988) adapted to a 96 well plate format. The LDH assay is based on the reduction of NAD to NADH (by the action of LDH) which activates the stoichiometric conversion of a tetrazolium dye to its formazan derivative, the colour of which is analyzed spectrophotometrically (Legrand *et al*, 1992). The enzymatic activity of LDH and generation of NADH is shown below (Figure 2.5):

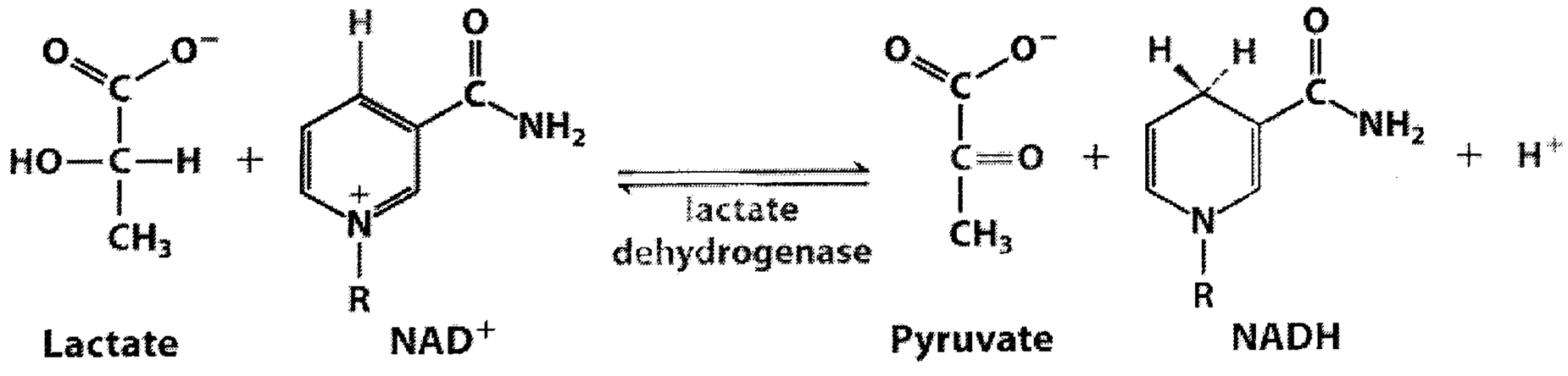

Figure 2.5: LDH catalysed conversion of lactate to pyruvate

(Adapted from www.bmb.psu.edu/.../ pratt/glycolysisreg.html with slight modifications)

In the Tox 7 assay (Sigma) used in this research, formazan concentrations are determined by measuring optical absorbance at 492nm. To measure the red formazan product accurately, adequate controls need to be included to compensate for the presence of phenol red in the tissue culture medium and for any endogenous LDH activity arising from animal serum (FCS) supplements in the tissue culture medium.

2.2.2.4.1 Lactate Dehydrogenase Assay Methodology

The LDH assay was performed on supernatant samples collected from control and treated cells. The supernatant was centrifuged for 4 mins at 2500 rpm at 4°C, to prevent cellular contamination and the TOX 7 assay (Sigma) conducted according to the manufacturers protocol. Briefly, the LDH assay mixture was prepared by mixing equal amounts of LDH assay substrate, enzyme and dye solutions. Microtitre 96 well plates were inoculated with 100µl of the supernatant to be tested and 50µl of the assay mixture, covered in aluminium foil (to exclude light) and incubated at RT for 30 mins. After such time, the reaction was terminated by the addition of 15µl of 1M HCL to each well and the absorbance measured spectrophotometrically at 490nm with background absorbance measured at 690nm.

2.2.2.5 Trypan Blue Dye Exclusion Assay

Trypan blue is one of several stains used in dye exclusion methods for assessing cell viability. The trypan blue dye only enters cells with impaired plasma membranes and is excluded from viable cells allowing both stained and unstained cells to be visualized and counted under a light microscope using a haemocytometer. This method is quick, inexpensive, and requires only a small fraction of total cells from a cell population.

2.2.2.5.1 Trypan Blue Assay Methodology

The trypan blue assay was performed by mixing 100µl of cell suspension (in PBS) with 100µl of 0.25%(w/v) trypan blue solution in PBS, incubating for 5 mins at room temperature, and then counting the cell populations in a haemocytometer. Cell numbers were counted in the 1mm centre square and four 1mm corner squares (not including cells touching the bottom and right-hand side lines of each square) and an average cell number for the squares counted calculated. With the coverslip in place, each large square of the haemocytometer represents a total volume of $0.1mm^3$ or 10^{-4} ml. Cell number was therefore calculated using the following equation:

$$\text{cell number} = \frac{\text{Cells counted x dilution factor x}10^4}{5}$$

The percentage cell viability can be determined using the following calculation:

$$\%\ \text{cell viability} = \frac{\text{Total viable cells (unstained)}}{\text{Total cells (stained and unstained)}} \times 100$$

For improved accuracy, the count for cell viability was repeated using at least 3 samples.

2.2.2.6 The Neutral Red dye uptake assay

The Neutral Red (3-amino-*m*-dimethylamino-2-methyl-phenazine hydrochloride) (NR) assay was developed as an *in vitro* cytotoxicity assay using mammalian cells in culture (Babich and Borenfreund, 1990; Babich and Borenfreund, 1993). This assay is based on the ability of viable, uninjured cells to uptake and bind neutral red, a supravital dye. NR is a weak cationic dye that readily penetrates cell membranes by non-ionic diffusion, accumulating intracellularly in lysosomes, where it binds with anionic sites in the lysosomal matrix of viable cells and hence can be used to demonstrate both increases and decreases in viable cell number (Babich *et al*, 1991). Damage to the plasma or lysosomal membrane decreases the uptake and subsequent retention of the dye. Following dye uptake, cells are washed and fixed and NR is then extracted from the lysosomes and measured spectrophotometrically. The intensity of dye colour following extraction has been shown to be linearly proportional to cell number both by direct cell counts and by protein determination of cell populations (Borenfreund and Puerner, 1986).

2.2.2.6.1 Neutral Red assay methodology

The neutral red assay was performed as follows: A neutral red working solution of 40µg ml^{-1} was freshly prepared each time by diluting the neutral red dye solution in culture media and centrifuging prior to use to remove fine dye crystals. Following treatment of cultured cells with exogenous agents, media was aspirated from the cultured cells and replaced with an equal volume of the neutral red containing medium. The cells were

then left to incubate for 3 hrs at 37°C, after which, the neutral red containing medium was aspirated and the attached cells rapidly rinsed and fixed with 100µl of 1%(w/v) $CaCl_2$ 0.5%(v/v) formaldehyde. The fixative solution was then removed and the cells solubilized with 100µl of 1%(v/v) acetic acid 50%(v/v) ethanol solution to release the NR incorporated into viable cells, yielding a red colour proportional to the number of viable cells. After a 10 min incubation period at RT, followed by 10 seconds of rapid agitation on a microtitre plate shaker, the absorbance of this final solution was measured at 540nm in a Dynatech MR5000 (Dynex Technologies Ltd. Worthing, U.K.) microtitreplate reader. All absorbance values for treated wells were compared against untreated control wells on the same plate and processed to give a viability count expressed as a percentage of the control cell viability.

2.2.3 Molecular Biology Techniques, RT-PCR and real time PCR.

The polymerase chain reaction (PCR) technique was originally presented by Khorana *et al* as early as 1971, but at the time seemed impractical before the advent of gene sequencing or the discovery of a viable thermostable DNA polymerase. It was not until about 12 years later that it was independently developed by Mullis (1983) and is now one of the most widespread methods for the analysis of DNA. PCR is a series of temperature and sequence-specific reactions resulting in the exponential amplification of short DNA sequences (from around 100 bases to around 3 Kb). When a sequence of DNA is amplified and repeated through 20 cycles, theoretically more than 2 million copies are made from just one copy (Wiley *et al*, 2003).

2.2.3.1 Reverse Transcription Polymerase Chain Reaction (RT-PCR)

The PCR technique now in routine use requires several basic components, but the crucial component is the DNA template, which contains the region of interest to be amplified. A variant on the standard PCR technique is reverse transcription PCR (RT-PCR). This technique is an extension to the PCR protocol which allows the analysis of gene expression using messenger RNA (mRNA) as the initial target for analysis. mRNA is the molecule into which the DNA code is transcribed prior to the production of protein at the ribosomes by translation of the RNA 'message'. If mRNA can be isolated it can be reverse transcribed back into complementary DNA (cDNA) by the enzyme reverse transcriptase (RT), first discovered by Temin and Baltimore in the 1970s (Raju,

1999). This enzyme works on a single strand of mRNA, generating cDNA based on the pairing of RNA nucleotides (adenine (A), uracil (U), guanine (G), cytosine (C)) to their DNA complements (thymine (T), adenine (A), cytosine (C), guanine (G)). When eukaryotic DNA is transcribed into mRNA, any introns are spliced out and a poly A-tail and GTP cap added to the mature mRNA strand. In the process of RT-PCR this poly A tail of the mature mRNA template is targeted with an oligo dT nucleotide which hybridizes and forms a 'starting point' for the process. The RT enzyme then synthesizes a sequence of DNA that complements the mRNA template, cDNA.

Once cDNA has been generated, this can then form the template for subsequent PCR reactions. PCR is performed in an ammonium (NH_4^+) buffer which provides a suitable environment for the DNA polymerase. The presence of magnesium (Mg^{2+}) ions is also required, with an optimum concentration in the 1-10mM range. This should be optimized for each individual target nucleotide sequence, too low a concentration of Mg^{2+} may result in no products, and an excess may result in a variety of unwanted products. The addition of nucleotides of the four bases (A, T, C, G), along with the DNA polymerase (which binds to single stranded DNA and synthesizes the complementary strand), completes the general PCR reagent cocktail. The DNA fragment to be amplified, is determined by the addition of specific, short DNA sequences that are complimentary to the beginning and end of the DNA fragment to be amplified. They anneal to the DNA template at these points, where the DNA polymerase also binds and begins synthesis of the complementary DNA strand.

Primer design depends on a number of considerations. The optimum length of a primer is generally from twenty to thirty nucleotides, with a melting temperature around 60°C, and should ideally contain relatively balanced GC vs AT content (e.g. 45%-55% GC) with no long stretches of any one base. Primers should also be designed such that the primer pairs used do not have complementary structures (more than two bp) to avoid "primer dimer" formation resulting from annealing of the two primers (especially at their 3' ends). The target nucleotide sequence defined by the two primers should ideally be 200-400bp in length, with an upper limit of around 3Kb.

The PCR process is effected by DNA polymerases obtained from thermophilic bacteria that grow at temperatures of above 110°C. The DNA polymerase from these organisms is thermostable and therefore is not degraded in the initial stage of the PCR reaction

when the reagent mixture is heated to 94°C to separate the double stranded DNA and produces the single stranded DNA template. One of the first themostable DNA polymerases isolated was Taq (obtained from *Thermus aquaticus*) and, although other thermostable polymerases have been used for example *Pwo* and *Pfu*, Taq remains the most popular.

The PCR reaction is carried out in a thermal cycler, which heats and cools the reaction tubes within it to the exact temperature needed for each step of the reaction. To prevent evaporation of the reaction mixture, a heated lid is placed on top of the reaction tubes or a layer of oil is added on the surface of the reaction mixture. The PCR technique comprises of a series of twenty to forty cycles, each of which consists of three stages.

Stage 1: The double stranded DNA is heated between 94°C-96°C for 1-2 minutes to denature the DNA (by breaking apart the hydrogen bonds that connect the two DNA strands) to yield single stranded DNA. Prior to the first cycle, the DNA is often denatured for an extended time to ensure that both the template DNA and the primers have completely separated and are single strand only.

Stage 2: After separating the DNA strands, the temperature is decreased to promote primer binding to the single DNA strands, a process known as annealing. The temperature of this stage depends on the primer composition and is usually 2-5°C below their combined melting temperatures. This step normally takes 1-2 minutes.

Stage 3: Once primer annealing has taken place, the DNA polymerase synthesizes the complementary strand to the template DNA. This process starts at the primer binding site and is known as extension or elongation. The extension temperature used depends on the DNA polymerase (usually 72°C for Taq) and the time is dependent on both the DNA polymerase and the length of the DNA fragment to be amplified. This step normally takes approximately 1 minute per 1Kb. These stages are represented graphically in figure 2.6 overleaf.

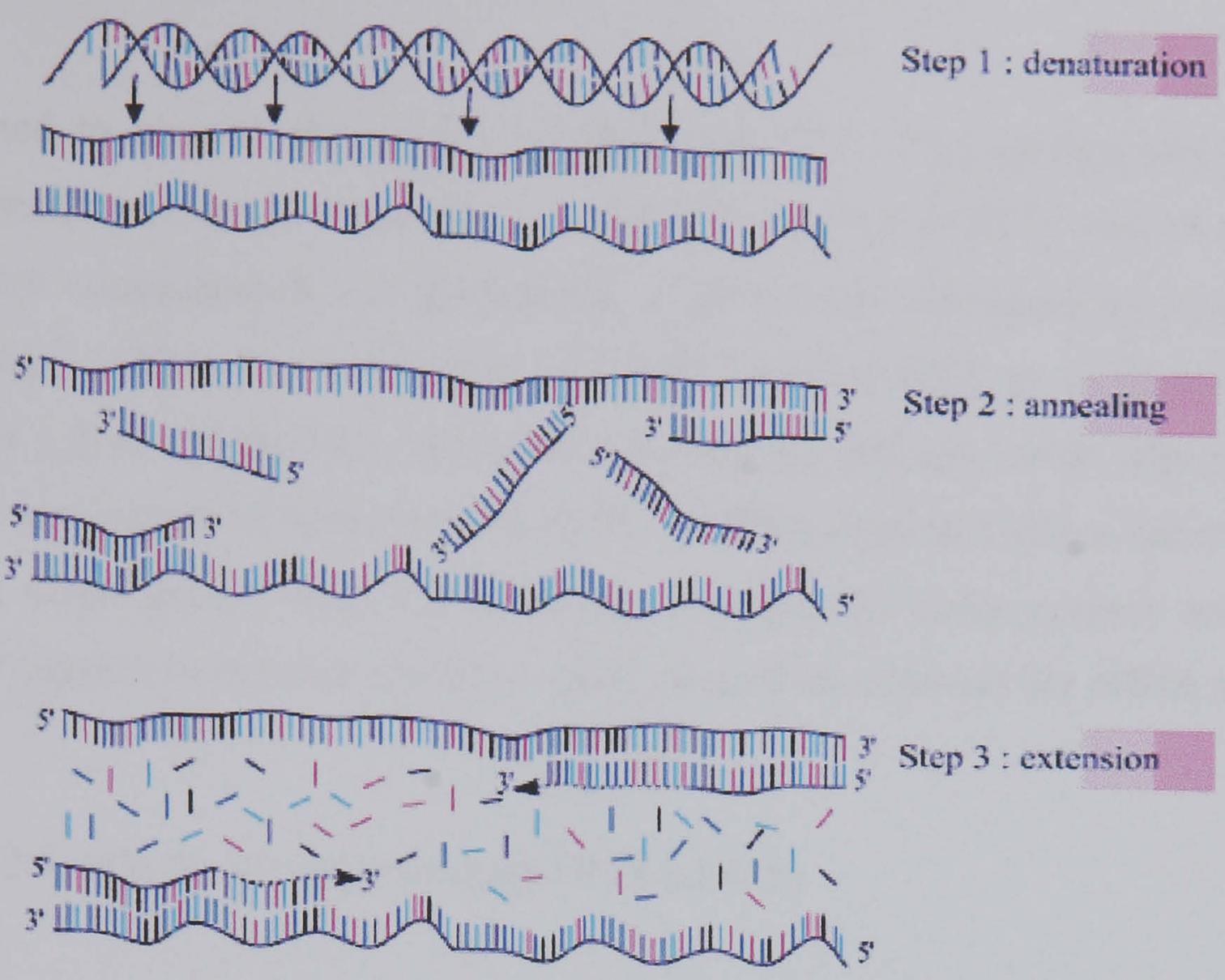

Figure 2.6: Graphical representation of the PCR process.

(Adapted from www.plantpath.wisc.edu/.../ virus/virustech.htm)

2.2.3.1.1 RNA isolation methodology

In order to perform the process of RT-PCR, RNA must first be extracted from the cells under study. Total cellular RNA was isolated from $3x10^5$ cultured C-20/A4 cells by the improved single step guanidium thiocyanate, phenol/chloroform method of Chomczynski (1993). All procedures were performed using ice cold reagents to reduce RNA degradation. Growth media was removed from cell cultures at approximately 95% confluency and cells were lysed with 1ml Sigma Tri–reagent (total RNA isolation reagent) per $10cm^2$ of culture flask surface area. A sterile pipette was used to aliquot 1ml of the lysate equally into sterile Eppendorf tubes and 200µl of chloroform added per ml of lysate. Samples were gently vortexed for 15 sec, incubated at room temperature for 15 min and then centrifuged at 12,000x g for 15 min at 4°C. Following centrifugation, the colourless upper aqueous phase (containing RNA) was transferred to a fresh tube, 500µl of isopropranol added, mixed gently and placed at –80°C for 30 min. After this time, the tubes were placed on ice for 5 min then centrifuged at 12,000 x g for 10 min at 4°C. The resulting RNA pellet was washed with 1ml of 75%(v/v) ethanol in 0.01%(v/v) DEPC treated water and centrifuged at 7,500 x g for 5 min at 4°C. The supernatant was discarded and the pellet dried at 37°C for 4 min in an Eppendorf 5301 Concentrator (Eppendorf, Cambridge, U.K), after which, the precipitated RNA was re-dissolved in 50µl 0.01% DEPC treated water. Agarose gel electrophoresis (AGE) was

performed to observe the quality of RNA and RNA concentration and purity were determined spectrophotometrically on a 1:50 dilution (in DEPC water) of the samples. The RNA concentration was determined at 260nm and calculated by multiplying the absorbance reading by 40 (40μg/ml of single stranded RNA gives an optical density (OD) of 1.0 at 260nm) and, taking into account the dilution factor. The purity of the sample was estimated from the ratio of OD_{260} (RNA content) / OD_{280} (protein content). With a value greater than 1.5 indicating, low protein contamination and sufficient purity. Samples were either stored at –80°C or used immediately for cDNA generation.

2.2.3.1.2 Synthesis of complementary DNA (cDNA)

cDNA synthesis, was effected by reverse transcription from 2µg of RNA. A volume of 1µl (0.5µg) of oligo $dT_{(18)}$ was added to 2µg of each sample, made up to a total volume of 12µl with UHQ water and heated at 70°C for 5 mins. Total cellular RNA was then converted to single stranded cDNA by adding 1µl (200 units) Moloney-murine Leukemia Virus reverse transcriptase (M-MLV–RT), 4µl Strand synthesis buffer (5x), 2µl deoxynucleotide triphosphate (dNTP) mixture (12.5mM) and 1µl (40 units) of recombinant RNase inhibitor (RNasin) to the initial reaction mixture. Larger amounts were synthesized using multiples of these figures. The cDNA generation was carried out for 1hr at 42°C followed by a further incubation period at 75°C for 10 mins to inactivate the M-MLV-RT. The cDNA generated was either used immediately for PCR or stored at –20°C until required.

2.2.3.1.3 Polymerase chain reaction (PCR) methodology

Target sequences in the cDNA were amplified by PCR, using published sequence specific oligonucleotide primers designed to amplify either urocortin (UCN), GAPDH or β-actin (GAPDH and β-actin are internal house keeping genes used as a reference control). PCR reactions were performed in an Eppendorf Master cycler gradient PCR machine (Eppendorf) using the primers and conditions documented in Table 2.3.

The reaction was performed in a 50µl reaction mixture containing 5µl (0.5µg) cDNA, 1µl $MgCl_2$ (5.0mM), 1µl (1.25mM) dNTP mix, 1µl (1µg) of each appropriate forward and reverse primer (UCN, GAPDH or β-actin) 1µl (5 units) of Bio-Taq polymerase, 5µl 10x ammonium buffer (pH 8.8) made up to the volume with 35µl of autoclaved UHQ

water. Finally, 30µl of mineral oil was overlaid in each reaction tube to prevent evaporation. A negative control reaction containing no cDNA (replaced with UHQ water) was run along-side each set of PCR reactions. All amplifications were performed with a denaturation temperature of 94°C for 1 min and an extension temperature of 72°C for 1 min. Annealing temperatures (employed for 1 min) and cycle details are shown in table 2.3 for each primer pair.

Table 2.3: Primer sequences and conditions for the amplification of UCN, GAPDH and β-actin.

Gene	Primer Sequence	Reference	Annealing Temperature (°C)	Number of cycles	Expected PCR Product Size (bp)
UCN	5" CAGGCGAGCGGCCGCG 3" 3" CTTGCCCACCGAGTCGAAT 5"	(Takahashi *et al*, 1998)	64°C	33	172
GAPDH	5"CCTGCTTCACCACCTTCTTG 3" 3"CATCATCTCTGCCCCCTCTG 5"	(Priglinger *et al*, 2003)	58°C	30	437
β-actin	5" GATTCCTATGTGGGCGACGAG 3" 3" CCATCTCTTGCTCGAAGTCC 5"	(Yasunari *et al*, 2000)	63°C	32	532

2.2.3.2 Real-time, quantitative PCR

During the course of this research, a more accurate and sensitive method of relative gene expression measurement has become available known as 'Real Time PCR', which allows the investigator to view the increase in the amount of DNA as it is amplified. The method allows the detection and quantitation of amplicon accumulation since it is performed using fluorogenic probes or intercalating dyes such as FAM and TAMRA (Bustin, 2002). As there is no need for gel electrophoresis, analysis can be completed quickly permitting a large sample throughput. As well as this, there is less risk of amplicon carry over as reaction tubes are unopened. Real-time quantitation of amplicon accumulation also allows determination of reaction efficiency and therefore permits the choice of more sensitive assays (Peters *et al*, 2004).

2.2.3.2.1 Real-time, quantitative PCR methodology

Experiments were performed using Real Time PCR, to confirm the data documented in section 4.3.4.1.2 cDNA was prepared for real Time PCR from 0.5μg RNA using the TaqMan reverse transcription reagent kit (Applied Biosystems, Warrington, U.K), according to the manufacturers instructions. Briefly, total RNA was extracted from C-20/A4 cells, and cDNA was generated from 0.5μg RNA. This was performed with the RNA sample containing 0.5μg RNA which was made up to 34.75µl with DEPC-treated water. Following this, 10µl of 10×RT buffer, 22µl (25 mM) $MgCl_2$, 20µl (10 mM) dNTPs, 5µl (50µM) oligo-dT, 2µl (20 units/µl) RNasin and 6.25µl (50 units/µl) MultiScribe RT were added. This complete mixture was incubated at 25ºC for 10 minutes, followed by a further incubation at 37ºC for 1 hr and a final incubation at 95ºC for 5 minutes, using a thermal cycler.

Real Time PCR was carried out for the amplification of UCN and GAPDH using the TaqMan universal PCR mastermix kit (Applied Biosystems) and the appropriate Assay-on-Demand primer and probe combinations for UCN (Cat. n° HS0017020-ml) or GAPDH (Cat. n° HS99999905-ml) according to the manufacturers protocol. 20-µl of each reaction mixture (containing 1 µl of 20× Ucn or GAPDH Assay-on-Demand mix) 9µl of cDNA (or 0.1% v/v DEPC-treated water for negative controls) and 10µl of 2×TaqMan universal mastermix were placed on a 96-well optical reaction plate and sealed using an optical adhesive cover. PCR was performed using an ABI Prism (model

7000) real-time PCR thermal cycler with the conditions shown in table 2.4. Results were plotted as mean ratio of Ucn cycle threshold (Ct) over GAPDH Ct ± SEM.

Table 2.4: Real Time PCR conditions

Stage	Step	Temperature (°C)	Time (minutes)	Cycle
Initial Denaturation	1	95 °C	10	1
Cycle Template Denaturation	2	95 °C	0.25	45
Annealing/Extension	3	60 °C	1	1

2.2.4 Electrophoretic and blotting techniques

2.2.4.1 Agarose Gel Electrophoresis (AGE)

Extracted RNA, and DNA products generated by PCR, are routinely assayed for quality and, in the case of PCR products, identified by size, using agarose gel electrophoresis with a TAE or TBE (Tris-acetate-EDTA / Tris buffered saline) buffer system. When an electric current is applied to nucleic acid molecules in an agarose gel, the negatively charged nucleic acids move through the gel matrix towards the anode. The rate of migration is affected by a number of factors including the concentration of agarose and the voltage applied to the gel. The voltage applied is usually in the range of 5-8 volts/cm with increases above this resulting in a decrease in resolution. Nucleic acid conformation is also a factor with RNA with the three main forms of DNA (superhelical, nicked and linear) running at different rates.

The Nucleic acid is loaded onto the agarose gel in a loading buffer which 'weights' the sample into the well and usually contains a visible, negatively charged indicator dye (e.g. Bromophenol blue (BPB), xylene cyanol FF), which give some indication of run progress. As the electrophoresis progresses, smaller molecules move towards the anode more rapidly than larger molecules (assuming all have the same conformation). The size of a PCR product can be estimated by comparison with a DNA ladder containing DNA fragments of known size, also loaded onto the gel. Nucleic acid molecules are visualized by the addition of ethidium bromide (EtBr) and observation under ultra violet (UV) light following EtBr intercalation into the nucleic acid structure.

2.2.4.1.1 AGE methodology

Extracted RNA was assessed for quality on 1%(w/v) agarose gels, whilst DNA PCR products were resolved on 2%(w/v) agarose gels. 1% agarose gels were prepared by heating 1.5g agarose in 150ml 1x TAE buffer in a 650w microwave for ~2 min and then cooling to ~45°C. Ethidium bromide, a fluorescent DNA intercalator was then added to the gel to a final concentration of 0.002%(v/v). The gel solution was set in a 10cm x 15cm gel casting tray with a 14 well comb and placed in an electrophoresis tank with 1x TAE running buffer. 2% agarose gels were prepared in a similar fashion using 3g agarose in 150ml 1x TAE. Molecular markers were included on all gels and loaded as supplied (3μl/well) whereas DNA samples were first mixed with loading buffer in a ratio of 10μl sample to 5μl buffer, prior to loading. The gel was electrophoresed at a continuous voltage of 100v for approximately 1 hour until the leading dye had migrated to midway of the gel. DNA was visualized under ultraviolet light with a Uvitec BTS-20 (Uvitec, Cambridge, U.K.) gel documentation system.

2.2.4.2 Sodium dodecyl sulphate polyacrylamide gel electrophoresis (SDS-PAGE)

Native polyacrylamide gel electrophoresis (PAGE) was first developed in 1964 by Ornstein as a replacement for the earlier support materials such as starch. The greater resolution and stability of polyacrylamide gels, enhanced by the introduction of the stacking gel, results in a much improved resolution with sample bands down to a few micrometres thick (Ornstein, 1964; Davis, 1964). A further development of the PAGE technique was the inclusion of sodium dodecyl sulphate (SDS), an ionic detergent which binds around the polypeptide backbone of protein molecules and allows for the separation of proteins according to their size (rather than a combination of both size and charge as occurs in native PAGE) (Weber and Osborn, 1969; Laemmli, 1970).

The binding of SDS to the polypeptide backbone denatures secondary and non-disulphide-linked tertiary protein structure, resulting in every protein carrying a net negative charge. Without the use of SDS, proteins with similar molecular weights may migrate differently because of charge differences and variation in folding. By heating the protein sample to 100°C in the presence of excess SDS and a reducing agent such as 2-mercaptoethanol or dithiothreitol, disulphide bonds are also cleaved, resulting in the complete dissociation of proteins and the removal of any remaining tertiary or

quaternary structure. As the intrinsic charges of proteins are small compared to the negative charges provided by the bound detergent, all SDS protein/polypeptide complexes have virtually the same negative charge and linear molecular shape. This results in all proteins migrating through the gel according to size only. The simplicity and speed of these methods, plus the fact that only μg quantities of proteins are required, has made SDS-PAGE one of the most widely used methods for the determination of molecular mass in a protein sample.

Once denatured in the loading buffer containing SDS and 2-mercaptoethanol, samples are loaded at one end of a polyacrylamide gel in contact with a suitable buffer. An electric current is applied across the gel, causing the negatively charged proteins to migrate towards the anode. After about an hour (depending on gel size) the proteins will have differentially migrated, with smaller proteins, moving further down the gel, while larger ones remain closer to the point of origin. Thus proteins may be separated according to size (and therefore molecular weight). A tracking dye (usually bromophenol blue) is often added to the loading buffer to indicate sample progress during the electrophoretic run.

PAGE/SDS-PAGE separations are typically performed using a discontinuous system composed of two distinct gels. Proteins migrate first through a low percentage stacking gel where they remain stacked, or unresolved, behind the moving boundary (dye front), until they reach a second, higher percentage resolving gel. At this point the proteins may unstack, or resolve, from the moving boundary. Unstacking can be achieved by;

a) Slowing down the protein after it has been stacked, or
b) Speeding up the trailing ions once the protein has been stacked.

Slowing the protein is achieved as it enters the higher percentage resolving gel, where its mobility is reduced so that it runs more slowly than the glycine ions. This results in the protein escaping the stack and migrating as if it were in a continuous gel at a lower local field strength. Simultaneously, the change in pH from the stacking gel to the resolving gel results in the acceleration of the trailing glycine ions as their net negative charge increases. As a result of this, the glycine ions overtake some of the proteins and now migrate directly behind the chloride ions.

These factors combine in the original methods of Ornstein (1964) and Davis (1964), to improve protein resolution with the use of a low percentage stacking gel at pH 6.8 over a higher percentage separation gel at pH 8.8. This system was later adapted by Laemmli (1970) for SDS-PAGE separation of proteins, keeping essentially the same features, and the technique has altered little since.

2.2.4.2.1 SDS-PAGE methodology

In the Laemmli (1970) system for SDS-PAGE, proteins are loaded into an upper (stacking) gel, then begin to separate when they reach a lower (separating) gel of different composition. The discontinuous gel is therefore cast in two stages. Acrylamide polymerizes best in the absence of oxygen, therefore each stage of gel casting is overlayed with distilled water to exclude air.

The glass plates and casting stand were assembled according to the manufacturers instructions and 10ml of gel mixture (prepared as in Table 2.5) added to each assembly. Prior to the pouring of the acrylamide solution, the Teflon comb was used to mark the glass plate for the stacking gel (the length of the comb teeth plus 1cm). Once the gel had been poured (leaving sufficient space for the stacking gel), the acrylamide solution was carefully overlayed with distilled water (using a Pasteur pipette) to exclude oxygen and to ensure a smooth distinct surface at the top of the separating gel in order to achieve optimum resolution.

Table 2.5: Composition of 15% resolving gels for Tris-glycine SDS-polyacrylamide gel Electrophoresis (PAGE).

Component	Volume
Distilled water	2.6ml
30 % (w/v) acrylamide/bisacrylamide (37:1) mix	12ml
1.5M Tris (pH 8.8)	5ml
10% SDS	0.2ml
10% Ammonium persulphate	0.2ml
TEMED	0.008ml

The gel was allowed to polymerise at room temperature for 30 minutes after which the overlay water was drained completely and the stacking gel, prepared as in Table 2.6, poured directly on top of the polymerized resolving gel. A clean Teflon comb (washed with distilled water) was immediately inserted into the stacking gel solution, avoiding trapping any air bubbles under the teeth and the gel allowed to polymerise at room temperature for at least 30 minutes. After polymerisation, the Teflon comb was removed and the wells rinsed immediately with distilled water to remove any un-polymerized acrylamide.

Table 2.6: Composition of 5% stacking gels for Tris-glycine SDS-polyacrylamide gel electrophoresis.

Component	Volume
Distilled water	3.4ml
30 % (w/v) acrylamide/bisacrylamide (37:1) mix	0.83ml
1.0M Tris (pH 6.8)	0.63ml
10% SDS	0.05ml
10% Ammonium persulphate	0.05ml
TEMED	0.005ml

Prior to sample loading the prepared gels were mounted and clamped in the electrophoresis apparatus and the SDS PAGE electrophoresis buffer prepared as in (Table 2.7) was added to the top and bottom reservoirs of the tank. Any bubbles trapped at the bottom of the gel between the glass plates were removed prior to commencing the electrophoretic run.

Table 2.7: Composition of SDS PAGE electrophoresis buffer

Component	Concentration
Trizma	0.025M
Glycine	0.192M
SDS	0.1% (w/v)

Prior to SDS-PAGE analysis cell extracts were prepared and their total protein content determined as detailed in section 2.2.5. Samples for SDS-PAGE analysis were

equalized for protein content then prepared for application by mixing with sample loading buffer (Table 2.8) in a 2:1 ratio and heating at 100°C for 3 minutes to ensure denaturation

Table 2.8: Composition of SDS PAGE electrophoresis loading buffer (20ml)

Component	Concentration
Glycerol	10%(v/v)
SDS	3%(w/v)
2-mercaptol-ethanol	0.5%(v/v)
Bromophenol blue	0.02%(w/v)

All protein resolution was performed on 15% acrylamide gels with 3µl of low molecular weight rainbow marker (Amersham, U.K.) or pre-stained protein marker (Biolabs, U.K) loaded into the second well of the gel and 20µl (equivalent to 30µg of whole cell extract) of each sample in loading buffer into other wells. The two outer wells were not used to eliminate 'edge effects' on samples run in these wells. The gels were run at a constant current of 87 volts per gel and the separation continued until the bromophenol blue marker dye had reached ~1cm from the bottom of the resolving gel (typically 1.5 hrs). Following electrophoresis, gels were removed from the apparatus and one stained for protein with picric acid/coomassie blue (to confirm uniform protein loading) whilst the other was subjected to Western blotting procedures.

2.2.4.2.2 Picric acid/Coomassie Brilliant Blue staining of SDS-PAGE gels

SDS-PAGE gels were first pre-washed with three changes of a solution of 45% (v/v) methanol / 10% (v/v) glacial acetic acid in distilled water, over the course of 1 hr in order to remove detergent from the gel to improve staining. Proteins were then stained with a picric acid/coomassie brilliant blue stain which binds nonspecifically to virtually all proteins. The stain was prepared from two solutions; a 0.5%(w/v) coomassie brilliant blue R-250 solution in 45%(v/v) methanol, 10%(v/v) glacial acetic acid and a picrate solution prepared by adding 132g of damp picric acid to approximately 2L of distilled water. The latter solution was stirred constantly and neutralized to pH 7 with 1M NaOH until the picrate had completely dissolved. A volume of 750ml of the coomassie

solution was then mixed with the picrate and made up to 3L with distilled water. This solution was used to stain SDS-PAGE gels by immersion of the gel in ~150ml of staining solution on a rocking platform for 1 hour at room temperature. The stain solution was then removed and stored in a Winchester bottle for future use and the gel de-stained. De-staining was performed by soaking gels in a 10%(v/v) methanol/ 7%(v/v) glacial acetic acid solution (in distilled water) on the rocking platform until excess dye was removed, changing the de-staining solution as necessary. Once fully de-stained, gels were preserved for future reference by drying at 80°C for 2 hours on a BIO-RAD Model 583 gel dryer (BIO-RAD, Hemel Hempstead, U.K.).

2.2.4.3 Western Blotting

Following electrophoretic separation it is often desirable to be able to identify a specific protein amongst those separated in the gel. This can be accomplished by a procedure known as Western blotting. Western blotting involves the use of a specific antibody to identify the protein of interest and is part of a family of blotting techniques including Southern blotting (for DNA) and Northern blotting (for RNA) (Burnette, 1981).

During the Western blotting procedure, proteins in the SDS-PAGE gel are transferred on to a membrane to allow immunoprobing. Several different membrane materials are available for Western blotting (e.g. poly-vinylidene difluoride (PVDF), nitrocellulose) but, regardless of their composition, these membranes bind proteins nonspecifically based upon hydrophobic and charged interactions between the membrane and protein. Following electrophoretic separation (e.g. SDS-PAGE) a sandwich of gel and membrane is compressed in a cassette and immersed in buffer between two parallel electrodes. A current is passed at right angles to the gel which causes the separated proteins to electrophorese out of the gel and onto the membrane which is then commonly referred to as 'the blot'. The efficiency with which a particular protein will be transferred is dependent on the protein binding capacity of the membrane used, the transfer method and conditions employed, as well as the nature of the proteins being transferred. Size and hydrophobicity are of particular importance with larger and more hydrophobic proteins generally transferring less well. Whilst the presence of SDS may be desirable for protein separation in the initial gel, it too can interfere with binding to the transfer membrane, especially for smaller proteins.

It is often desirable to have some visual confirmation of protein transfer to the membrane which may be simply achieved by the inclusion of a lane of pre-stained protein markers on the gel. Alternatively, a total protein stain such as Ponceau S may be used which is fast, reversible and does not interfere with subsequent immuno- detection.

After transfer of the proteins from the gel, the remaining protein-binding sites on the membrane must be blocked to avoid non-specific binding of the detection antibodies to the membrane. This is usually achieved by placing the membrane in a solution of casein (or non-fat dried milk powder) in the presence of the detergent Tween^{TM} 20.

Following blocking, a primary antibody specific for the protein of interest is incubated with the membrane at an appropriate dilution to achieve high specificity, and low non-specific background. After washing the membrane to remove unbound primary antibody a secondary antibody is employed to detect the first and is usually produced in different species e.g. a goat anti-rabbit antibody might be used if the primary antibody was produced in rabbits. This secondary antibody is usually linked to an enzyme to allow detection of its binding location with the use of a suitable substrate. Secondary antibodies are typically conjugated with enzymes such as horseradish peroxidase (HRP) (as used in this research) or alkaline phosphatase (AP). Secondary antibodies may also be biotinylated, where a final stage with avidin HRP or AP complexes is necessary. The western blotting process is summarized in Figure 2.7

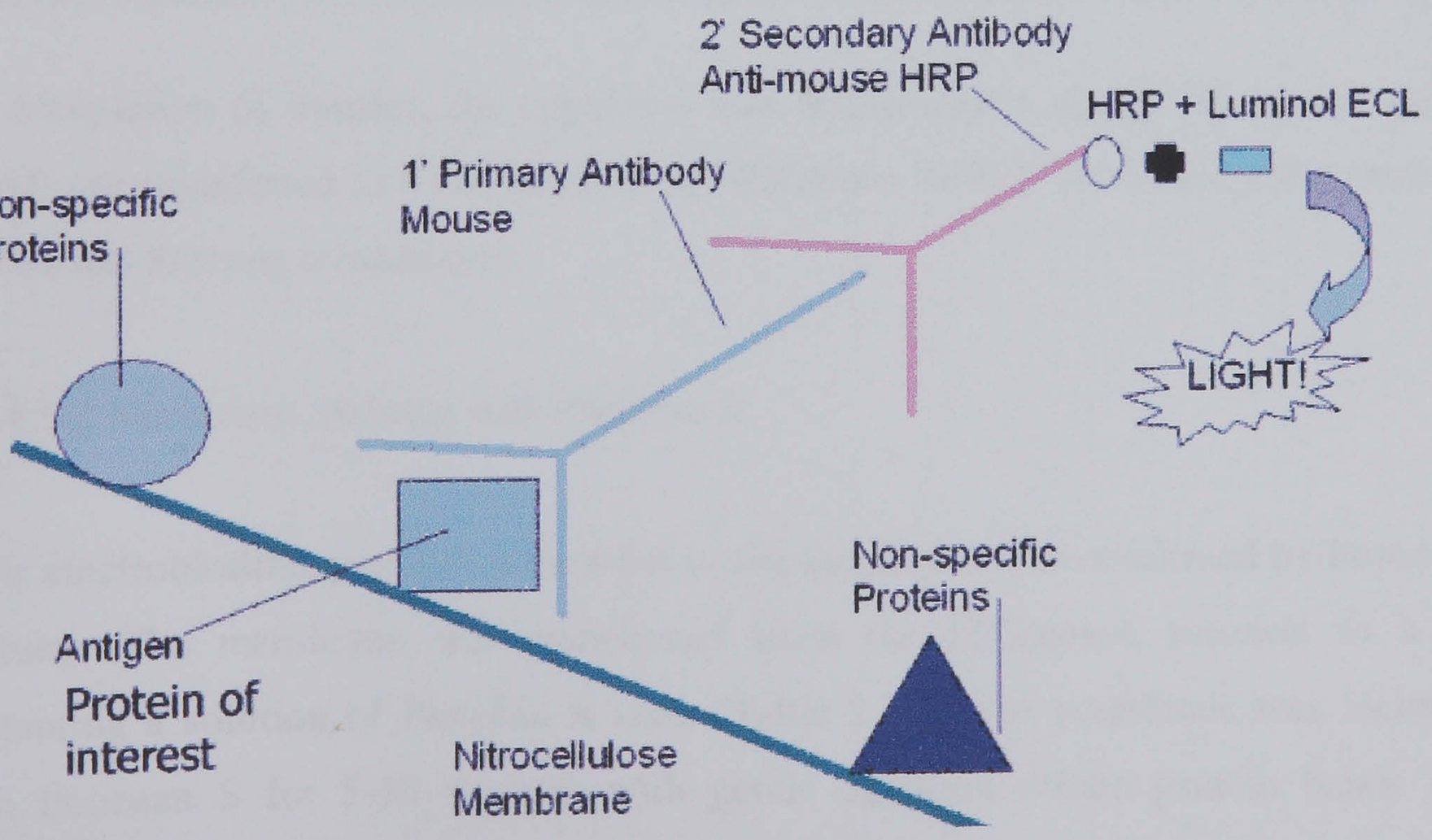

Figure 2.7: Principles of the Western blotting technique

(Adapted from www.google.com/western blotting)

2.2.4.3.1 Western blotting methodology

On completion of the electrophoretic separation, gels were removed from the apparatus and washed in transfer buffer (Table 2.9) for 10 minutes to remove excess SDS from the gel surface. The transfer (blot) was performed using a mini Trans-Blot SB wet Transfer Cell apparatus (BIO-RAD) according to the manufacturers specifications, with the components assembled as follows: anode, 'scotchbrite' sponge (pre-soaked in transfer buffer), 3 squares of filter paper (also pre-soaked in transfer buffer) the washed SDS-PAGE gel, Hybond^{TM} C membrane (pre-soaked in transfer buffer and added with tweezers), 3 further pre-soaked filter papers, an additional pre-soaked sponge pad, cathode. The complete 'sandwich' was placed in the electrophoresis tank, topped up with transfer buffer, an ice pack added to keep the tank cool, and the proteins transferred at a constant voltage of 310 milliamps for 2 hours.

Table 2.9: Composition of Transfer buffer (1L)

Component	Concentration
Glycine	39mM
Trizma	48mM
SDS	0.037%(w/v)
Methanol	20%(v/v)

On completion of transfer, the apparatus was disassembled, the gel discarded and the membrane transferred to a container with PBS/tween (0.01% (v/v)) and left to rinse for 10 minutes at room temperature.

2.2.4.3.2 Membrane staining with Ponceau S

After electroblotting, transfer of proteins to the membrane was confirmed by Ponceau S staining. The membrane was transferred from the PBS/tween solution to a tray containing a solution of Ponceau S stain (Table 2.10). The membrane was incubated with Ponceau S for 5-10 minutes with gentle agitation. When protein bands were visible, the Ponceau S solution was poured back into its bottle and stored for future use. The membrane was then washed in several changes of PBS/tween solution at room

temperature, until membrane background staining was minimal. Protein transfer was confirmed by visual inspection.

Table 2.10: Composition of Ponceau S stain (aqueous solution).

Component	Concentration
Ponceau S	2%(w/v)
Trichloroacetic acid	30%(w/v)
Sulfosalicyclic	30%(w/v)
Water made to 100ml	

2.2.4.3.3 Immunoprobing methodology

Prior to immunoprobing for specific proteins, the membrane was blocked with 2% (w/v) non-fat dried milk powder dissolved in 0.01%(v/v) PBS/tween for 30 minutes at room temperature with continuous agitation. Following the blocking period, the milk was discarded and the membrane was probed with primary antibodies against the protein of interest (anti-phosphorylated P42/P44 MAPK and p-ERK (P42/P44 MAPK total, anti-caspase 3, 8, or 9, and GAPDH) diluted 1:500 in 2% nonfat milk at 4°C with gentle agitation overnight. Following incubation with the primary antibody, the membrane was washed three times (10 minutes per change) with PBS/tween, and was then immediately incubated for 2 hours at 4°C with the secondary antibody, polyclonal rabbit anti-mouse Ig HRP (Dako Cytomation, Ely, U.K.) (for the MAP Kinase phosphorylated P42/P44 antibody) or polyclonal goat anti-rabbit Ig HRP (for the caspases, GAPDH and p-ERK antibodies) both diluted 1:500 in 2% milk. The membrane was then washed a further three times with PBS/tween, placed on saran wrap and remaining buffer drained off. Specific antibody binding was detected using 1ml of ECL (enhanced chemiluminescence) substrate solution (prepared according to the manufacturer's instructions) distributed evenly over the membrane. After 1 minute incubation at room temperature, the ECL substrate solution was drained off the membrane with a paper towel and wrapped in saran wrap, eliminating any visible air bubbles. The chemi-illuminescence reaction was detected using Kodak BioMax X-ray film exposed to the blot in a sealed cassette for 5-20 minutes at room temperature.

Following exposure, the film was developed and fixed using Kodak developing and fixing solutions according to the manufacturer's instructions. Subsequently, the film was washed with tap water and hung to dry. The relative intensities of the P42/P44 MAPK protein bands of each sample were normalized by the intensity of the total P42/P44 MAPK protein band per lane were determined using densitometry, normalizing the P42/P44 MAPK with the total P42/P44 MAPK and caspase 3 with the GAPDH.

2.2.4.3.4 Membrane stripping and re-probing

One of the major advantages of chemiluminescent detection, is the ability to strip antibodies from a blot and then re-probe the same blot. A blot may be stripped and reprobed several times to visualize other proteins or to optimize detection of a protein (i.e. antibody concentrations), without the need to re-run gels. During the procedure, some antigen is lost from the membrane, but this maybe minimized by stripping the membrane as gently as possible.

Where used, the Hybond^{TM} C membrane was stripped by subjecting it to three washes of 5 minutes each in 0.2M NaOH. After stripping, the membrane was washed three times in 1x PBS/tween (5 minute intervals) and then blocked in 2% non fat milk and re-probed.

2.2.5 Preparation of cell extracts and determination of protein concentration

2.2.5.1 Preparation of cell extracts

Cell lysis is the first step in cell fractionation and protein purification. Many techniques are available for the disruption of cells, including physical (sonication, French press or vortexing) and detergent-based methods. Physical lysis requires expensive, awkward equipment and involves protocols that can be difficult to repeat due to apparatus variability. Detergent-based lysis (as used in this research) has become the method of choice in recent years due to convenience, low cost and efficient protocols. Sigma CelLytic (as used in this research) is one such detergent based protein extraction reagent.

2.2.5.1.1 CelLytic™ methodology

Prior to cell extract preparation, spent medium was removed from the cell culture, the adherent cells rinsed with cold DPBS (4°C) and then detached with a further volume of DPBS and pelleted by centrifugation. Following removal of the supernatant, 125µl of Sigma CelLytic buffer was added per $1x10^6$ cells, the resulting suspension was transferred to an eppendorf tube and 10µl of protease inhibitor cocktail added to prevent the breakdown of protein during the procedure. This combination was then mixed on a rotary mixer (40 rpm) for 15mins at 4°C followed by centrifugation at 20,000xg for 15mins at 4°C. Supernatants were collected and transferred to a fresh cold eppendorf tube and frozen immediately at -80°C.

2.2.5.2 The Bradford protein assay

The Bradford assay is a rapid protein assay which has been adapted to a microtitre plate format in order to use a minimum amount of sample. The assay is based on the observation that the absorbance maximum for an acidic solution of Coomassie Brilliant Blue R-250 shifts from 456nm to 595nm when binding to protein occurs. Both hydrophobic and ionic interactions stabilize the anionic form of the dye, causing a stable visible colour change. It is a very versatile assay since the extinction coefficient of a dye-albumin complex solution is constant over a wide concentration range and is recommended for the determination of protein content prior to gel electrophoresis (Stoscheck, 1990)

2.2.5.2.1 Bradford assay methodology

The Bradford reagent was prepared by dissolving 600mg of Coomassie Brilliant Blue R-250 in 1L of 2%(w/v) perchloric acid overnight followed by filtration to remove any undissolved dye.

Prior to the assay, a set of BSA standards were prepared over the range of 0.005 to 100mg ml^{-1} protein. These standards were analysed along with the treated samples to calibrate the assay each time. All standards and samples were run in triplicates in a 96 well microtitre plate. The assay was performed by mixing 10μl of sample or standard

with 190μl of Bradford reagent and, following 5 minutes incubation at RT, the titre plate was read at 595nm to determine protein concentration of the samples.

2.2.6 Statistical Analysis

Data values shown in the figures are expressed as mean ± SD of n independent experiments. The experiments were repeated at least 9 times. All data were subjected to one way ANOVA with Bonferroni's correction for post hoc t-tests. Probabilities of $P \leq 0.05$ were considered statistically significant. The Prism GraphPad software (San Diego, U.S.A) version 3 (5.1.2600.2180) for windows, was used to perform all the statistics described. Data analysis was performed using Microsoft Excel.

CHAPTER 3

THE RESPONSE OF C-20/A4 CELLS TO PRO-APOPTOTIC STIMULI

3.1 Introduction

Chondrocyte apoptosis, a potential factor in the pathogenesis of OA may be initiated *in vitro* by NO (Kim *et al*, 2002), TNF-α (Petterson *et al*, 2002) and IL-1β (Singh *et al*, 2003) as discussed more fully in chapter 1. Previous studies have linked increased levels of NO and cell death in arthritic cartilage, but its not known if NO is the primary inducer of chondrocyte apoptosis. Apoptotic cell death has been identified in chondrocytes *in vitro* following exposure to NO in the presence of oxygen radical scavengers (Blanco *et al*, 1995; Notoya *et al*, 2000). Experimental evidence is also emerging that pro-inflammatory, catabolic cytokines TNF-α and IL-1β may be involved in the pathophysiology of many joint diseases and are mediators of joint damage in OA (Westacott and Sharif, 1996). Additionally, these cytokines IL-1β and TNF-α, have been reported to play important roles in cartilage and bone degradation (Kobayashi *et al*, 2005).

In order to further investigate the response of chondrocytes to these stimuli *in vitro*, the experiments detailed in this chapter were designed to assess chondrocyte apoptosis when treated with a range of concentrations of the NO donor SNAP, TNF-α and IL-1β. The concentrations of these stimuli used in these experiments were designed to cover normal levels through to the elevated levels of SNAP, IL-1β and TNF-α which have been, reported in the synovial fluid in OA patients (Greisberg *et al*, 2002).

3.2 Methods

A chondrocyte cell suspension at a density of $3x10^6$ cells/ml, was transferred to 6 well tissue culture plates. An equal volume of cells re-suspended in media were added into each well containing 1ml of 10% FCS complete medium. Cell monolayers were incubated for 24–48 hours (hrs) in this 10% FCS complete medium until they reached ~80% confluency (Figure 3.1a). The cells were then 'serum starved' for 24 hrs by substituting the 10% FCS complete medium for a growth medium containing 1% FCS. This has the effect of reducing cell division and promoting a more 'metabolic phenotype' in the C-20/A4 chondrocytes (Figure 3.1b). The cultured cells were then re-supplied with the 1% FCS supplemented medium containing varying concentrations of SNAP (0mM-10mM), TNF-α (0-100pg/ml) or IL-1β (0-20pg/ml) for 6hours treatment. SNAP was chosen as the NO donor because it releases pure NO spontaneously, as opposed to other frequently used NO, donors like SNP, SIN-1 *etc.* which release the potentially toxic substances peroxynitrite and cyanide ions. TNF-α and IL-1β were chosen for these studies as they are pro-inflammatory and pro-apoptotic stimuli that have been implicated in the pathogenesis of OA. A six hour incubation time was employed for all stimuli as the optimum cell activation time for many cytokines has been established to be 6-8hours (Seid *et al*, 1993). These experiments were performed to establish 'a dose response' curve for each of the stimuli and to determine the optimum concentration of these stimuli required to achieve suitable levels of chondrocyte death for future experiments. Control experiments with untreated cells were also run alongside all treated experiments. Chondrocyte cell death was quantified by Annexin V/PI and TUNEL assay for apoptosis and LDH release for necrosis as documented in chapter 2, section 2.2.2.

(a)

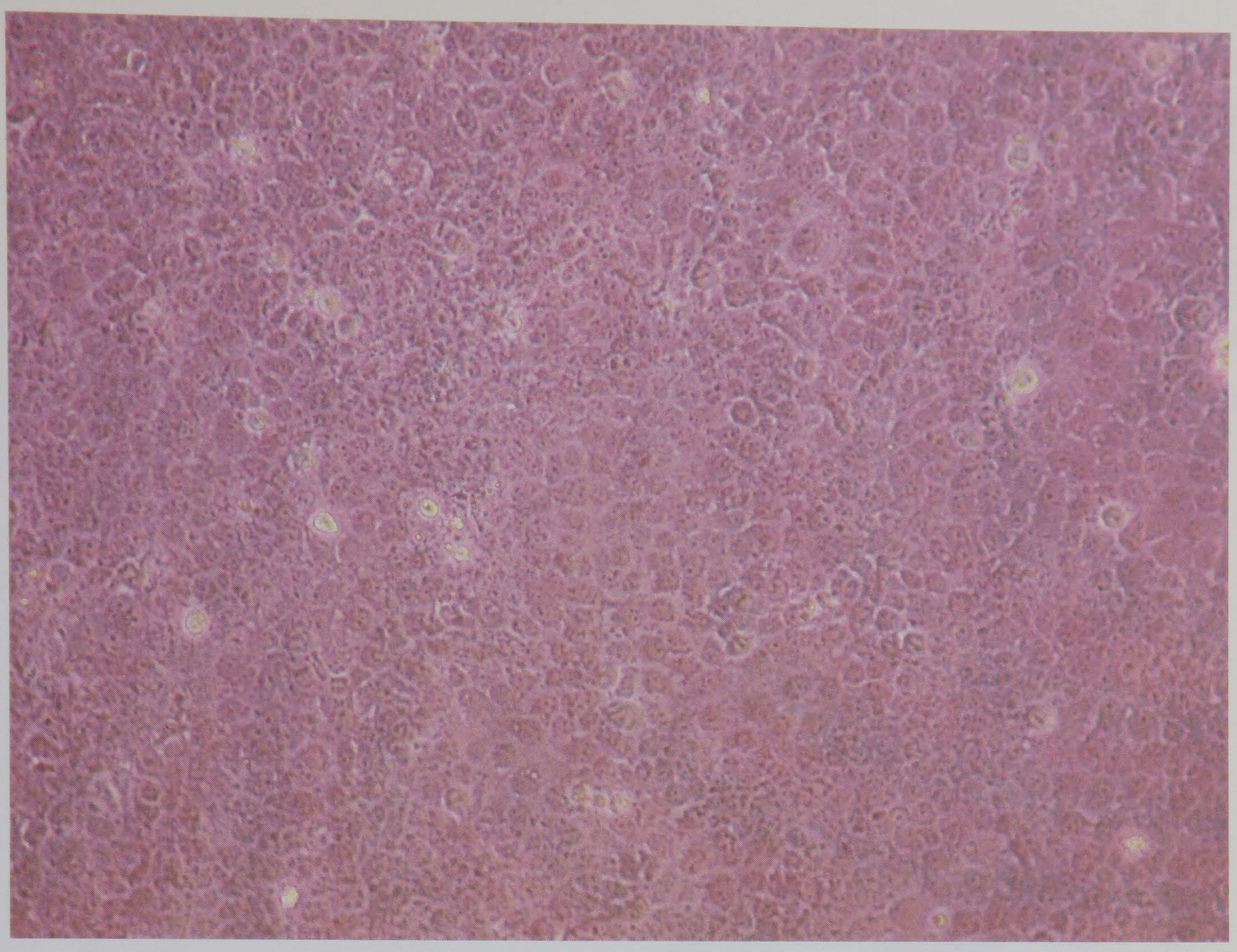

(b)

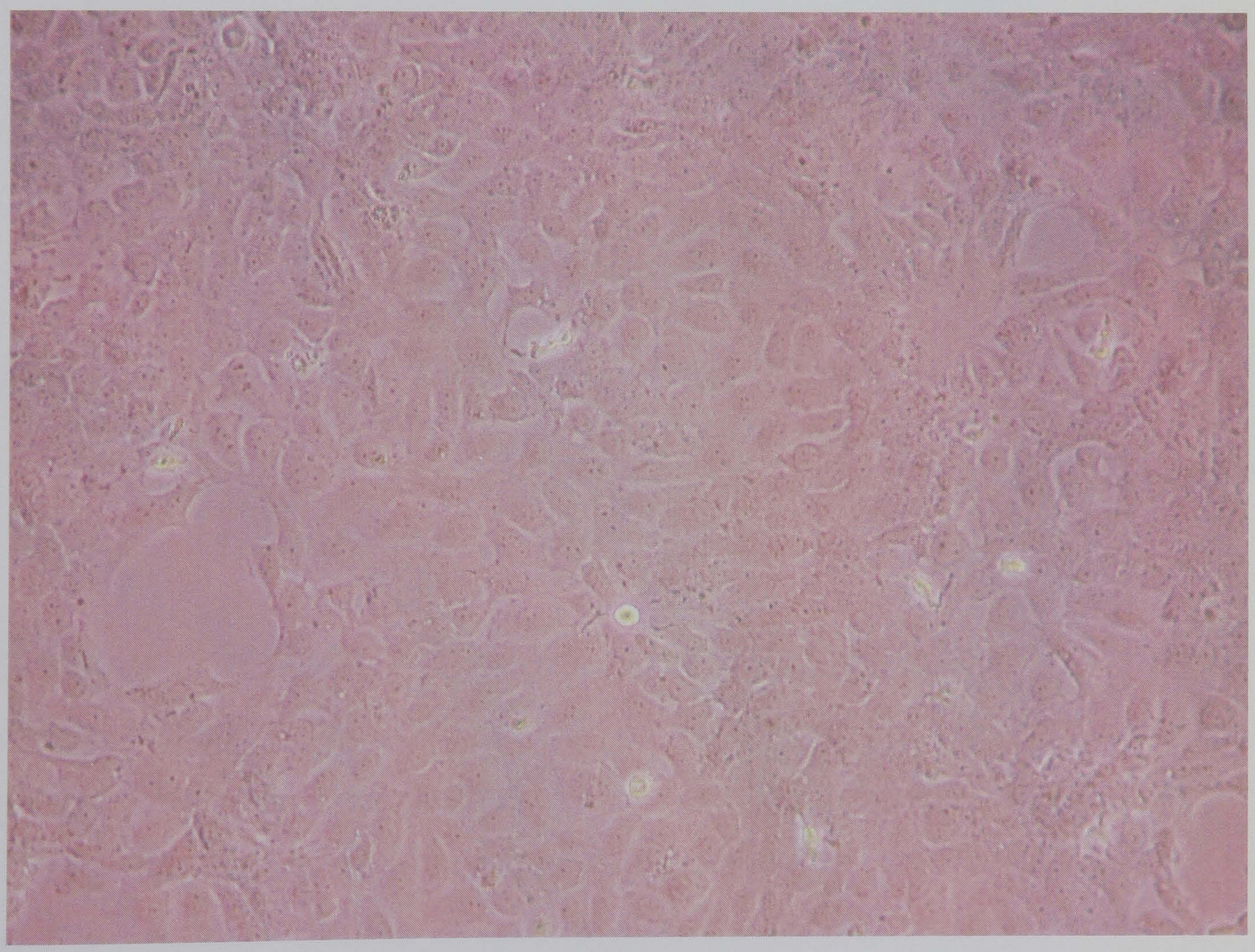

Figure 3.1: Microscopic photographs (400x magnification) demonstrating morphology of immortalized C-20/A4 chondrocyte cells grown in 10% FCS medium (a) and (b) 1% FCS medium.

3.3 Results

To determine whether apoptosis or necrosis was the underlying mechanism of SNAP, TNF-α and IL-1β induced cell death, chondrocyte apoptosis was determined by the Annexin V/Propidium Iodide (Annexin V/PI) and TUNEL assays and necrosis by LDH release. Annexin V/PI and TUNEL data are expressed as the percentage of positive cells and LDH release as optical density (OD) at 490nm. All results are the average of at least 9 experiments with the standard deviation (SD) represented by the error bars.

3.3.1 The effects of SNAP on C-20/A4 cells.

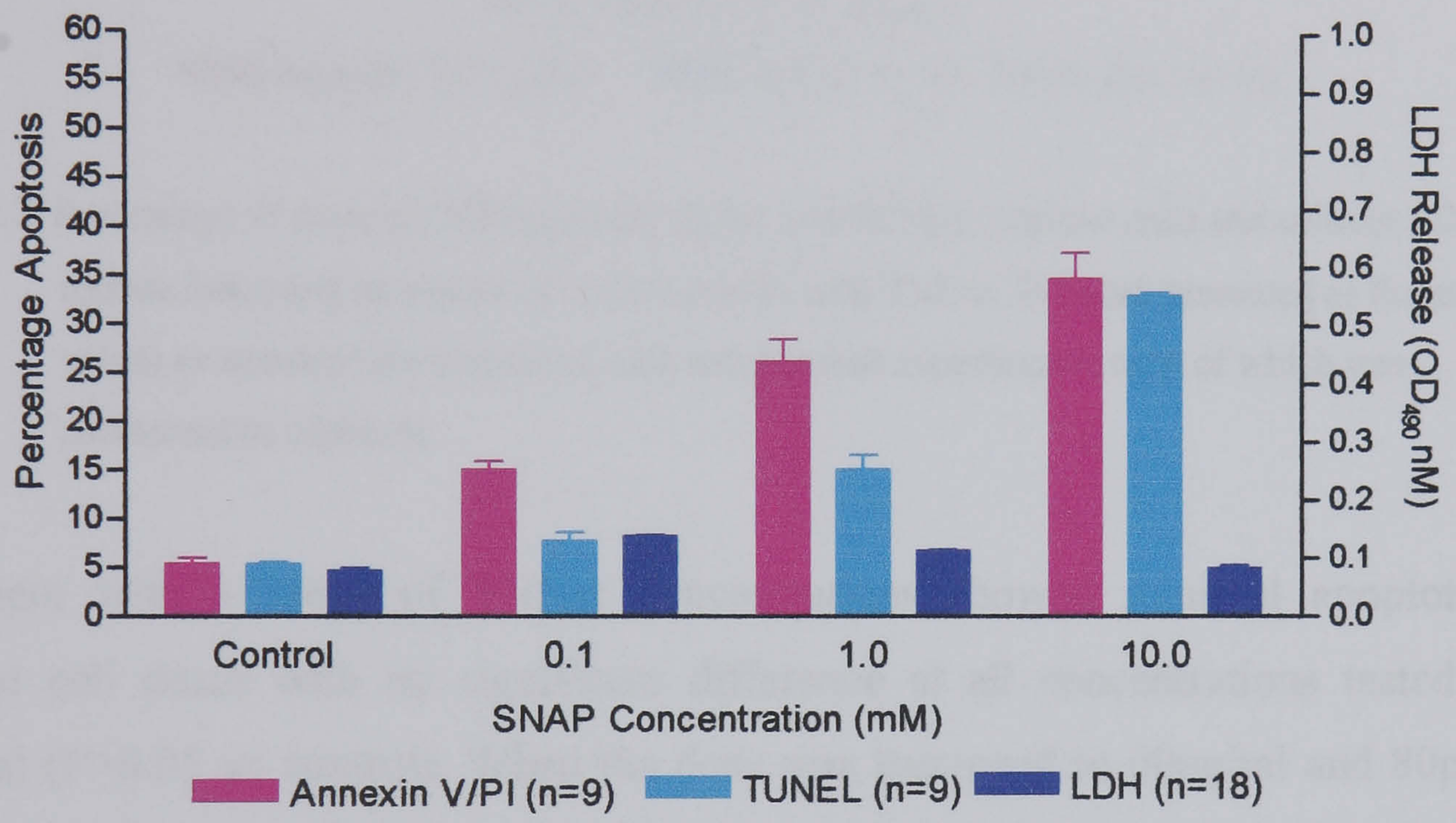

Figure 3.2: Percentage of Annexin V/Propidium Iodide and TUNEL positive cells and cellular LDH release following treatment of C-20/A4 cells with increasing SNAP concentrations. Data are presented as the mean values (± standard deviations) of nine independent experiments, each of which was performed in triplicate.

Treatment with 0.1mM SNAP showed a minimal but significant increase in the level of Annexin V/PI staining ($P<0.05$ vs control), but the increase in TUNEL positivity was not significant ($P>0.05$ vs control). As the dose of SNAP increased, apoptotic levels increased also, whilst necrotic cell death was unchanged from control levels. At 1mM SNAP a significant increase in apoptosis was also observed (26% Annexin V/PI and 15% TUNEL positive cells) ($P<0.001$ vs control), with a further increase observed at 10mM SNAP (35% Annexin V/PI and 33% TUNEL positive cells) ($P<0.001$ vs control). No significant difference in necrotic levels were observed through out the experiments (One way ANOVA, Bonferroni's correction, all P values >0.05).

3.3.2 The effects of TNF-α on C-20/A4 cells

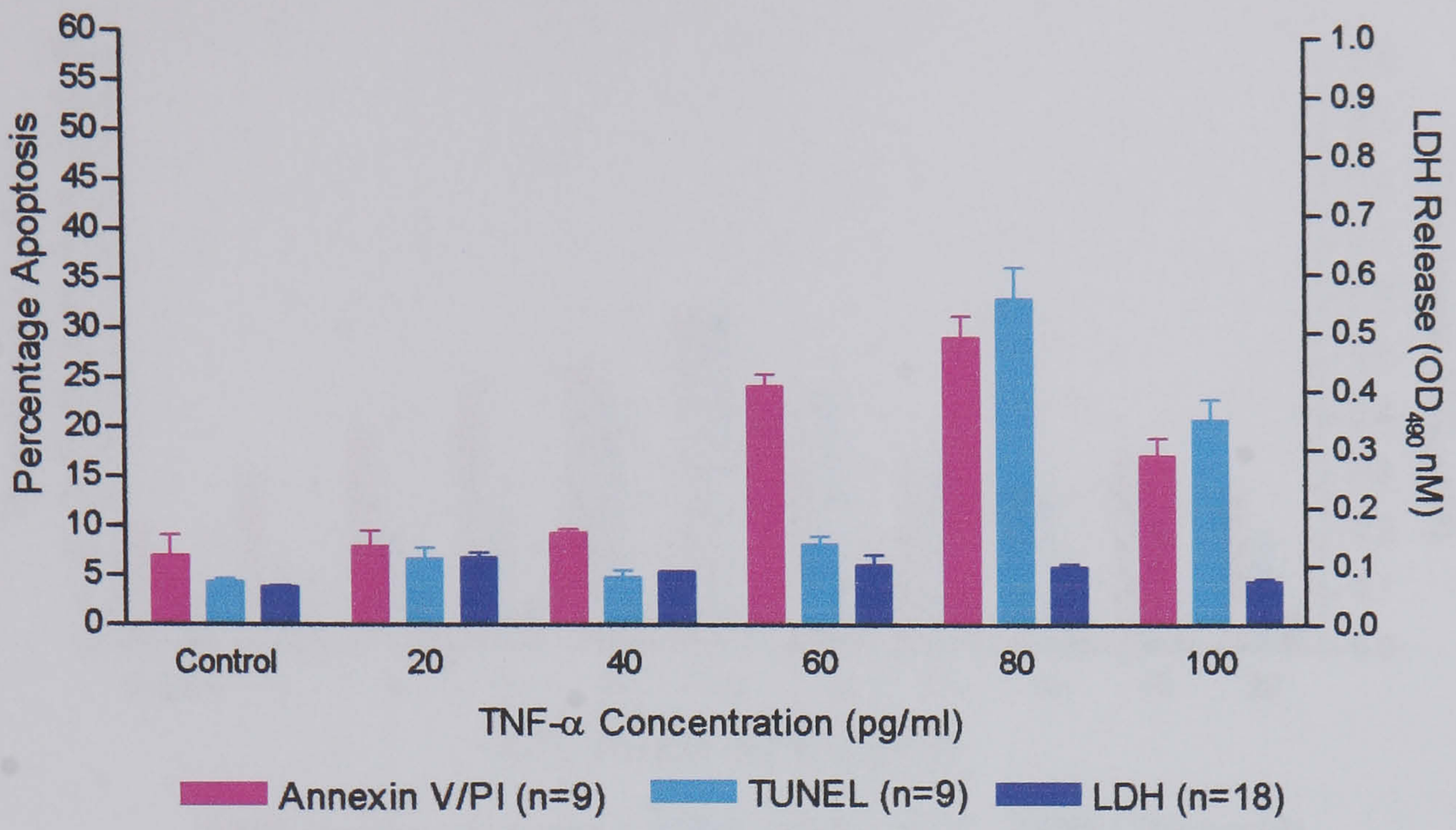

Figure 3.3: Percentage of Annexin V/Propidium Iodide and TUNEL positive cells and cellular LDH release following treatment of C-20/A4 cells with TNF-α. Data are presented as the mean values (± standard deviations) of nine independent experiments, each of which was performed in triplicate.

Treatment with a range of TNF-α concentrations showed minimal apoptotic and necrotic cell death with no significant difference at all concentrations tested up to 40pg/ml ($P>0.05$ vs control). When the dose was increased to 60pg/ml and 80pg/ml a significant increase in C-20/A4 chondrocyte apoptosis was observed in TUNEL stained cells ($P<0.001$, 60pg/ml vs 80pg/ml), but not Annexin V/PI stained cells ($P>0.05$, 60pg/ml vs 80pg/ml). At greater concentrations (100pg/ml) a significantly decreased level of apoptosis was observed ($P<0.05$ 80pg/ml vs 100pg/ml) but this was still significantly greater than the control ($P<0.001$). LDH release (necrosis) remained minimal throughout and was not significantly different from the control at any concentrations tested ($P>0.05$).

3.3.3 The effects of IL-1β on C-20/A4 cells

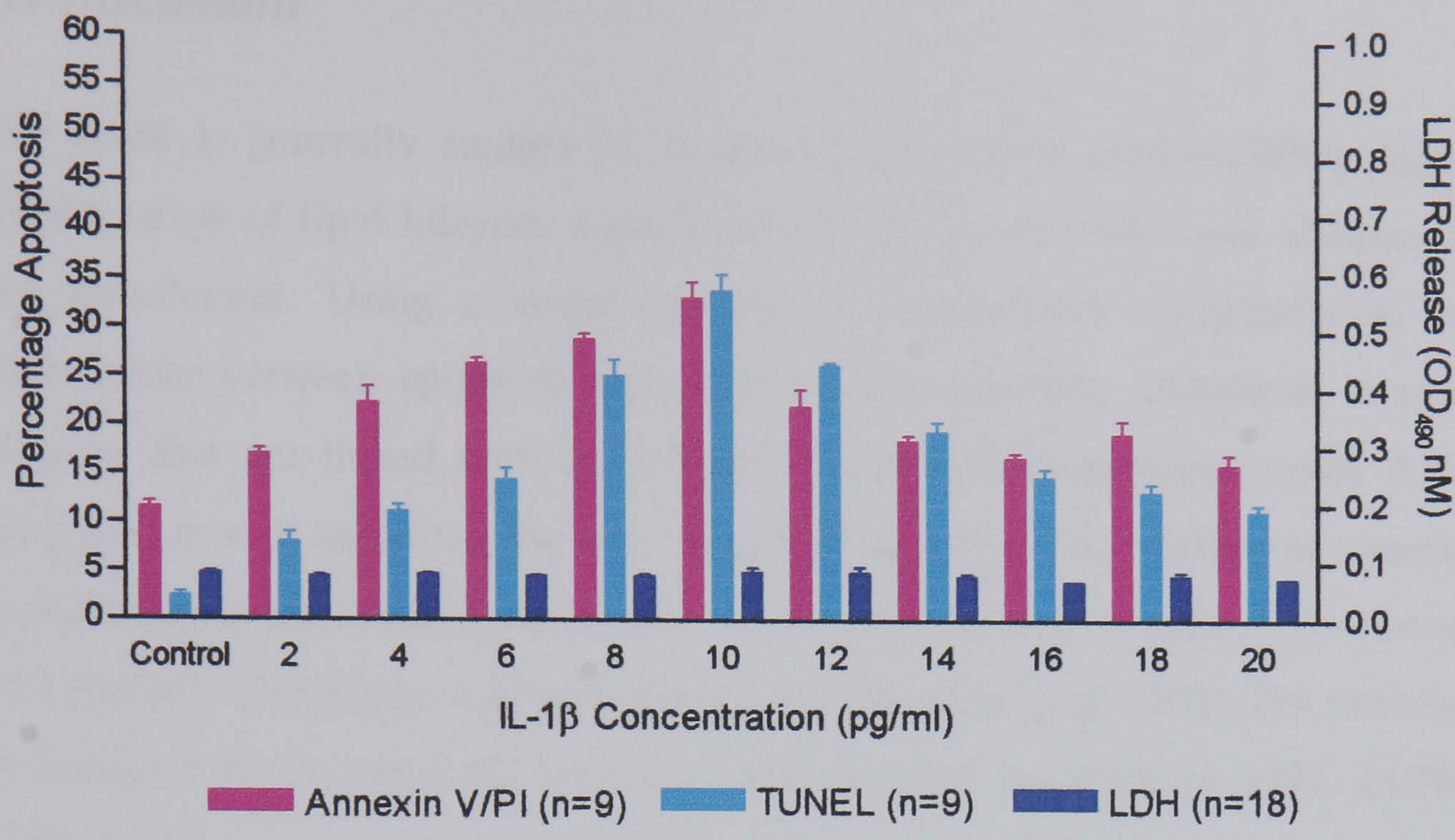

Figure 3.4: Percentage of Annexin V/Propidium Iodide and TUNEL positive cells and cellular LDH release following treatment of C-20/A4 cells with IL-1β. Data are presented as the mean values (± standard deviations) of nine independent experiments, each of which was performed in triplicate.

Treatment with various concentrations of IL-1β showed a significant increase in Annexin V/PI assay positive cells up to 10pg/ml ($P<0.001$ vs control). The TUNEL assay also showed significant increases but these were small up to 6pg/ml (22% Annexin V/PI and 11% TUNEL) ($P<0.001$ vs control). As the dose increased between 6-10pg/ml a significantly higher level of TUNEL positivity was observed with each increase when compared to the previous concentration ($P<0.001$). At greater concentrations between 12-20pg/ml a significant decrease occurred up to 16pg/ml in both Annexin V/PI and TUNEL positive cells ($P<0.001$) after which no further significant reduction was demonstrated. Necrotic cell death remained minimal with increasing concentrations of IL-1β and were not significantly different from the control ($P>0.05$).

3.4 Discussion

Cell death is generally studied by measuring parameters such as DNA degradation, disintegration of lipid bilayers, mitochondrial activity or, in the case of adherent cells, cell detachment. Using a single technique is sometimes insufficient to correctly differentiate between apoptosis and necrosis. For example, alterations in membrane integrity that are linked with the release of cytosolic components occur during late apoptosis as well as during the early stages of necrosis. The binding of Annexin V to phosphatidylserine residues can be seen in apoptotic as well as necrotic or oncotic cells with partially disintegrated plasma membranes (Lecoeur *et al*, 2001). For this reason the chondrocyte death measured here has been assessed by Annexin V/PI, TUNEL and LDH release.

A decline in cartilage deposition and in chondrocyte numbers are hallmarks of OA. Blanco *et al*, (1998) reported that changes in OA cartilage lesions are directly related to *in situ* apoptosis and indeed apoptosis has been suggested to be one of the mechanisms for increased level of cell death in ageing and osteoarthritic cartilage (Stockwell, 1991; Loeser and Shakoor, 2003; Blanco *et al*, 2004). There are many mediators that will induce apoptosis in chondrocyte cultures, however very few are likely to be physiologically significant *in vivo* (Goggs *et al*, 2003). The mediators that may be significant in OA include NO (Blanco *et al*, 1995), TNF-α (Rath and Aggarwal, 1999) fas L (CD95L) (Hashimoto *et al*, 1997) and IL-1β (Pelletier *et al*, 1999).

Nitric oxide (NO), TNF-α and IL-1β are all present in osteoarthritic cartilage and may be important mediators involved in osteoarthritis (Archer *et al*, 1994). NO in particular is produced in large amounts in osteoarthritic cartilage when compared with the normal state, both spontaneously and in proinflammatory cytokine-stimulated conditions. TNF-α, IL-1β, IL-6, IL-17 have been found in the middle or deep layers of the cartilage, suggesting that the chondrocytes themselves may produce them and NOS II/iNOS is expressed by a variety of cells, including chondrocytes, following exposure to cytokines like TNF-α and IL-1β. NOS II is a high output enzyme capable of generating elevated, sustained levels of NO which is known to contribute to chondrocyte death in two ways either by directly inducing apoptosis or promoting necrosis (Spina *et al*, 1996).

This study examined the effects of NO, TNF-α and IL-1β exposure on apoptosis and necrosis levels in monolayer culture of a human chondrocyte cell line (C-20/A4). The data presented here shows that all three of these major mediators of cartilage destruction induced apoptosis in phenotypically normal cells.

Several studies have demonstrated that NO is able to induce apoptosis in a large number of cell types, which include mouse and human chondrocytes (Blanco *et al*, 1995). Hayashi *et al*, (1997) demonstrated that larger amounts of NO may be produced by superficial chondrocytes than by their deep counterparts, showing the important role of NO at the cartilage-synovial membrane interface. In order to investigate this phenomenon further, NO was delivered to cells in culture by exposing them to millimolar concentrations of an NO releasing compound (NO donor) SNAP. Chondrocytes were treated with increasing concentrations (0.1-10mM) of the stable *S*-nitrosothiol NO donor SNAP, a dose range based on preliminary, wider dose response experiments (data not shown). These concentrations were shown to be effective in this human chondrocyte cell line and demonstrated increasing levels of apoptosis. Low, but significant levels of apoptosis were observed in cells treated with 0.1mM SNAP ($P<0.05$ vs control) indicating that even the low NO levels generated by this concentration of SNAP are capable of inducing chondrocyte apoptosis. Apoptotic cell death was more significant however when 1mM and 10mM SNAP were used ($P<0.001$ vs control for both concentrations) and moreover a dose dependent increase in Annexin V/PI and TUNEL positive FITC staining was observed, as the dose increased so did the level of apoptosis. Annexin V/PI staining showed significantly higher levels of apoptotic cell death than TUNEL following treatment with 1mM SNAP (26% Annexin V/PI and 15% TUNEL), whilst at 10mM SNAP, both assays showed almost the same level of cell death (35% Annexin V/PI and 33% TUNEL). These apparent differences are due to the fact that Annexin V/PI measures both early and late apoptosis whereas TUNEL only measured late apoptosis, resulting in lower TUNEL positivity than AnnexinV/PI positivity. Necrotic cell death, however was not significantly different ($P>0.05$) throughout the experiments (as measured by low LDH leakage into the medium), indicating that SNAP/NO induces chondrocyte apoptosis only with minimal necrotic cell death. These data have demonstrated that SNAP treatment of human C-20/A4 chondrocytes induced apoptotic cell death in a dose dependent manner at SNAP concentrations between 0.1mM and 10mM (Figure 3.2). This is in agreement with the data of several authors (Blanco *et al*, 1995; Kim and Chun, 2003; Kim *et al*, 2005;

Maneiro *et al*, 2005) who demonstrated that at 1mM NO treatment of primary articular chondrocyte culture results in apoptosis and dedifferentiation. This data is also in agreement with the data of Kühn *et al*, (2004) who showed that the application of an NO donor (SNP) resulted in a dose dependent increase in chondrocyte apoptosis and was most significant above 1mM. The data presented here is also comparable to that of Borderie *et al*, (1999) who showed that the treatment of synoviocytes (cells in the synovial membrane) with 0.5mM SNAP resulted in a 20% induction of apoptosis as measured by TUNEL. The differences between the data of this study and that of Borderie *et al*, (1999) would appear to indicate that synoviocytes may be more susceptible to NO-induced apoptosis than chondrocytes.

The level of biological activity of an NO donor is dependent on the total amount of NO delivered, the rate of NO delivery, and the exposure time to NO. Once released, the probability of NO reaching a target cell is dependent on the activity of chemical species that can protect it, (e.g. superoxide dismutase) and the activity of chemical species that can scavenge it, such as O_2, superoxide, transition metals and thiols (discussed in chapter 1). In any event, various factors regulate the cytotoxicity of a NO donor, with its half life value being only one of a large number of variables (Babich and Zuckerbraun, 2001). Following these dose-response experiments it was decided that the concentration of SNAP to be used for all future experiments would be 1mM as this results in a significant induction of apoptosis that may be easily monitored for change when co-treatments are introduced. Matthews *et al*, (1996) reported at 1mM concentration, SNAP releases 60nM free NO, indicating that millimolar concentrations of pharmacological NO donors are required to generate sub-micromolar concentrations of free NO in cells. SNAP is however one of the more productive NO donors and in support of this, Kim *et al*, (2005) reported that the NO produced by SNAP is 8.9 fold higher than other NO donors.

Fernandes *et al*, (2002) showed that at certain clinical stages of OA, proinflammatory cytokines such as TNF-α and IL-1β, which are produced by activated synoviocytes and chondrocytes, are vital factors for the progression of morphological changes. TNF-α is a well characterized cytokine that mediates a wide range of cellular inflammatory responses to stress, infection, or injury. In the early stages of injury, TNF-α plays an important role in inflammation, although if the stimulus for the injury is not eliminated or the cytokine network becomes dysregulated, prolonged or excessive levels of TNF-α

result in significant inflammatory pathology and cell death. TNF-α has been shown *in vitro* to contribute to accelerated damage of articular cartilage and to amplify the inflammatory response in developing OA (Horton *et al*, 1998).

C-20/A4 chondrocytes were treated with various concentrations of TNF-α in the range of 0-100pg/ml. These concentrations were based on the work of Bellometti *et al*, (1997) who reported TNF-α levels of this magnitude in OA synovial fluid. Treatment of C-20/A4 cells with these various concentrations of TNF-α failed to reveal any significant degree of TUNEL positive cells at concentrations between 0-40pg/ml ($P>0.05$). This observation is also supported by the data from the Annexin V/PI assay which also detected low levels of apoptosis up to this dose. This would indicate that these concentrations of TNF-α are too low to induce significant cell death in these cells, although very small increases in Annexin V/PI staining indicating a possible induction of early apoptosis, were observed. These were not however significant when compared to the control ($P>0.05$). In contrast, concentrations of 60pg/ml and 80pg/ml TNF-α induced significantly high levels of apoptotic cell death (24% Annexin V/PI, 8% TUNEL and 29% Annexin V/PI, 33% TUNEL respectively) ($P<0.001$ vs control). The level of apoptotic cell death detected by the Annexin V/PI and TUNEL assays varied, however at these concentrations. At 60pg/ml, higher levels of early apoptosis (as demonstrated by Annexin V/PI binding), than late (TUNEL) were observed whereas at 80pg/ml TUNEL results are similar to Annexin V/PI indicating a higher number of apoptotic cells in the later stages of apoptosis. At 100pg/ml apoptotic levels had decreased to 17% Annexin V/PI and 21% TUNEL positive cells, and were observed as significantly different compared to chondrocytes treated at 80pg/ml ($P<0.05$). Necrotic cell death remained minimal throughout and was not significantly different to the control ($P>0.05$). Whilst these results at first appear contradictory they demonstrate a known phenomenon whereby TNF-α activity is mediated via two separate pathways, an apoptotic pathway and an anti-apoptotic pathway (Aizawa *et al*, 2001).

Whilst TNF-α is known to induce cell death via TNF-R1 binding and activation of caspase 8 it can also activate NF-κB, a ubiquitously expressed transcription factor that has been implicated in suppression of apoptosis, and promotion of cell survival/proliferation (Garg and Aggarwal, 2002). NF-κB activation usually follows the pro-apoptotic effects of TNF-α, and as TNF-α activates NF-κB in all cell types, it rarely

induces apoptosis in the absence of other pro-apoptotic stimuli. The binding of TNF-α to TNF-R1, activates TRAF-2 and TRAF-6 which then interact with MAPKKK, also known as NF-κB-inducing kinase (NIK). NIK phosphorylates IκB kinase B (IKK-B) resulting in IκB degradation and the release of NF-κB, which translocates into the nucleus and activates its target genes, some of which play a role in mediating the anti-apoptotic effect of NF-κB (Escobar *et al*, 2006). Lianxu *et al*, (2006) reported that exposure of 10ng/ml of IL-1β and TNF-α in rat cartilage significantly increased NF-κB binding, and the effect of TNF-α was greater than that of IL-1β. The authors clarified that other transcriptional factors, including signal transducer and activator of transcription (STAT)-1 and AP-1 took part provoking inflammatory factors in chondrocytes stimulated with IL-1β. The data presented here and that of Lianxu *et al*, indicates that at high concentrations TNF-α induces the NF-κB survival pathway and at lower concentrations TNF-α induces the death receptor pathway.

TNF-α may also influence chondrocyte survival by inducing chondrocyte cell surface adhesion molecule expression, of which the α1β1 integrin is the major collagen receptor that is expressed by chondrocytes (Loeser *et al*, 2000). There is evidence to suggest that the presence of matrix components such as collagen (and possibly also cell-cell contact) may provide chondrocyte survival signals as *in vitro* chondrocyte death may be prevented by the presence of collagen (Kuhn *et al*, 2004). Chondrocyte survival has also been shown by others to be dependent on integrins containing the α2, α3 or β1 subunits (Pulai *et al*, 2002). This may occur as a result of integrin initiated NF-κB activation. Integrins can activate, by tyrosine phosphorylation, many cytoskeleton-associated proteins at focal adhesion sites, including focal adhesion kinase and the src family protein tyrosine kinases. Focal adhesion kinase in particular is strongly associated with a link between integrin receptors and the activation of downstream targets including P42/P44 MAPK which in turn will activate NF-κB. C-20/A4 cells are known to have a 10-fold increased expression of β1 integrins, increased α2, α3 and highly increased α5 integrin subunit (Loeser, 2002).

Based on the data from the TNF-α experiments, it was decided that the optimum concentration for TNF-α to be used in future experiments would be 70pg/ml as a suitably elevated level of apoptosis was observed between 60-80pg/ml as indicated by the TUNEL and Annexin V/PI assays. The level of apoptosis observed at 70pg/ml TNF-α are of a suitable magnitude to allow easy detection of any changes during co-

treatment experiments. Similarly to the SNAP experiments, the dose response of chondrocytes to TNF-α has not previously been demonstrated, but these observations are supported by Meldrum *et al,* (1998) who demonstrated induction of TNF-α during simulated ischaemia-reperfusion where a level of 67 ± 3.6 pg/ml TNF-α was observed with corresponding apoptotic renal cell death. The data presented in this thesis is also supported by that of Kim *et al,* (2002) who reported that treatment of human OA chondrocytes with high concentrations of TNF-α (10ng/ml) did not result in any significant level of cell death (8.2 ± 4.3) as compared to the control (7.2 ± 2.6) when assessed by Annexin V/PI FACS. This data fits with that presented here in that higher levels of TNF-α (100pg/ml) result in decreases in apoptosis. López-Armada, (2006) also reported that at 10ng/ml TNF-α did not induce significant levels of cell death, which was measured by the 3-[4,5-dimethylthiazol-2yl] 2,5-diphenyl tetrazolium bromide (MTT) assay. Schuerwegh *et al,* (2003) demonstrated in their *in vitro* studies that 100 ng/ml TNF-α induced apoptosis (24%) of bovine chondrocytes which was measured by the TUNEL and Annexin V assays.

Interleukin-1 (IL-1) is a cytokine produced mainly by activated mononuclear phagocytes but also by OA chondrocytes, and functions in mediating host inflammatory responses and has a major catabolic effect on chondrocytes. IL-1 stimulates resorption of cartilage both *in vivo* and *in vitro* and may contribute to the pathogenesis of OA (Yasuhara *et al*, 2005). The two forms of IL-1 (α and β) bind to the same receptors and have identical biological effects. However, IL-1β is the predominant circulating isoform in humans (Bazan *et al*, 1996). IL-1β also stimulates chondrocytes and synoviocytes to generate other cytokines (TNF-α, IL-1β, IL-6, IL-8, and IFN-γ) that stimulate the inflammatory response leading to more cartilage loss. It has been shown that the gradual release of cytokines in OA, especially IL-1β and TNF-α, may be due to micro-inflammation or local involuntary damage of the cartilage (Blanco *et al*, 2004). Immunohistochemical studies of normal cartilage indicated the presence of IL-1β in a small number of chondrocytes present in the superficial layer. However, a strong positive staining for IL-1β and TNF-α is observed in the upper half of OA cartilage for both chondrocytes and the ECM.

An *in vitro* study by Verschure and Van Noorden, (1990) showed that IL-1β increases the synthesis and release of many proteases capable of breaking down the cartilage

matrix in human articular chondrocytes. This was also observed similarly in bovine articular cartilage (Tattersall *et al*, 2005). Synthesis of collagen type II (the major collagen in cartilage) is decreased after exposure to IL-1β in healthy articular cartilage, whilst synthesis of collagen types I and III is increased and proteoglycan synthesis is decreased (Goldring, 2000). All of these factors would suggest that IL-1β may mediate aspects of OA pathogenesis.

To determine whether C-20/A4 chondrocyte apoptosis is inducible by IL-1β and what form that induction may take, chondrocyte cultures were exposed to various concentrations (0-20pg/ml) also based on levels reported by Bellometti *et al*, (1997) for 6 hrs. C-20/A4 cells have been previously shown to exhibit responses to IL-1 similar to those described in primary human chondrocytes (Goldring *et al*, 1994) but no detailed study of its apoptotic effects has been made. IL-1β induced significant increases in Annexin V/PI and TUNEL positive cells up to a concentration of 10pg/ml. Cells exposed to 2pg/ml showed a significant increase in apoptosis (17% Annexin V/PI, 8% TUNEL) when compared to control treated cells ($P<0.001$), which increased further with increasing IL-1β concentration ($P<0.01$, 4pg/ml vs control and $P<0.001$, 6pg/ml vs control). A further significant increase in apoptosis compared to control cells was observed at concentrations between 8pg/ml (29% Annexin V/PI, 25% TUNEL) ($P<0.001$ vs control) and 10pg/ml (33% Annexin V/PI, 34% TUNEL) ($P<0.001$ vs control). The increase in cell death at 10pg/ml were significant when compared to 8 pg/ml with respect to TUNEL staining ($P<0.01$) but not for Annexin V/PI staining ($P>0.05$). Annexin V/PI staining was generally higher than TUNEL staining due to its increased sensitivity for early apoptosis except at 10pg/ml where they were similar. Induction of apoptosis peaked at 10pg/ml, and then decreased dose-dependently to almost control level as the dose increased up to 20pg/ml. The gradual decrease in apoptosis was observed up to 14pg/ml, after which no further significant changes were detected. Necrotic cell death (as measured by LDH release) remained low throughout.

Our experiments documented a dose dependent increase in chondrocyte apoptosis up to 10pg/ml, after which apoptotic levels decreased with high IL-1β concentrations, possibly indicating chondroprotection at higher concentrations. Oliver *et al*, (2005) have similarly demonstrated that exposure of immortalized chondrocytes to high levels of extracellular IL-1β (1ng/ml) induces a stress response that is protective against apoptosis adding support to our data. Concentration dependent IL-1β activation of

chondrocytes may be important in the context of actual concentrations of IL-1β present in normal or diseased joints. OA synovial fluid, concentrations averaging 28pg/ml have been reported (Westacott *et al*, 1990), but no information exists at present about the actual concentration of IL-1β in articular cartilage (Fan *et al*, 2005). Martel-Pelletier *et al*, (1992) reported that the levels of IL-1β receptor type I expressed in OA chondrocytes are higher than in normal chondrocytes, and Palmer *et al*, (2002) have shown that IL-1Ra (IL-1 receptor antagonist) is produced by C-20/A4 human chondrocyte cells in response to IL-1β treatment. IL-1Ra would prevent the interaction between IL-1 and its cell surface receptors, and competitively inhibit the biological effects of IL-1. The induction of this endogenous antagonist may well explain the results obtained in this research and local production of IL-1Ra might thus be part of a negative feedback mechanism initiated by these cytokines *in vivo*. Such a mechanism may exert a chondroprotective effect against IL-1 mediated cartilage lesions during physiologic and pathological processes (inflammatory and catabolic), including RA and OA.

This data disagrees with that of Schuerwegh *et al*, (2003) who showed that IL-1 induced apoptosis of bovine chondrocytes in a dose dependent manner at concentrations from 0.1-100ng/ml and Heraud *et al*, (2000) who showed that IL-1β treatment of normal human chondrocytes induced apoptosis at concentrations of 1, 3 and 10ng/ml. This may be explained however by the work of Guerne *et al*, (1994), and Fan *et al*, (2005) who showed that the response of IL-1 in primary and sub-cultured chondrocytes and chondrocyte cell lines are different in terms of TNF-α and IL-1β stimulation. The data presented in this thesis is however in agreement with these authors in so far as IL-1β treatment induced chondrocyte apoptosis and not necrosis. These data indicate that the cell type and culture conditions should be considered when interpretating data.

Similar to TNF-α, IL-1β has also been reported to prevent apoptosis in chondrocytes (Kothny-Wilkes *et al*, 1998), osteoclasts (Schmidt *et al*, 1999), and other cell types via a mechanism that probably involves activation of NF-κB (Tatsuna *et al*, 1996) and it is possible that NF-κB activation may, at least in part be responsible for the anti-apoptotic effect of IL-1β (Grutkoski *et al*, 2002). This suggests that cytokines which trigger ECM breakdown could also protect chondrocytes against apoptosis when survival promoting effects of ECM are reduced during the matrix remodeling process (Fischer *et al*, 2000).

Both IL-1β and TNF-α also appear to induce quick activation of transcription factors, such as NF-κB and AP-1, and potentiates MAP kinase phosphorylation and activation in synovial fibroblasts, although TNF-α and IL-1β bind to distinct cellular receptors (Ogura *et al*, 2005). Recently, Barchowsky *et al*, (2000) showed that IL-1β is more effective than TNF-α at inducing MMP-1 gene expression in rabbit primary synovial fibroblasts. They thought that this maybe because TNF-α is less effective than IL-1β at activating the MAPK/AP-1 pathway. Anti-apoptotic effects of IL-1β in chondrocytes by the involvement of the P38 MAPK pathway and NF-κB has also been reported by Kühn *et al*, (2000; 2003). Interestingly, Aigner *et al*, (2005) showed that IL-1β (1ng/ml) treatment of articular chondrocytes up-regulates IAP 1 which may also explain the lack of cell death at high concentrations of IL-1β.

Based on this data, the optimum concentration for IL-1β induction of apoptosis in future experiments would be 8pg/ml as maximum apoptosis was observed between 8-10pg/ml by TUNEL and Annexin V/PI staining although this data also represents a full study of the dose response of human C-20/A4 chondrocytes to a range of IL-1β concentrations not previously documented.

Based on the data in this chapter, it is reported that apoptosis is the major form of cell death in C-20/A4 human chondrocytes treated with SNAP (NO), TNF-α and IL-1β as shown by two independent parameters, Annexin V/PI binding and DNA fragmentation, which reflect early and late phases of programmed cell death. None of these stimuli, at the concentrations tested, induce significant levels of necrosis. The optimum concentrations of SNAP, TNF-α and IL-1β for use in subsequent experiments detailed in this thesis were determined to be 1mM, 70pg/ml and 8pg/ml respectively. IL-1β, will not, however be investigated further in these studies, largely due to time constraints. It is also expected that there would be similarities in the mode of action of these two stimuli, indeed Fischer *et al*, (2000) suggest that TNF-α, and IL-1β act through a common cell death pathway in human articular chondrocytes. The rest of this study will therefore concentrate on the role of NO and TNF-α in chondrocyte cell death and the survival factors which may counter these stimuli.

CHAPTER 4

THE PROTECTIVE ROLE OF UCN IN C-20/A4 CHONDROCYTE

4.1 Introduction

In order to study further the involvement of chondrocyte death in OA, along with possible endogenous mechanisms that may be manipulated to reduce/prevent that death, the role of UCN in chondrocytes has been investigated. Production of UCN has been shown in other cell types (Brar *et al*, 1999; Latchman, 2002; Lawrence *et al*, 2005) and has been recognized as a cytoprotective peptide inhibiting apoptotic cell death (Brar *et al*, 2002; Chanalaris *et al*, 2003), as discussed in more detail in chapter 1. It is therefore possible that such a mechanism may also exist in chondrocytes. If so, this may represent an endogenous mechanism for preventing chondrocyte death and perhaps therefore an opportunity for therapeutic intervention to prevent/ameliorate disease progression in OA.

Studies were first conducted to determine if UCN is endogenously produced by chondrocytes (using the RT-PCR technique documented in section 2.2.3.1) and then the effects of various stimuli on the level of UCN production were investigated. The optimum concentrations of SNAP and TNF-α established in chapter 3 were used to treat C-20/A4 cells both alone, and in the presence of the CRH antagonist α helical $CRH_{(9-41)}$, to determine the role of endogenously produced UCN. These experiments were supplemented with UCN depletion studies and then extended with the addition of exogenous UCN.

4.2 Methods

4.2.1 The endogenous production of UCN by C-20/A4 chondrocytes

4.2.1.1 Optimisation of PCR conditions

Initial RT-PCR experiments, using published primer sequences and conditions, proved unreliable for the experiments performed here with the C-20/A4 chondrocyte cell line. Following the determination of initial PCR conditions by empirical means, it was therefore deemed necessary to further optimize annealing temperature, cycle number and magnesium content of the reaction mixture. For each pair of primers, PCR was performed at various annealing temperatures either side of the calculated average melting point of the two primers. The mean melting temperatures were calculated as 64°C for all primer pairs used (UCN, GAPDH and β-actin) and the Eppendorf master cycler gradient PCR machine was set as follows (Table 4.1):

Table 4.1: PCR programme for establishing the annealing temperature for UCN, GAPDH and β-actin

Stage	Annealing Temperature (°C)	Time (mins)	Cycle
Initial Denaturation	94°C	3	1
Denaturation	94°C	1	30
Annealing	54°C-74°C	1	30
Extension	72°C	1	30
Final Extension	72°C	10	1

30 cycles were employed for the temperature gradient studies and after establishing the optimum annealing temperatures for UCN, GAPDH and β-actin primers, multiple PCR reactions were performed to establish the optimum cycle number for each set of primers. In order to establish the number of amplification cycles necessary to detect basal levels of UCN expression, PCR experiments were performed at the optimal annealing temperature for 20-40 cycles and the intensity of the resulting product band was analysed by densitometry following 2% agarose gel electrophoresis. This was repeated for all three target nucleotide sequences.

Once the optimum annealing temperature and cycle number were established for each target sequence, PCR's were performed under these conditions with varying $MgCl_2$ concentrations (1-5mM) to establish the optimum Mg^{2+} concentration to be used in future PCR experiments. The final PCR conditions used for all subsequent experiments are shown in table 4.2 below (collated from data presented in section 4.3.1).

4.2.1.2 RT-PCR analysis of UCN expression by C-20/A4 cells following treatment with pro-apoptotic stimuli

C-20/A4 cells grown in 6 well tissue culture plates were treated with the pro-apoptotic stimuli SNAP (NO donor) and TNF-α for six hours at concentrations of 1mM and 70pg/ml respectively (based on the data documented in chapter 3). Cells were also treated with 10^{-8}M α helical CRH for 6 hours (similarly determined as the optimum concentration for use, described later in this chapter). Once these treatments were complete, the media were removed and cellular RNA extracted and processed for RT-PCR as documented in chapter 2 section 2.2.3.1.1. The cDNA generated from treated and control cells was then used to perform PCR to determine the expression of UCN and the 'house keeping genes' β-actin and GAPDH using the conditions detailed in Table 4.2. These results were further confirmed by real time PCR as detailed in chapter 2, section 2.2.3.2.

Table 4.2: PCR program for the amplification for UCN, GAPDH and β-actin

Gene	Time (minutes)	Annealing Temperature	Cycle	Mg^{2+} Concentration
UCN	1	64°C	33	1mM
GAPDH	1	58°C	30	1mM
β-actin	1	63°C	32	1mM

4.2.1.3 Real-time PCR analysis of UCN expression by C-20/A4 cells following treatment with pro-apoptotic stimuli

Real time PCR amplification for UCN and GAPDH was performed as detailed in section 2.2.3.2.1 using the following ABI 'Assay-on-Demand' primer and probe combinations for UCN (HS0017020-ml) and for GAPDH (HS99999905-ml).

4.2.1.4 Purification of PCR products.

The PCR products generated were purified using the Spin Prep™ PCR clean up kit (Novagen, U.K.) according to the manufacturer's instructions. Briefly, 40µl of each of the completed PCR reactions was transferred to a clean 1.5ml microcentrifuge tube, and 400µl of Spin Prep bind buffer added. This was vortexed, transferred to a Spin Prep PCR filter in a 2ml receiver tube and centrifuged at 10,000 x g for 1 minute. Following centrifugation, the filtrate in the receiver tube was discarded, a further 400µl of Spin Prep bind buffer added, and the unit centrifuged again at 10,000 x g for 1 minute. The filtrate was again discarded and 500µl of reconstituted Spin Prep wash buffer was added. Following a further centrifugation step (10,000 g for 1 minute) the supernatant was discarded and the spin unit centrifuged again at 10,000 x g for 2 minutes to remove residual Spin Prep wash buffer. The Spin Prep filter was then transferred to a 1.5ml Eluate receiver tube, a volume of 50µl of pre-warmed (70°C) Spin Prep Elute buffer added onto the Spin Prep filter membrane, the cap closed and the unit incubated for 3 mins at 65°C. After the incubation period, the tube was immediately centrifuged for 1 minute to collect the eluted PCR product. A recovery of 60-90% of the input material is typical for this method.

4.2.1.5 Sequencing of purified PCR samples

Representative PCR products for each target nucleotide sequence (UCN, GAPDH and β-actin) were purified as documented in 4.2.1.4 and sent to The John Innes Centre, Norwich, U.K. for sequencing. Sequencing was performed using a standard automated protocol on the PRISM 7000 3730 DNA analyzer. The returned sequence data were analysed using BLAST (basic local alignment search tool) nucleic acid database searches from the National Centre for Biotechnology Information (www.ncbi.nlm.nih.gov/BLAST/).

4.2.2 CRH antagonist studies

4.2.2.1 The effects of α helical $CRH_{(9-41)}$ on C-20/A4 cells

C-20/A4 cells were serum starved in 1% FCS media for 24 hours (as detailed in section 2.2.1.1) then treated with various concentrations of α helical $CRH_{(9-41)}$ (10^{-6} - 10^{-12}M) for 6 hours exposure. This procedure was performed to establish if CRH receptor blockade would induce cell death and to assess if α helical $CRH_{(9-41)}$ induced cell death was dose dependent. Control experiments with untreated cells were also run alongside treated experiments.

4.2.2.2 Co-treatment of C-20/A4 cells with α helical $CRH_{(9-41)}$ and pro-apoptotic stimuli

Experiments were performed with α helical $CRH_{(9-41)}$ at a concentration of 10^{-8}M (established in section 4.2.2.1 above) along with the pro-apoptotic stimuli (SNAP or TNF-α). Cells were cultured as described previously, transferred from a 75cm^2 flask to 6 well plates, and allowed to grow to ~80% confluency. Prior to treatment, cells were cultured and starved of serum (1% FCS media) for 24 hrs, then re-supplied with 1% FCS DMEM containing the appropriate stimulus for a 6 hour exposure. Cells were treated with 1mM SNAP alone (the optimum concentration established in section 3.2), 10^{-8} α helical $CRH_{(9-41)}$ alone (the optimum established concentration in section 4.2.2.1) or SNAP and α helical $CRH_{(9-41)}$. A similar procedure was repeated for TNF-α but with the SNAP being replaced by 70pg/ml TNFα, (also established in section 3.2).

4.2.3 Endogenous UCN depletion studies

UCN specific depletion was performed by the addition of 100μg/ml rabbit anti-human UCN antibody and the effects on chondrocyte cell death compared to an isotype control, anti-human albumin antibody. Prior to experimentation, the UCN antibody and albumin antibody were first desalted (due to the presence of sodium azide) using the Sephadex G50 nick columns. Chondrocytes were starved of serum (1% FCS media) for 24 hours which is detailed in section 2.2.1.1. Chondrocytes were then treated with anti-human UCN antibody, anti-human albumin antibody, and helical $CRH_{(9-41)}$ (10^{-8}M) for a 6 hour exposure.

4.2.4 Preconditioned media studies

Prior to these experiments three types of preconditioned media were generated and designated PC, PS and PT. PC represents media in which a culture of ~80% confluent C-20/A4 cells had grown for 6 hours in the absence of any exogenous pro-apoptotic stimuli. PS represents media from ~80% confluent C-20/A4 culture that had been exposed to 1mM SNAP for 6 hours. PT represents media from an 80% confluent C-20/A4 culture that had been exposed to 70pg/ml TNF-α for 6 hours. These pre-conditioned media were then used to treat fresh cultures of C-20/A4 cells under a variety of conditions.

4.2.4.1 100% preconditioned media treatment of C-20/A4 cells

100% preconditioned media studies were performed similarly to the experiments detailed in section 4.2.2.2 but with the complete exchange of normal growth medium for the preconditioned medium (PC, PS or PT) for the duration of the experiment. The preconditioned media used was dependent on the subsequent stimulus applied to the second culture, i.e. cells treated with SNAP were cultured in PS preconditioned medium and those treated with TNF-α were cultured in PT preconditioned medium. For both stimuli a further set of cells were treated in the presence of PC pre-treated medium to act as a control

4.2.4.2 10% preconditioned media treatment of C-20/A4 cells

Preconditioned media studies were carried out corresponding to the experiments mentioned in the α helical $CRH_{(9-41)}$ studies (4.2.2.2). With the prior exchange, of normal growth medium for the 10% preconditioned medium (preconditioned (PC), pre-conditioned SNAP (PS) or preconditioned TNF-α (PT)) for the duration of the experiment. Experiments were performed as described in 4.2.4.1 where cells were grown for 6 hrs, in the presence and absence of pro-apoptotic stimuli (SNAP or TNF-α). The neat preconditioned media (PC, PS or PT) were then diluted to 10% with normal media (90%) to treat additional cell cultures.

4.2.5 Exogenous UCN studies

4.2.5.1 The effects of exogenous UCN on C-20/A4 cells.

Serum starved C-20/A4 cells were treated with human UCN at various concentrations (10^{-6} - 10^{-12}M) for a 6 hour exposure. This was performed in order to establish the optimum concentration of UCN for achieving suitable levels of cell protection. Control experiments with untreated cells were also carried out alongside treated experiments.

4.2.5.2 The competitive inhibition of exogenous UCN by α helical $CRH_{(9-41)}$

Whilst a concentration of 10^{-8}M α helical $CRH_{(9-41)}$ was used for all other experiments, a lower concentration of $5x10^{-10}$M was used here. The data presented in section 4.3.2 shows that levels of apoptosis start to increase with concentrations of α helical $CRH_{(9-41)}$ between 10^{-9}M and 10^{-10}M. $5x10^{-10}$M represents a midway point between these concentrations and was used in conjunction with various concentrations of UCN (10^{-6}M to 10^{-12}M) to determine if a competitive CRH-R binding occurred between these two peptides and to observe the effect on cell death. The procedure followed was similar to that in 4.2.5.1, but with the addition of $5x10^{-10}$M α helical $CRH_{(9-41)}$.

4.2.5.3 The effects of exogenous UCN co-treatment on C-20/A4 cells subjected to pro-apoptotic stimuli

Experiments were performed with exogenous UCN at the established concentration of 10^{-8}M alone and in conjunction with the stimuli (SNAP & TNF-α). Cultured cells were transferred from a 75cm^2 flask to 6 well plates, each plate representing each condition. Cells were treated with 1mM SNAP alone, SNAP with 10^{-8} M UCN, and SNAP, 10^{-8} M UCN and 10^{-8} M α helical $CRH_{(9-41)}$. Cells were treated as described previously in 2.2.1.1 The procedure was repeated for TNF-α with SNAP being replaced by 70pg/ml TNF-α.

4.2.5.4 The effects of exogenous UCN pre-treatment on C-20/A4 cells subjected to pro-apoptotic stimuli.

Prior to treatment, cells were cultured and starved of serum for 24 hrs, re-supplied with 1% FCS DMEM media for a 6 hour exposure. Once the optimum concentration of UCN was established to be 10^{-8} M, this concentration was then used to treat C-20/A4 cells at various time intervals prior to the addition of the pro-apoptotic stimuli. Cells were subcultured as described previously (section 2.2.1.1) and then pre-treated with UCN at 0 min, 30 min, 1 hour and 2 hour interval after which pro-apoptotic stimuli (SNAP or TNF-α) were added.

4.2.6 The effects of exogenous UCN on cell proliferation

The neutral red assay was used in these experiments to investigate any change in cell number over time following treatment with various concentrations of exogenous UCN (10^{-6}M, 10^{-8}M and 10^{-10}M). Experiments were performed as described in 2.2.1.1. A volume of 100µl of chondrocyte cell suspension was inoculated to individual wells of sterile 96 well microtitre tissue culture plates and allowed to grow to 60-70% confluency (approx. 48 hrs). At this point, the growth medium was replaced with media containing 10^{-6}M, 10^{-8}M and 10^{-10}M UCN concentrations. Sixteen replicate wells were used per concentration and half the plate (48 wells), were used as control. This procedure was repeated for time periods of 6hr, 12hr, 24hr, 48hr and 96hr. After exposure, to UCN for the appropriate time period, cell number was assessed by the NR assay as described in 2.2.2.6.1.

4.3 Results

4.3.1 The endogenous production of UCN by C-20/A4 chondrocytes

RT-PCR was used to establish the possible existence of the CRH-like peptide UCN in C-20/A4 cells. PCR conditions for UCN were first optimized with regard to annealing temperature, cycle number and magnesium (Mg^{2+}) concentration. This was also performed for the housekeeping genes β-actin and GAPDH.

4.3.1.1 Optimisation of PCR conditions for UCN amplification

4.3.1.1.1 Optimisation of annealing temperature.

Figure 4.1 shows AGE analysis of PCR products generated using an annealing temperature gradient for UCN primers. Annealing temperatures ranged from 54°C-74°C (lane 3–12) and amplification was performed for 30 cycles. UCN bands at 172 bp were observed from 54°C - 69°C, after which no bands were observed.

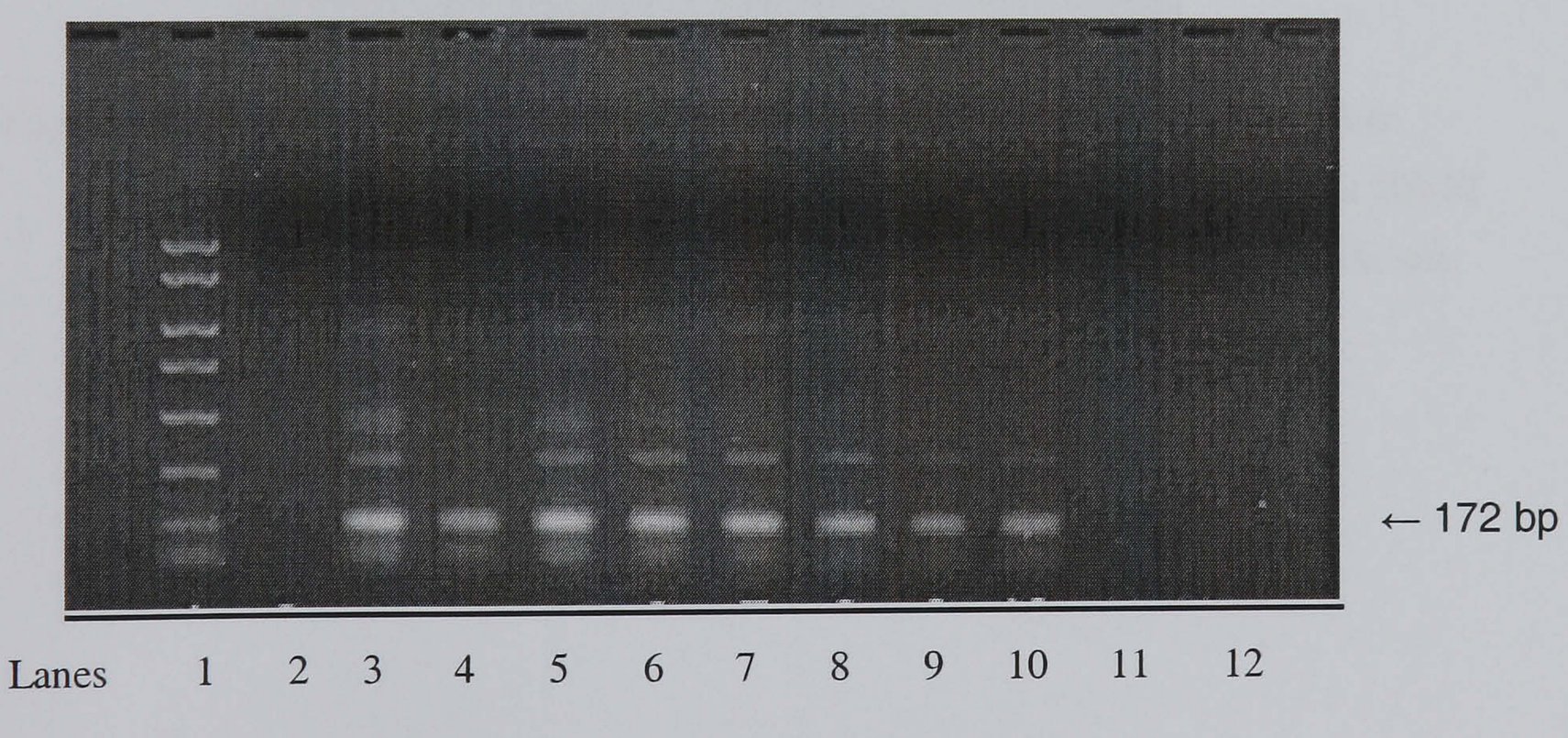

Figure 4.1: PCR annealing temperature gradient for UCN amplification.
Lane 1- 2Kb ladder (Sigma), lane 2- Negative Control, lane 3-54°C, lane 4-55°C, lane 5-56°C, lane 6-58°C, lane 7-61°C, lane 8-64°C, lane 9-66°C, lane 10-69°C, lane 11-71°C, lane 12- 74°C.

4.3.1.1.2 Optimisation of cycle number

Figure 4.2a shows AGE analysis of PCR amplification of UCN over 20-40 cycles at 64°C annealing temperature. UCN bands at 172 bp were observed from cycle 25 (lane 8) onwards with band intensity increasing with cycle number. Figure 4.2b represents the densitometry analysis of the UCN band for each cycle.

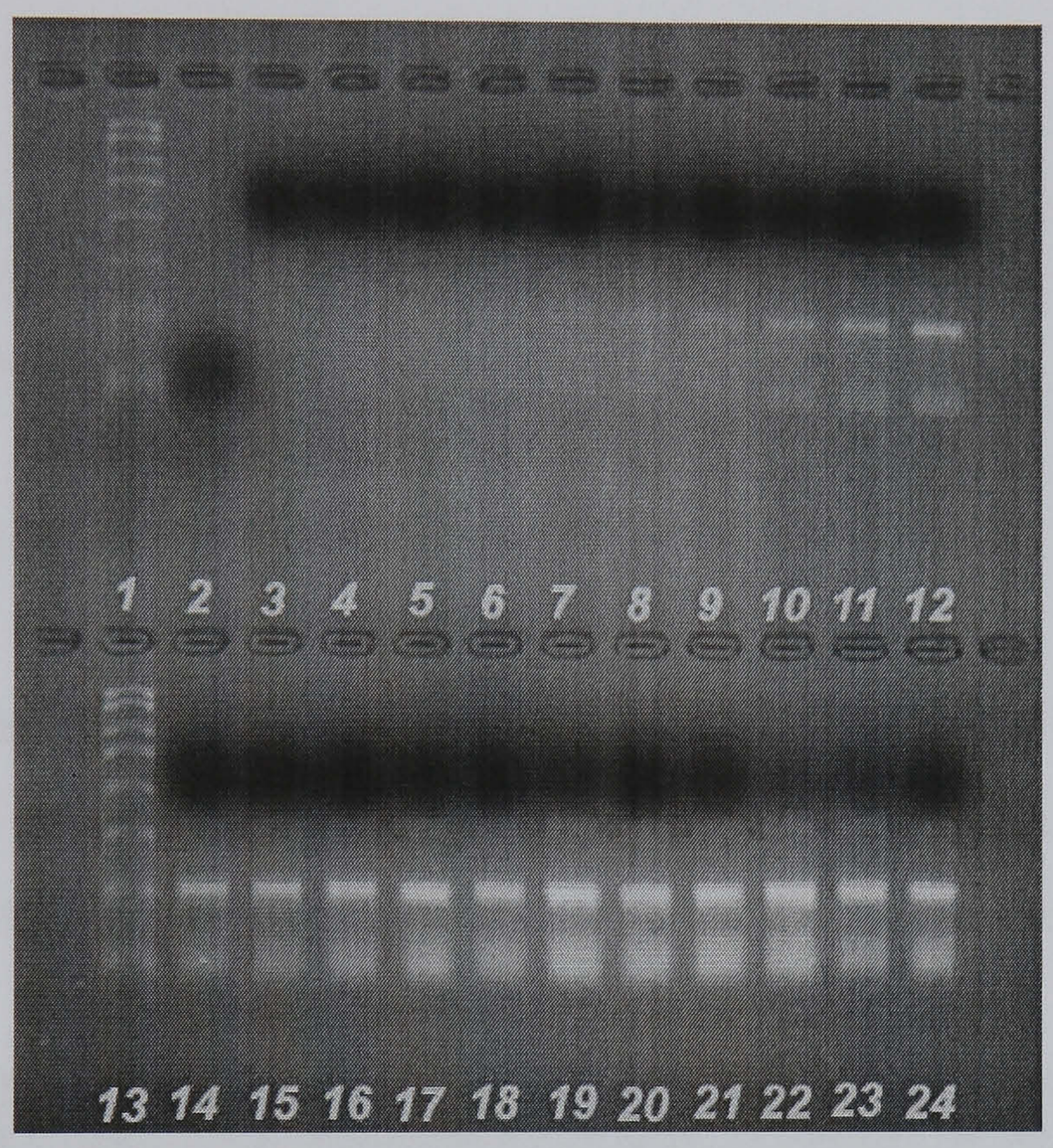

Figure 4.2a: Gel photograph depicting UCN PCR products at varying cycle number.
Lane 1- 2Kb ladder (Sigma), lane 2- Negative Control, lane 3 (cycle 20)-12 (cycle 29), lane 13-2Kb ladder (Sigma), lane 14 (cycle 30)-24 (Cycle 40).

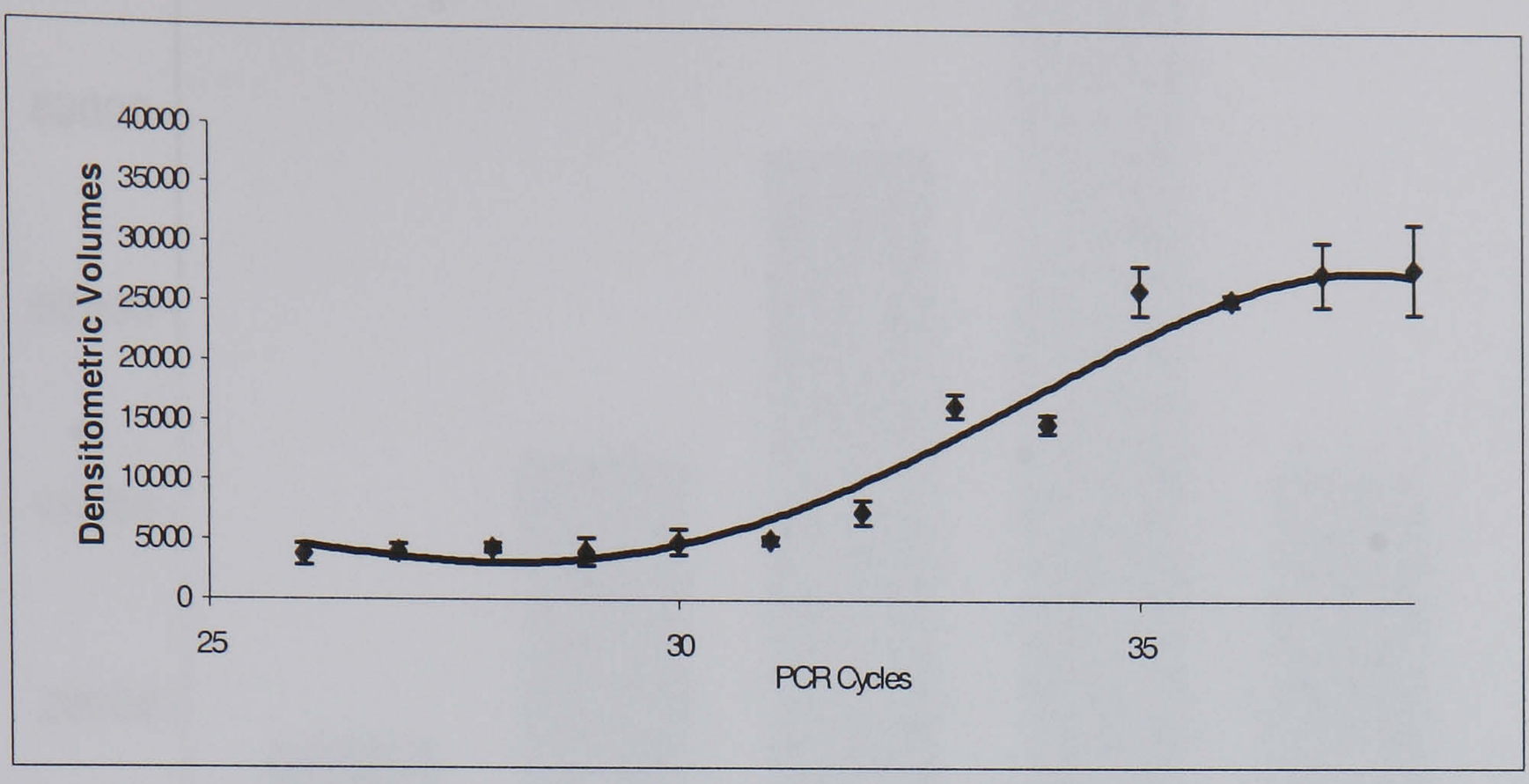

Figure 4.2b: Densitometric analysis of agarose gel electrophoresis of UCN PCR products at corresponding cycle number. Data are presented as the mean values (± standard deviations) of five independent experiments.

4.3.1.1.3 Optimisation of Mg^{2+} concentration

Figure 4.3a represents an AGE analysis of RT-PCR of UCN (at 172 bp) with 33 cycles at 64°C annealing temperature with varying magnesium concentration. Figure 4.3b represents the densitometry analysis of the UCN band for each cycle.

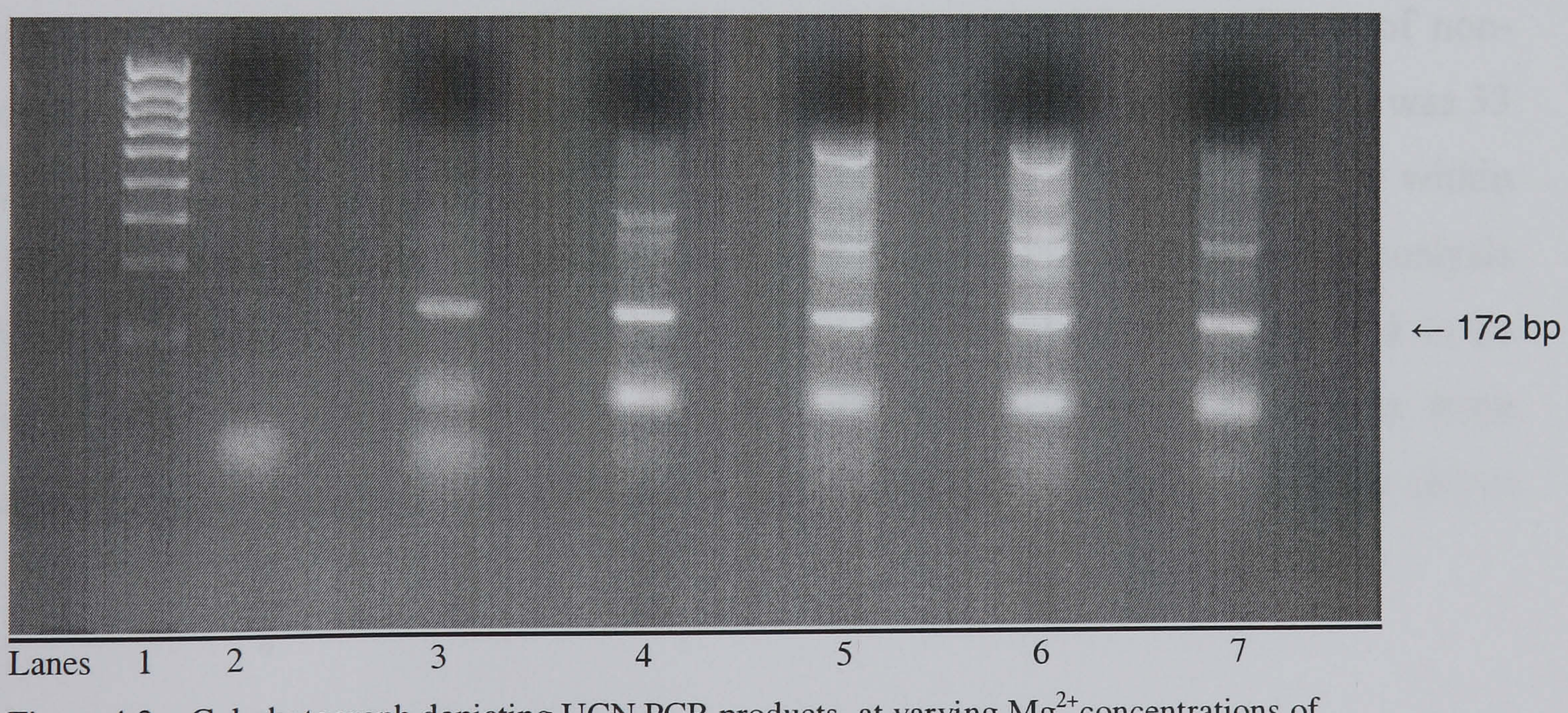

Figure 4.3a: Gel photograph depicting UCN PCR products, at varying Mg^{2+} concentrations of C-20/A4 cells. Lane 1- 1Kb ladder (Invitrogen), lane 2- Negative Control, lane 3- 1mM, lane 4- 2mM, lane 5- 3mM, lane 6- 4mM, lane 7- 5mM.

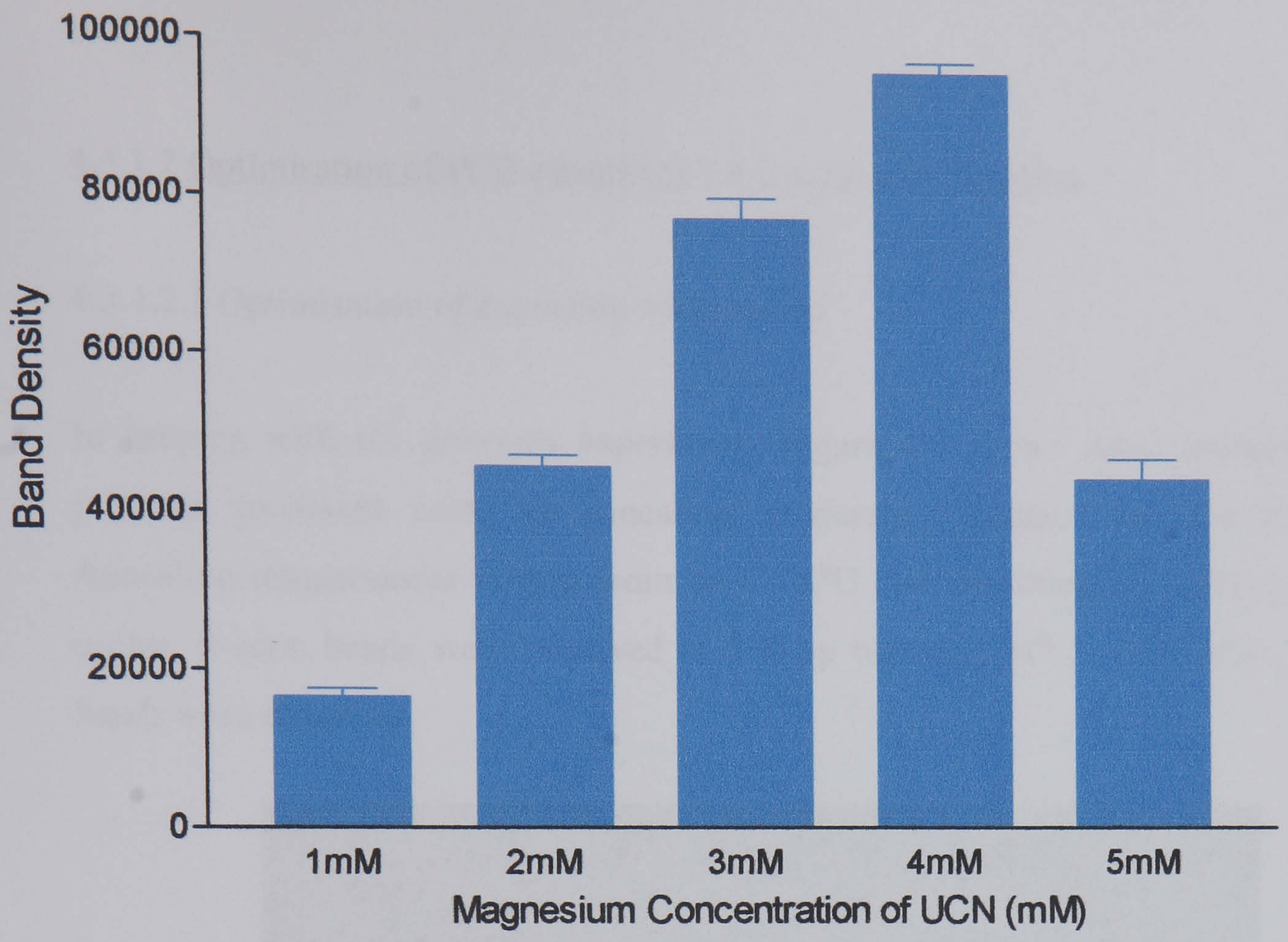

Figure 4.3b: Densitometric analysis of agarose gel electrophoresis of UCN, PCR products at varying Mg^{2+} concentrations of C-20/A4 cells. Data are presented as the mean values (± standard deviations) of three independent experiments.

Based on data obtained for the experiments documented in section 4.3.1.1, the optimum annealing temperature for the UCN primers was determined to be 64°C (as this temperature gives a good amplification of the target gene with lower levels of non-specific amplification). The optimum cycle number determined from the studies was 33 cycles as the amount of UCN product produced at this cycle number is clearly within the linear part of the amplification curve and therefore suitable for expression analysis in future experiments. The optimum magnesium concentration was determined to be 1mM for the UCN primers although higher Mg^{2+} concentrations resulted in a more intense UCN band, as multiple products were also observed at concentrations above this.

4.3.1.2 Optimisation of PCR conditions for β-actin amplification

4.3.1.2.1 Optimisation of annealing temperature

In keeping with the previous experiment, Figure 4.4 shows AGE analysis of PCR products generated using an annealing temperature gradient for β-actin primers. Annealing temperatures ranged from 54°C-74°C and amplification performed for 30 cycles. β-actin bands were observed at 532 bp between 54°C - 66°C after which no bands were observed.

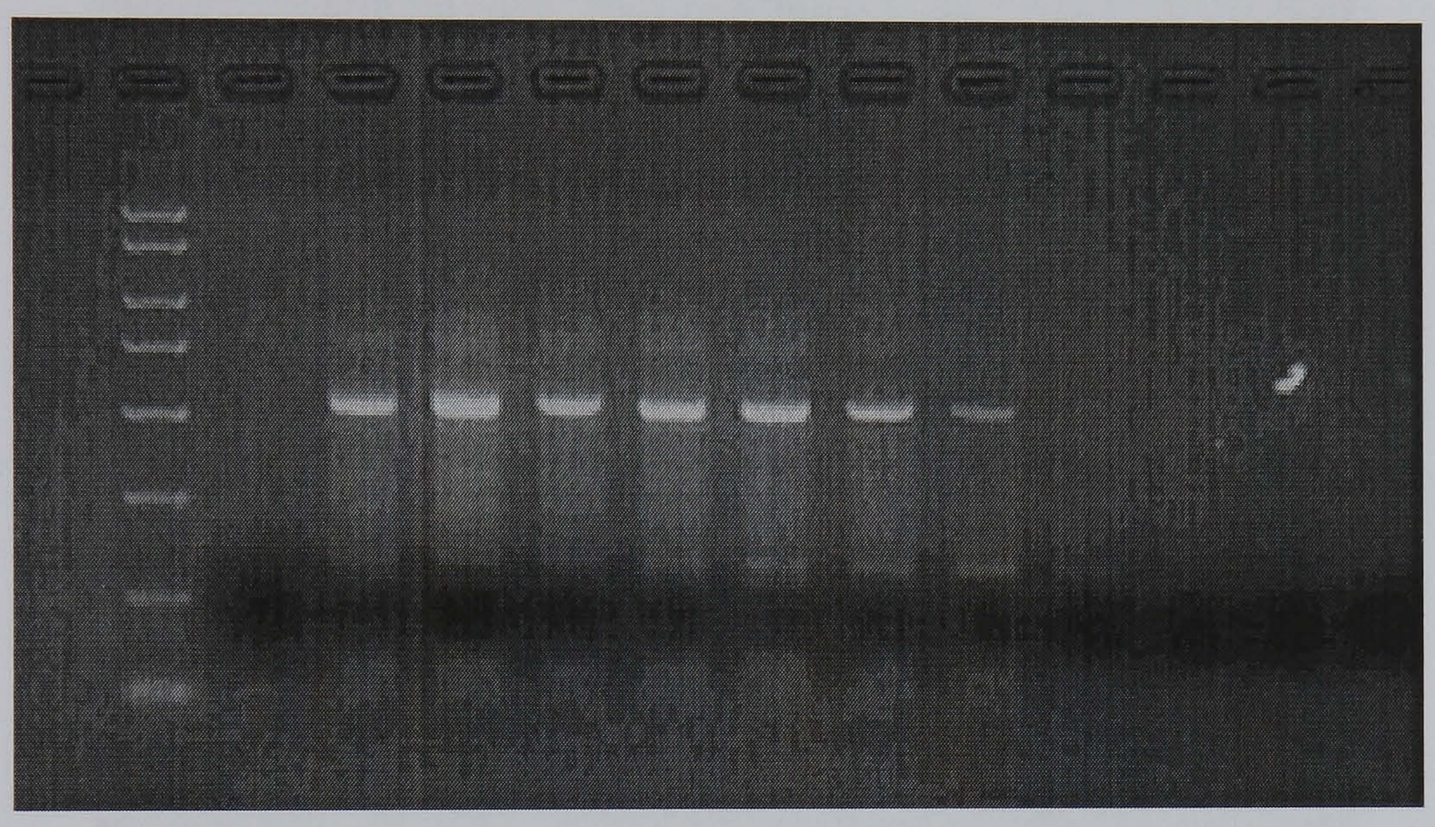

Figure 4.4: PCR annealing temperature gradient for β-actin amplification.
Lane 1- 2Kb ladder (Sigma), lane 2- Negative Control, lane 3- 54°C, lane 4- 55°C, lane 5- 56°C, lane 6- 58°C, lane 7- 61°C, lane 8- 64°C, lane 9- 66°C, lane 10-69°C, lane 11- 71°C, lane 12- 74°C.

4.3.1.2.2 Optimisation of cycle number

Again, in keeping with the previous experiments, Figure 4.5a shows AGE analysis of PCR amplification of β-actin over 20-40 cycles at 63°C annealing temperature. β-actin bands at 532 bp in length (Figure 4.5a) was observed from cycle 27 (lane 10) onwards with band intensity increasing as cycle number increased. Figure 4.5b represents the densitometry volume of each cycle.

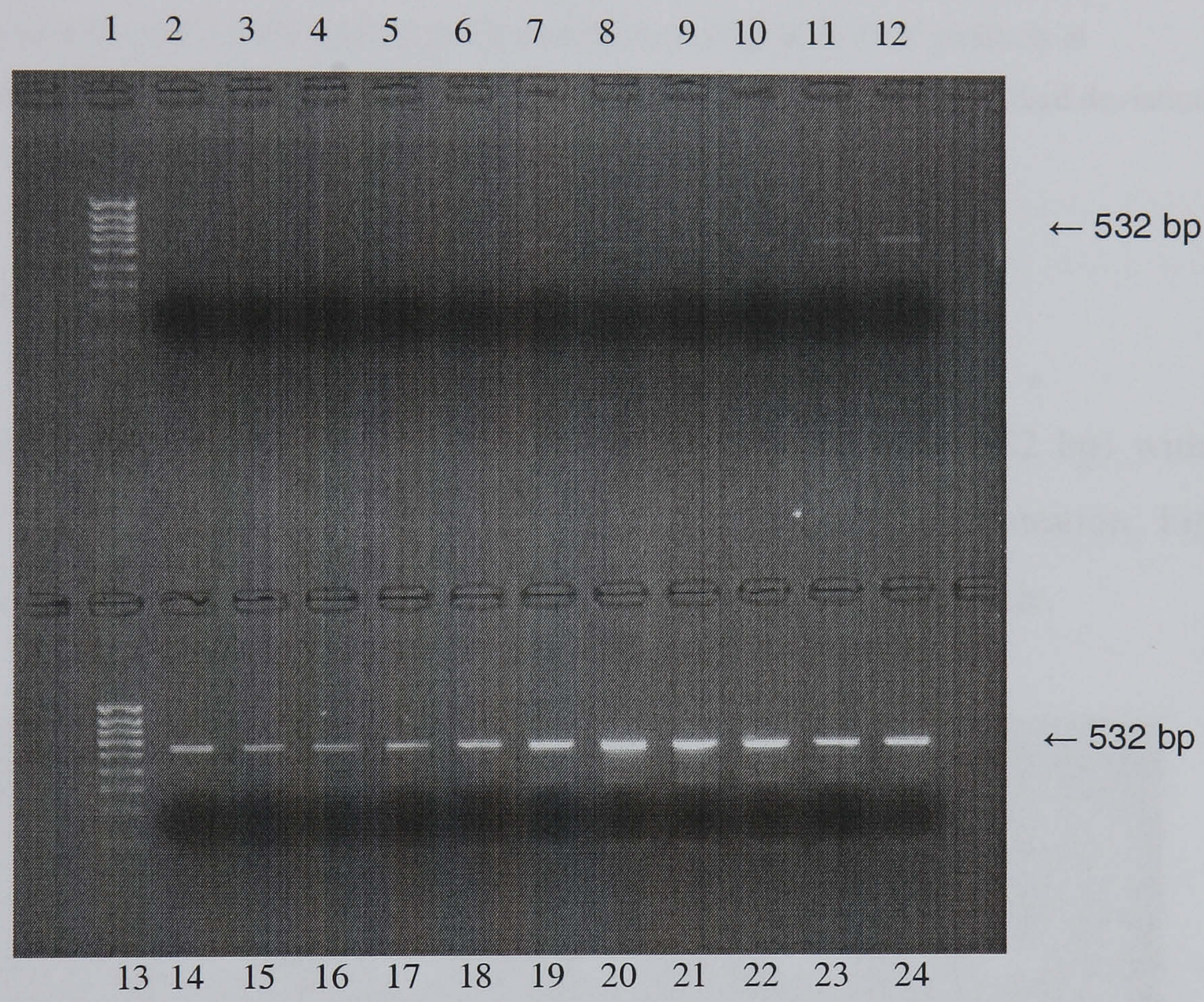

Figure 4.5a: Gel photograph depicting β-actin PCR products at varying cycle number.
Lane 1- 1Kb ladder (Sigma), lane 2- Negative Control, lane 3 (cycle 20)-12 (cycle 29), lane 13- 1Kb ladder (Sigma), lane 14 (cycle 30)-24 (Cycle 40).

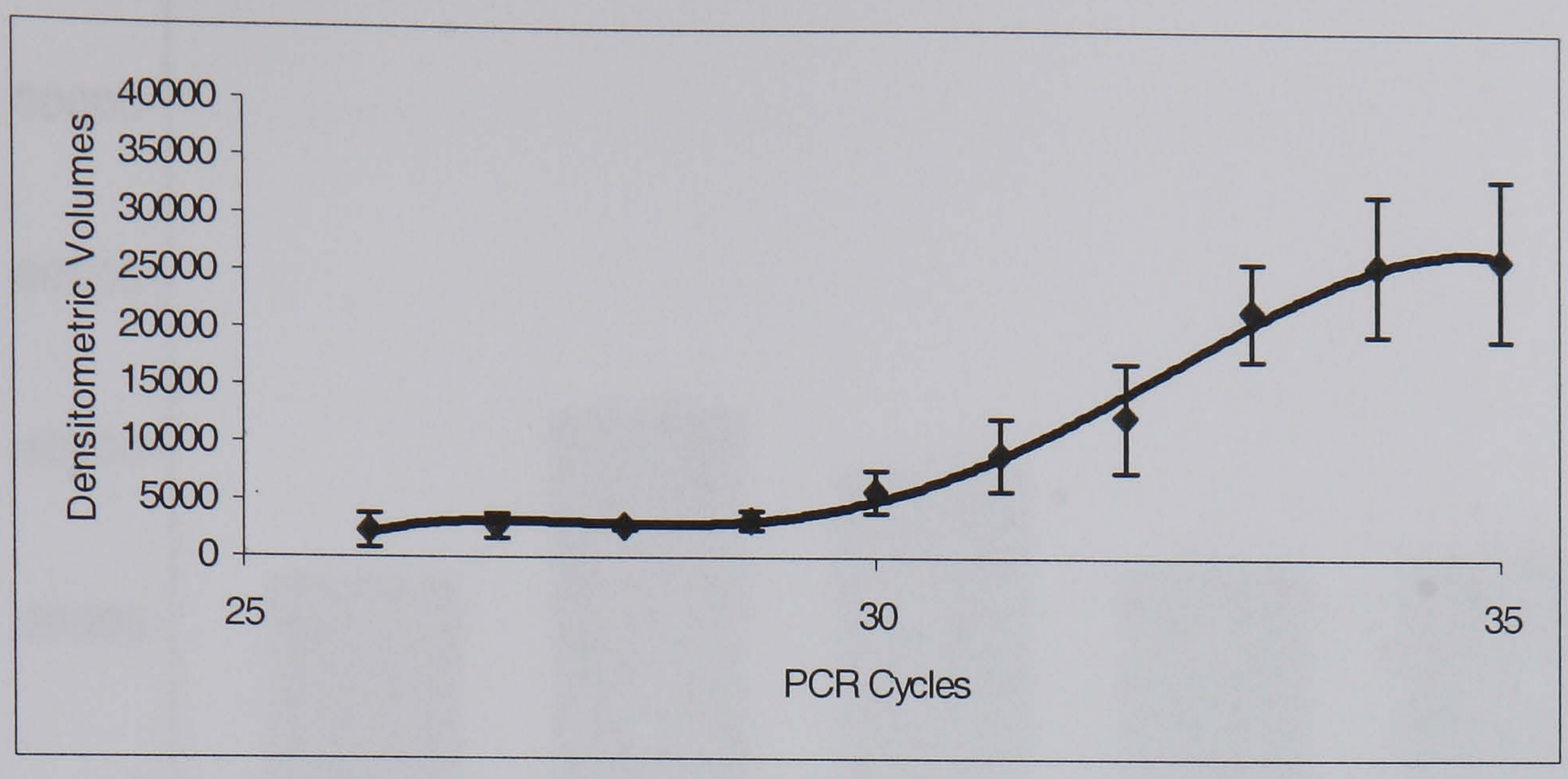

Figure 4.5b: Densitometric analysis of agarose gel electrophoresis of β-actin PCR products at corresponding cycle number. Data are presented as the mean values (± standard deviations) of five independent experiments.

4.3.1.2.3 Optimisation of Mg^{2+} concentration

Figure 4.6a represents an AGE analysis of RT-PCR of β-actin (at 532 bp) with 32 cycles at 63°C annealing temperature with varying magnesium concentration. Figure 4.6b represents the densitometry analysis of the β-actin band for each cycle.

Figure 4.6a: Gel photograph depicting β-actin PCR products, at varying Mg^{2+}concentrations of C-20/A4 cells. Lane 1- 1Kb ladder, lane 2- Negative Control, lane 3- 1mM, lane 4- 2mM, lane 5- 3mM, lane 6- 4mM, lane 7- 5mM.

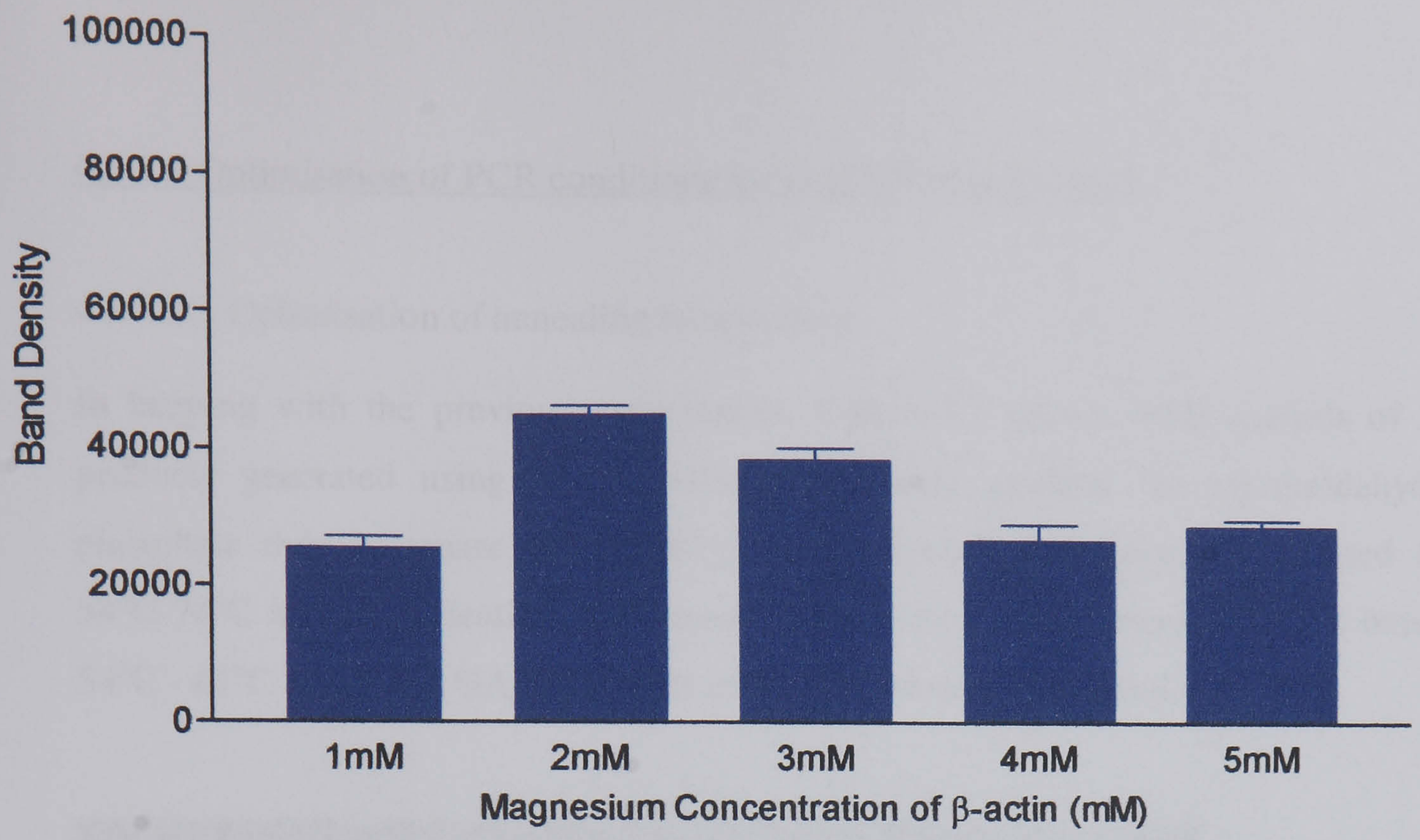

Figure 4.6b: Densitometric analysis of agarose gel electrophoresis of β-actin PCR products at varying Mg^{2+} concentrations of C-20/A4 cells. Data are presented as the mean values (± standard deviations) of three independent experiments.

Overall, from data obtained from the experiments detailed in section 4.3.1.2, the optimum annealing temperature for the β-actin primers was established to be 63°C (since this temperature provides a good amplification of the target gene with minimal contaminating bands). The optimum cycle number established from the studies was 32 cycles as the amount of β-actin product generated at this cycle number is within the linear part of the amplification curve and consequently suitable for expression analysis in future experiments. The optimum magnesium concentration established for β-actin was 1mM, because above this concentration, extra bands in the products were observed, which are not visibly clear from the gel picture.

4.3.1.3 Optimisation of PCR conditions for GAPDH amplification

4.3.1.3.1 Optimisation of annealing temperature

In keeping with the previous experiments, Figure 4.7 shows AGE analysis of PCR products generated using an annealing temperature gradient for glyceraldehyde-3-phosphate dehydrogenase (GAPDH) primers. Annealing temperatures ranged from 54°C-74°C and amplification performed for 30 cycles. Bands were observed between 54°C - 61°C at 437 bp. GAPDH bands after 61°C were not observed.

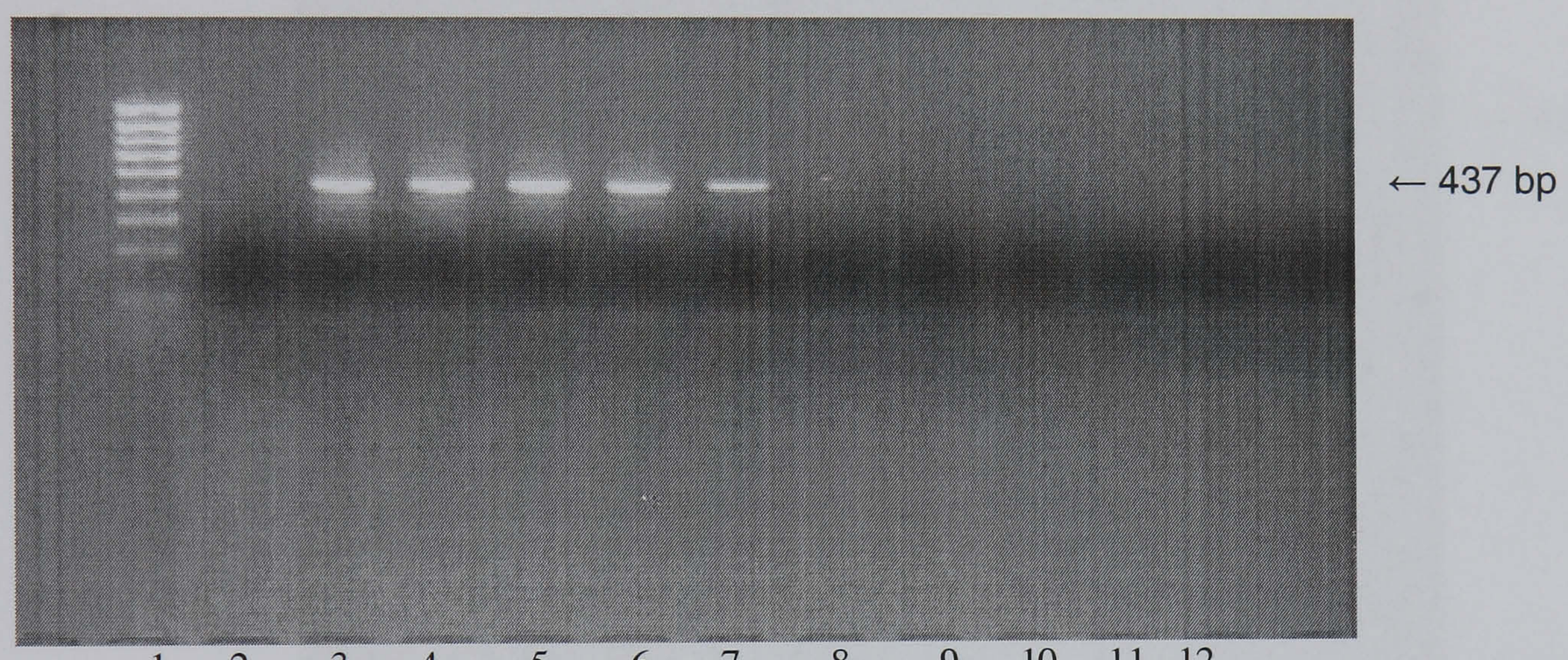

Figure 4.7: PCR annealing temperature gradient for GAPDH amplification.
Lane 1- 1Kb ladder (Invitrogen), lane 2- Negative Control, lane 3- 54°C, lane 4- 55°C, lane 5- 56°C, lane 6- 58°C, lane 7- 61°C, lane 8- 64°C, lane 9- 66°C, lane 10- 69°C, lane 11- 71°C, lane 12- 74°C.

4.3.1.3.2 Optimisation of cycle number

Again, in keeping with the previous experiments, Figure 4.8a shows AGE analysis of PCR amplification of GAPDH over 20-40 cycles at 58°C. GAPDH bands at 437 bp in length were observed from cycle 25 (lane 8) onwards with band intensity increasing as cycle number increased. Figure 4.8b represents the densitometry volume of each cycle number.

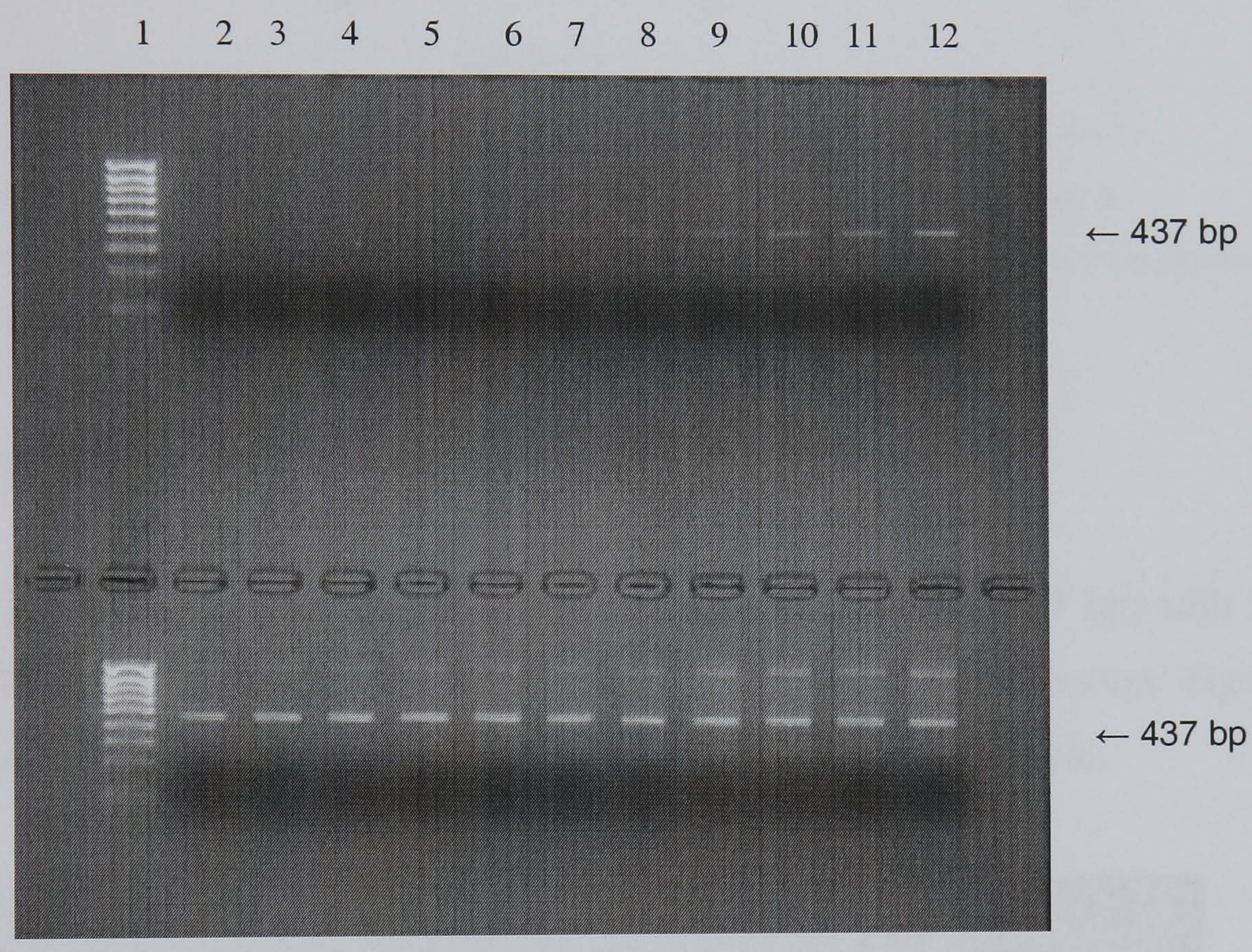

Figure 4.8a: Gel photograph depicting GAPDH PCR products at varying cycle number. Lane 1- 1Kb ladder (Invitrogen), lane 2- Negative Control, lane 3 (cycle 20)-12 (cycle 29), lane 13-1Kb ladder (Invitrogen), lane 14 (cycle 30)-24 (Cycle 40).

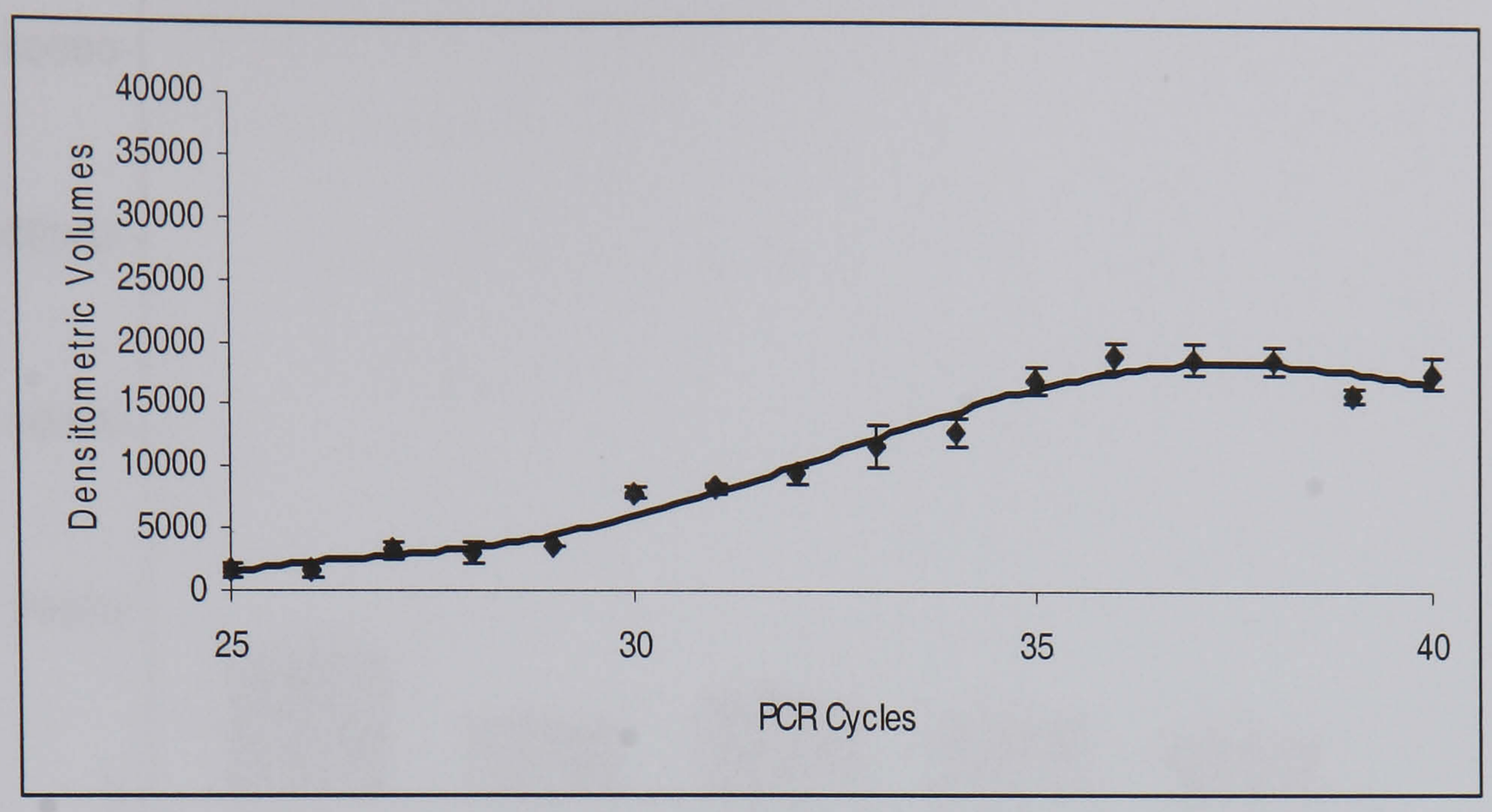

Figure 4.8b: Densitometric analysis of agarose gel electrophoresis of GAPDH PCR product at corresponding cycle number. Data are presented as the mean values (± standard deviations) of four independent experiments.

4.3.1.3.3 Optimisation of Mg^{2+} concentration

Figure 4.9a represents an AGE analysis of RT-PCR of GAPDH (at 437 bp) with 30 cycles at 58°C annealing temperature with varying magnesium concentration. Figure 4.9b represents the densitometry analysis of the GAPDH band for each cycle.

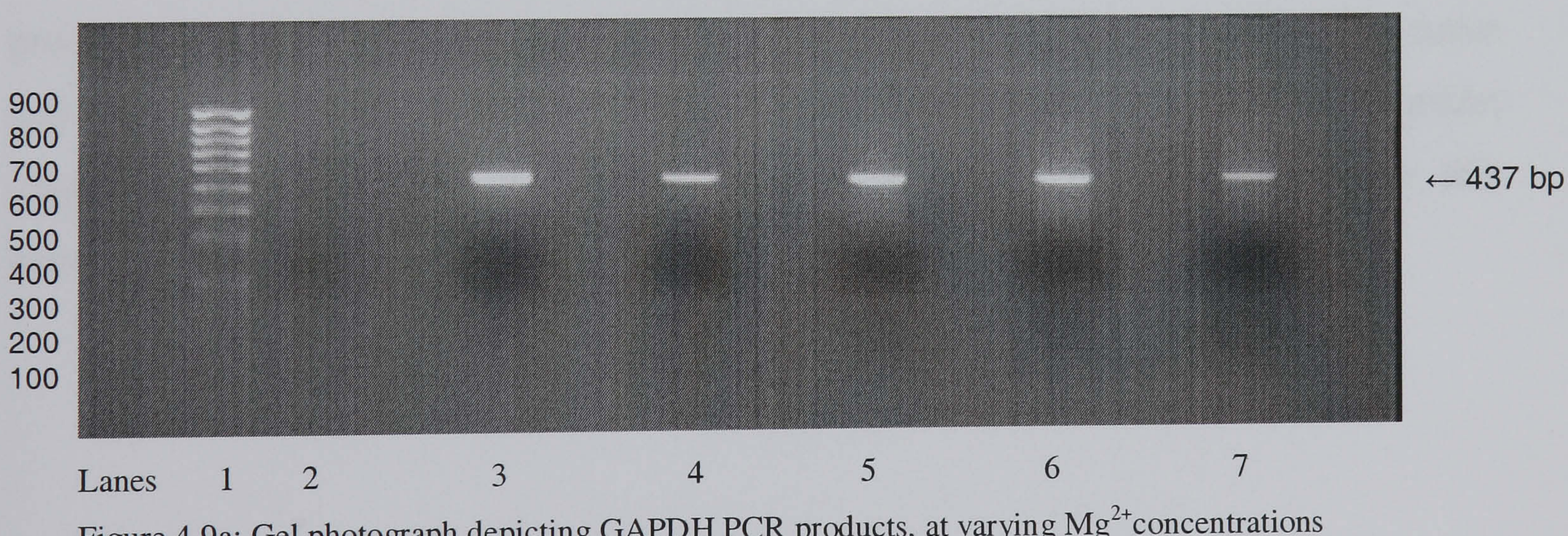

Figure 4.9a: Gel photograph depicting GAPDH PCR products, at varying Mg^{2+} concentrations of C-20/A4 cells. Lane 1- 1Kb ladder (Invitrogen), lane 2- Negative Control, lane 3- 1mM, lane 4- 2mM, lane 5- 3mM, lane 6- 4mM, lane 7- 5mM.

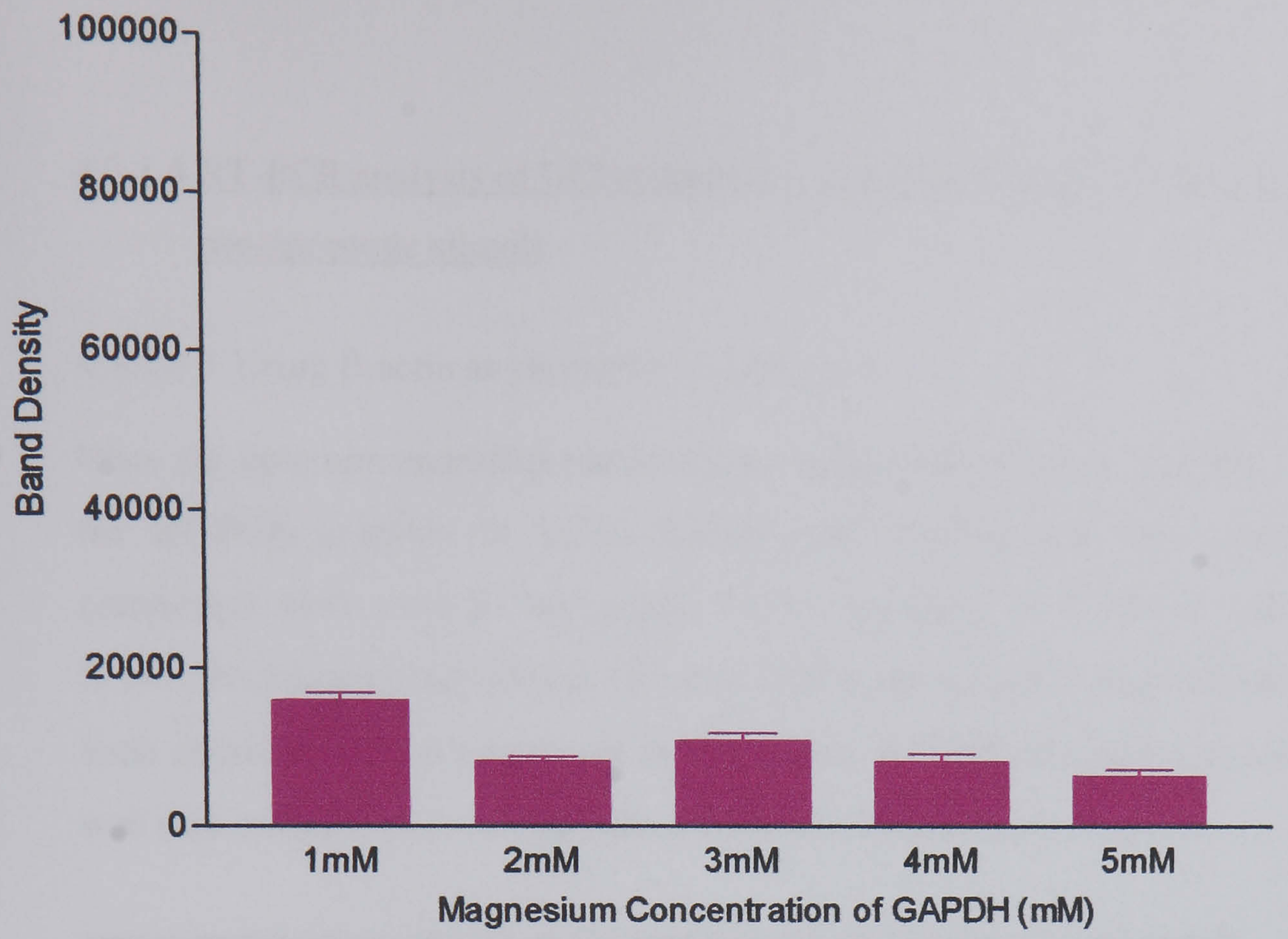

Figure 4.9b: Densitometric analysis of agarose gel electrophoresis of GAPDH PCR products at varying Mg^{2+} concentrations of C-20/A4 cells. Data are presented as the mean values (± standard deviations) of three independent experiments.

Overall, data gathered for the experiments reported in section 4.3.1.3, shows that the optimum annealing temperature for the GAPDH primers was 58°C (since this temperature provides a good amplification of the target gene). The optimum cycle number established from the studies was 30 cycles as the amount of GAPDH product produced at this cycle number is visibly within the linear part of the amplification curve and consequently suitable for expression analysis in future experiments. The optimum magnesium concentration determined for GAPDH was 1mM, because above this concentration a gradual decrease in GAPDH in the products were observed.

4.3.1.4 RT-PCR analysis of UCN expression by C-20/A4 cells following treatment with pro-apoptotic stimuli

4.3.1.4.1 Using β-actin as an internal control

Once the optimum annealing temperatures, amplification cycles and Mg^{2+} concentration for RT-PCR analysis of UCN, β-actin and GAPDH had been determined, these parameters were used to investigate UCN expression in C-20/A4 cells treated with SNAP (NO donor) and TNF-α. NO and TNF-α are both pro-apoptotic stimuli that have been demonstrated to be present in OA joints. A CRH antagonist, α helical $CRH_{(9-41)}$ was also included to investigate the effects of CRH receptor blockade.

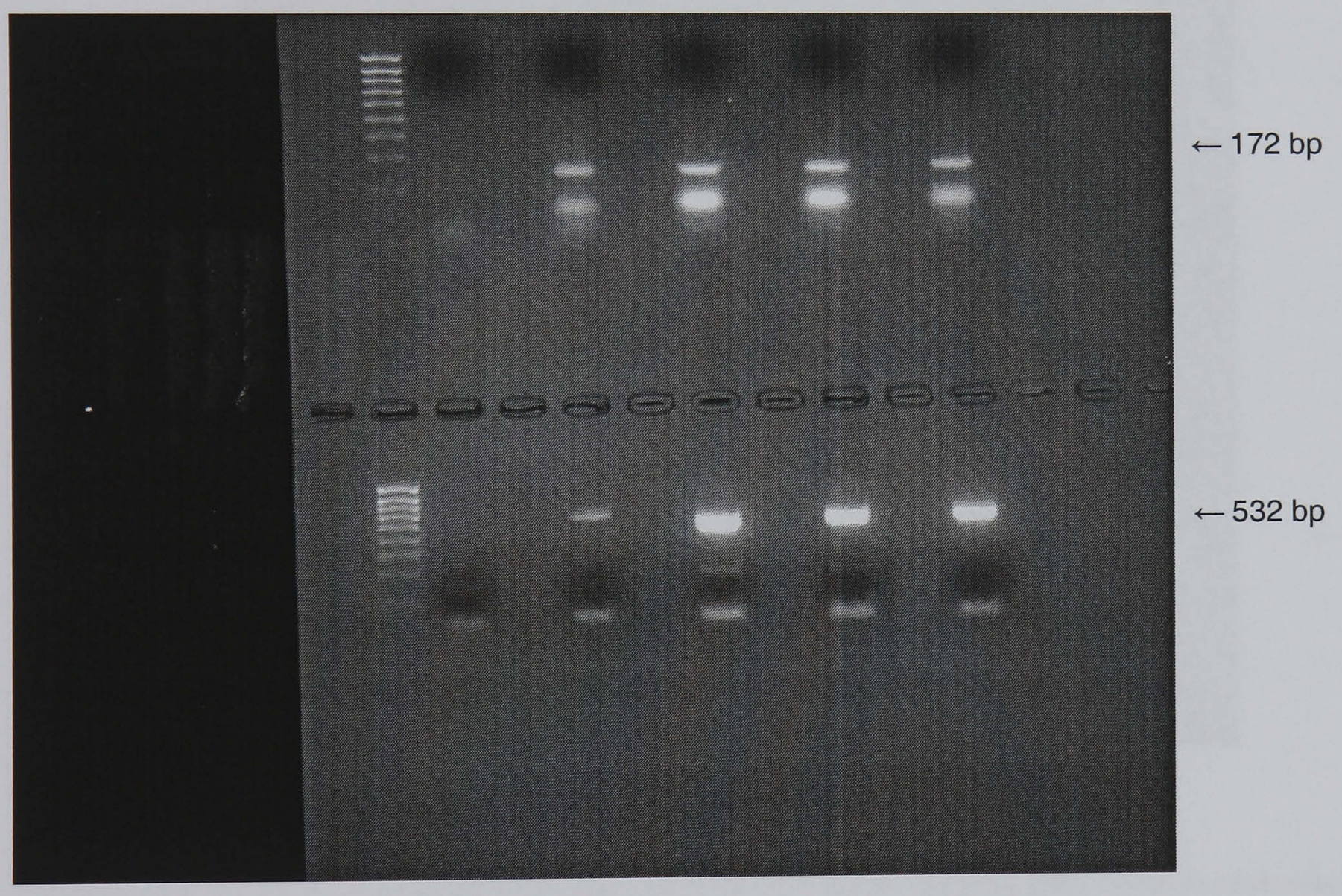

Figure 4.10: RT-PCR analysis of UCN and β-actin (as a house keeping gene control) expression in C-20/A4 chondrocytes. Lane 1- Hyperladder IV molecular size marker (Invitrogen), lane 2 is the negative control, lanes 3-6 shows expression of UCN (top) and β-actin (bottom) in Control, SNAP, TNF-α, and α helical $CRH_{(9-41)}$ treated cells respectively.

Densitometric analysis (data not shown) of the agarose gels shown in Figure 4.10 shows an increased expression of UCN (172 bp product, top) following SNAP and TNF-α treatment of C-20/A4 cells. It is also clear from these results however that β-actin gene expression (532 bp, bottom) is also variable, making this 'house keeping' gene unreliable for these experiments. β-actin expression should be consistent in all

conditions as expected from a control 'housekeeping' gene (Figure 4.10). This observation prompted the use of an alternative housekeeping gene, GAPDH. GAPDH is also one of the best known and most extensively used housekeeping genes (along with β-actin), with a constant level of transcription (Hanauer and Mandel, 1984).

4.3.1.4.2 Using GAPDH as an internal control

Figure 4.11a shows the results of an experiment analogous to that shown in figure 4.10 with the substitution of GAPDH for β-actin as a house keeping gene.

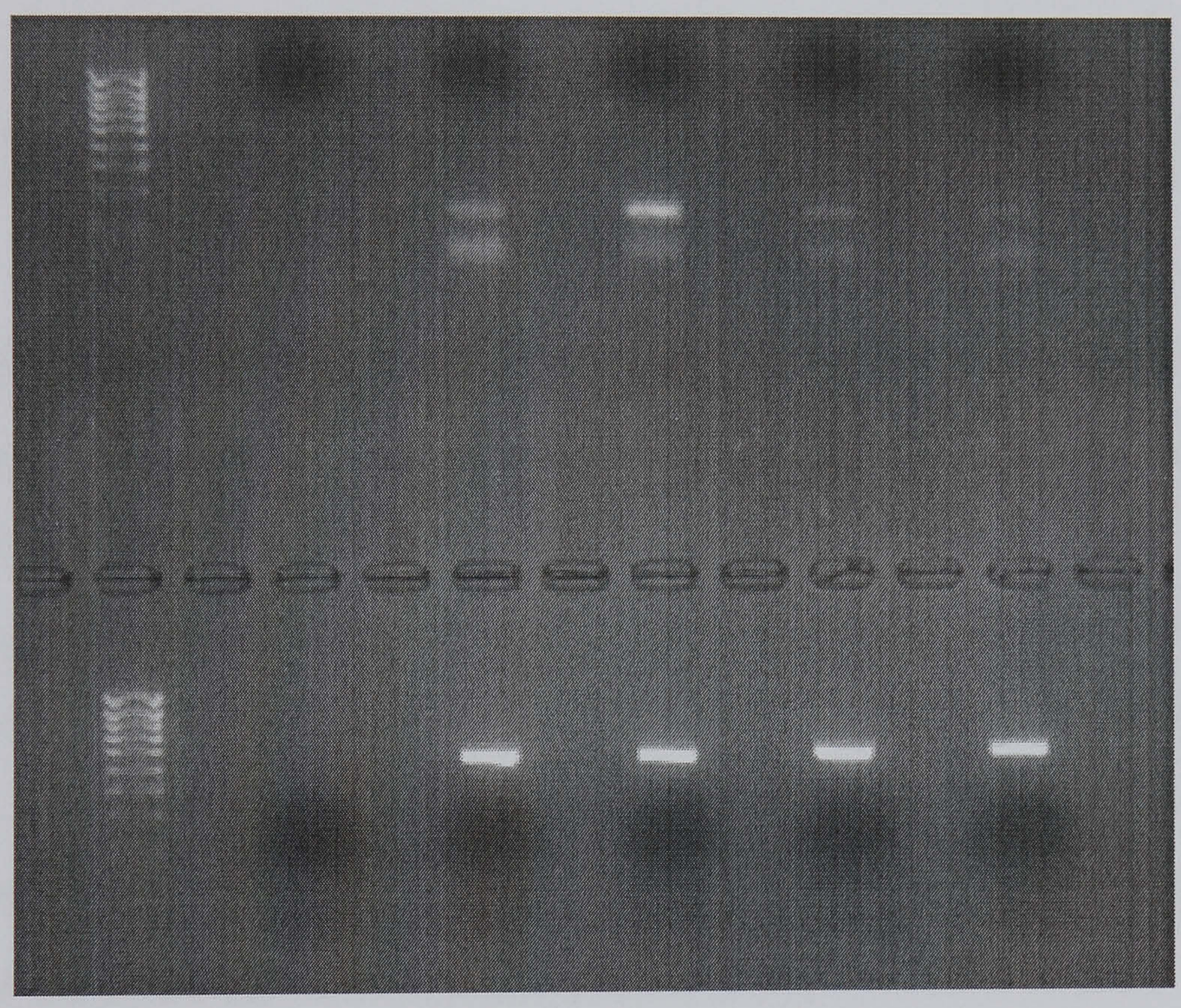

Figure 4.11a: RT-PCR analysis of UCN and GAPDH (as a house keeping gene control) expression in C-20/A4 chondrocytes. Lane 1- Hyperladder IV DNA markers (Invitrogen), lane 2– negative control, lanes 3-6- expression of UCN (top) and GAPDH (bottom) in Control, SNAP, TNF-α, and α helical $CRH_{(9-41)}$ treated cells respectively.

Densitometric analysis of the data in Figure 4.11a demonstrates variable UCN expression under the different treatment regimes but constant GAPDH expression. This allows the confident calculation of expression ratios of UCN gene against the GAPDH housekeeping gene as shown in Figure 4.11b.

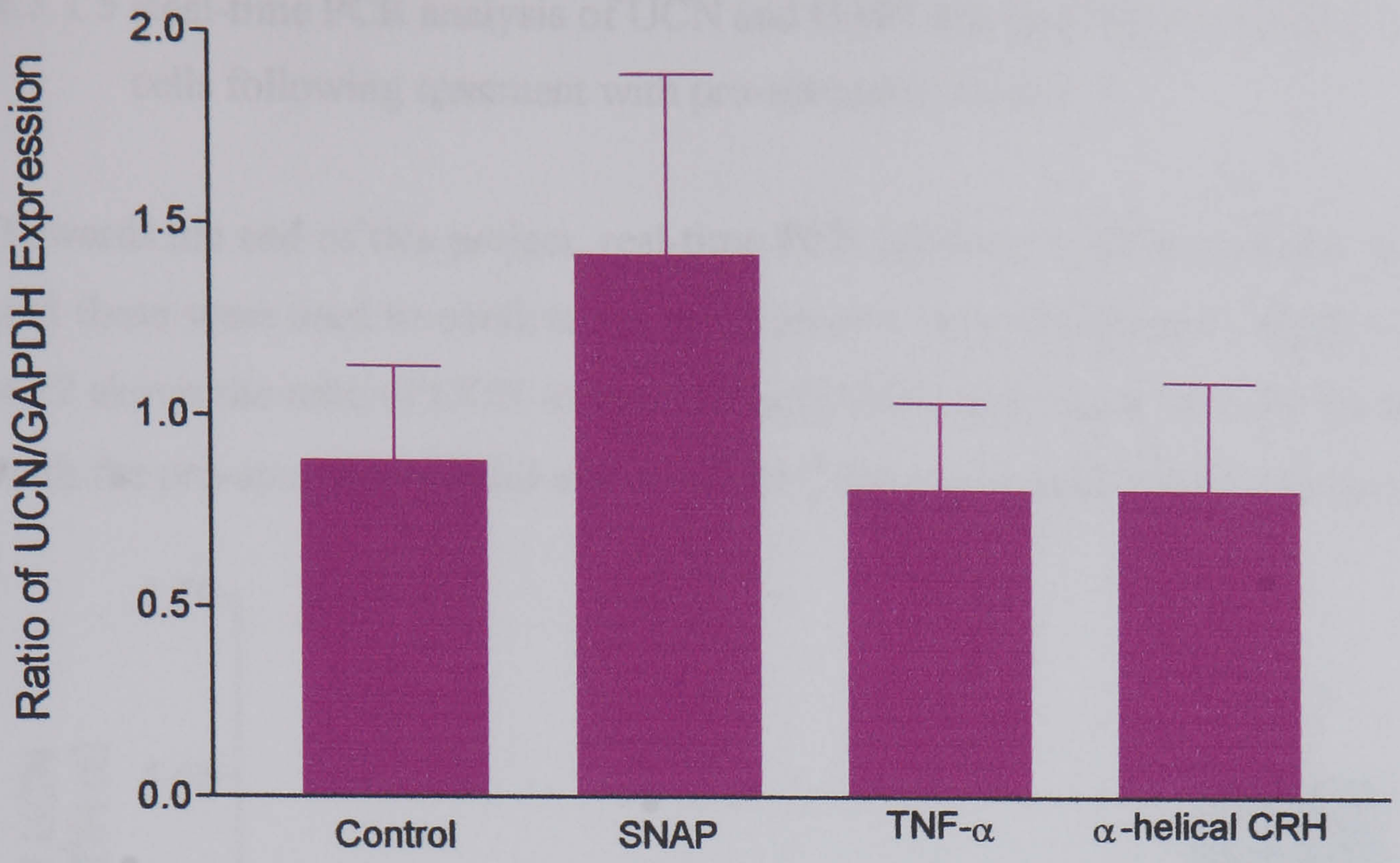

Figure 4.11b: Ratio of UCN/GAPDH expression in pro-apoptotic stimuli treated C-20/A4 cells. Data are presented as the mean values (± standard deviations) of nine independent experiments.

Figure 4.11a and 4.11b show that SNAP treated cells exhibited an increased expression of UCN as compared to control, TNF-α and α helical $CRH_{(9-41)}$ treated cells. The area under curve (AUC) ratio of UCN-GAPDH expression for SNAP was significantly different as compared to the control ($P<0.01$), whereas TNF-α, and α helical $CRH_{(9-41)}$ were not significantly different to the control ($P>0.05$). Control cells demonstrated an expression ratio of 0.88 (UCN:GAPDH) whilst SNAP treated cells showed a ratio of 1.42 (UCN:GAPDH) clearly indicating that NO treatment stimulates the production of UCN in C-20/A4 cells, whilst TNF-α treatment does not.

4.3.1.5 Real-time PCR analysis of UCN and GAPDH expression by C-20/A4 cells following treatment with pro-apoptotic stimuli

Towards the end of this project, real-time PCR facilities became available to the author and these were used to confirm the densitometric data presented in Figure 4.12. Figure 4.12 shows the ratio of UCN expression to GAPDH expression in C-20/A4 cells treated with the pro-apoptotic stimuli and α helical $CRH_{(9-41)}$ as analysed by real-time PCR.

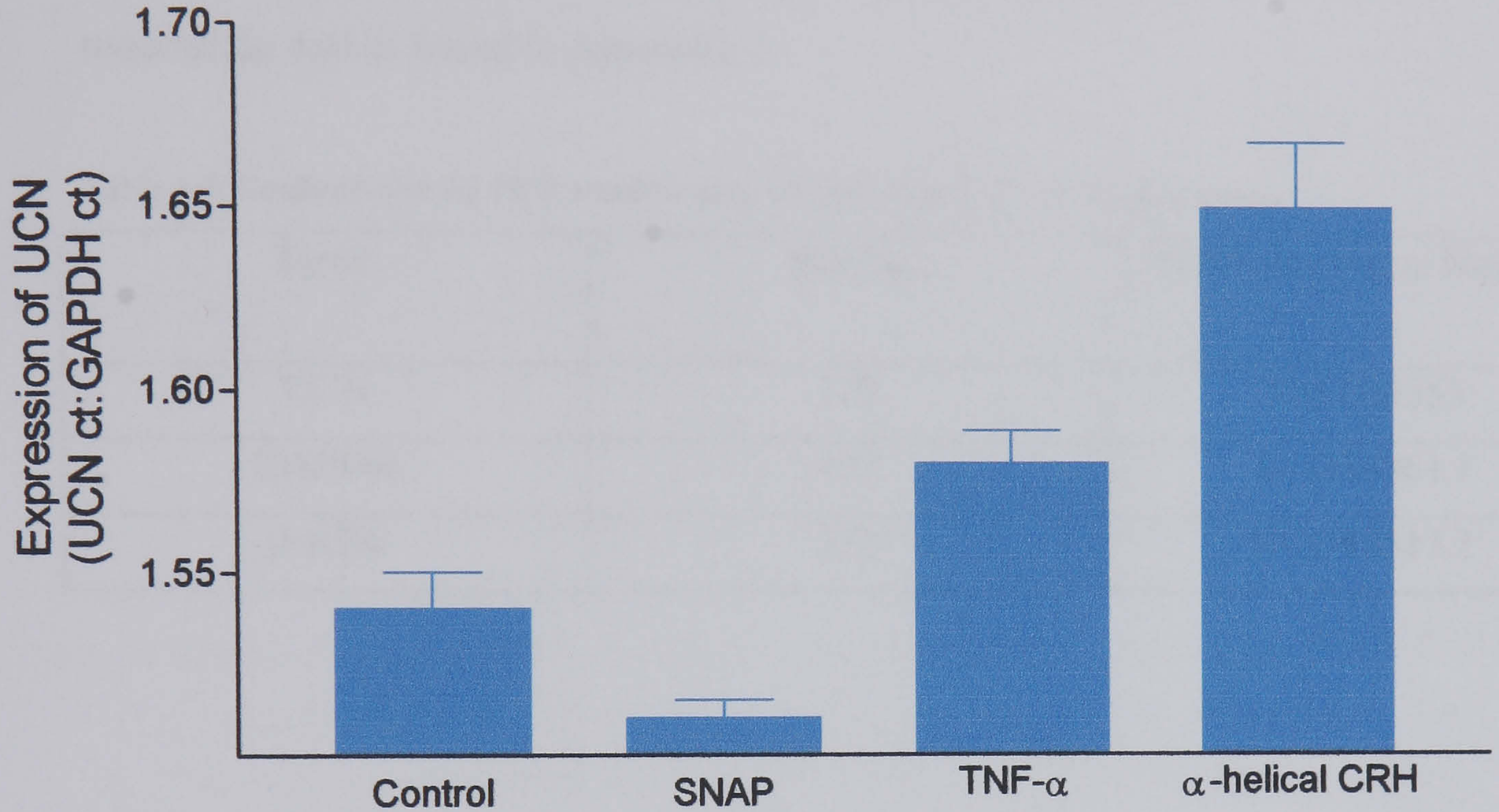

Figure 4.12: Ratio of UCN/GAPDH expression in PCR products of pro-apoptotic stimuli treated C-20/A4 cells using real time PCR. Data are presented as the mean values (± standard deviations) of four independent experiments.

It is worth noting here that interpretation of real-time PCR data is somewhat counter-intuitive. A decrease in the cycle threshold (ct) of gene expression, and also therefore any calculated ratios, indicates an increased expression of the gene of interest. With this in mind, Figure 4.12 shows that C-20/A4 cells treated with SNAP exhibited a significant increase in expression of UCN ($P<0.01$, SNAP vs control) whereas those treated with TNF-α and α helical $CRH_{(9-41)}$, actually showed a decrease which were both significant compared to control ($P<0.001$). The control cells presented a ratio of 1.54. These data support to a certain extent that shown in Figure 4.11b but, with the exception of the α helical $CRH_{(9-41)}$ data ($P<0.001$) compared to the control.

4.3.1.6 Sequence analysis of purified PCR samples

Sequence analysis confirmed the identity of all of the PCR products when sequence data were analysed using BLAST nucleic acid database searches from the National Centre for Biotechnology Information (www.ncbi.nlm.nih.gov/BLAST/). The relevant accession numbers for matching nucleotide sequences are given in table 4.3 and full sequencing data is found in Appendix 1.

Table 4.3: Confirmation for PCR amplification of cDNA in C-20/A4 chondrocytes.

Gene	Size bp	NCBI Accession Number
UCN	172	NM 003353
GAPDH	437	BCO14861.1
β-actin	532	BCO83511.1

4.3.2 CRH antagonist studies

4.3.2.1 The effects of α helical $CRH_{(9-41)}$ on C-20/A4 cells

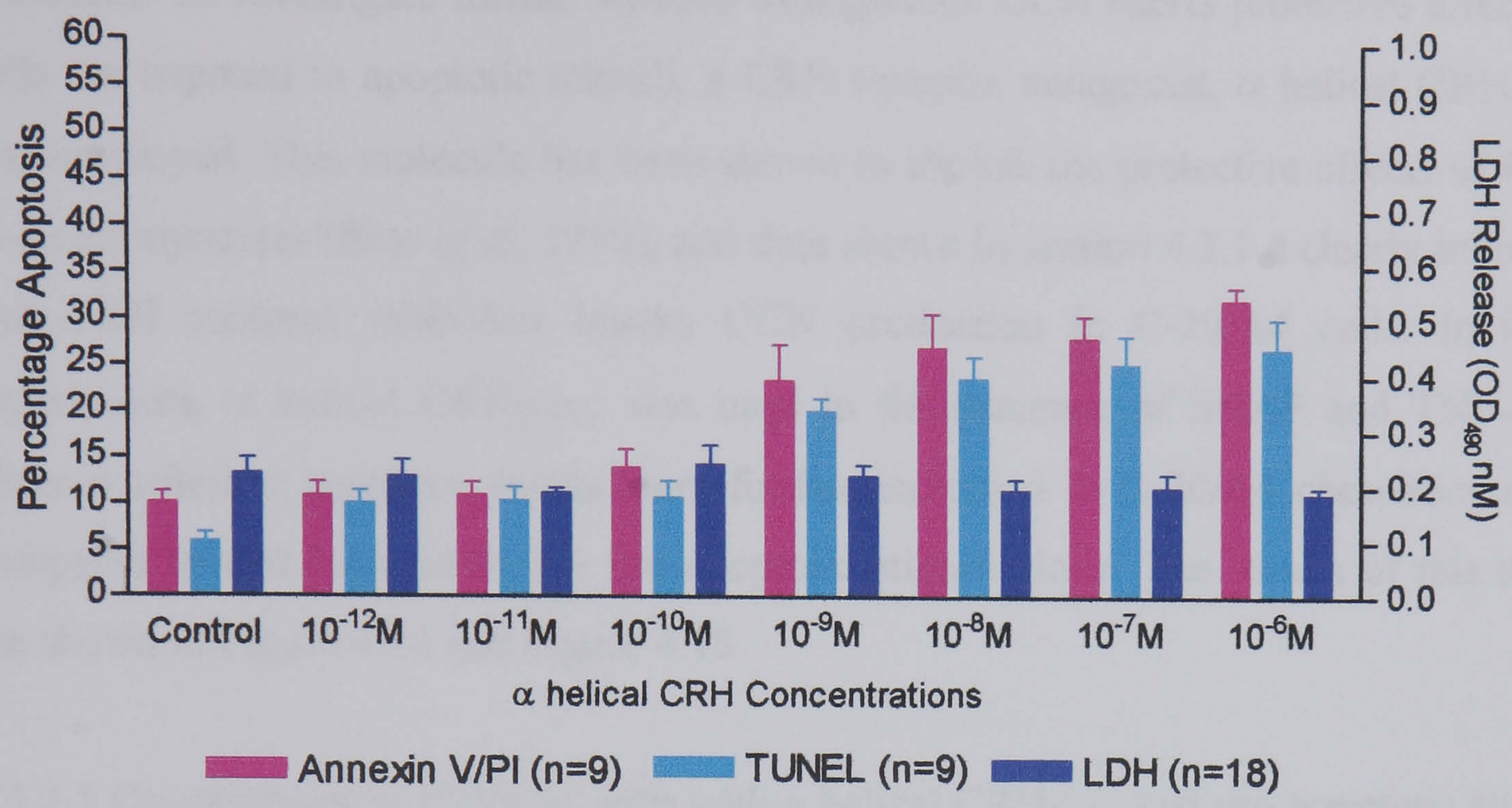

Figure 4.13: Percentage of Annexin V/Propidium Iodide and TUNEL positive cells and cellular LDH release following treatment of C-20/A4 cells with concentrations of α helical $CRH_{(9-41)}$.
Data are presented as the mean values (± standard deviations) of three independent experiments, each of which was performed in triplicate.

Treatment with a range of α helical $CRH_{(9-41)}$ concentrations showed minimal level of Annexin V/PI and TUNEL staining up to 10^{-11}M and low levels of necrotic cell death both of which were not significant compared to the control ($P>0.05$). As the dose of α helical $CRH_{(9-41)}$ increased from 10^{-10}M however, the level of both early and late apoptotic cell death had gradually increased significantly ($P<0.001$ 10^{-10}M vs 10^{-9}M), whilst necrotic cell death remained constant and shown not to be significant ($P>0.05$).

The optimum concentration of α helical $CRH_{(9-41)}$ for use in further experiments was established to be 10^{-8} M as a suitable level of apoptosis was observed between 10^{-9} M-10^{-6} M. No significant difference in the level of apoptosis between these concentrations was noted ($P>0.05$).

4.3.2.2 Co-treatment of C-20/A4 cells with α helical $CRH_{(9-41)}$ and pro-apoptotic stimuli

Experiments shown in sections 4.3.1.4 clearly demonstrated the production of the CRH family peptide, namely UCN by C-20/A4 chondrocytes especially after SNAP treatment. To investigate further whether endogenous UCN exerts protective effects in cells are exposed to apoptotic stimuli, a CRH receptor antagonist, α helical $CRH_{(9-41)}$, was employed. This molecule has been shown to abolish the protective effects of UCN in cardiomyocytes (Brar *et al*, 1999), and data shown in section 4.3.1.4 clearly indicates that CRH receptor inhibition blocks UCN production in C-20/A4 cells. In these experiments, α helical $CRH_{(9-41)}$, was used in the presence of SNAP and TNF-α to observe whether apoptotic levels were further increased in C-20/A4 chondrocytes as compared to that induced by the pro-apoptotic stimuli alone. The results of this study are shown in Figure 4.14 and Figure 4.15.

4.3.2.2 Co-treatment of C-20/A4 cells with α helical $CRH_{(9-41)}$ and pro-apoptotic stimuli

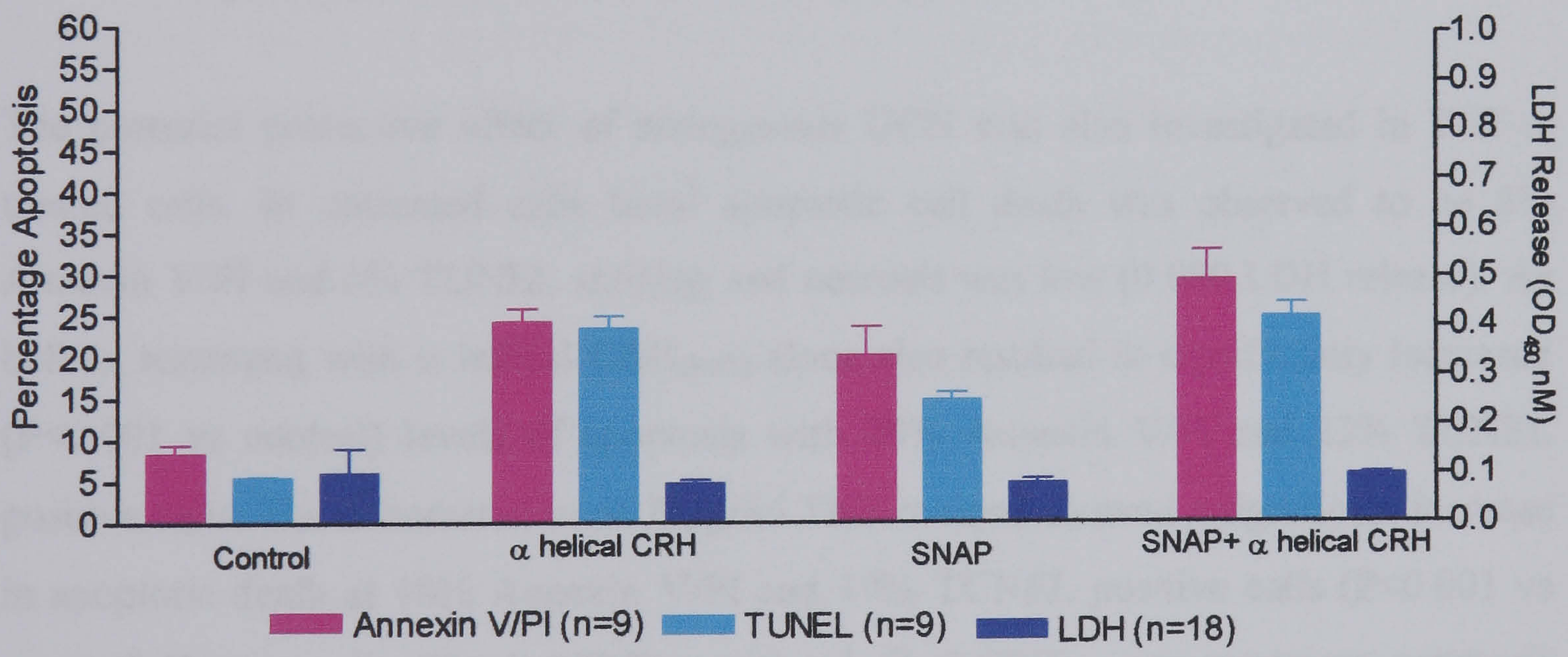

Figure 4.14: Percentage of Annexin V/Propidium Iodide and TUNEL positive cells and cellular LDH release following co-treatment of C-20/A4 cells with 1mM SNAP and 10^{-8}M α helical $CRH_{(9-41)}$. Data are presented as the mean values (± standard deviations) of three independent experiments, each of which was performed in triplicate.

Control cells showed minimal level of apoptosis and necrosis (8% Annexin V/PI, 6% TUNEL and 0.100 LDH release), whilst the addition of α helical $CRH_{(9-41)}$ alone resulted in significantly higher ($P<0.001$ vs control) levels of apoptosis (25% Annexin V/PI and 24% TUNEL). Treatment with 1mM SNAP alone also resulted in a significantly increased ($P<0.01$ vs control) level of apoptosis (20% Annexin V/PI and

15% TUNEL) but treatment with both SNAP and α helical $CRH_{(9-41)}$ showed maximum apoptosis (30% Annexin V/PI and 25% TUNEL), which was significantly different ($P<0.05$) from that induced by SNAP alone. Necrosis remained low in all experiments and was not significantly different from the control ($P>0.05$).

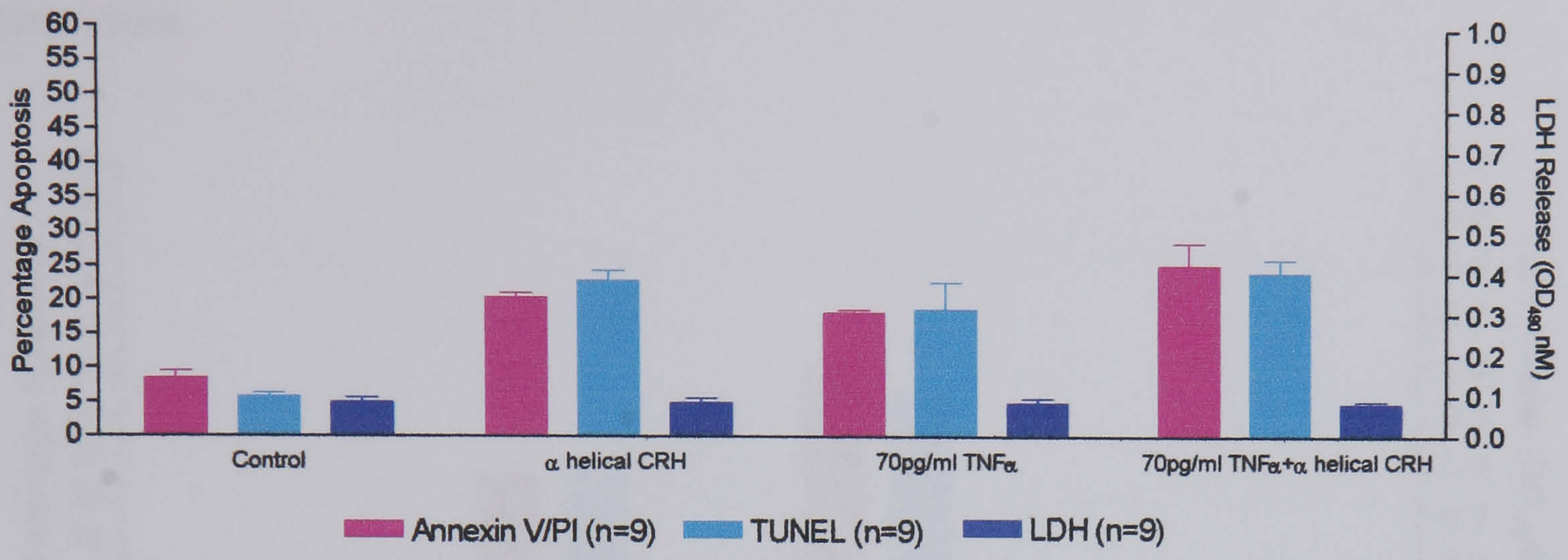

Figure 4.15: Percentage of Annexin V/Propidium Iodide and TUNEL Positive cells and cellular LDH release following co-treatment of C-20/A4 cells with 70pg/ml TNF-α and α-helical $CRH_{(9-41)}$ Data are presented as the mean values (± standard deviations) of three independent experiments, each of which was performed in triplicate.

The potential protective effect of endogenous UCN was also investigated in TNF-α treated cells. In untreated cells basal apoptotic cell death was observed to be 8% Annexin V/PI and 6% TUNEL staining and necrosis was low (0.080 LDH release). As before, treatment with α helical $CRH_{(9-41)}$ alone also resulted in significantly increased ($P<0.001$ vs control) levels of apoptosis with 20% Annexin V/PI and 23% TUNEL positive cells. The concentration of 70pg/ml TNF-α alone showed a significant increase in apoptotic death at 18% Annexin V/PI and 19% TUNEL positive cells ($P<0.001$ vs control). However, for 70pg/ml TNF-α with α helical $CRH_{(9-41)}$ co-treatment, apoptosis was shown to be further increased at 25% Annexin V/PI and 24% TUNEL ($P<0.01$ vs TNF-α alone). Necrotic levels remained low throughout all experiments and were not significantly different from the control ($P>0.05$).

4.3.3 Endogenous UCN depletion studies

In these experiments an anti-human UCN antibody was used to investigate the endogenous production of UCN in C-20/A4 cells. An isotype control antibody (anti-human albumin) and the CRH antagonist, α helical $CRH_{(9-41)}$ were included for comparison.

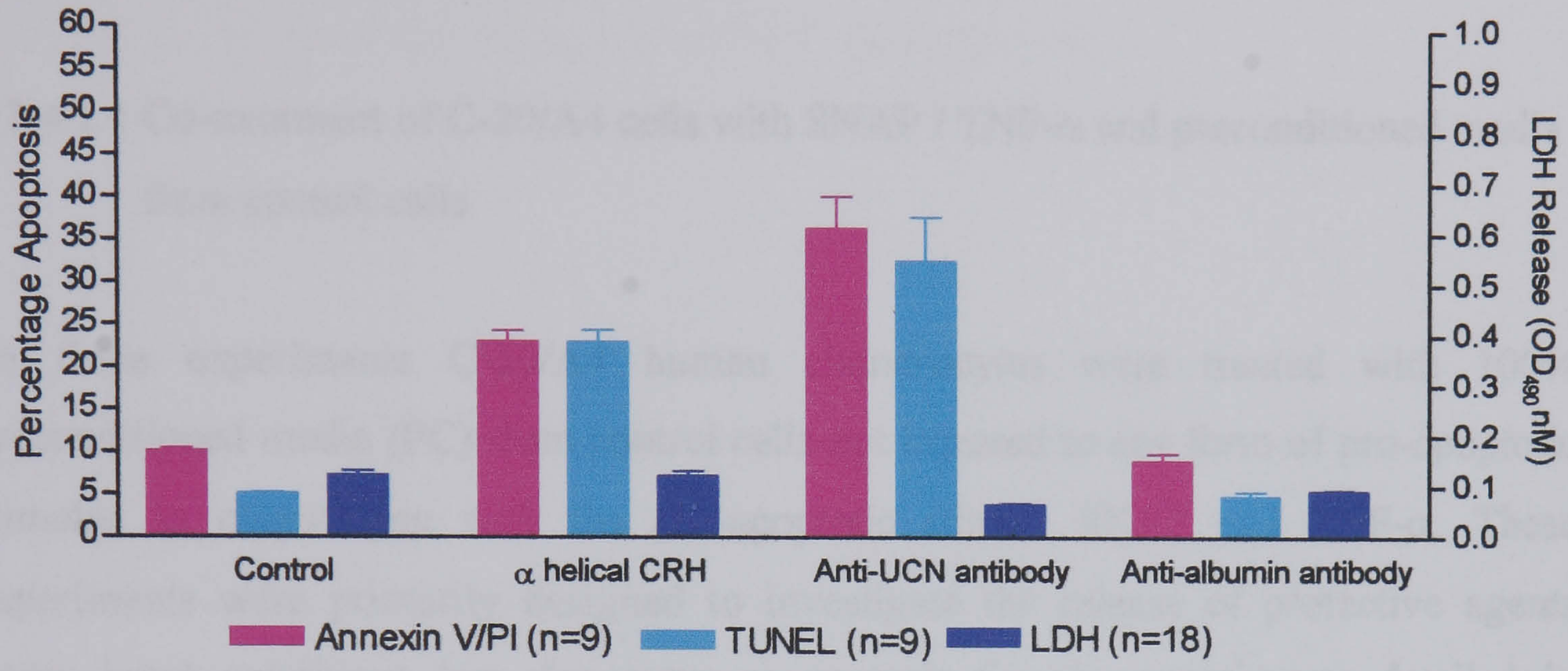

Figure 4.16: Percentage of Annexin V/Propidium Iodide and TUNEL positive cells and cellular LDH release following treatment of C-20/A4 cells, with α helical $CRH_{(9-41)}$, anti-UCN antibody and anti-albumin antibody. Data are presented as the mean values (± standard deviations) of three independent experiments, each of which was performed in triplicate.

In untreated cells, a low level of basal apoptotic cell death was recorded (10% Annexin V/PI and 5% TUNEL), with minimal necrosis as measured by LDH release. Treatment with α helical $CRH_{(9-41)}$ resulted in a significant ($P<0.001$ vs control) increase of apoptotic cell death (23% Annexin V/PI and 23% TUNEL) with an even greater increase noted on the addition of an anti-UCN antibody, significantly greater than α helical $CRH_{(9-41)}$ ($P<0.01$) to 37% Annexin V/PI and 33% TUNEL. However, anti-albumin antibody did not produce any increased apoptosis compared to the control with 9% Annexin V/PI and 5% TUNEL ($P>0.05$). Necrotic cell death remained constantly low in all conditions. These data support a role for endogenous UCN as an autocrine/paracrine growth factor for C-20/A4 cells, as well as endogenous UCN having a cytoprotective effect when the cells are exposed to apoptotic stimuli.

4.3.4 Preconditioned Media Studies

The data presented in this section are the results of a series of experiments designed to investigate whether a protective agent is released into the cell growth medium which enhances chondrocyte survival.

4.3.4.1 100% preconditioned media studies

4.3.4.1.1 Co-treatment of C-20/A4 cells with SNAP / TNF-α and preconditioned media from control cells

In these experiments C-20/A4 human chondrocytes were treated with 100% preconditioned media (PC) from control cells not exposed to any form of pro-apoptotic stimulus in conjunction with the pro-apoptotic stimuli SNAP and TNF-α. These experiments were primarily designed to investigate the release of protective agents under basal conditions but also serve as controls for the experiments detailed in 4.3.4.1.2 and 4.3.4.1.3.

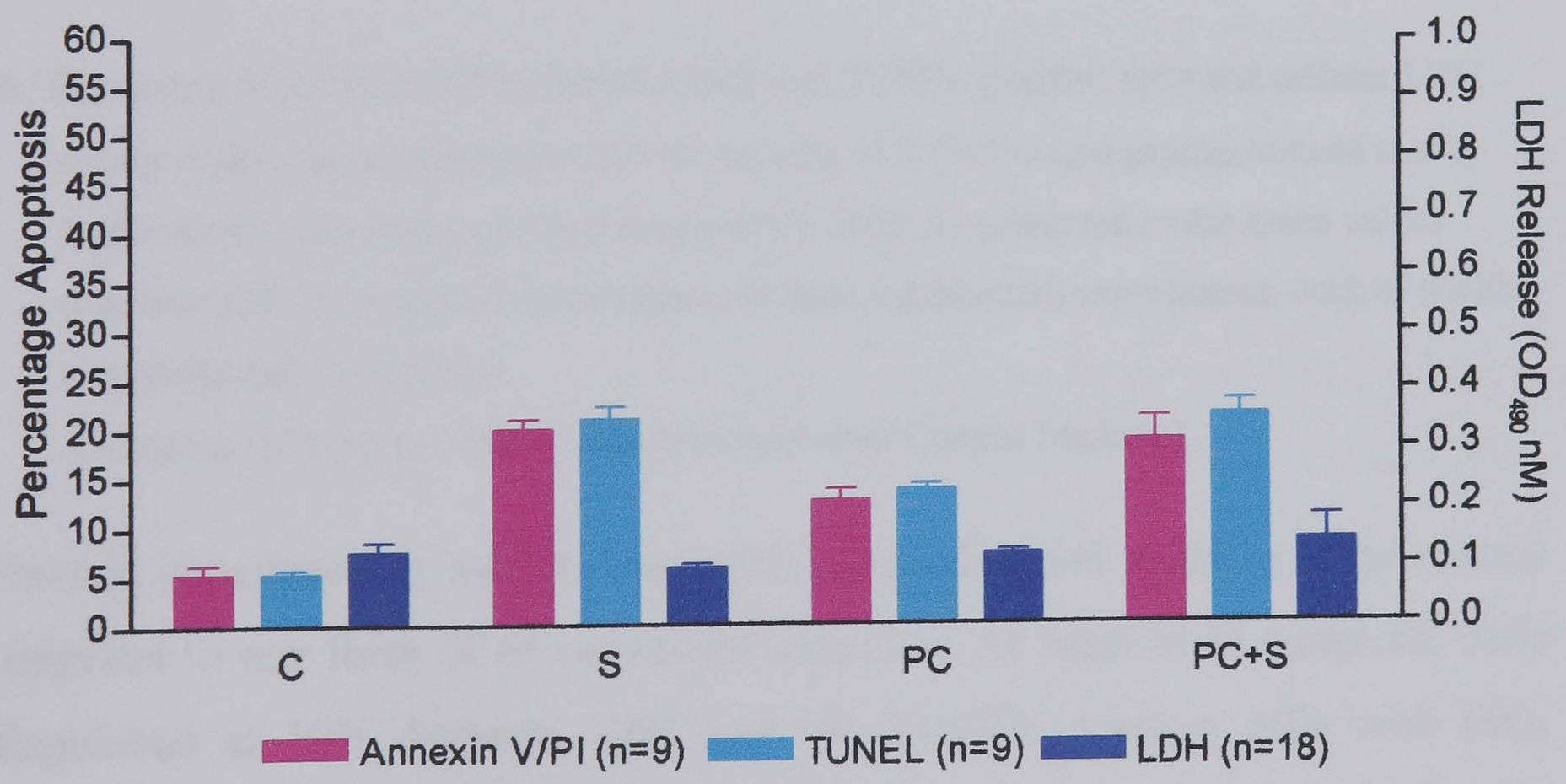

Figure 4.17a: Percentage of Annexin V/Propidium Iodide and TUNEL positive cells and cellular LDH release following co-treatment of C-20/A4 cells with SNAP and preconditioned medium from control cells unexposed to stimulus (PC). Data are presented as the mean values (± standard deviations) of three independent experiments, each of which were performed in triplicate.
(C-control, S-1mM SNAP, PC-Preconditioned Control Medium)

In untreated C-20/A4 cells apoptosis was observed at 5% for both Annexin V/PI and TUNEL assays with low LDH release. SNAP alone (S) treatment resulted in a significant increase in apoptotic cell death ($P<0.05$) but not necrosis when compared to the control. The addition of preconditioned control medium (PC) alone also showed a significant increase in apoptosis ($P<0.05$ vs control) but not necrosis ($P>0.05$ vs control). Combinations of preconditioned control and SNAP (PC+S) resulted in a significant increase in cell death compared to preconditioned control alone (PC) ($P<0.01$) but no significant change over SNAP alone ($P>0.05$).

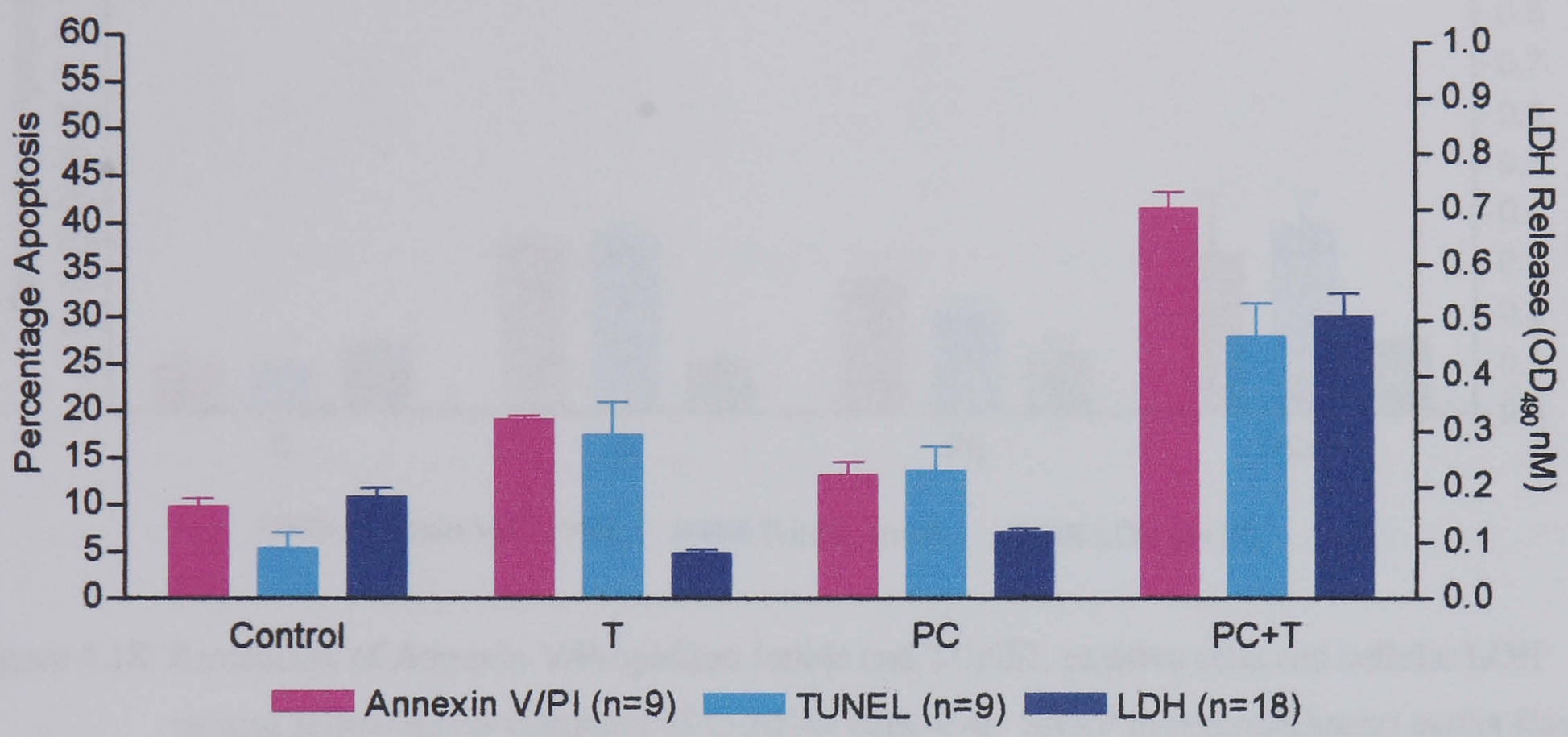

Figure 4.17b: Percentage of Annexin V/Propidium Iodide and TUNEL positive cells and cellular LDH release following co-treatment of C-20/A4 cells with TNF-α and preconditioned media from control cells unexposed to stimulus (PC). Data are presented as the mean values (together with the ± standard deviations) of three independent experiments, each of which was performed in triplicate.
(C-control, T-70 pg/ml TNF-α, PC-Preconditioned Control Medium)

C-20/A4 human chondrocytes were treated with preconditioned medium from control cells not exposed to any form of pro-apoptotic stimulus. At basal level apoptotic cells were distinguished at 10% Annexin V/PI and 5% TUNEL positive cells with little necrosis (0.180 LDH release). TNF-α alone (T), treatment resulted in a significant increase in apoptosis ($P<0.001$) but not necrosis when compared to the control. Preconditioned control (PC) treated cells indicated a slightly higher level of apoptosis as compared to control, which was especially noted for late apoptosis. Minimal necrosis, was observed which was not statistically significant ($P>0.05$). Combinations of preconditioned control and TNF-α (PC+T) resulted in a significant increase in apoptotic death (especially Annexin V/PI staining) compared to preconditioned control (PC) alone

($P<0.001$) and TNF-α alone (T) ($P<0.01$). Necrotic level in preconditioned control and TNF-α (PC+T) treated cells was significantly increased compared to preconditioned control and TNF-α ($P<0.001$ respectively).

4.3.4.1.2 Co-treatment of C-20/A4 cells with SNAP and preconditioned media from cells subjected to SNAP

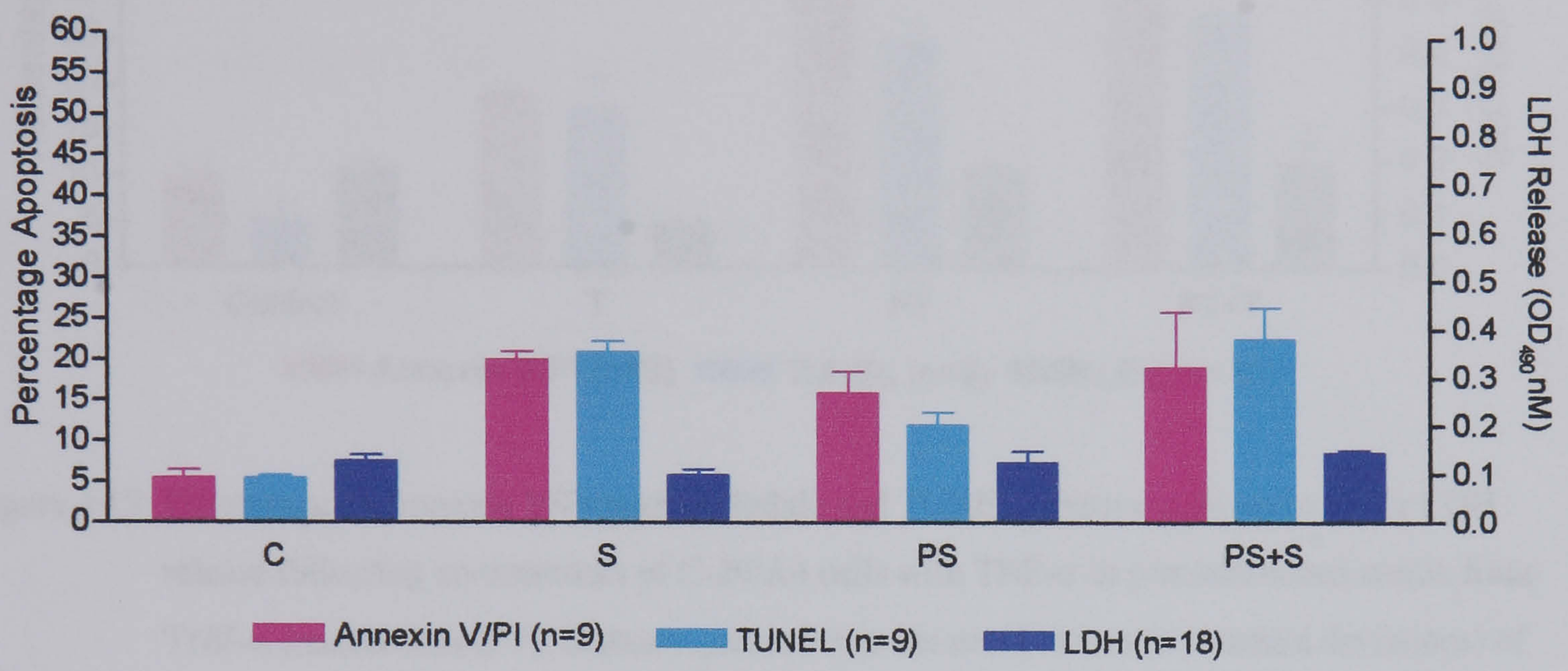

Figure 4.18: Percentage of Annexin V/Propidium Iodide and TUNEL positive cells and cellular LDH release following co-treatment of C-20/A4 cells with SNAP in preconditioned media from SNAP treated cells (PS). Data are presented as the mean values (± standard deviations) of three independent experiments, each of which was performed in triplicate.
(C-control, S-1mM SNAP, PS-Preconditioned SNAP Medium)

Preconditioned SNAP medium (100%) from cells exposed to SNAP was used to treat additional C-20/A4 cells (PS). At basal level, apoptosis was noticed at 5% for Annexin V/PI and 5% TUNEL positive cells. The effect of preconditioned SNAP media (PS) alone revealed 16% Annexin V/PI and 12% TUNEL positive cells, which were observed to be significantly lower than SNAP alone ($P<0.05$), especially TUNEL staining. Combinations of preconditioned SNAP + SNAP (PS+S) showed a significant increase in TUNEL staining, but not Annexin V/PI staining and shown to be significantly different against preconditioned SNAP (PS) ($P<0.05$) but not significant against SNAP (S) alone ($P>0.05$).

4.3.4.1.3 Co-treatment of C-20/A4 cells with TNF-α and preconditioned media from cells subjected to TNF-α

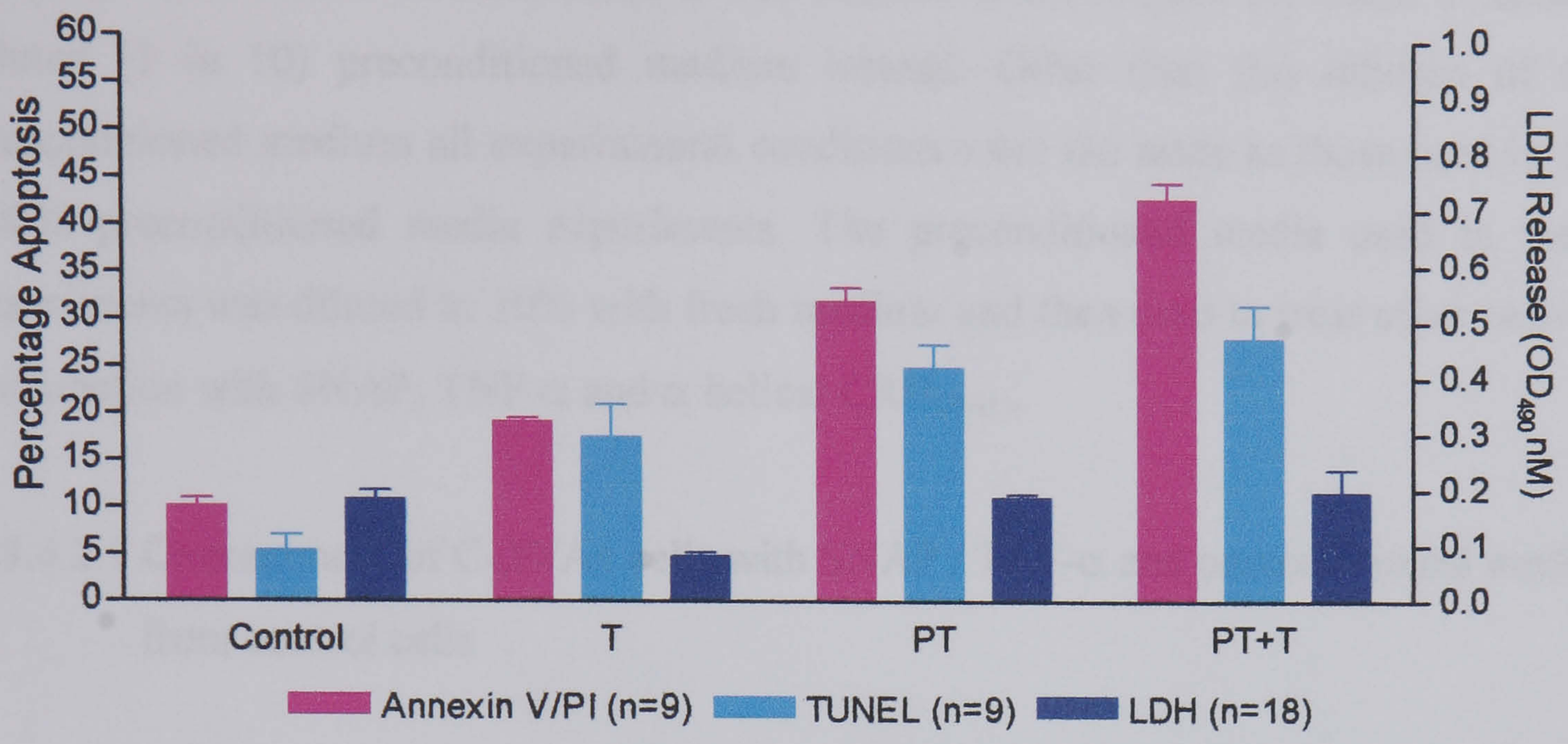

Figure 4.19: Percentage of Annexin V/Propidium Iodide and TUNEL positive cells and cellular LDH release following co-treatment of C-20/A4 cells with TNF-α in preconditioned media from TNF-α treated cells (PT). Data are presented as the mean values (± standard deviations) of three independent experiments, each of which was performed in triplicate.
(C-control, T-70pg/ml TNF-α, PT-Pre-conditioned TNF-α Medium)

Preconditioned TNF-α medium (100%) from cells exposed to TNF-α was used to treat additional C-20/A4 cells. Control experiments showed minimal level of apoptosis at 10% for Annexin V/PI and 5% TUNEL positive cells. The results of preconditioned TNF-α media (PT) were observed at 32% Annexin V/PI and 25% TUNEL ($P<0.001$) positive cells with low necrotic death, which was significantly increased ($P<0.05$) against TNF-α alone (T). A significantly increased level of Annexin V/PI staining was observed in preconditioned TNF-α + TNF-α (PT+T) compared to preconditioned TNF-α medium alone (PT) ($P<0.05$) and in TNF-α alone (T) ($P<0.001$).

4.3.4.2 10% Preconditioned media studies

As all the experiments in section 4.3.4.1 show an increase in cell death on the addition of the preconditioned medium alone it was decided to investigate the effect of adding diluted (1 in 10) preconditioned medium instead. Other than this dilution of the preconditioned medium all experimental conditions were the same as those used in the 100% preconditioned media experiments. The preconditioned media used in these experiments was diluted to 10% with fresh medium and then used to treat other cells in conjunction with SNAP, TNF-α and α helical $CRH_{(9-41)}$.

4.3.4.2.1 Co-treatment of C-20/A4 cells with SNAP / TNF-α and preconditioned media from control cells

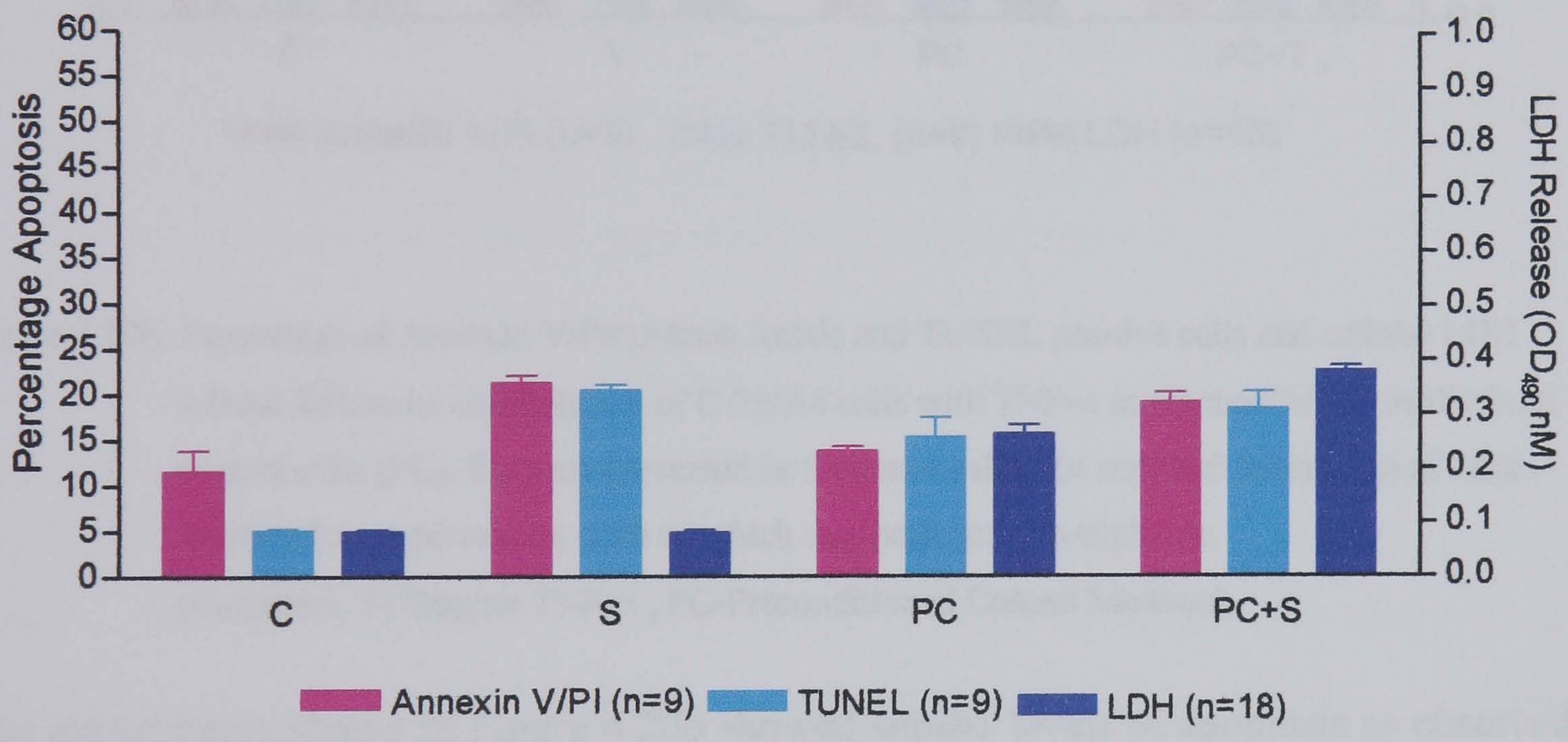

Figure 4.20a: Percentage of Annexin V/Propidium Iodide and TUNEL positive cells and cellular LDH release following co-treatment of C-20/A4 cells with SNAP in preconditioned media from control cells (PC). Data are presented as the mean values (± standard deviations) of three independent experiments, each of which was performed in triplicate.
(C-control, S-1mM SNAP, PC-Preconditioned Control Medium)

The experiments shown in Figure 4.20a indicated similar levels of apoptosis as observed with the preconditioned 100% media studies. In untreated C-20/A4 cells (control), apoptosis was observed at 12% for Annexin V/PI and 5% TUNEL positive cells. SNAP alone (S) treatment had resulted in a significant increase in apoptotic cell death ($P<0.05$) but not necrosis when compared to the control. Whilst, preconditioned control media (PC) showed 14% Annexin V/PI and 15% TUNEL positive cells and low

necrosis (P<0.001), this was shown to be significantly different as compared to control treated cells. High apoptotic and low necrotic levels were also observed in preconditioned control media + SNAP (PC+S) and shown not to be significantly different against SNAP (S) alone (P>0.05), but was significant against preconditioned control media (PC) (P<0.01), especially with Annexin V/PI treated cells. Whilst, necrotic levels were significant as compared to SNAP (S) alone (P<0.001).

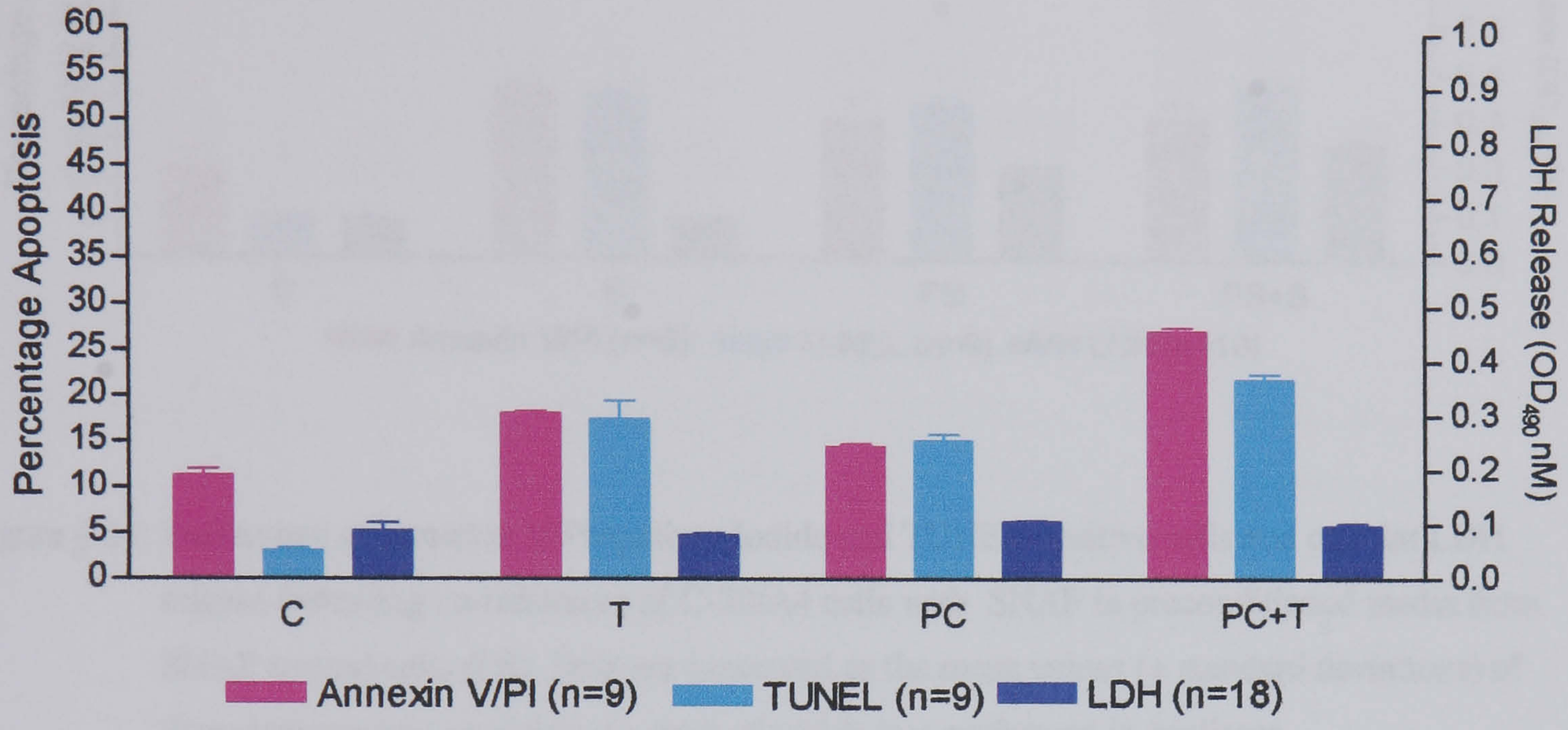

Figure 4.20b: Percentage of Annexin V/Propidium Iodide and TUNEL positive cells and cellular LDH release following co-treatment of C-20/A4 cells with TNF-α in preconditioned media from control cells (PC). Data are presented as the mean values (± standard deviations) of three independent experiments, each of which was performed in triplicate.
(C-control, T-70pg/ml TNF-α , PC-Preconditioned Control Medium)

The experiments shown in Figure 4.20b showed similar levels of apoptosis as observed with the preconditioned 100% media studies. At basal level apoptotic cells were observed at 11% Annexin V/PI and 3% TUNEL positive cells with little necrosis. Preconditioned control media (PC) treated cells indicated a significantly higher (P<0.001) level of TUNEL staining but not Annexin V/PI staining (P>0.05) as compared to control cells, with low necrosis. TNF-α alone (T), treatment resulted in a significant increase in apoptosis (P<0.001) but not necrosis when compared to the control. Significantly increased apoptotic and low necrotic levels were observed in preconditioned control media and TNF-α (PC+T) as compared to preconditioned control (PC) alone (P<0.05) and TNF-α (T) (P<0.05), which was especially noted for Annexin V/PI treated cells.

4.3.4.2.2 Co-treatment of C-20/A4 cells with SNAP and preconditioned media from cells subjected to SNAP

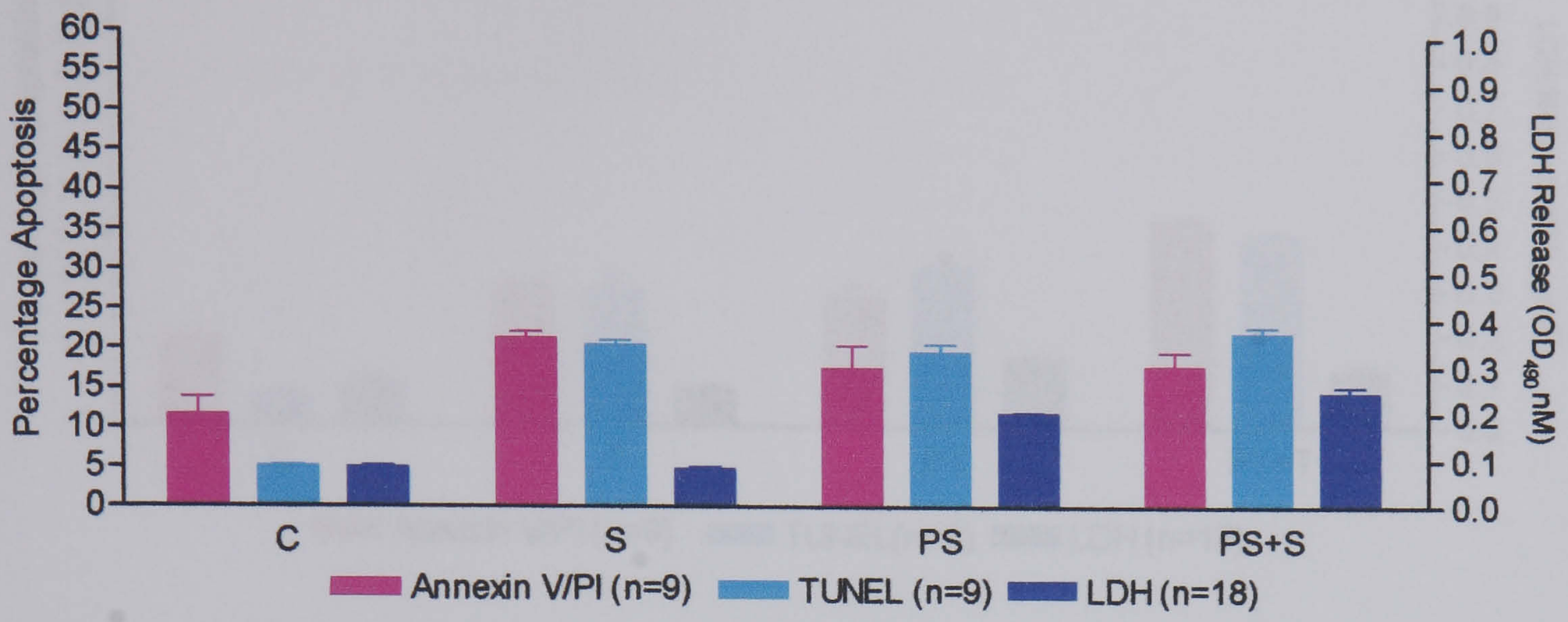

Figure 4.21: Percentage of Annexin V/Propidium Iodide and TUNEL positive cells and cellular LDH release following co-treatment of C-20/A4 cells with SNAP in preconditioned media from SNAP treated cells (PS). Data are presented as the mean values (± standard deviations) of three independent experiments, each of which was performed in triplicate.
(C-control, S-1mM SNAP, PS-Preconditioned SNAP Medium)

Preconditioned SNAP medium (10%) from cells exposed to SNAP was used to treat additional C-20/A4 cells. At basal level, apoptotic cell death was low. Significantly high apoptotic and low necrotic levels were observed in preconditioned SNAP media (PS) alone as compared to control ($P<0.01$). High levels of apoptosis was observed in preconditioned SNAP+SNAP (PS+S), but shown not to be significantly different against SNAP alone ($P>0.05$) or preconditioned SNAP (PS) alone ($P>0.05$), whilst necrotic levels were high and observed as significantly different against SNAP alone and control ($P<0.001$ respectively).

4.3.4.2.3 Co-treatment of C-20/A4 cells with TNF-α and preconditioned media from cells subjected to TNF-α

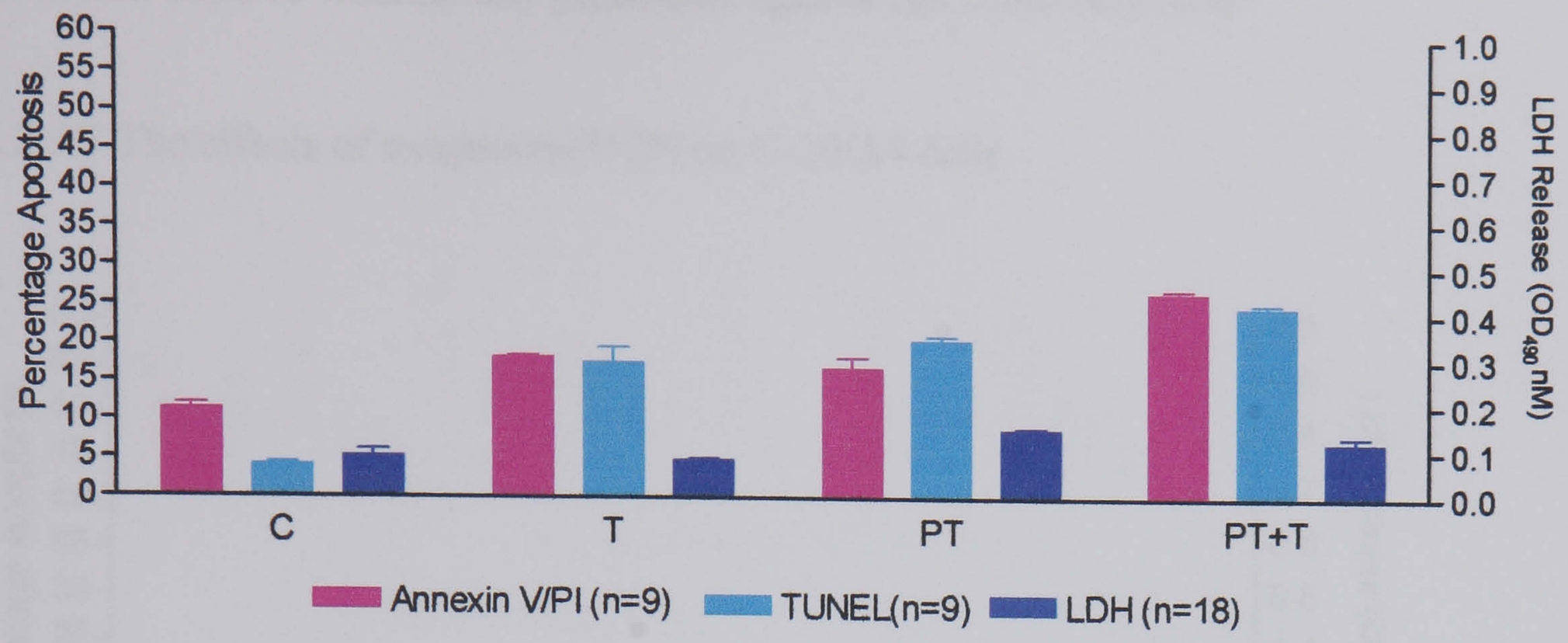

Figure 4.22: Percentage of Annexin V/Propidium Iodide and TUNEL positive cells and cellular LDH release following co-treatment of C-20/A4 cells with TNF-α in preconditioned media from TNF-α treated cells (PT). Data are presented as the mean values (± standard deviations) of three independent experiments, each of which was performed in triplicate.
(C-control, T-70pg/ml TNF-α, PT-Preconditioned TNF-α Medium)

Preconditioned TNF-α medium (10%) from cells exposed to TNF-α was used to treat additional C-20/A4 cells. These experiments showed similar levels of apoptosis as observed with the preconditioned TNF-α media (100%) studies with the difference of lower apoptotic levels observed with 10% preconditioned TNF-α than 100%. Preconditioned TNF-α media (PT) revealed significantly increased ($P<0.05$) apoptotic level as compared to the control, but was not significant in comparison to TNF-α alone ($P>0.05$). Combinations of preconditioned TNF-α and TNF-α (PT+T) resulted in further significant increases in apoptotic death when compared to TNF-α alone ($P<0.001$) especially noted for Annexin V/PI stained cells and preconditioned TNF-α alone ($P<0.001$).

4.3.5 Exogenous Urocortin studies

Experiments detailed in sections 4.3.2 demonstrated that in the presence of a CRH receptor antagonist, α helical $CRH_{(9-41)}$, apoptotic levels increased significantly in C-20/A4 cells, indicating that this antagonist may be abolishing the protective effect of a CRH-R binding peptide on these cells. Experiments documented in section 4.3.3 indicate that UCN is a strong candidate for this putative, protective CRH-R binding

peptide. To further investigate this possibility a series of experiments were performed adding exogenous UCN to C-20/A4 cells in the presence and absence of pro-apoptotic stimuli to observe whether any protection against cell death occurred.

4.3.5.1 The effects of exogenous UCN on C-20/A4 cells

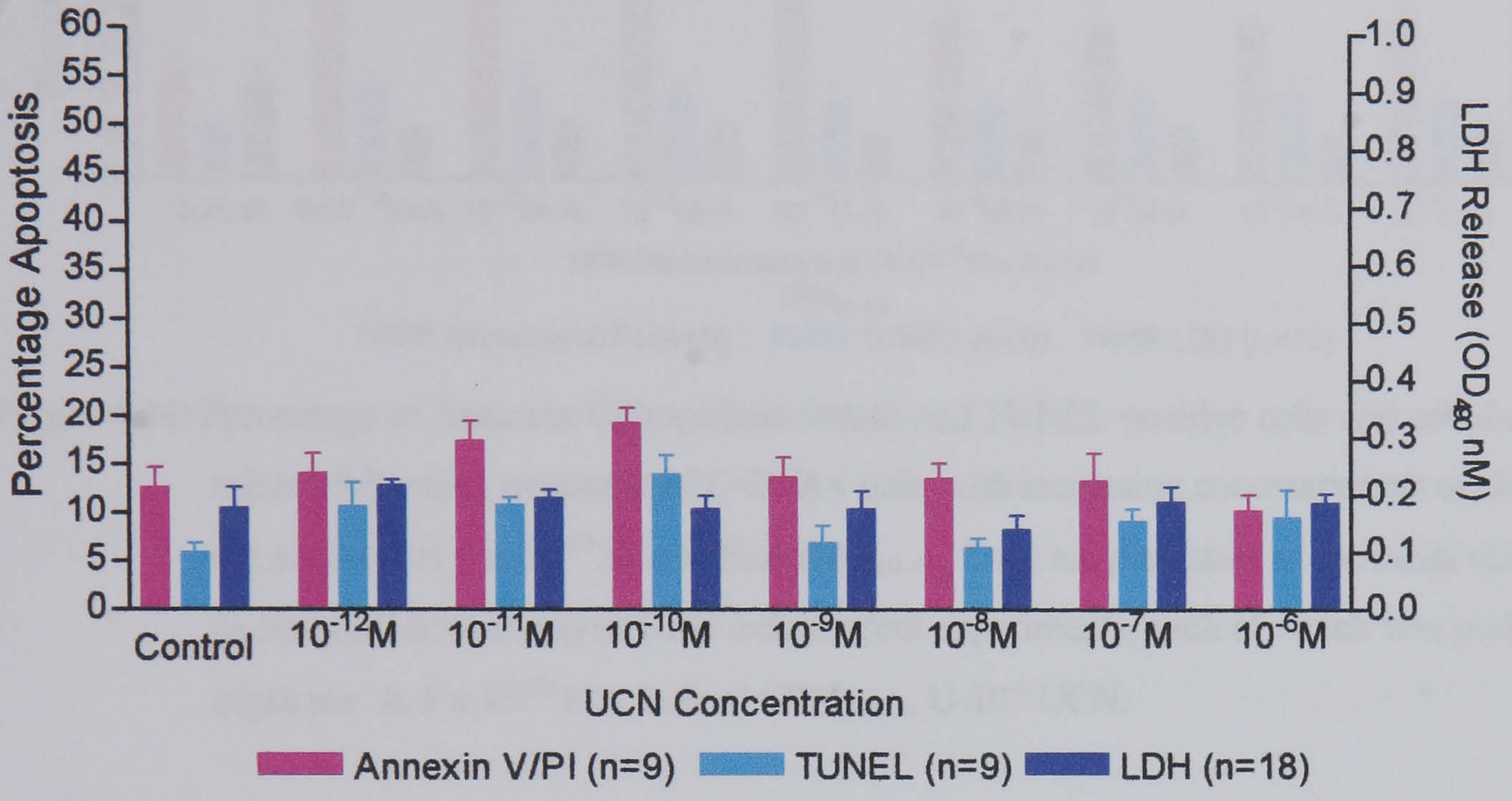

Figure 4.23: Percentage of Annexin V/Propidium Iodide and TUNEL positive cells and cellular LDH release following treatment of C-20/A4 cells with increasing concentrations of exogenous UCN. Data are presented as the mean values (± standard deviations) of three independent experiments, each of which was performed in triplicate.

UCN was used at various concentrations to treat C-20/A4 cells. Firstly, we assessed whether a range of concentrations of exogenous UCN influenced basal cell death. While significant increases in Annexin V/PI and TUNEL staining were seen with 10^{-12}M to 10^{-10}M concentrations, no significant changes in cell death parameters were seen with lower concentrations. The optimum concentration for UCN was established to be 10^{-8}M as a suitable level of protection was observed between 10^{-9}M-10^{-6}M and showed no significant apoptosis as compared to control up to 10^{-6} M UCN ($P>0.05$).

4.3.5.2 The competitive inhibition of UCN by α helical $CRH_{(9-41)}$

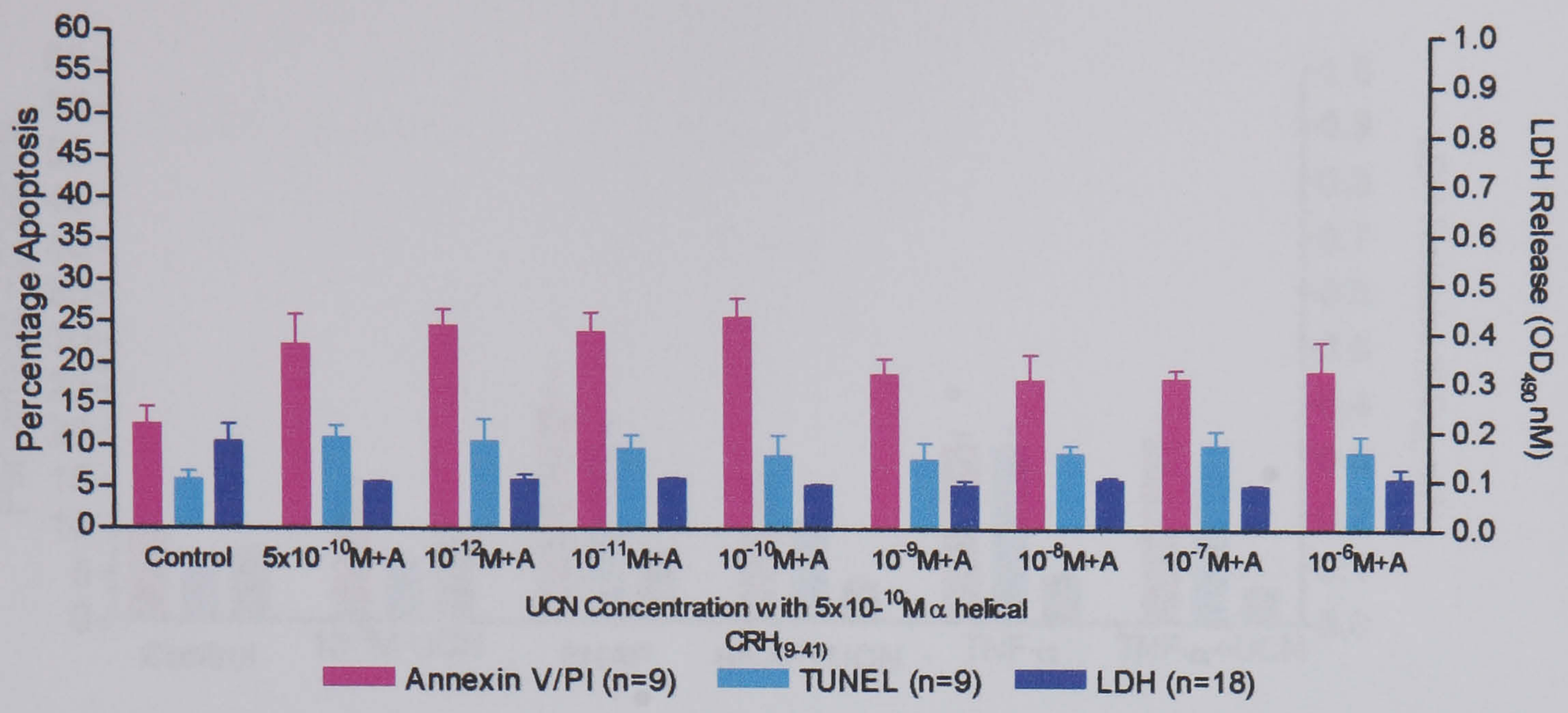

Figure 4.24: Percentage of Annexin V/Propidium Iodide and TUNEL positive cells and cellular LDH release following treatment of C-20/A4 cells with increasing concentrations of UCN and the addition of 5×10^{-10} M α helical $CRH_{(9-41)}$. Data are presented as the mean values (± standard deviations) of three independent experiments, each of which was performed in triplicate. A-5×10^{-10} M α helical $CRH_{(9-41)}$, U-10^{-n} UCN.

The concentration for α helical $CRH_{(9-41)}$ used for most experiments was 10^{-8} M, a concentration which induced high levels of apoptosis. Figure 4.13 had shown that a more modest level was observed between 10^{-9} M-10^{-10} M. A concentration in the middle of this range, 5×10^{-10} M was used to investigate the ability of various concentrations of UCN to lower the apoptotic cell death in α helical $CRH_{(9-41)}$ treated C-20/A4 cells to determine if UCN and α helical $CRH_{(9-41)}$ were competitively occupying CRH receptors. 5×10^{-10} M α helical $CRH_{(9-41)}$ produced a modest, but significant increase in Annexin V/PI but not in TUNEL staining, which was, however, not significantly reduced ($P>0.05$) by addition of 10^{-12} M to 10^{-10} M exogenous UCN. Whilst at 10^{-10} M U+A - 10^{-9} M U+A, a significant decrease ($P<0.01$) in apoptosis was observed for Annexin V/PI staining only, after which no significant changes in cell death parameters was observed ($P>0.05$).

4.3.5.3 The effects of UCN co-treatment on C-20/A4 cells subjected to pro-apoptotic stimuli

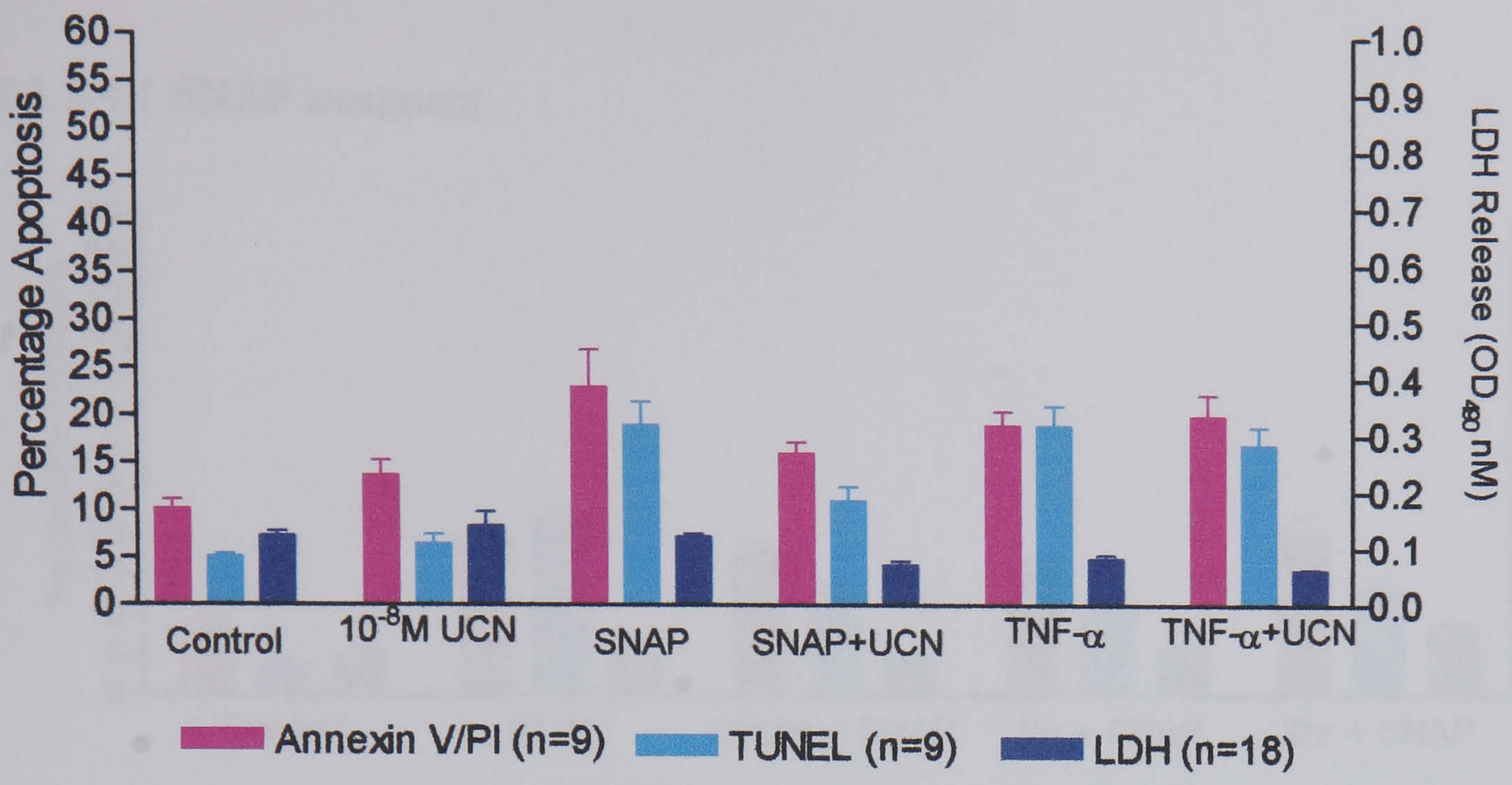

Figure 4.25: Percentage of Annexin V/Propidium Iodide and TUNEL positive cells and cellular LDH release following treatment of C-20/A4 cells with SNAP and TNF-α with/without UCN. Data are presented as the mean values (± standard deviations) of three independent experiments, each of which was performed in triplicate.

Figure 4.25 shows the results of UCN treatment of C-20/A4 cells in the presence of 1mM SNAP and 70pg/ml TNF-α. 10^{-8}M UCN was added together with the pro-apoptotic stimuli for 6 hours. Treatment with UCN alone showed a minimal level of apoptosis (14% Annexin V/PI and 6% TUNEL) which, although slightly increased compared to control treated cells was not significantly different ($P>0.05$). C-20/A4 cells treated with both UCN and SNAP showed significantly lower levels of apoptosis (16% Annexin V/PI and 11% TUNEL) compared to those treated with SNAP alone ($P<0.001$) indicating a degree of protection. Co-treatment of UCN and TNF-α however did not show any significant difference in apoptotic cell death compared to TNF-α alone.

4.3.5.4 The effects of UCN pre-treatment on C-20/A4 cells subjected to pro-apoptotic stimuli.

4.3.5.4.1 SNAP treatment

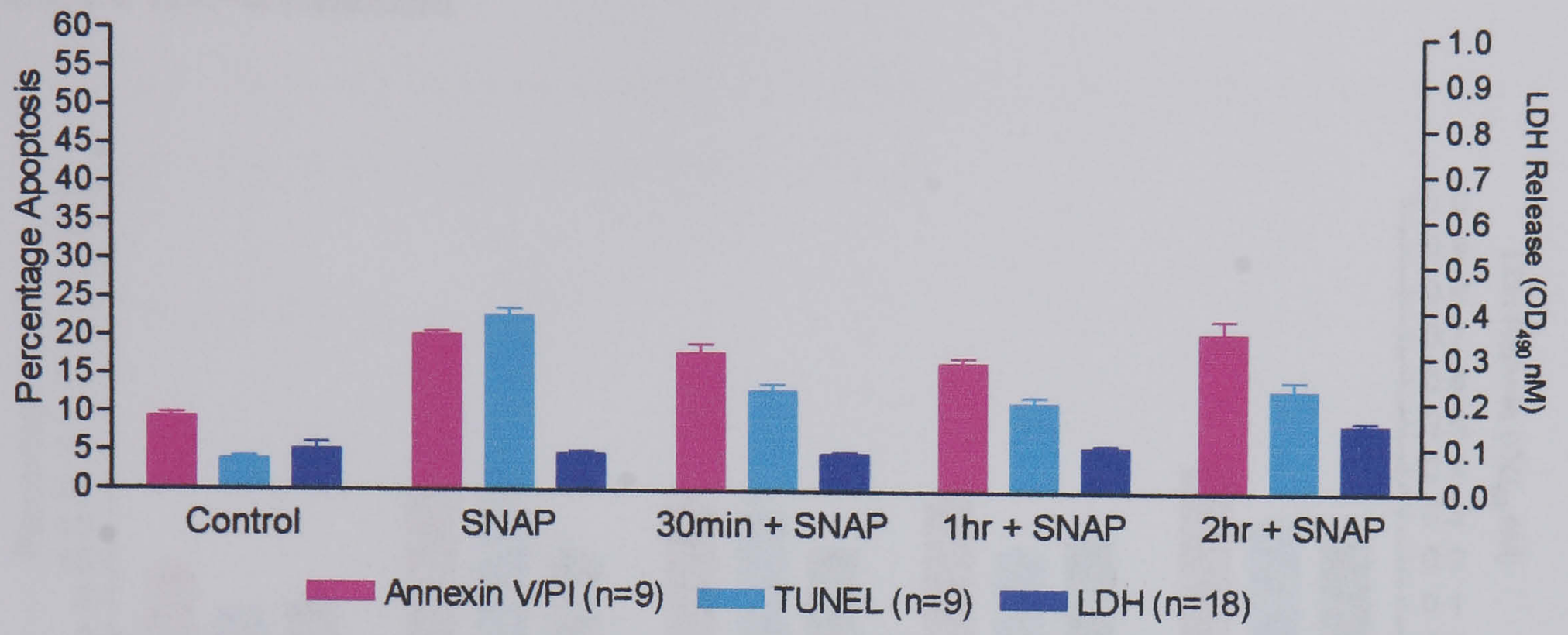

Figure 4.26: Percentage time course of Annexin V/Propidium Iodide and TUNEL positive cells and cellular LDH release after pre-treatment of C-20/A4 cells with UCN prior to 1mM SNAP treatment. Data are presented as the mean values (± standard deviations) of three independent experiments, each of which was performed in triplicate.

30 min + SNAP – UCN pre-treated 30 minutes prior to the addition of SNAP
1 hr + SNAP – UCN pre-treated 1 hour prior to the addition of SNAP
2 hr + SNAP – UCN pre-treated 2 hour prior to the addition of SNAP

As shown in Figure 4.25, co-treatment of C-20/A4 cells with SNAP and UCN results in a degree of protection against apoptosis induced by SNAP alone. The experiments shown in Figure 4.26 were designed to assess if pre-treatment with UCN before the addition of SNAP results in increased levels of protection. UCN co-treatment of TNF-α did not however induce any significant protection (Figure 4.25) and so a similar pre-treatment study was performed for TNF-α to see if this conferred protection (Figure 4.27). Treatment with SNAP alone demonstrated a significant increase in apoptotic death compared to untreated cells ($P<0.001$). A 30 minute exposure to UCN showed a significantly lower level of TUNEL but not Annexin V/PI staining compared to SNAP alone ($P<0.001$) and was also significant compared to control ($P<0.05$). At 1 hour treatment with SNAP, apoptotic levels remained unchanged and were not significantly different to the 30 minute treatment ($P>0.05$), but significant against control ($P<0.05$). Whilst at 2 hour treatment apoptotic levels slightly increased, but were not significantly different to 30 minute treatment ($P>0.05$) or 1hr treatment ($P>0.05$), but significant

against control ($P<0.05$). Since pre-treatment of UCN had made no significant difference in protection of C-20/A4 cells, it was decided that UCN would be added to cultures at the same time as SNAP in future experiments.

4.3.5.4.2 TNF-α treatment

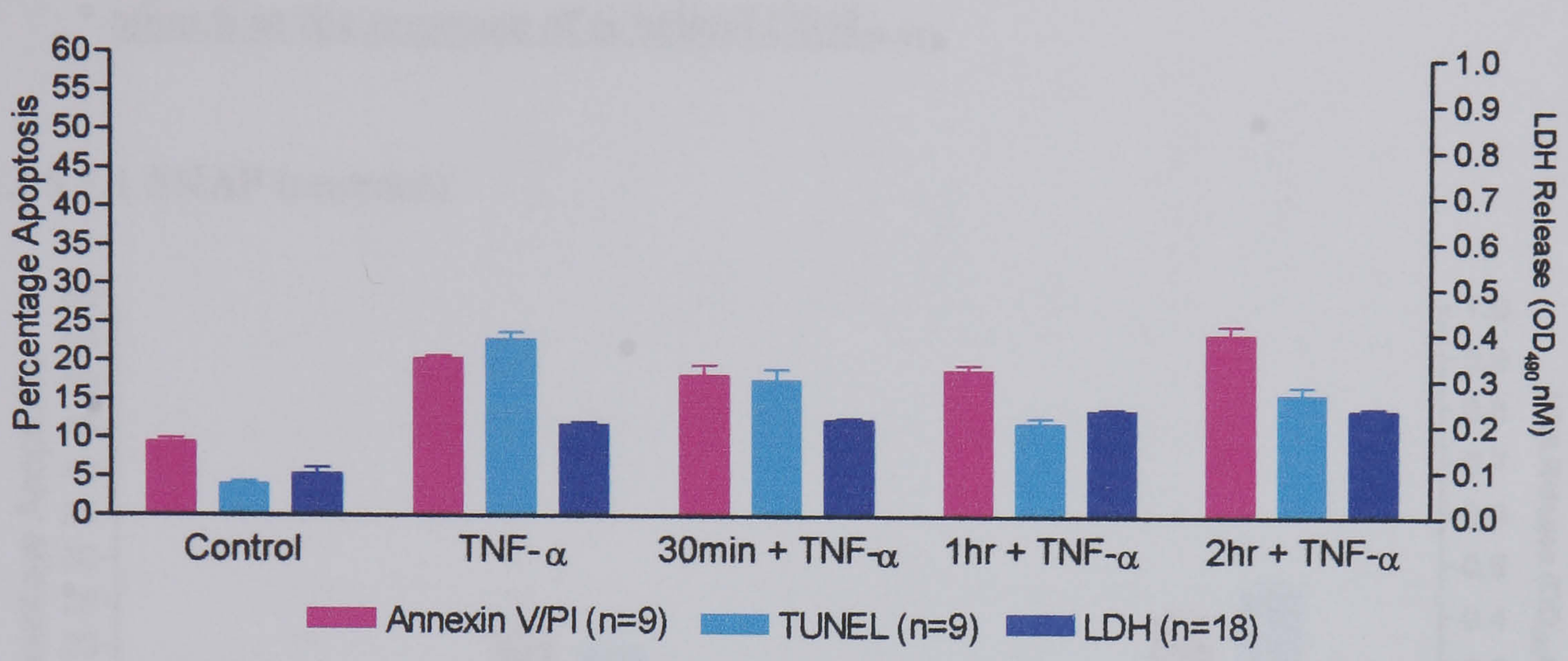

Figure 4.27: Percentage time course of Annexin V/Propidium Iodide and TUNEL positive cells and cellular LDH release after pre-treatment of 10^{-8}M UCN followed by 70pg/ml TNF-α in C-20/A4 cells. Data are presented as the mean values (± standard deviations) of three independent experiments, each of which was performed in triplicate.

30 min + TNF-α – UCN pre-treated 30 minutes prior to the addition of TNF-α
1 hr + TNF-α – UCN pre-treated 1 hour prior to the addition of TNF-α
2 hr + TNF-α – UCN pre-treated 2 hour prior to the addition of TNF-α

Control experiments showed minimal level of apoptosis and necrosis. Treatment with TNF-α alone showed a significantly higher level of apoptotic and low necrotic death as compared to basal level ($P<0.001$). Pre-treatment for 30 minutes did not show decrease apoptotic death for both Annexin V/PI and TUNEL staining compared to control ($P<0.001$) but was still observed to be significant. Whilst significantly decreased levels (30 min + TNF-α) were observed in TUNEL staining compared to TNF-α alone ($P<0.01$). Pre-treatment for 1 hr did not result in low apoptotic levels compared to control, but was observed to be significant ($P<0.01$). However, a significant reduction in apoptosis was observed in TUNEL staining ($P<0.01$) as compared to TNF-α alone with no significance observed for Annexin V/PI ($P>0.05$). Pre-treatment at 2 hr again did not result in low apoptotic cell death compared to control ($P<0.01$). Although apoptotic levels were significantly decreased with TUNEL staining ($P<0.01$) compared to TNF-α

alone, with no significance observed with Annexin V/PI ($P>0.05$) even though apoptotic levels were higher. Due to the fact that UCN pre-treatment made no significant difference in protection of C-20/A4 cells as compared to Figure 4.25, it was decided that UCN would be added to cultures at the same time with TNF-α in future experiments.

4.3.5.5 The effects of UCN co-treatment on C-20/A4 cells subjected to pro-apoptotic stimuli in the presence of α helical $CRH_{(9-41)}$

4.3.5.5.1 SNAP treatment

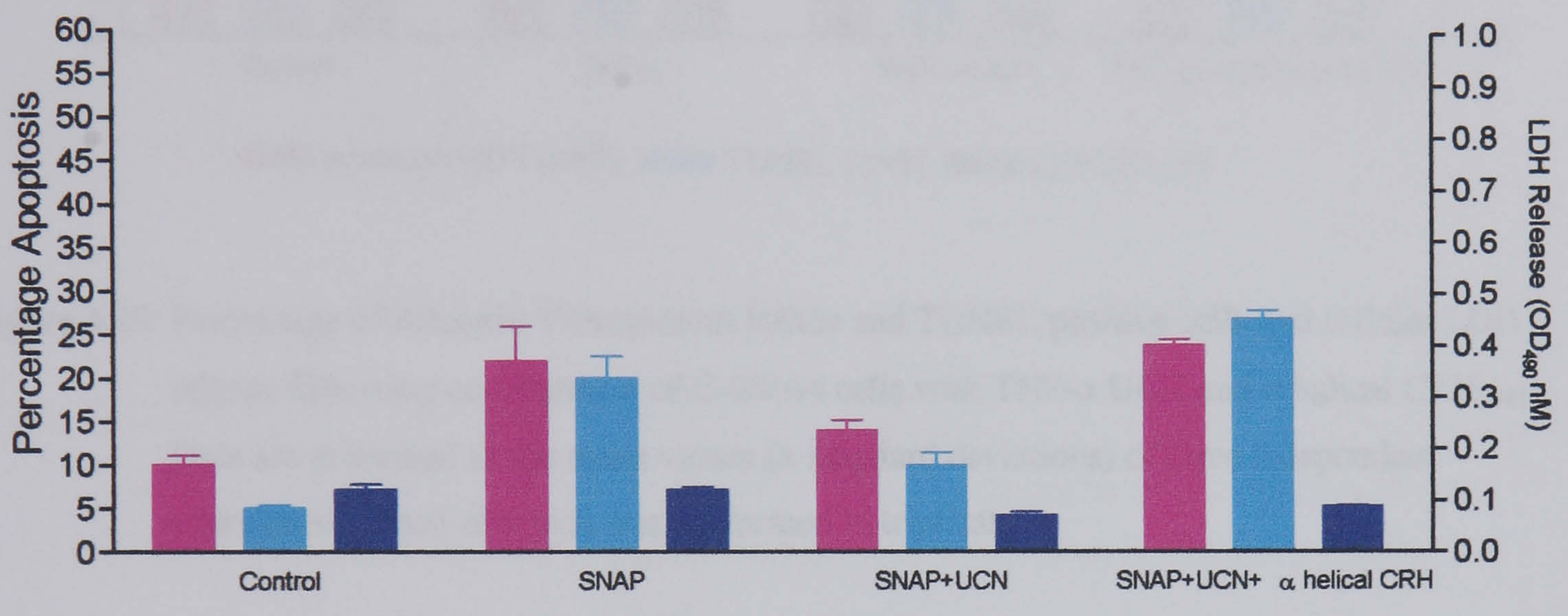

Figure 4.28: Percentage of Annexin V/Propidium Iodide and TUNEL positive cells and cellular LDH release following co-treatment of C-20/A4 cells with SNAP, UCN and α helical $CRH_{(9-41)}$. Data are presented as the mean values (± standard deviations) of three independent experiments, each of which was performed in triplicate.

As shown in Figure 4.28, and confirming previous data (Figure 4.25) significantly decreased levels of apoptosis (14% Annexin V/PI and 10% TUNEL) were observed with the co-treatment of both SNAP and 10^{-8} M UCN ($P<0.001$). This cytoprotective effect however was reversed when α helical $CRH_{(9-41)}$ was added to the cultures with levels of 24% Annexin V/PI and 27% TUNEL staining, a significant increase when compared to SNAP+UCN ($P<0.001$).

4.3.5.5.2 TNF-α treatment

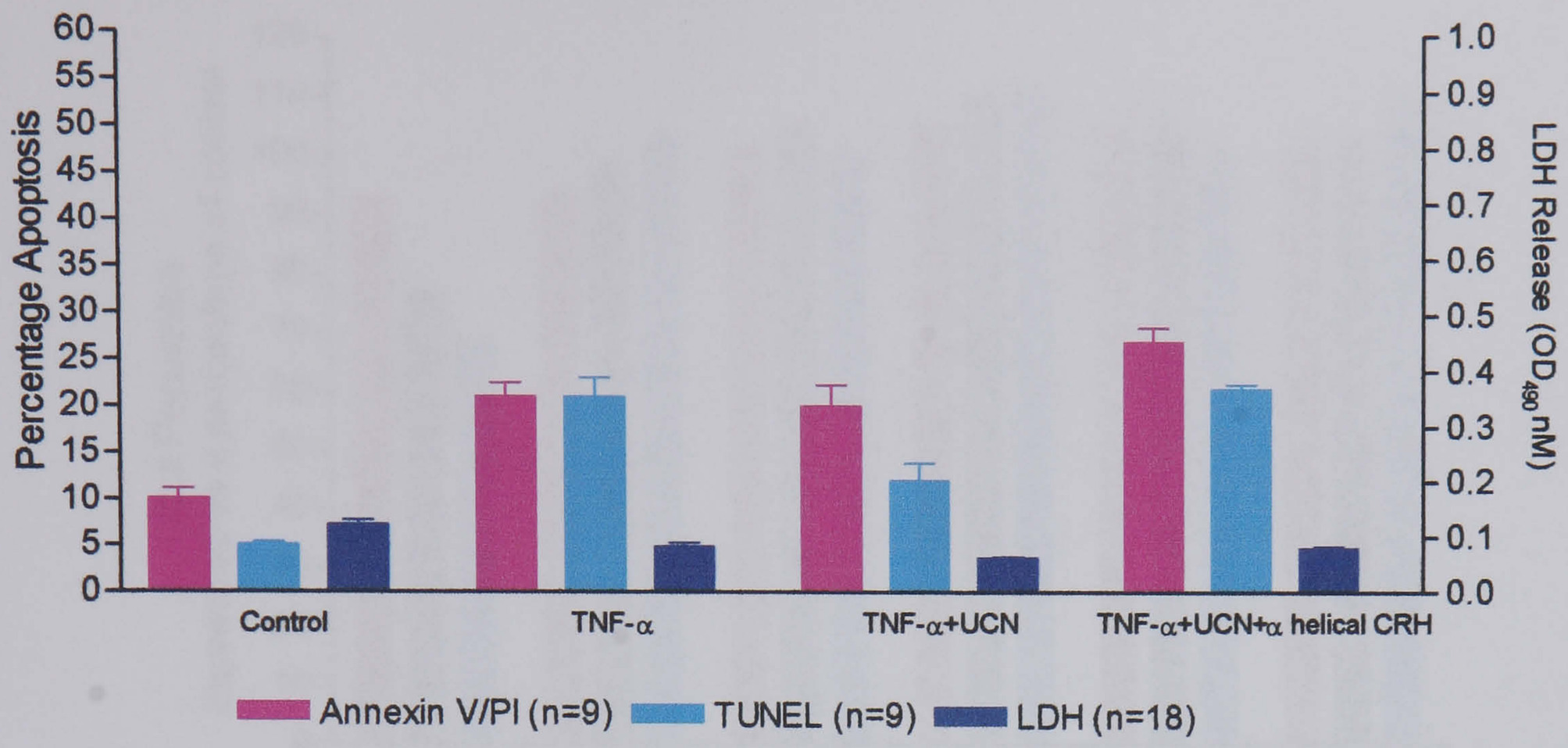

Figure 4.29: Percentage of Annexin V/Propidium Iodide and TUNEL positive cells and cellular LDH release following co-treatment of C-20/A4 cells with TNF-α UCN and α helical $CRH_{(9-41)}$. Data are presented as the mean values (± standard deviations) of three independent experiments, each of which was performed in triplicate.

As observed in Figure 4.29, TNF-α alone treated cells showed a significant increase in apoptosis ($P<0.001$) in C-20/A4 cells, as compared to control cells. With the co-treatment of TNF-α and UCN levels of TUNEL but not Annexin V/PI staining was significantly reduced ($P<0.05$). Again, the reduction in TUNEL positivity in response to UCN treatment was significantly reversed by α helical $CRH_{(9-41)}$ ($P<0.001$, TNF-α+UCN+α helical $CRH_{(9-41)}$ vs TNF-α+UCN).

4.3.5.6 The effects of exogenous UCN on cell proliferation

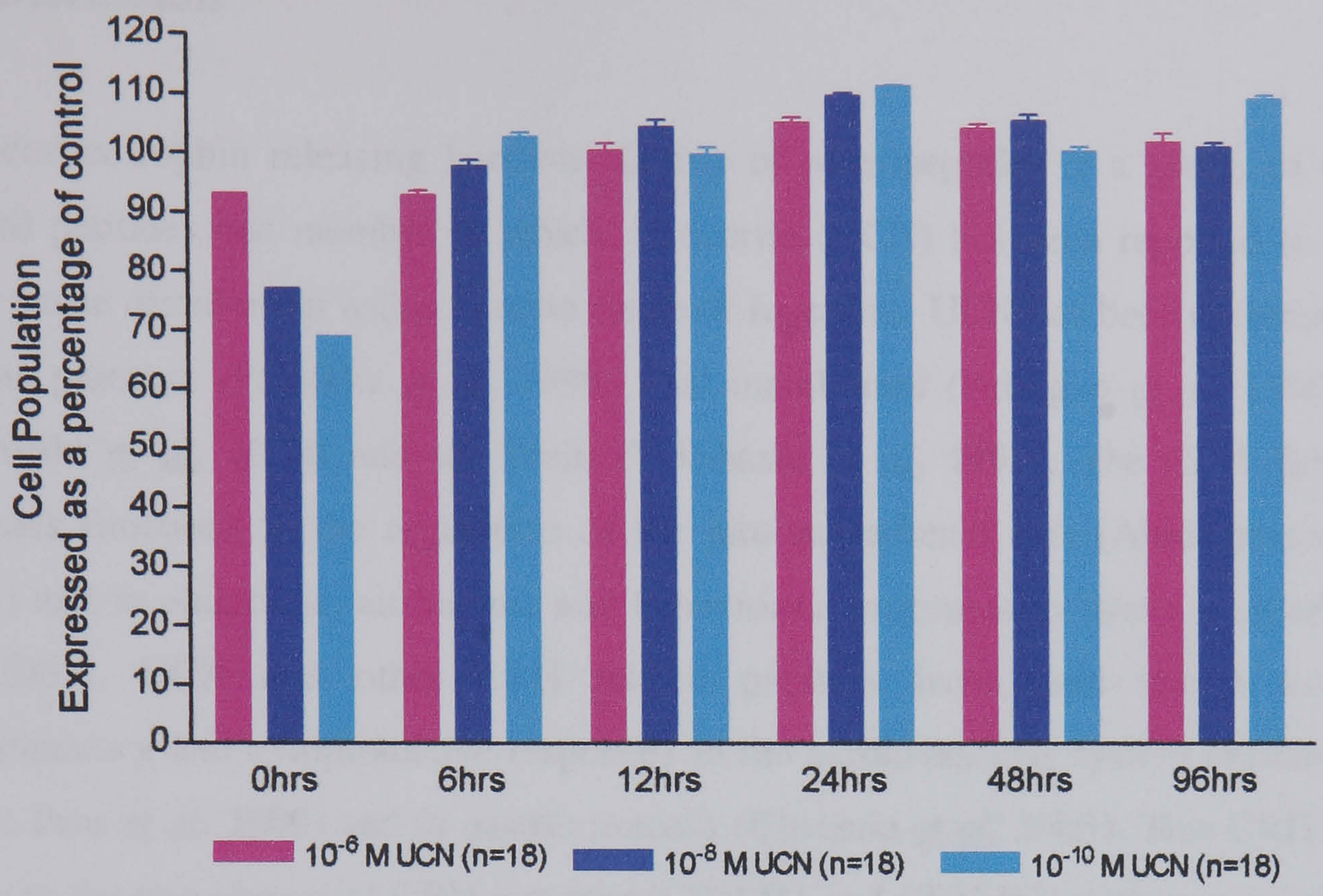

Figure 4.30: C-20/A4 cell numbers following treatment with various concentrations of UCN expressed as a percentage of the growth of a control (untreated populations). Data are presented as the mean values (± standard deviations) of three independent experiments, each of which was performed in triplicate.

The neutral red assay was used to monitor the effects of various concentrations of UCN, on the growth rate of C-20/A4 cells in monolayer. Since, previous experiments detailed here have shown that UCN may be a growth factor as well as a cytoprotective agent on C-20/A4 chondrocytes, these experiments were designed to assess whether exogenous UCN also had an effect on cell growth rate. As observed in Figure 4.30, cell number remained relatively stable, and cell proliferation was not affected significantly when compared to the control population. No significant changes were observed over time ($P>0.05$).

4.4 Discussion

The corticotrophin releasing hormone family of neuropeptides is a group of closely related peptides one member of which, Urocortin (UCN) has been reported to have a wide tissue distribution with a diverse range of functions. UCN has been detected in the human placenta (Petraglia *et al*, 1996) fetal membranes (Petraglia *et al*, 1996), skin (Slomiski *et al*, 2000) and the brain (Takahashi *et al*, 1998). The CRH family of peptides functions in the regulation of the pituitary-adrenal axis (Abrahamson *et al*, 2001) and in endocrine, autonomic and behavioural responses to stress (Lubomirov *et al*, 2001). UCN and other CRH related peptides have been shown to affect inflammatory and cytoprotective responses in the cardiovascular system (Kohno *et al*, 2001; Brar *et al*, 2000) and in gastric mucosa (Chatzaki *et al*, 2003). This CRH family binds to the two classes of CRH receptor (CRH-R1 and CRH-R2) with varying affinity. CRH and UCN bind to the CRH-RI receptor with similar potency, whereas UCN, UCN II and UCN III bind to the CRH-R2 subtype with higher affinity than CRH. UCN II and UCN III are exclusive CRH-R2 ligands and do not bind to CRH-R1 (Reyes *et al*, 2001; Lewis *et al*, 2001).

This chapter first investigated the basal expression of UCN in C-20/A4 chondrocyte cells and variations in expression in response to stimuli. Endogenous UCN expression was established by reverse transcription-polymerase chain reaction (RT-PCR) in C-20/A4 cells, the first demonstration of UCN mRNA (and therefore, by inference, protein) in chondrocytes to the best of our knowledge. In order to perform further experiments, PCR optimization was performed with regard to annealing temperature, cycle number and Mg^{2+} concentration. These conditions were established as an annealing temperature of 64°C for 33 amplification cycles with 1mM magnesium ion concentration. For UCN these conditions resulted in strong bands for the gene of interest when analysed by AGE with minimal extraneous products. Optimum conditions were similarly established for the β-actin and GAPDH housekeeping genes using 63°C, 32 cycles, 1mM Mg^{2+} concentration (β-actin) and 58°C, 30 cycles, 1mM Mg^{2+} concentration (GAPDH), although β-actin subsequently proved to be an inappropriate housekeeping gene in these studies.

These PCR parameters were used throughout this study to examine the expression of UCN mRNA in C-20/A4 cells treated with a variety of stimuli. UCN mRNA was

expressed and easily detected in all conditions investigated, as can be seen in Figures 4.10 and 4.11. The original intention was to normalize UCN expression against the β-actin housekeeping gene. However, as the bands in Figure 4.10 clearly show, β-actin expression fluctuates following treatment with the various stimuli making it unreliable as a housekeeping gene for these experiments. A house keeping gene (internal control primer) such as β-actin should not vary under experimental conditions and is used to ensure consistency in sample preparation and loading despite differences in tissue type and localisation. The use of β-actin as a housekeeping gene has also been shown to be problematic by other authors (Harrison *et al*, 2000; Nishida *et al*, 2006) and with these considerations in mind β-actin was abandoned as a housekeeping gene for the studies in this thesis and GAPDH was adopted. GAPDH is one of the glycolytic enzymes involved in energy production, but has many different biological properties including DNA repair and replication, translational control of gene expression, endocytosis, and apoptosis (Harrison *et al*, 2000). The data shown in Figure 4.11a indicates a much more stable level of GAPDH expression in C-20/A4 chondrocytes exposed to various stimuli, than that observed for β-actin in Figure 4.10 which validates the use of this gene as an alternative housekeeping gene. The amplification products were compatible with the expected sizes for UCN (172 bp) and GAPDH (437 bp) and their identity was further confirmed by sequencing and subsequent BLAST searches of the human genome, (accession numbers given in table 4.3) verifying the presence of UCN mRNA in C-20/A4 cells. PCR data was normalized by expressing data as a ratio of UCN:GAPDH densitometry readings (4.11b). Several important observations may be made from this normalized data. UCN is expressed at a basal level in untreated C-20/A4 chondrocytes but, this data also clearly shows that UCN mRNA expression increases when C-20/A4 cells are treated with SNAP/NO and that this increase is statistically significant ($P<0.01$). Treatment with TNF-α and α helical $CRH_{(9-41)}$, a CRH receptor antagonist however, does not result in any significant increase in UCN above the basal levels. This data was further supported by real time PCR using commercial 'assay on demand' primer/probe kits (Figure 4.12). This method also showed that SNAP treatment of C-20/A4 cells stimulated the production of UCN whereas TNF-α and α helical $CRH_{(9-41)}$ did not. The real time PCR data actually suggest that TNF-α and α helical $CRH_{(9-41)}$ reduce UCN expression which was statistically significant when compared to the control cells.

The data would suggest that UCN may be a specific cytoprotective agent produced in response to certain stimuli/apoptotic pathways only. As well as the presence of UCN in C-20/A4 cells, the beneficial effects of UCN mRNA has been reported in many other tissues including brain, heart, spleen, skeletal muscle, kidney, liver, adipose tissue, intestine, lungs, stomach, skin, adjuvant-induced arthritic joints, placenta and the ovary (Boorse and Denver, 2006). The present data is consistant with the data of Okosi *et al*, (1998) who also demonstrated increased endogenous mRNA UCN expression in rat cardiac myocytes, which was increased further by thermal shock resulting in UCN protection of cardiac myocytes from cell death triggered by hypoxia. The present data is also supported by Brar *et al*, (1999), who demonstrated that simulated ischeamia (which caused both necrotic and apoptotic death of neonatal rat cardiac myocytes) is linked with increased expression of UCN mRNA and peptide production. Kohno *et al*, (2001) and Uzuki *et al*, (2001) have both reported that UCN mRNA and immunoreactivity was expressed in synovial lining cell layer, synovial fibroblast like cells, blood vessel endothelial cells and infiltrating mononuclear inflammatory cells in human arthritic joints. They also established that the expression of UCN mRNA in synovial tissues in RA was more significant than that in OA and correlated with the level of inflammation. This could be due to the higher level of cytokines and NO in RA. They also demonstrated that synovium from healthy patients showed a decreased level of UCN expression. They suggested UCN in the inflamed joints may be secreted by the terminals of peripheral neurons as well as immune cells. This data may also suggest that UCN may play an important role as an autocrine and/or paracrine regulator of synovial inflammation (Oki and Sasano, 2004). However, the present data disagrees with the data of Honjo *et al*, (2006), who reported the presence of TNF-α (10 ng/ml) had resulted in increased UCN mRNA levels in HUVECs observed in a time and dose dependent manner. Clearly, this was not observed with C-20/A4 cells. This could be due to Honjo *et al*, using a higher dose of TNF-α which could indicate that UCN is expressed at increased TNF-α concentration, whilst in this study, the concentration of TNF-α was much lower (70pg/ml), which could explain why UCN was not expressed.

To investigate the endogenous production of UCN further, cells were treated with various concentrations of the CRH antagonist α helical $CRH_{(9-41)}$. In order to first establish a suitable concentration of α helical $CRH_{(9-41)}$ to use, C-20/A4 cells were treated with a range of concentrations (10^{-12}M to 10^{-6}M) which resulted in a dose dependent increase in apoptosis (Figure 4.13). Low concentrations of α helical

$CRH_{(9-41)}$ from 10^{-12}M to 10^{-10}M resulted in no significant increase in apoptotic or necrotic cell death as compared to control cells ($P>0.05$). A gradual dose dependent increase in apoptosis was observed however from 10^{-9}M to 10^{-6}M α helical $CRH_{(9-41)}$ with no change in necrosis. It is likely that receptor saturation with ligands occurs at higher concentrations of α helical $CRH_{(9-41)}$ than at low concentrations, since apoptotic levels remained unchanged from 10^{-9}M to 10^{-6}M. These data suggest that the endogenous UCN is produced even by resting C-20/A4 cells which is secreted and acts in an autocrine/paracrine fashion to promote cell growth/survival. For the purposes of further experiments, a concentration of 10^{-8}M α helical $CRH_{(9-41)}$ was used, since this was apoptogenic. This dose is in agreement to the data of Brar *et al*, (1999), who established that the dose 10^{-8}M α helical $CRH_{(9-41)}$ was effective in abolishing the protective effect of UCN in cardiac myocytes exposed to simulated ischaemia.

The increase in apoptotic death with α helical $CRH_{(9-41)}$ alone would support the existence of a CRH-R mediated protective mechanism. Whilst this data would indicate a basal expression of UCN which could contribute to cell survival, the data from section 4.3.1.4.2 indicates that UCN expression is induced by pro-apoptotic stimuli. Experiments were therefore conducted to investigate the nature of this UCN induction further and to determine if this too could be blocked by α helical $CRH_{(9-41)}$. Chondrocyte cells were therefore treated with 1mM SNAP and 10^{-8}M α helical $CRH_{(9-41)}$. Figure 4.14 shows low levels of apoptosis in control cells, but a high level of apoptosis in cells treated with 10^{-8} M α helical $CRH_{(9-41)}$ which was significantly different from control cells ($P<0.001$). This would indicate an endogenous basal production of a member or members of the CRH family of peptides (CRH, UCN, UCN II, or UCN III). The addition of α helical $CRH_{(9-41)}$ would block the binding of these CRH peptides to the CRH receptor (at present it is not known which type of CRH receptor CRH-R1 or CRH-R2 is expressed by chondrocytes, but α helical $CRH_{(9-41)}$ inhibits both receptor subtypes). SNAP treatment of C-20/A4 cells resulted in an increase level of apoptosis, however, apoptotic levels in SNAP treated cells were significantly less than those treated with α helical $CRH_{(9-41)}$ alone, ($P<0.01$). Treatment with both SNAP and α helical $CRH_{(9-41)}$ showed a further increase of apoptosis to 30% Annexin V/PI and 25% TUNEL positive cells, ($P<0.05$) against SNAP alone. These data and that from section 4.3.1.4.2 therefore suggest that the increased endogenous urocortin induced by SNAP is also released, and may exert, a cytoprotective effect by

possibly binding to a CRH receptor on the C-20/A4 cell surface due to the antagonist used α helical $CRH_{(9-41)}$ (blocks either CRH-R1/2). This increase in chondrocyte death following CRH receptor blockade is a novel observation and would support the presence of a CRH receptor-dependent protective mechanism in C-20/A4 cells. This hypothesis is supported by the work of Brar *et al,* (1999), who demonstrated that α helical $CRH_{(9-41)}$ treatment of cardiac myocytes significantly reduced the protective effect of preconditioned media.

In experiments performed with TNF-α (Figure 4.15), untreated cells showed low levels of apoptosis whilst α helical $CRH_{(9-41)}$ alone, as in the SNAP experiments, significantly increased ($P<0.001$) apoptotic levels. Treatment with 70pg/ml TNF-α showed an induction of apoptosis. Similarly to the SNAP experiments, a further increase in cell death was achieved in the presence of both TNF-α and α helical $CRH_{(9-41)}$ and this was again observed to be significantly different compared to TNF-α alone ($P<0.01$), correlating with the results observed with the SNAP experiments. This may indicate that some CRH family peptide binding to CRH receptors was taking place resulting in a degree of protection from the stimulus although the data from Figure 4.15 indicates that, unlike SNAP, TNF-α does not stimulate the production of UCN. Data from these experiments would indicate that chondrocytes may synthesise and release a member of the CRH family (possibly UCN, as suggested by the RT-PCR data), which protects from apoptosis by binding to a CRH receptor. The involvement of a CRH family peptide is further supported by the data of Okosi *et al,* (1998) who showed that UCN expression in rat heart is increased by thermal shock and that exogenous UCN protects primary cardiac myocytes from cell death induced by simulated ischaemia suggesting that UCN may work as an endogenous cardioprotective agent. This is further supported by Scarabelli *et al,* (2003) who reported that myocytes which expressed UCN at the protein level resulted in no TUNEL positive cells, suggesting that endogenous UCN effectively protects those myocytes in which it is produced. It has been suggested by Vaughan *et al*, (1995), Kozicz *et al*, (1998) and Oki *et al*, (1998) that UCN may be the endogenous mammalian ligand for the CRH-R2 receptor and binds to this receptor with high affinity, although the identity of the CRH receptors on chondrocytes has not been established.

As the α helical $CRH_{(9-41)}$ studies described here clearly suggest the existence of a UCN/CRH-R circuit, an alternative approach was sought using selective depletion of UCN from the culture medium of growing C-20/A4 cells, using an anti human UCN antibody. Figure 4.16, shows that, the selective depletion of UCN with an anti-UCN antibody results in an increased level of cell death, even greater than that caused by the addition of α helical $CRH_{(9-41)}$ and shown to be significant against the control ($P<0.001$) and α helical $CRH_{(9-41)}$ ($P<0.001$). The addition of anti-albumin antibody (isotype control) did not result in a significant increase ($P>0.05$) in cell death, with a similar level of apoptosis observed to that of the control cells. These data support that from the α helical $CRH_{(9-41)}$ studies suggesting the existence of an endogenous cytoprotective mechanism involving UCN in chondrocytes.

The data from the UCN depletion studies and the RT-PCR data indicate that UCN may be endogenously produced and released to act in an autocrine/paracrine manner as a cytoprotective mechanism. This hypothesis is supported by the cardiac myocyte data of Brar *et al*, (1999) who showed that preconditioned media from cardiac myocytes exposed to brief simulated ischaemia significantly protected other cardiac myocytes from cell death. Experiments were therefore designed to investigate whether similar phenomenon occurred in C-20/A4 chodrocyte cells.

The protective effects of preconditioned media were evaluated by growing C-20/A4 cells for 6 hours in the presence of 1mM SNAP (PS) or 70pg/ml TNF-α (PT), harvesting the medium and using it to treat other cells. Control medium was also generated from cells grown for 6 hours without SNAP or TNF-α (PC). These preconditioned media were used to treat additional C-20/A4 cells in conditions similar to those used in the SNAP and TNF-α experiments previously. However, no protection was observed using any of the preconditioned media, at either 10% or 100% concentration (Figures 4.17-4.22). Even if endogenous UCN was being released, any potential effect is presumably being masked by the presence of other pro-apoptotic factors also present. This whole series of experiments does not, therefore contribute to the confirmation or reflection of the hypothesis for an autocrine/paracrine endogenous UCN-CRH-R protective pathway.

As selective depletion of endogenous UCN results in increased cell death, the chondroprotective role of UCN was examined further, by first incubating C-20/A4 cells

in various concentrations of exogenous UCN to investigate the response of these cells to UCN in the absence of pro-apoptotic stimuli. After 6 hours the cells were assessed for cell death by the three assays. Figure 4.23 illustrates that, after an initial rise in apoptosis between the concentrations 10^{-12}M-10^{-10}M a gradual decrease to control levels occurs at higher concentrations. For the purposes of further experiments, a concentration of 10^{-8}M UCN was used, since this was not apoptogenic. This dose is in agreement to the data of Okosi *et al*, (1998), Brar *et al*, (1999), Schulman *et al*, (2002) and Chanalaris *et al*, (2005), who established a dose of 10^{-8}M UCN to be potective in cardiac cells, and further supported by Honjo *et al*, (2006) who also found this dose was protective in HUVECs.

The data in Figure 4.24 indicates that UCN cytoprotective action is competitively inhibited by α helical $CRH_{(9-41)}$. Whilst a concentration of 10^{-8}M α helical $CRH_{(9-41)}$ (Figure 4.13) was used for most experiments, a lower concentration of $5x10^{-10}$M was used for these experiments to give increased sensitivity. This experiment was designed to investigate whether varying concentrations of UCN are able to lower the apoptotic cell death in α helical $CRH_{(9-41)}$ treated C-20/A4 cells and therefore by inference whether UCN and α helical $CRH_{(9-41)}$ are competitively occupying CRH receptors. At lower concentrations (10^{-12} M-10^{-10} M) of UCN it appears that α helical $CRH_{(9-41)}$ occupies the CRH receptors to a greater extent than UCN, resulting in increased cell death. As the concentration of UCN increased, levels of apoptosis decreased demonstrating that UCN is likely to be competing with α helical $CRH_{(9-41)}$ for the binding of its receptors. No inference can be made as to the subtype of CRH receptor present since this has not been established in this study, however UCN is known to bind to the CRH-R2 at high potency and efficacy (~5 fold higher) than CRH-R1 (Bale and Vale, 2004).

Once an optimum UCN concentration for further experiments had been decided upon, cells were treated as before with SNAP and TNF-α, but this time with the addition of exogenous UCN at 10^{-8}M (Figure 4.25), in order to investigate any possible protective effects. C-20/A4 cells were co-treated both with SNAP and UCN, and TNF-α and UCN. It can be seen that treatment with SNAP + UCN, showed a decreased level of apoptosis as compared to SNAP alone showing a significant level of protection against cell death ($P<0.01$). With TNF-α + UCN however, no significant protection was observed when compared with TNF-α alone ($P>0.05$). These data clearly show that

exogenous UCN protects C-20/A4 cells from apoptosis, where SNAP (NO) is the stimulus but not where TNF-α is the stimulus. As previously shown in this study, UCN is constitutively expressed and is also inducible by SNAP treatment. The addition of exogenous UCN would increase the pool present in the medium increasing CRH receptor binding and hence protection observed in SNAP treatment. The production of UCN in the presence of TNF-α was previously shown to be significantly lower as compared to SNAP. It is possible that the difference in response of SNAP and TNF-α to UCN could arise from various expressions of the receptors (CRH or calcium channels, because at present the identity of the CRH-R on chondrocytes is not known (discussed later). Whilst Agnello *et al*, (1998) did report that the effect on TNF-α producing cells may be the reason for UCN inhibition, which indicated a lack of protection from TNF-α in the presence of UCN in C-20/A4 chondrocytes.

As discussed earlier, protection is observed when cells were co-treated with SNAP (NO) and UCN but not TNF-α and UCN (Figure 4.25). Studies were also performed to determine if pre-treatment with UCN resulted in further increases in protection. For this reason, cells were pre-treated with UCN at several time points prior to the addition of SNAP (Figure 4.26) and TNF-α (Figure 4.27) and the level of cell death determined. Cell death increased with increased pre-treatment time. Indeed the studies with SNAP (Figure 4.26) indicate the pre-treatment for 30 minutes or 1 hour makes no significant difference to the level of cell death when compared to the level observed with co-treatment of SNAP and UCN (Figure 4.25) ($P<0.001$). Pre-treatment for longer times than this e.g. 2 hours, results in a significant reduction in UCN mediated cytoprotection against SNAP ($P<0.01$). In experiments, where TNF-α provided the pro-apoptotic stimulus (Figure 4.27) UCN pre-treatment had little effect on levels of cell death showing no significant decrease in death at any time point, including co-treatment (Figure 4.25) ($P>0.05$). These data indicate that UCN does not protect chondrocytes further when pretreated. It is possible that at increased treatment times UCN may bind to other sites other than CRH receptors resulting in changed intracellular signals and biological effects. However because receptor ligation was not studied in this thesis, it is not possible to fully conclude on this. It is equally possible however that UCN may have a short half life (plasma half life in normal humans is 52± 3 minutes (Davis *et al* 2004) and may be degraded and no longer biologically active after extended incubations. For this reason it was decided that C-20/A4 chondrocytes would be treated with UCN and the pro-apoptotic stimulus concurrently in future experiments as pre-

treatment with UCN did not protect cells further. The present data disagrees with the data of Brar *et al*, (2000) who showed that a 30 minute pre-treatment with UCN was effective in protecting primary cardiac myocyte culture exposed to lethal simulated hypoxia/ischeamia from apoptotic death as measured by Annexin V/PI and TUNEL staining.

In order, to investigate the protective role of UCN further, C-20/A4 cells were co-treated with exogenous UCN at the established concentration of 10^{-8}M with the pro-apoptotic stimuli (SNAP and TNF-α), but the specificity of the UCN effects were also assessed by the addition of the CRH-R antagonist α helical $CRH_{(9-41)}$ (10^{-8}M). The data observed in Figure 4.28 shows that with the addition of exogenous UCN, apoptotic levels induced by SNAP are notably decreased. Treatment with UCN and SNAP showed a significantly ($P<0.001$) decreased level of apoptosis compared to SNAP alone. However, treatment with SNAP, UCN and α helical $CRH_{(9-41)}$ showed high levels of apoptosis ($P>0.05$), which were not significant against SNAP alone. Therefore the protective effects of UCN are abrogated by this receptor antagonist. C-20/A4 cells were also treated with TNF-α in the absence and presence of 10^{-8}M UCN (Figure 4.29). Observations from Figure 4.29 shows that when cells were treated with TNF-α in the presence of UCN, TUNEL, but not Annexin V/PI staining was significantly reduced ($P<0.05$) as compared to TNF-α alone. This may suggest that UCN is delaying the progression of the apoptotic programme in response to TNF-α. Again, the protective effects of UCN on DNA fragmentation were inhibited by the receptor antagonist.

These data show that with the addition of α helical $CRH_{(9-41)}$, the chondroprotective effect of UCN is abolished in C-20/A4 cells, suggesting that the effects of UCN are possibly CRH receptor mediated (Xu *et al*, 2006). In comparison to Figure 4.14 and 4.15, the main difference observed, is that a CRH peptide appears to be present at basal level because with the addition of α helical $CRH_{(9-41)}$ alone, apoptotic levels had increased considerably. Subsequently, the data obtained in Figures 4.28 and 4.29 shows when UCN was added exogenously the level of UCN content in these media would have increased. Indicating UCN was at a more concentrated level, which helped protect these cells from death especially in SNAP treated cells. Until now, a direct link between UCN and NO has not been reported in C-20/A4 human chondrocytes and as observed previously in this study, UCN production in the presence of TNF-α is small. As shown in the SNAP treated cells α helical $CRH_{(9-41)}$ abolished any protective effects exerted by

this peptide. UCN has also been shown to exert cytoprotective effect in several tissues. This data is in agreement with results obtained from Okosi *et al*, (1998) and Brar *et al*, (1999) who demonstrated UCN to be protective against cardiac myocytes cultured from neonatal rat against lethal ischaemic injury and reduces the infarct size of the intact rat heart prior to and following ischaemic insult and it is therefore possible that UCN also performs a similar protective function in chondrocytes. Brar *et al*, (2002) later reported that UCN generated significant protection against hypoxia/reoxygenation both in terms of total cell death (measured by Trypan blue) and of apoptosis (as measured by Annexin V and TUNEL staining). The present data is also supported by Scarabelli *et al*, (2002) who reported that the addition of UCN (10^{-8}M) reduced necrotic and apoptotic cell death in the isolated rat heart exposed to ischaemia/reperfusion. Cardioprotective effects of UCN on cardiac myocytes stimulated by hypoxia or by ischaemia indicate that calcium channels could take part since ischaemia and hypoxia damage is linked with calcium overload (Scarabelli *et al*, 2002). Tao *et al*, (2004; 2005) reported that UCN may exert the inhibitory effect directly on L-type calcium channels or K_{ATP} channels instead of through binding primarily to its CRH-R receptors (by using CRH-R antagonist) in rat cardiac myocytes. These authors also reported that UCN can directly block L-type calcium currents. This blocking effect of UCN on L type calcium channels would be possible to exert a cardioprotective action by reducing calcium overload via the calcium voltage gated calcium channels, consistent with the studies of Scarabelli *et al*, (2002) who reported that UCN protected the cardiomyocytes against apoptosis which is known to be linked with calcium overload. These reports were further supported by their *in vivo* studies (Tao *et al*,) indicating UCN, similar to the L type calcium channel blocker, verapamil, significantly diminished the infarct size of adult rat hearts. Since calcium plays a vital role in apoptosis, and the evidence suggested by Tao *et al*, it is possible these human chondrocytes could be exerting its inhibitory effects directly on the L-type calcium channels before binding to the CRH receptors, but since the existence of CRH receptors or L-type calcium channels has not been shown in this study, this remains inconclusive. In regards to this Kohno *et al*, (2001) reported that UCN on inflammation is mediated by CRH-R1 in RA and OA patients, and acts in an autocrine or paracrine manner. Webster *et al*, (1996) reported that most of the inflammatory actions of UCN are mediated by CRH-R1 rather than CRH-R2 in rat pituitary, frontal cortex and cerebellum, but not heart, (by using the CRH-R1 antagonist antalarmin). It is possible that C-20/A4 cells could be mediated by CRH-R1 also, because of the antagonist used in this study which recognises both receptor forms. The

present data also agrees with the data of Nishikimi *et al*, (2000), who showed exogenous UCN is potent in protecting cardiac myocytes from necrotic and apoptotic death induced by ischeamia. The present data is also consistant with the data of Pederson *et al*, (2002) who showed that UCN exert its potent protective effect on cultured rat hippocampal neurons with concentrations in the range 0.5-5.0pM, increasing the resistance of these cells to oxidative and excitotoxic stresses via CRH-R1. In this report, however the concentration of UCN had protected cultured hippocampal neurons from cell death was lower than that used with chondrocytes indicating that UCN is cytoprotective even at low doses. The present data is also supported by Facci *et al*, (2003) who reported that the protective effect of UCN (30nM) was abolished by a CRH receptor antagonist in cerebellar granule neurons. The data obtained in this study would indicate that SNAP and TNF-α are both involved in the pathogenesis of OA, and may exert their pro-apoptotic effects via alternative pathways. Since TNF-α is known to induce apoptosis via the death receptor pathway and NO is known to induce apoptosis via the mitochondrial pathway.

The final experiments documented in this chapter (Figure 4.30) were designed to assess whether UCN treatment was showing apparent decreases in cell death by increasing C-20/A4 chondrocyte growth rate or by actually protecting existing cells. The data in Figure 4.30 show no increase in cell growth for UCN treated cells as compared to control, untreated cells, suggesting that UCN is exerting a genuine cytoprotective effect.

Data in this thesis demonstrates, for the first time, the endogenous production of UCN by a human chondrocyte cell line and reveals a cytoprotective role of UCN in chondrocytes subjected to the pro-apoptotic mitochondrial stimulus NO, but not to the death receptor mediated stimulus TNF-α. Many mechanisms may take part in this protective effect of UCN in C-20/A4 cells such as activation of PI3K (Brar *et al*, 2002b), P38 MAPK (Kageyama *et al*, 2003), P42/P44 MAPK (Schulman *et al*, 2002; Brar *et al*, 2002b), or activation of mitochondrial ATP-sensitive potassium channels (K_{ATP}) (Lawrence *et al*, 2002). Whilst the identification of upstream kinases (MAPKs) that are activated by UCN have been established in C-20/A4 cells and other cells, the identification of end effector molecules has not. Lawrence *et al*, (2002; 2004) used Affymetrix gene chip technology to search for global gene changes linked with a 24 hour exposure of rat neonatal primary cardiac myocytes to UCN. They investigated three gene products by this technique, the first one being an ATP sensitive inwardly

rectifying potassium channel (K_{ATP}) subtype, Kir6.1 that is increased 2.6-fold at the protein level in UCN treated cells compared to controls. The mitochondrial K_{ATP} channel blockers further increased apoptotic cell death during ischaemia/reperfusion (I/R) and blocked the protective effect of UCN. The authors reported these channel blockers to be cardioprotective. The second protein they identified was a specific calcium independent phospholipase A_2 ($iPLA_2$) enzyme which was lowered by UCN (2.3 fold). This protein has been shown to enhance its activities during I/R, with a simultaneous increase in its metabolites arachidonic acid (AA) and lysophosphatidylcholine (LPC). LPC has been implicated in cell death during I/R insult and the authors recently discovered that the concentration of LPC in the heart is lowered by a 24 hour UCN treatment. The third and final gene discovered as being altered during UCN treatment is the protein kinase C epsilon (PKCε). The transcript level of this enzyme in cardiac myocytes after UCN treatment were increased 3.6 fold compared to untreated cells. No other isoform of PKC present on the gene chip was changed following UCN treatment. The PKCε is the only isoform of PKC that is protective during ischaemic injury. Since these proteins were not examined in C-20/A4 cells, and the evidence of chondroprotection observed with SNAP treatment (possibly mitochondrial pathway), it is possible these proteins, present in the mitochondria could be activated in these cells with UCN treatment, to endure chondroprotection. It has also been reported that these three proteins can interact, e.g. LPC can alter both K_{ATP} channels and PKCε, whilst PKCε can interact with K_{ATP} channels and $iPLA_2$ (Steer *et al*, 2002).

The protective effect of UCN has been demonstrated to be dependent on the activation of the PI3K (Brar *et al*, 2002b), P38 MAPK (Kageyama *et al*, 2003) and P42/P44 MAPK (Brar *et al*, 2002a) in other cell types. As a result, chapter 5 documents the investigation and possible beneficial effects of UCN via these pathways in C-20/A4 chondrocytes. As well as these pathways, the apoptotic pathway observed in chondrocytes was also investigated using specific antibodies for caspases.

CHAPTER 5

INTRACELLULAR SIGNALLING IN UCN MEDIATED C-20/A4 CHONDROCYTE PROTECTION

5.1 Introduction

Others have previously identified signal transduction pathways associated with urocortin-mediated cytoprotection. Firstly, therefore I wished to establish whether the same pathways were also implicated in the protection of chondrocyte apoptosis by UCN. Secondly, although TNF-α is known to induce apoptosis primarily by binding to TNF-R, and activation of caspase 8, I have investigated which initiator caspase was initially activated by SNAP, to evaluate whether NO-induced chondrocyte apoptosis is mediated by mitochondrial or death receptor pathways.

Inhibitors of the kinase family of signal pathways, are used in research in order to establish specific signaling leading to changes in gene expression. The majority of the protein kinase inhibitors are small molecules that either interfere with phosphorylation or bind (competitively) in the ATP binding site, an area within the activation loop of the kinase in which the dual phosphorylation (especially MAPK) takes place (Hommes *et al*, 2003).

In the present study, three selective inhibitors of different pathways were studied, LY294002 (for P13K inhibition), SB202190 (for P38 MAPK inhibition), and PD98059 (for P42/P44 MAPK inhibition) (Dudley *et al*, 1995). By using selective inhibitors for each pathway, it was possible to study the potential importance of these pathways in C-20/A4 chondrocytes.

LY294002 (2-(4-morpholinyl)-8-phenyl-4H-1-benzopyran-4-one) is a potent and selective cell permeable inhibitor of PI3K which inhibits purified PI3K with an IC_{50} of 1.4μM on purified preparations (Vlahos *et al*, 1994). LY294002, is a compound originated from the naturally occurring bioflavinoid quercetin, and is known to prevent PI3K activity through competitive inhibition of an ATP binding site on the p85α subunit (Vlahos *et al*, 1994). LY294002 is an effective compound for the identification of cellular events that are controlled by the PI3K/Akt axis, and has been shown to enhance apoptosis in a variety of cells by blocking the PI3K/Akt anti-apoptotic pathway (Bancroft *et al*, 2002). LY294002 was shown to totally eliminate PI3K activity in stimulated human neutrophils, as well as inhibiting proliferation of smooth muscle cells in cultured rabbit aortic segments (Vlahos *et al*, 1994). LY294002 was also used to treat

C-20/A4 chondrocytes to establish if the PI3K is involved in the protective mechanism of UCN.

Ever since selective inhibitors of the P38 MAPK and P42/P44 MAPK cascades were first described, they have been extensively used to study the relative contribution of different intracellular signal transduction pathways. The pyridinylimidazole compound 4-(4-fluorophenyl)-2-(4-hydroxyphenyl)-5-(4-pyridyl)1H-imidazole (SB202190) is primarily a specific inhibitor of P38α and P38β (Jiang *et al*, 1996) via competition with ATP for the same binding site on the P38 kinase (Wilson *et al*, 1997). This selective P38 inhibitor is extensively used in investigations of the physiological functions of the P38 MAPK pathway, including lipopolysaccharide, UV, anisomycin-induced *c-jun* and *c-fos* expression (Hazzalin *et al*, 1996), and B cell antigen receptor-induced apoptosis (Graves *et al*, 1998). The P38 MAPK inhibitor is also known to control cytokine production and is anti-inflammatory *in vivo* (Beyaert *et al*, 1996). P38 MAPK inhibitors have been reported to suppress TNF-α mRNA translation (Young *et al*, 1993). However, the inhibitory step that is blocked by P38 inhibitors depends on the cytokine and cell type used (Chin and Kostura, 1993). SB202190 is also known to be a membrane permeable inhibitor of P38 MAPK, and was used to treat C-20/A4 cells to establish if the P38 MAPK is involved in the protective mechanism of UCN. It has been reported that in RA, P38 MAPK and P42/P44 MAPK are activated in rheumatoid synovial tissues (Jackson *et al*, 1998).

The flavone compound 2-(2'-amino-3'-methoxyphenyl)oxanaphthalen-4-one (PD98059) is a cell permeable selective inhibitor of the mammalian MEK-1/2 and has been used widely for investigating the physiological function of P42/P44 MAPK (Pang *et al*, 1995). PD98059 selectively inhibits MEK activation, leading to the inhibition of phosphorylation and the activation of MAPK. In PC12 cells, it blocks the increase in MAPK activity produced by NGF. PD98059 is a very useful tool to assist in the clarification on the role of the MAPK cascade in many biological systems (Yeh *et al*, 2002). As with the other inhibitors, PD98059 was also used to treat C-20/A4 chondrocytes to establish if the P42/P44 MAPK is involved in the protective mechanism of UCN.

Caspases are the main effectors of apoptosis. The caspases are a group of cysteine proteases present in the cell as inactive pro-forms or zymogens, which can be cleaved to

form active enzymes after apoptotic induction. Induction of apoptosis via death receptors and mitochondrial pathways results in the activation of an initiator caspase such as caspase 8 and caspase 9 respectively. These caspases can then activate other caspases in a cascade, which leads to the activation of the effector caspase, caspase 3. These caspases are responsible for the cleavage of the key cellular proteins that leads to the typical morphological changes observed in cells undergoing apoptosis and are discussed in detail in chapter 1.

5.2 Methods

5.2.1 Electrophoresis / Western blotting technique

The SDS-PAGE electrophoresis and Western blot procedure was followed as set in chapter 2 (section 2.2.4.2 and 2.2.4.3 respectively) for P42/P44 MAPK as well as the caspases 3, 8 and 9. The P42/P44 MAPK inhibitor, PD98059 was administered to C-20/A4 cells in the presence and absence of stimuli for a period of 30 minutes. This time point was chosen following initial experiments with exposure lines of 30 and 60 minutes (data not shown). The induction of P42/P44 MAPK activities were clearly detected in C-20/A4 cells at 30 minutes, whilst at 60 minutes the activation had not enhanced any further. This was also observed by Brar *et al*, (2002a) who showed that P42/P44 MAPK actually occurs in the presence of stimuli as early as 5 minutes (weak response) and is further enhanced with the increase in time up to 1 hour (Brar *et al*, 2004). The blots were probed for phosphorylated/total ERK 1/2 using 1:500 dilutions of polyclonal rabbit antibodies specific for the ERK 1/2 proteins and followed as explained in chapter 2.

Western blotting was performed with polyclonal rabbit antibodies (1:500) to caspase 3 (recognizes cleaved active form only, purchased from Cell Signaling), caspase 8 and caspase 9 (recognise both the inactive precursors and the activated forms of either caspase, purchased from Santa Cruz Biotechnology). Analysis is presented as ratio densitometry values of active caspase 3 to GAPDH.

5.2.2 Co-treatment of C-20/A4 cells with signal transduction pathway inhibitors and pro-apoptotic Stimuli.

The LY294002 (PI3K inhibitor) was used to treat C-20/A4 cells along with the pro-apoptotic stimuli (1mM SNAP or 70pg/ml TNF-α) and the CRH family peptide UCN. Cells were cultured as described previously (2.2.1.1) and transferred from a 75cm^2 flask to 6 well plates. Cells were treated at a final concentration of 25μM LY294002 alone (concentration established in a study by Gavaldà *et al,* (2004)), pro-apoptotic stimuli alone (1mM SNAP or 70pg/ml TNF-α), pro-apoptotic stimulus plus 10^{-8}M UCN, or LY294002 with either of the pro-apoptotic stimulus and UCN. Prior to treatment, cells

were cultured and starved of serum for 24 hrs, then re-supplied with either 1% FCS DMEM media for a 6 hr exposure. A similar procedure was repeated with either the P38 MAPK pathway inhibitor SB202190 being replaced by LY294002 at a final concentration of 3μM (established in a study by Wang *et al*, (1999)) or PD98059 (P42/P44 MAPK pathway inhibitor) at a final concentration of 50μM (concentration established in a study by Dudley *et al*, (1995)).

5.3 Results

5.3.1 The investigation of the UCN mediated protective pathways in C-20/A4 cells

5.3.1.1 The effects of PI3K inhibition in C-20/A4 cells treated with pro-apoptotic stimuli and UCN

5.3.1.1.1 SNAP and UCN treatment

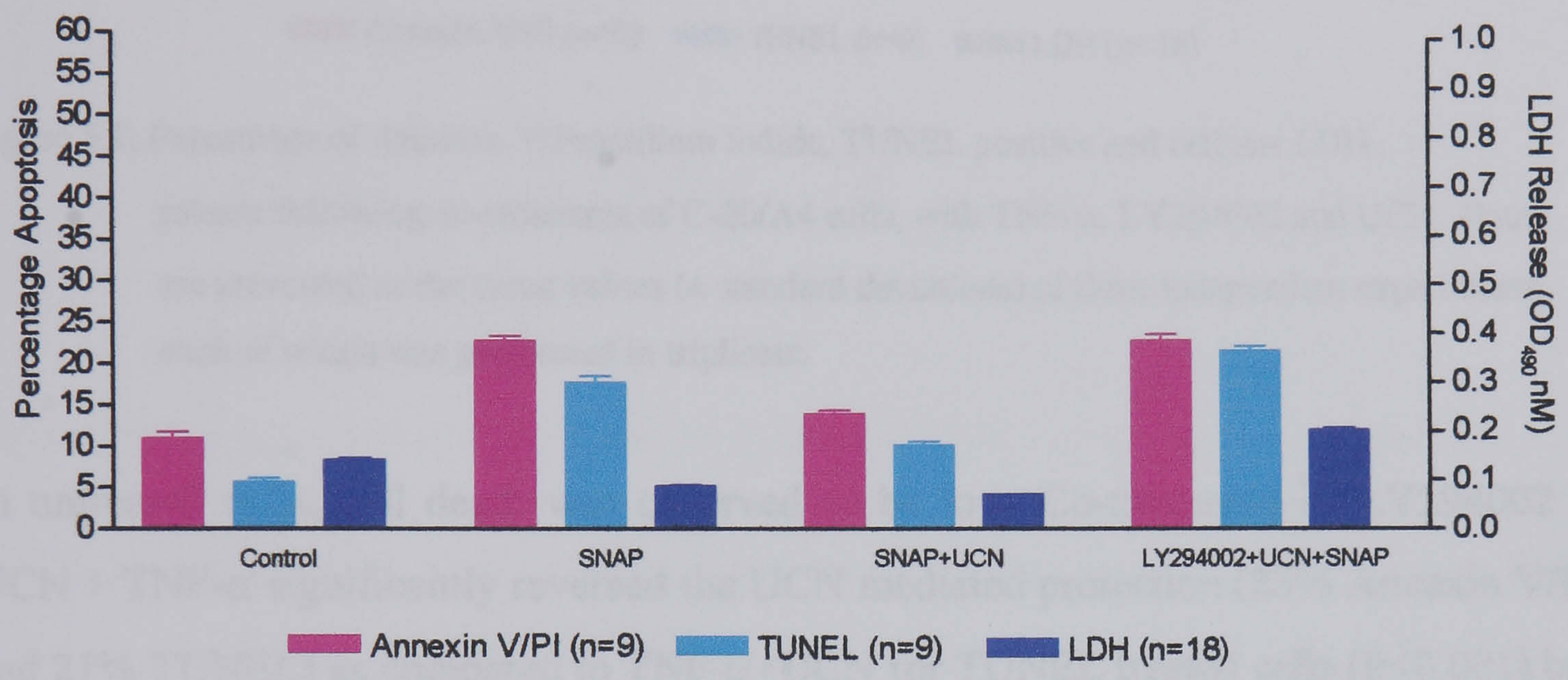

Figure 5.1: Percentage of Annexin V/Propidium Iodide, TUNEL positive and cellular LDH release following co-treatment of C-20/A4 cells, with SNAP, LY294002 and UCN. Data are presented as the mean values (± standard deviations) of three independent experiments, each of which was performed in triplicate.

Control experiments showed low levels of apoptosis. Significantly high apoptotic and low necrotic levels were observed with SNAP alone as compared to SNAP + UCN ($P<0.001$). However, the addition of LY294002 to SNAP and UCN significantly reversed the UCN mediated protection ($P<0.001$).

5.3.1.1.2 TNF-α and UCN treatment

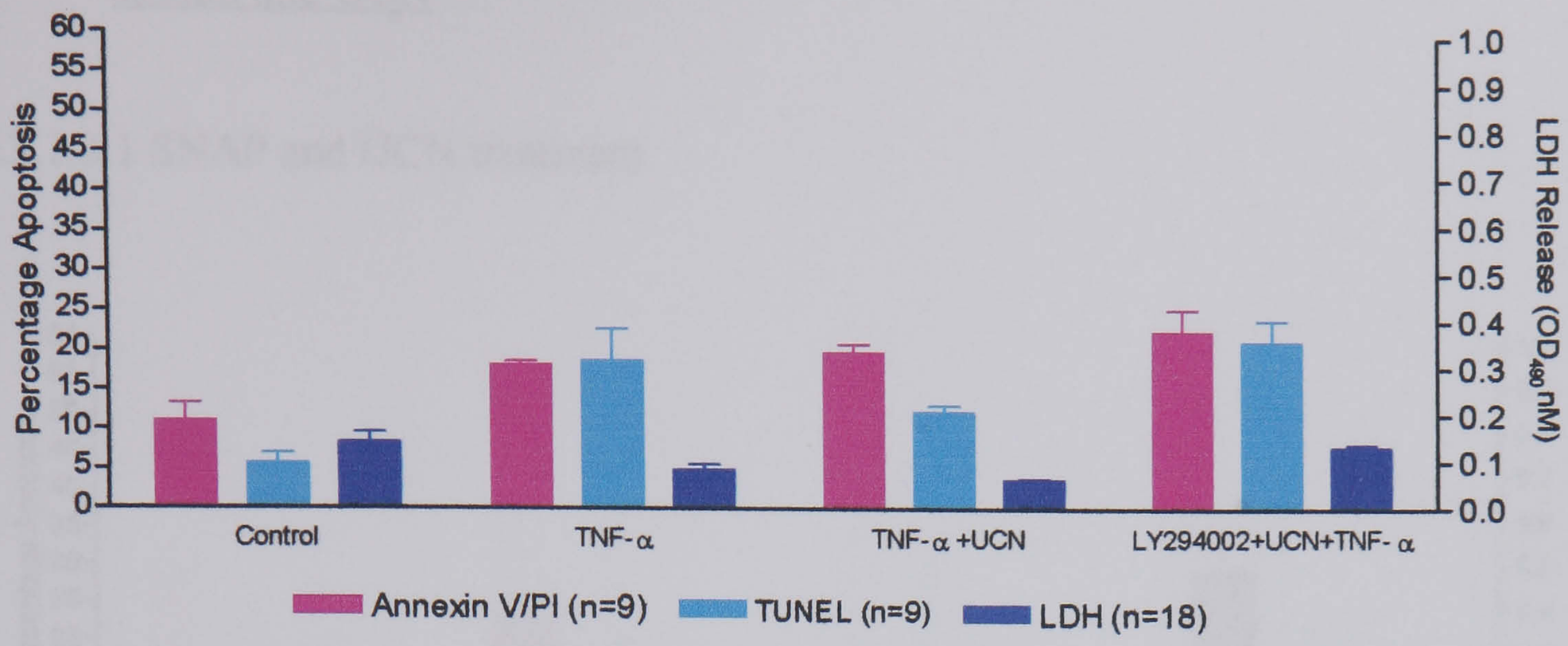

Figure 5.2: Percentage of Annexin V/Propidium Iodide, TUNEL positive and cellular LDH release following co-treatment of C-20/A4 cells, with TNF-α, LY294002 and UCN. Data are presented as the mean values (± standard deviations) of three independent experiments, each of which was performed in triplicate.

In untreated cells, cell death was observed to be low. Co-treatment of LY294002 + UCN + TNF-α significantly reversed the UCN mediated protection (23% Annexin V/PI and 21% TUNEL) as compared to TNF-α+UCN for TUNEL treated cells ($P<0.001$) but not Annexin V/PI treated cells ($P>0.05$), and was not significantly different to TNF-α alone ($P>0.05$) for both Annexin V/PI and TUNEL staining.

5.3.1.2 The effects of P38 MAPK inhibition in C-20/A4 cells treated with pro-apoptotic stimuli and UCN

5.3.1.2.1 SNAP and UCN treatment

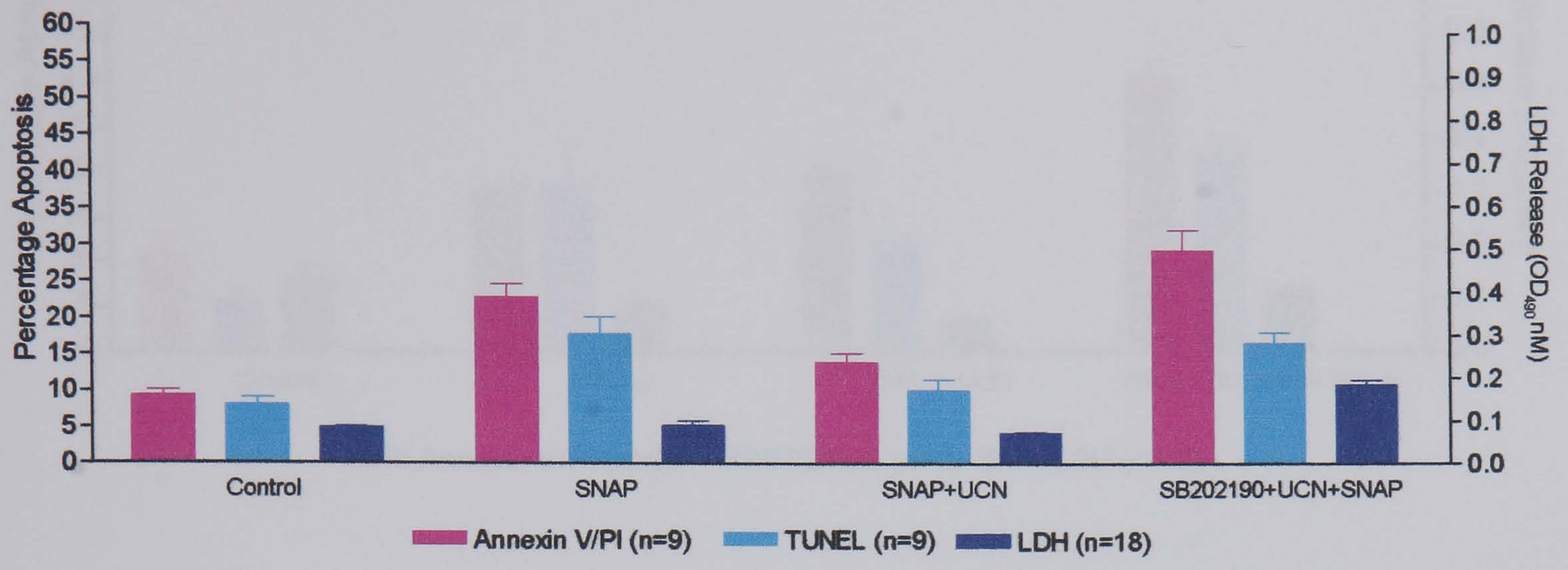

Figure 5.3: Percentage of Annexin V/Propidium Iodide and TUNEL positive cells and cellular LDH release following co-treatment of C-20/A4 cells, with SNAP, SB202190 and UCN. Data are presented as the mean values (± standard deviations) of three independent experiments, each of which was performed in triplicate.

Co-treatment with UCN and SNAP resulted in significantly low ($P<0.001$) apoptotic levels as compared to SNAP alone ($P<0.001$). However, the addition of SB202190 + UCN + SNAP (30% Annexin V/PI, 17% TUNEL) significantly reversed the UCN mediated protection compared to SNAP+UCN ($P<0.001$) for Annexin V/PI treated cells. Necrotic levels remained low throughout the experiment.

5.3.1.2.2 TNF-α and UCN treatment

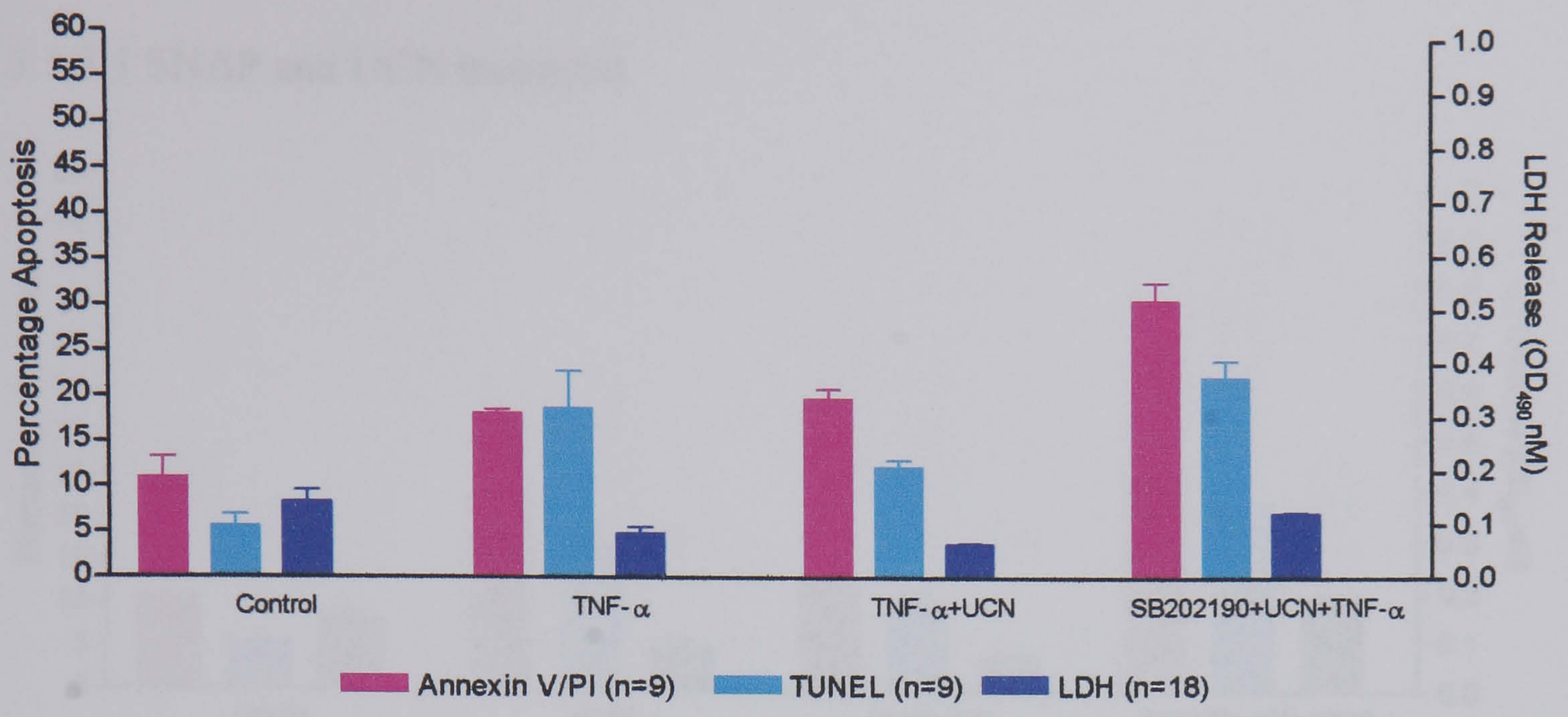

Figure 5.4: Percentage of Annexin V/Propidium Iodide, TUNEL positive and cellular LDH release following co-treatment of C-20/A4 cells, with TNF-α, SB202190 and UCN. Data are presented as the mean values (± standard deviations) of three independent experiments, each of which was performed in triplicate.

Co-treatment of SB202190 + UCN + TNF-α reversed the UCN mediated protection (23% Annexin V/PI and 21% TUNEL) as compared to TNF-α+UCN for Annexin V/PI and TUNEL staining ($P<0.001$), and was significantly different to TNF-α alone ($P<0.001$) for Annexin V/PI staining.

5.3.1.3 The effects of P42/P44 MAPK inhibition in C-20/A4 cells treated with pro-apoptotic stimuli and UCN

5.3.1.3.1 SNAP and UCN treatment

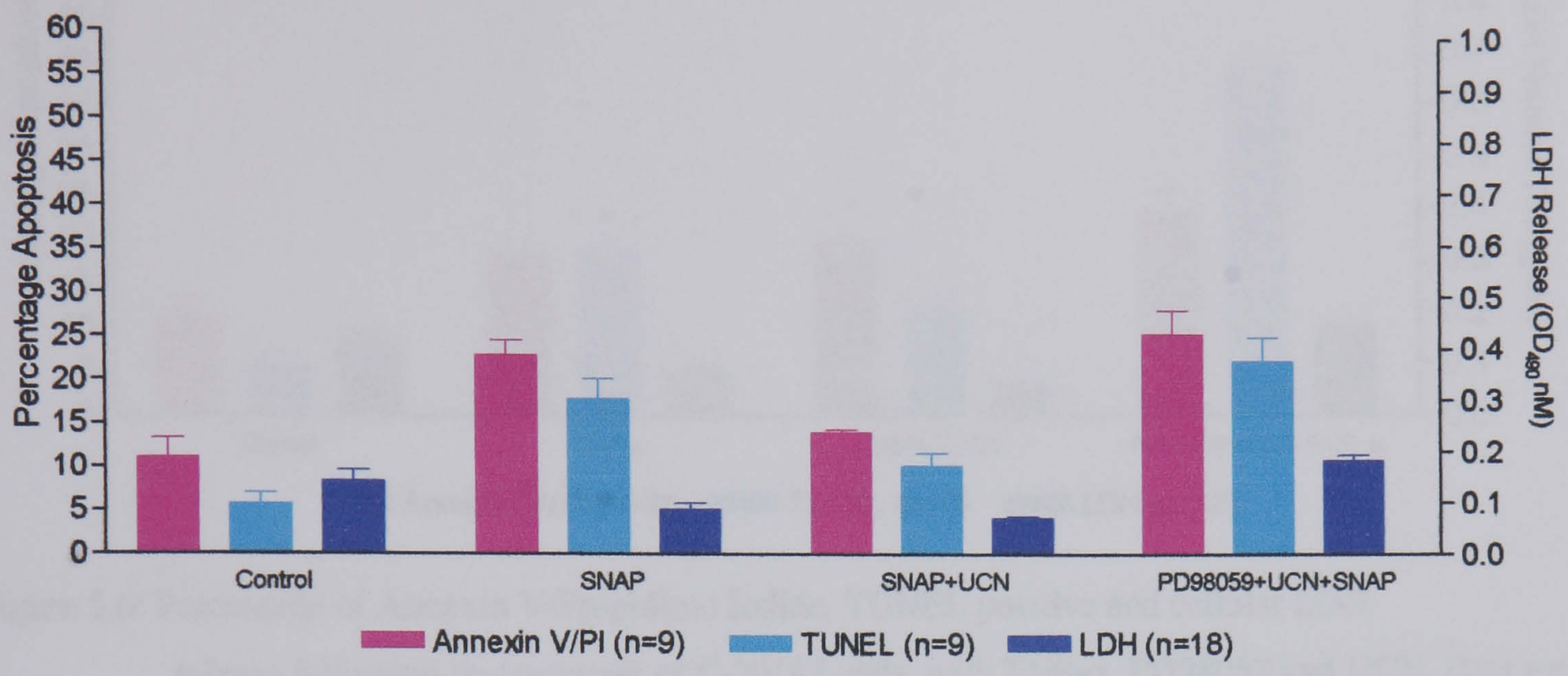

Figure 5.5: Percentage of Annexin V/Propidium Iodide, TUNEL positive and cellular LDH release following co-treatment of C-20/A4 cells, with SNAP, PD98059 and UCN. Data are represented as the mean values (± standard deviations) of three independent experiments, each of which was performed in triplicate.

Control experiments showed low levels of apoptosis. SNAP+UCN showed significantly low levels of apoptosis as compared to SNAP alone ($P<0.01$), but in PD98059 + UCN + SNAP, apoptotic level was observed to be significant increased as compared to SNAP+UCN ($P<0.001$), but not in SNAP alone ($P>0.05$), indicating that PD98059 reversed the UCN mediated protection

5.3.1.3.2 TNF-α and UCN treatment

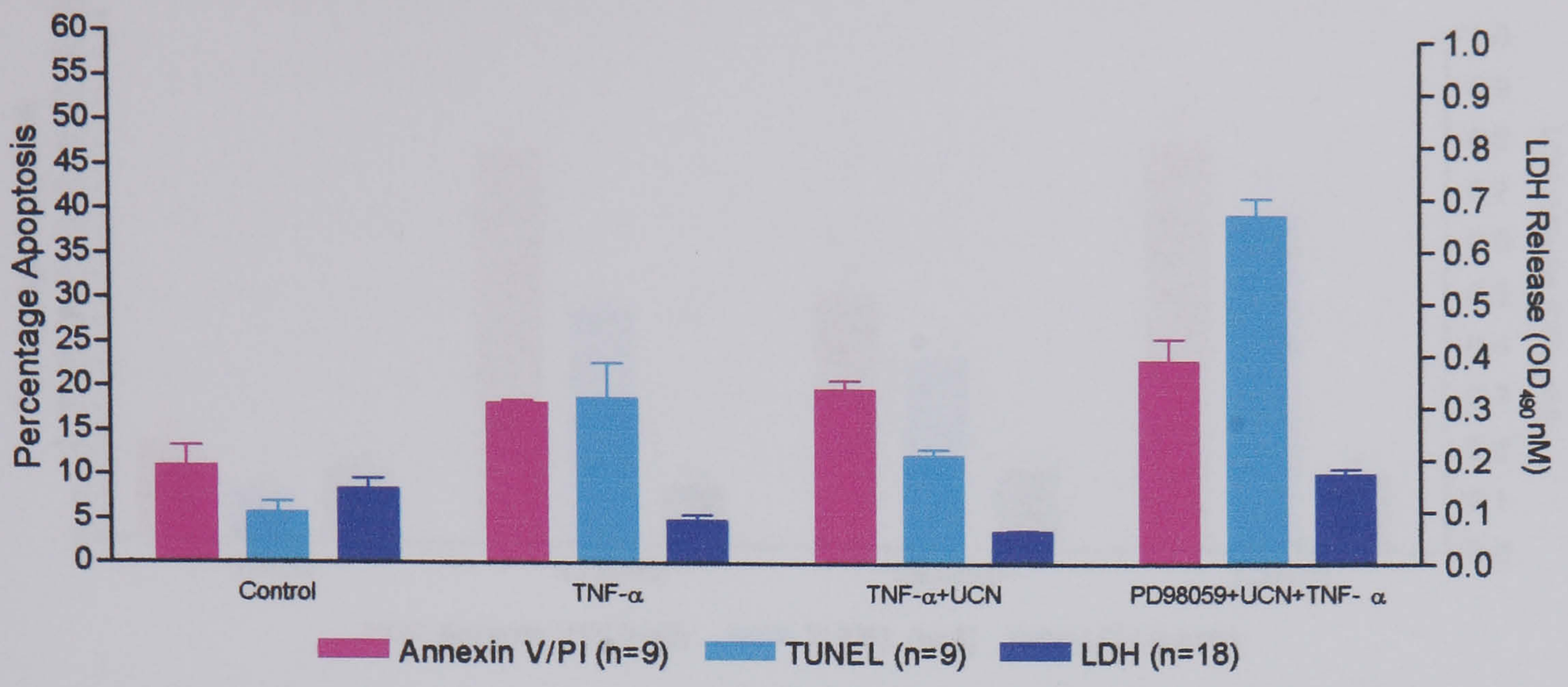

Figure 5.6: Percentage of Annexin V/Propidium Iodide, TUNEL positive and cellular LDH release following co-treatment of C-20/A4 cells, with TNF-α, PD98059 and UCN. Data are presented as the mean values (± standard deviations) of three independent experiments, each of which was performed in triplicate.

Co-treatment of PD98059+UCN+TNF-α showed an increased level of apoptosis at 23% Annexin V/PI, 40% TUNEL, which was more prominent for TUNEL than Annexin V/PI staining. These were significantly different as compared to TNF-α+UCN ($P<0.001$) and TNF-α alone ($P<0.001$), which both showed a decreased level of apoptosis especially for TUNEL staining. This data again indicated that PD98059 had reversed the UCN mediated protection in C-20/A4 cells more for TUNEL staining than Annexin V/PI staining.

5.3.1.4 The effects of LY294002, SB202190 and PD98059 inhibition alone in C-20/A4 cells

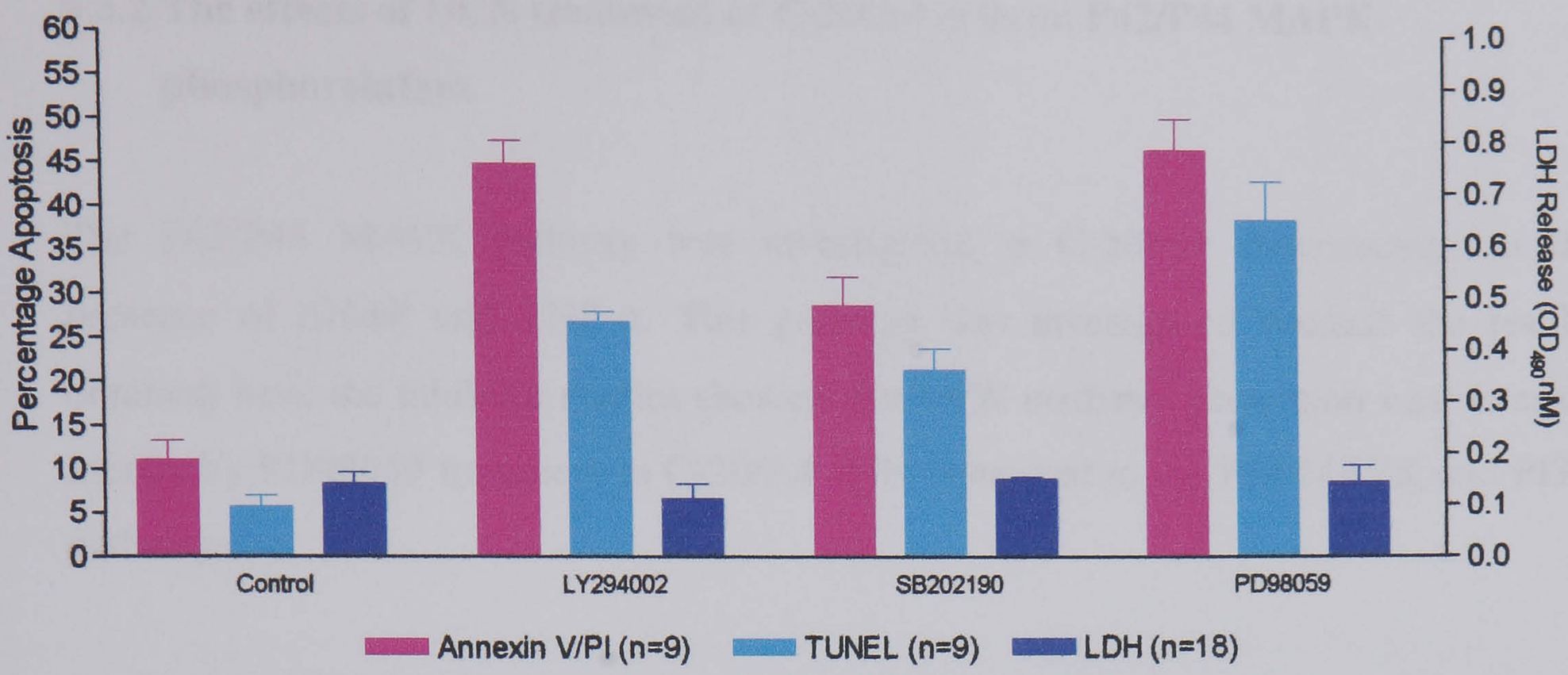

Figure 5.7: Percentage of Annexin V/Propidium Iodide, TUNEL positive and cellular LDH release following treatment of C-20/A4 cells, with LY294002, SB202190 and PD98059. Data are presented as the mean values (± standard deviations) of three independent experiments, each of which was performed in triplicate.

The inhibitors used in this study for the various pathways were then used to treat C-20/A4 cells alone. This was to observe whether these inhibitors were exerting a toxic effect in these cells. Treatment of LY294002, SB202190 and PD98059 were all significantly increased against the control respectively ($P<0.001$).

5.3.2 The effects of UCN treatment of C-20/A4 cells on P42/P44 MAPK phosphorylation

The P42/P44 MAPK pathway was investigated in C-20/A4 chondrocytes in the presence of SNAP and TNF-α. This pathway was investigated because the results obtained from the inhibitor studies showed that UCN mediated protection was reversed mostly by PD98059 treatment in C-20/A4 cells compared to the P38 MAPK and PI3K pathways.

5.3.2.1 P42/P44 MAPK phosphorylation in the absence of pro-apoptotic stimuli.

MAPK activation in C-20/A4 cells were investigated in the presence of various stimuli. Chondrocytes were subjected to the P42/P44 MAPK inhibitor PD98059 with UCN, as well as the P38 MAPK inhibitor SB202190 with UCN, PD98059 alone and UCN alone before cells were harvested and constituent proteins probed with dual phospho-P42/P44 and total P42/P44 antibodies.

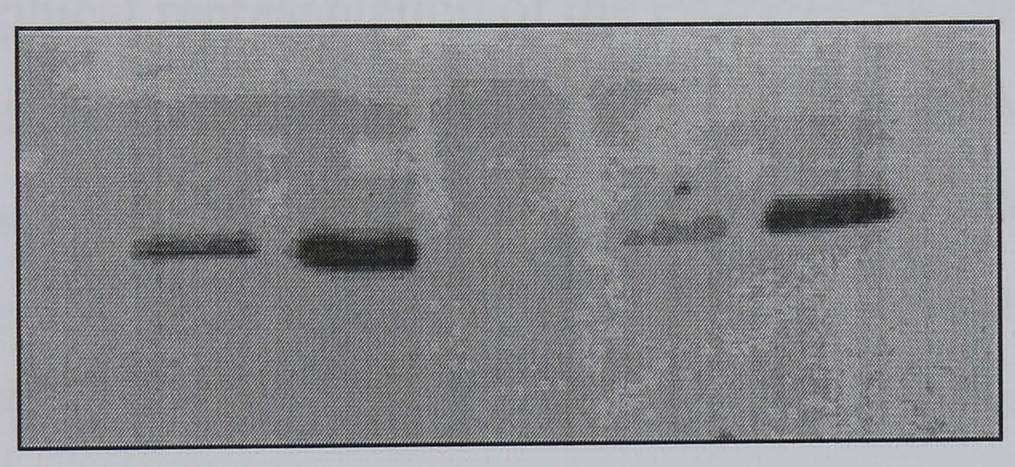

Figure 5.8: Activation of P42/P44 MAPK in C-20/A4 cells. Samples are probed with dual phospho-specific MAPK antibodies for P42/P44. From left to right, C-control, U-UCN, PD-PD98059, PD+U-PD98059+UCN, SB+U-SB202190+UCN.

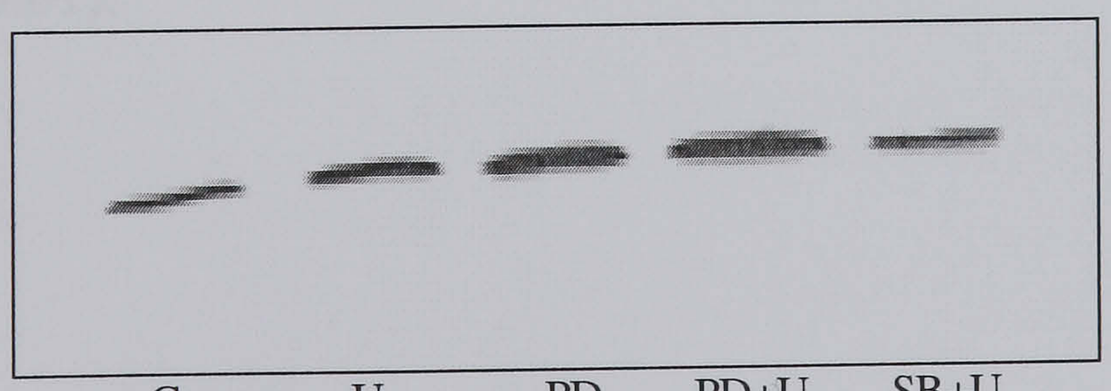

Figure 5.9: Total levels of P42/P44 MAPK in C-20/A4 cells. Samples are probed with antibodies detecting total P42/P44 MAPK. From left to right, C-control, U-UCN, PD-PD98059, PD+U-PD98059+UCN, SB+U-SB202190+UCN.

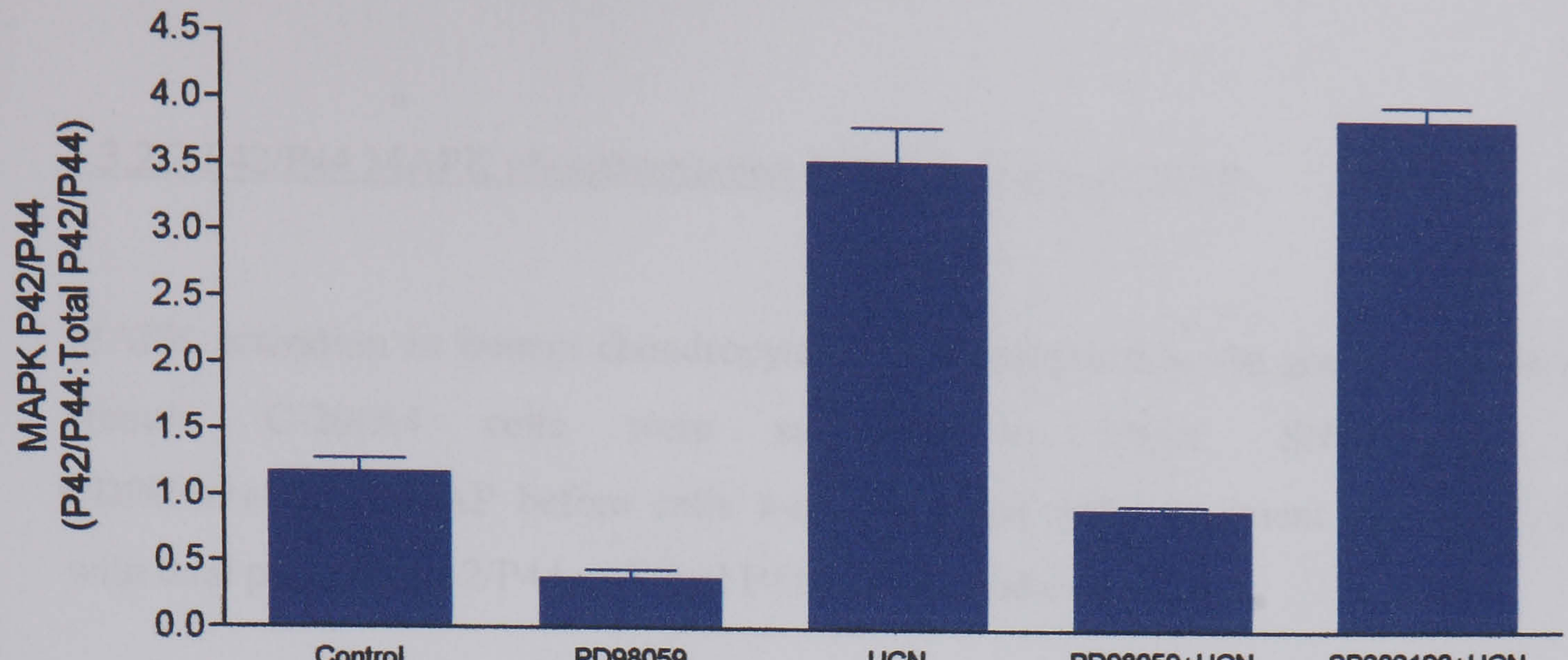

Figure 5.10: Ratio of P42/P44 MAPK expression of UCN, PD98059 and SB202190 in Western blot analysis. Data are presented as the mean values (± standard deviations) of three independent experiments.

Figure 5.8 represents C-20/A4 chondrocytes treated with UCN, PD98059, PD98059+UCN and SB202190+UCN. Figure 5.9 shows equal protein loading after the membranes were stripped and re-probed with the ERK 2 (total P42/P44) antibody. Figure 5.10 shows a graphical representation of the P42/P44 phosphorylated against the P42/P44 total ratio of the different treatments. P42/P44 MAPK activation was evaluated biochemically using an antibody which recognizes the activated form of P42/P44 MAPK. PD98059 alone and with treatment was added to ensure its effectiveness in blocking P42/P44 MAPK activation. Some activation was observed in control treated cells, which was significantly blocked by PD98059 alone ($P<0.001$). Cells treated with UCN alone showed increased phosphorylation of P42/P44 MAPK ($P<0.001$ UCN vs control) which was significantly blocked by the addition of PD98059 ($P<0.001$), but not SB202190+UCN ($P>0.01$).

5.3.2.2 P42/P44 MAPK phosphorylation in the presence of SNAP

MAPK activation in human chondrocytes was investigated in the presence of various stimuli. C-20/A4 cells were subjected to SNAP, SNAP+UCN and PD98059+UCN+SNAP before cells were harvested and constituent proteins probed with dual phospho-P42/P44 and total P42/P44 antibodies.

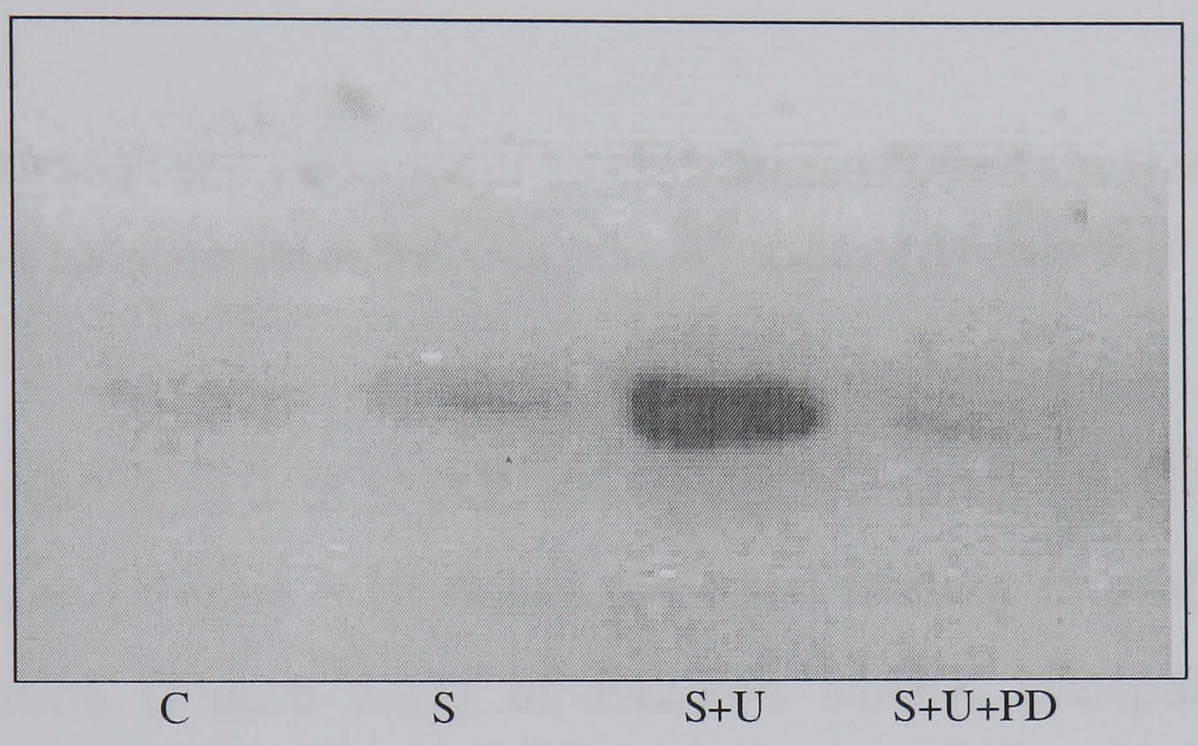

Figure 5.11: Activation of P42/P44 MAPK in C-20/A4 cells. Samples are probed with dual phospho-specific MAPK antibodies for P42/P44. From left to right, C-control, S-SNAP, S+U-SNAP+UCN, S+U+PD-SNAP+UCN+PD98059.

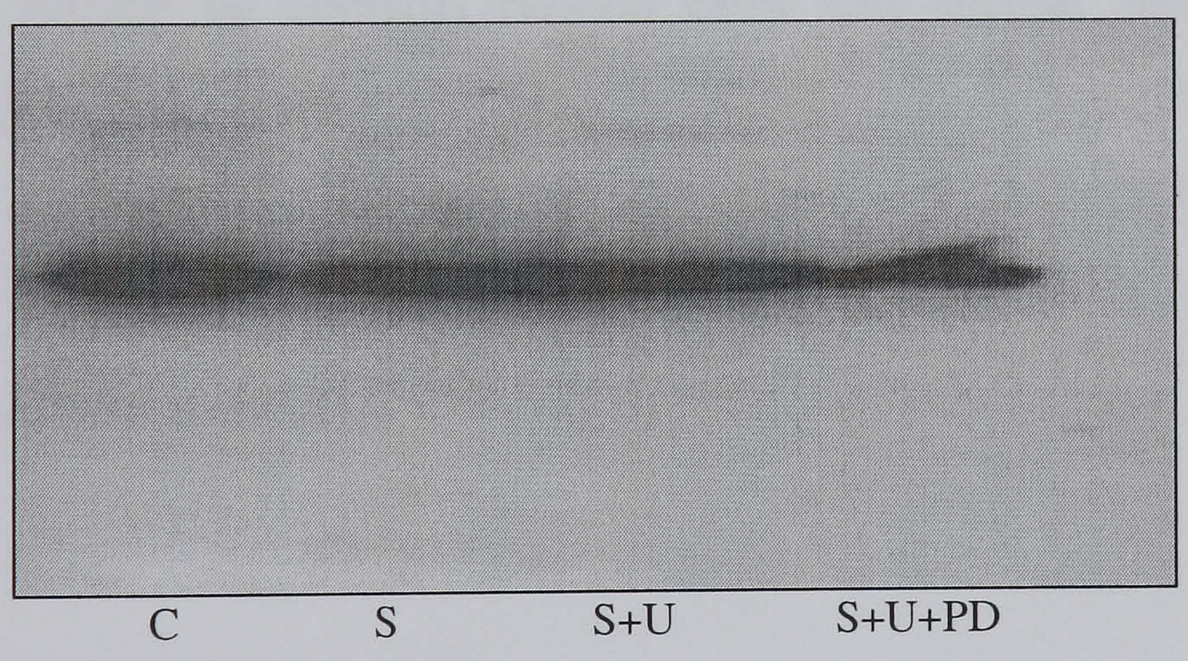

Figure 5.12: Total levels of P42/P44 MAPK in C-20/A4 cells. Samples are probed with antibodies detecting total P42/P44 MAPK. From left to right, C-control, S-SNAP, S+U-SNAP+UCN, S+U+PD-SNAP+UCN+PD98059.

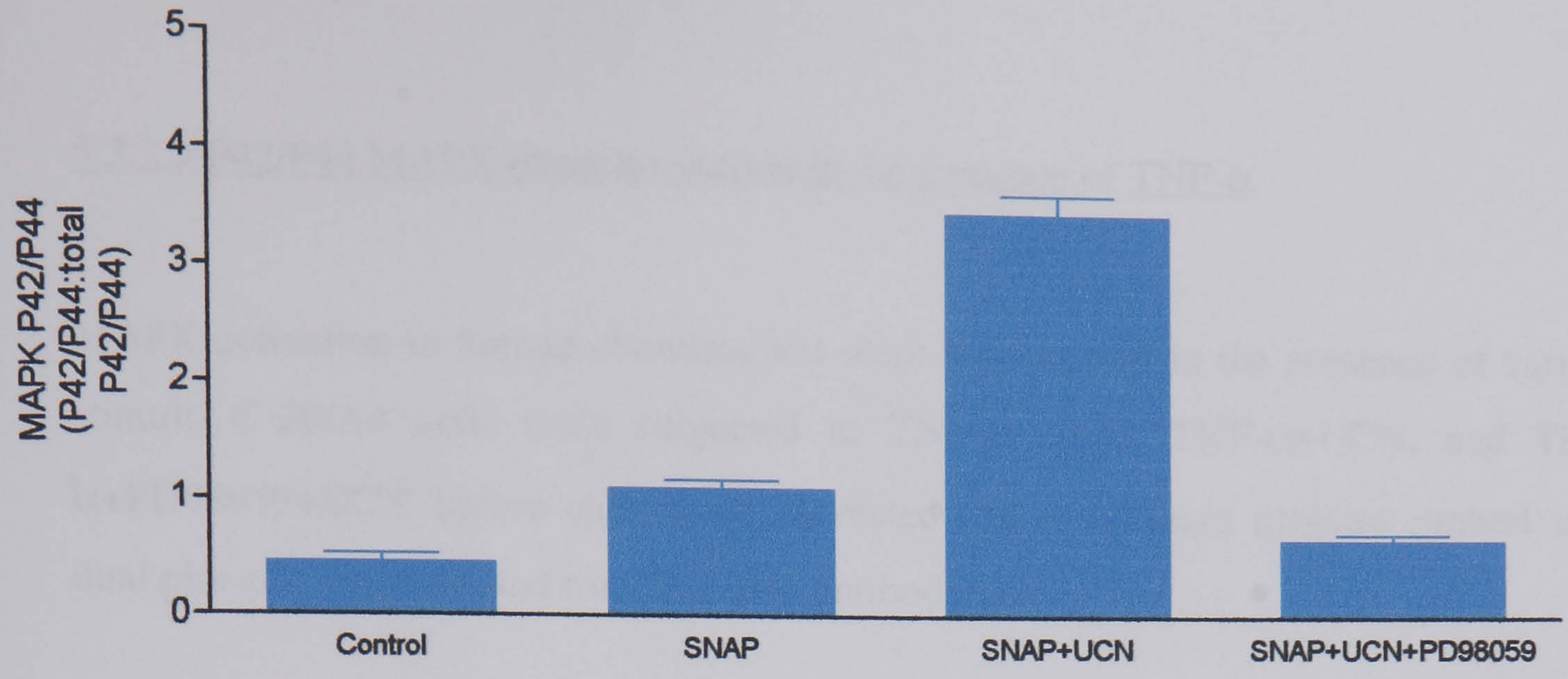

Figure 5.13: Ratio of P42/P44 MAPK expression of SNAP, UCN and PD98059 in Western blot analysis. Data are presented as the mean values (± standard deviations) of three independent experiments.

Figure 5.11 denotes treatment with SNAP, SNAP+UCN and SNAP+UCN+PD98059 in human chondrocytes and Figure 5.12 shows the equal loading of protein followed by graphical representation (Figure 5.13) of P42/P44 MAPK phosphorylated against P42/P44 MAPK total ratio of the various treatments. Untreated cells showed the least P42/P44 MAPK activation in C-20/A4 cells. P42/P44 MAPK activation was increased in SNAP ($P<0.001$ SNAP vs control) treated cells and further increased with the addition of UCN ($P<0.001$, SNAP vs SNAP+UCN), which was then significantly blocked by the addition of PD98059 ($P<0.001$, SNAP+UCN+PD98059 vs SNAP+UCN), and observed not to be significant compared to control ($P>0.05$ SNAP+UCN+PD98059 vs control).

5.3.2.3 P42/P44 MAPK phosphorylation in the presence of TNF-α

MAPK activation in human chondrocytes were investigated in the presence of various stimuli. C-20/A4 cells were subjected to TNF-α alone, TNF-α+UCN, and TNF-α+PD98059+UCN before cells were harvested and constituent proteins probed with dual phospho-P42/P44 and total P42/P44 antibodies.

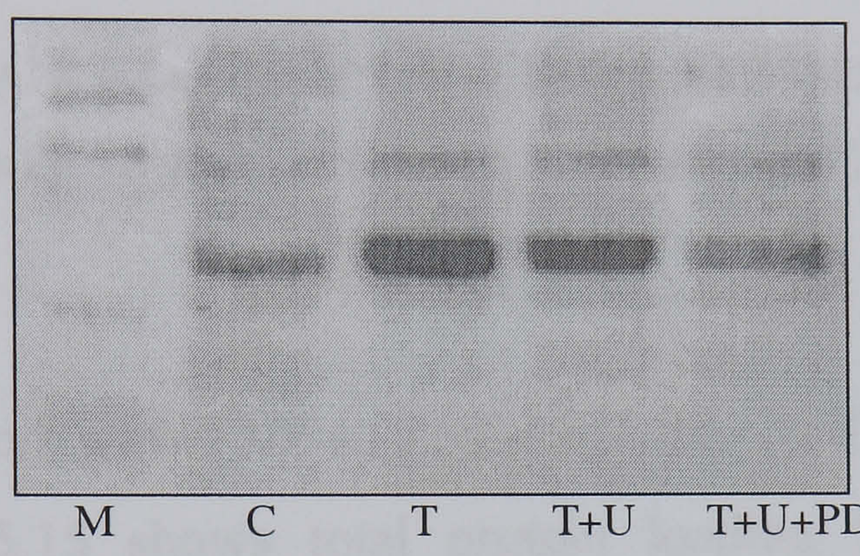

Figure 5.14: Activation of P42/P44 MAPK in C-20/A4 cells. Samples are probed with dual phospho-specific MAPK antibodies for P42/P44. From left to right, M-Pre-stained protein marker (Biolabs), C-control, T-TNF-α, T+U-TNF-α+UCN, T+U+PD-TNF-α+UCN+PD98059.

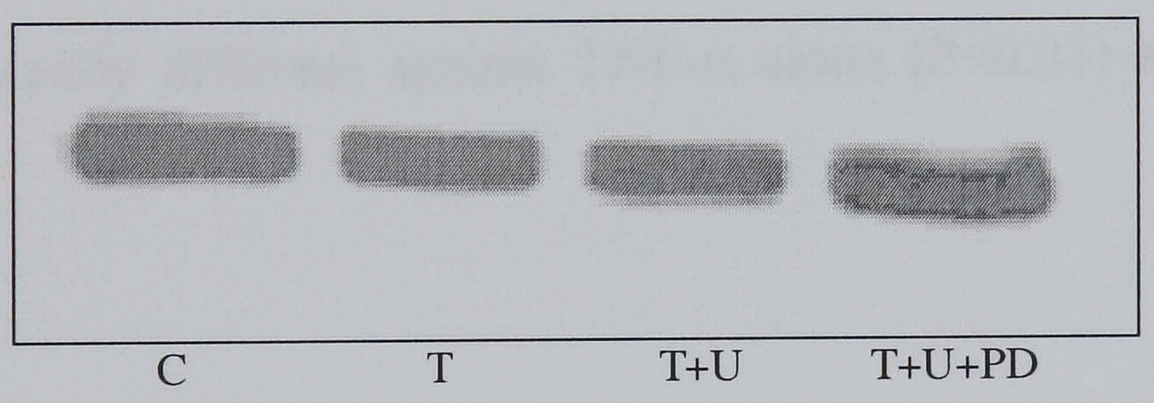

Figure 5.15: Total levels of of P42/P44 MAPK in C-20/A4 cells. Samples are probed with antibodies detecting total P42/P44 MAPK. From left to right, C-control, T-TNF-α, T+U-TNF-α+UCN, T+U+PD-TNF-α+UCN+PD98059.

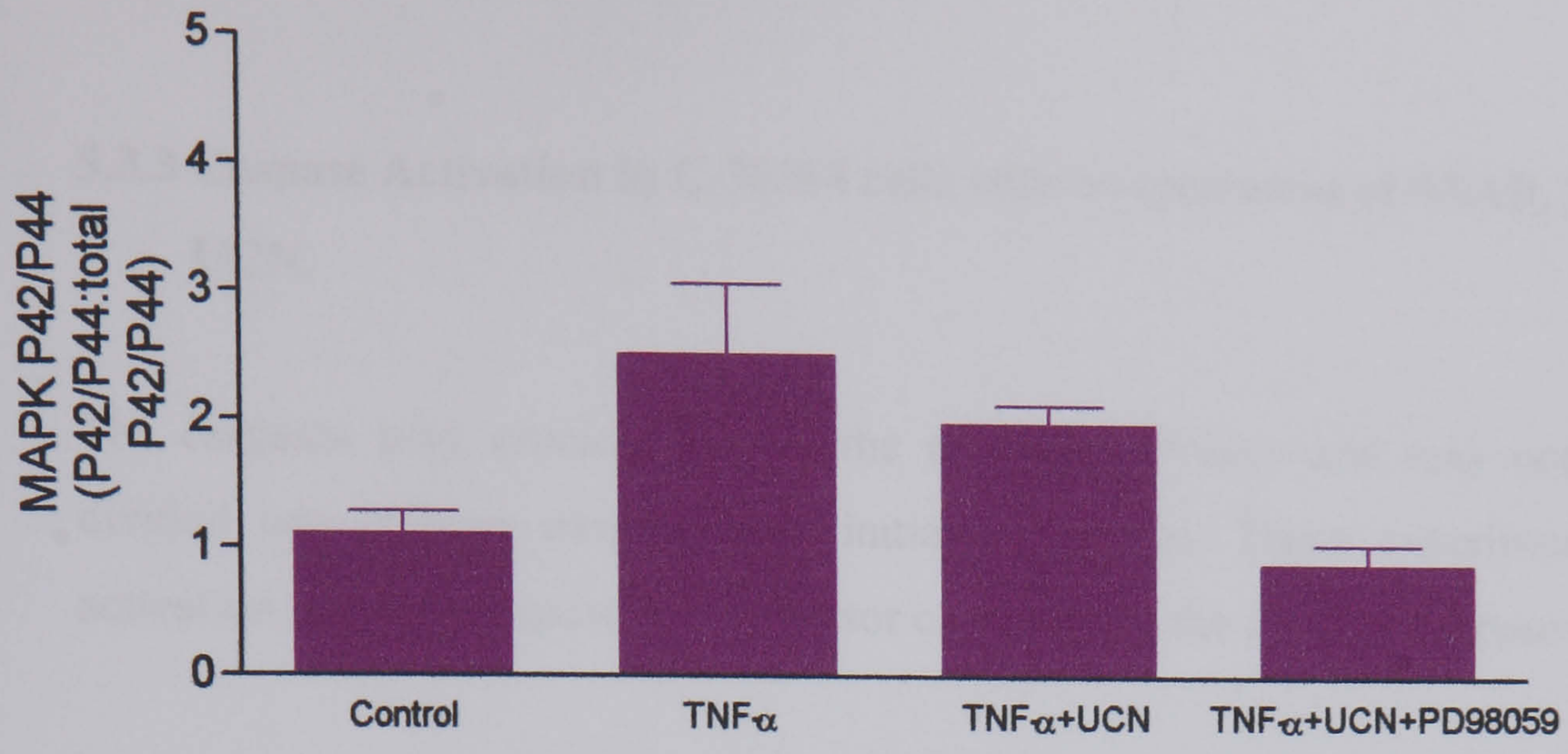

Figure 5.16: Ratio of P42/P44 MAPK expression of TNF-α, UCN and PD98059 in Western blot analysis. Data are presented as the mean values (± standard deviations) of three independent experiments.

Figure 5.14 shows treatments with TNF-α, TNF-α+UCN and TNF-α+UCN+PD98059 in chondrocytes. Figure 5.15 shows total protein loading followed by graphical representation (Figure 5.16) of P42/P44 phosphorylated against P42/P44 MAPK total. Treatment of TNF-α alone increased activation against control ($P<0.001$), which was not increased further with TNF-α+UCN, but activation of P42/P44 MAPK was blocked by the addition of PD98059 which was not significantly increased compared to control ($P>0.05$), but significantly different against TNF-α alone ($P<0.01$) and TNF-α+UCN ($P<0.001$).

5.3.3 Caspase Activation in C-20/A4 cells with co-treatment of SNAP, TNF-α and UCN.

The caspases play crucial roles in the apoptotic process and may conveniently be divided into effector caspases and initiator caspases. These experiments detail the activation status of caspase 3, an effector caspase, and the initiator caspases 8 and 9.

5.3.3.1 Caspase 3 activation

C-20/A4 cells were investigated for caspase 3 activation after stimulation with SNAP, SNAP+UCN, TNF-α and TNF-α+UCN before cells were collected, subjected to Western blotting and then probed with an antibody for activated caspase 3.

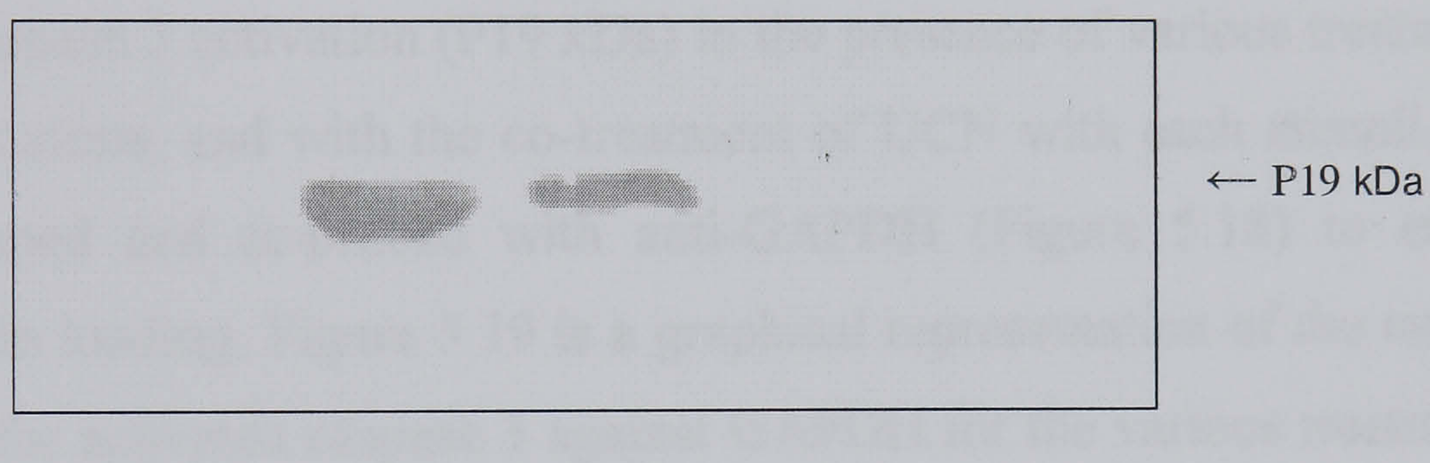

Figure 5.17: Activation of caspase 3 in C-20/A4 cells. Samples are probed with anti-caspase 3 antibody, which recognizes only the active form. From left to right, C-control, S-SNAP, S+U-SNAP+UCN, T-TNF-α, T+U-TNF-α+UCN.

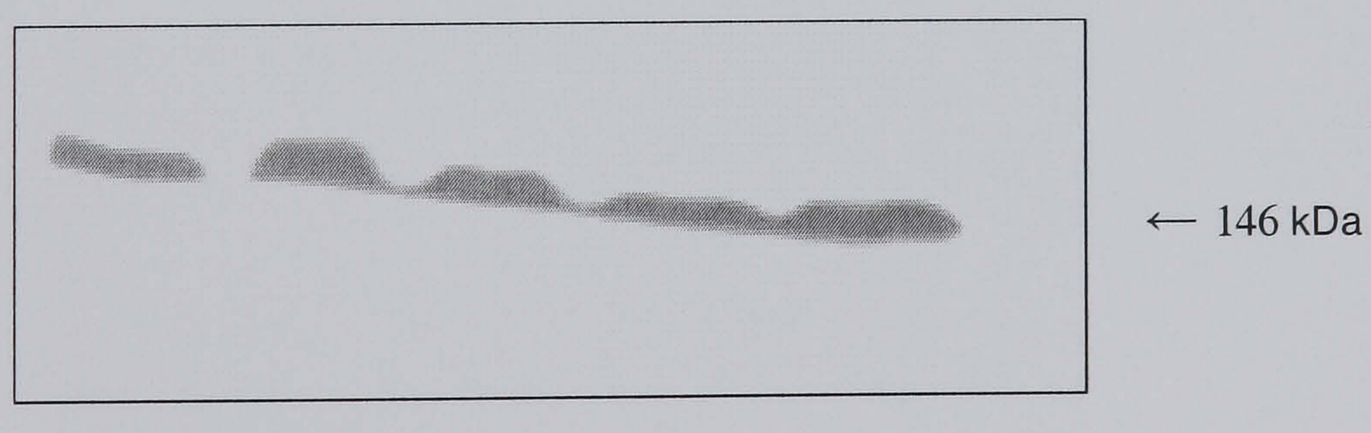

Figure 5.18: Total level of GAPDH in C-20/A4 cells. From left to right, C-control, S-SNAP, and S+U-SNAP+UCN, T-TNF-α, T+U-TNF-α+UCN.

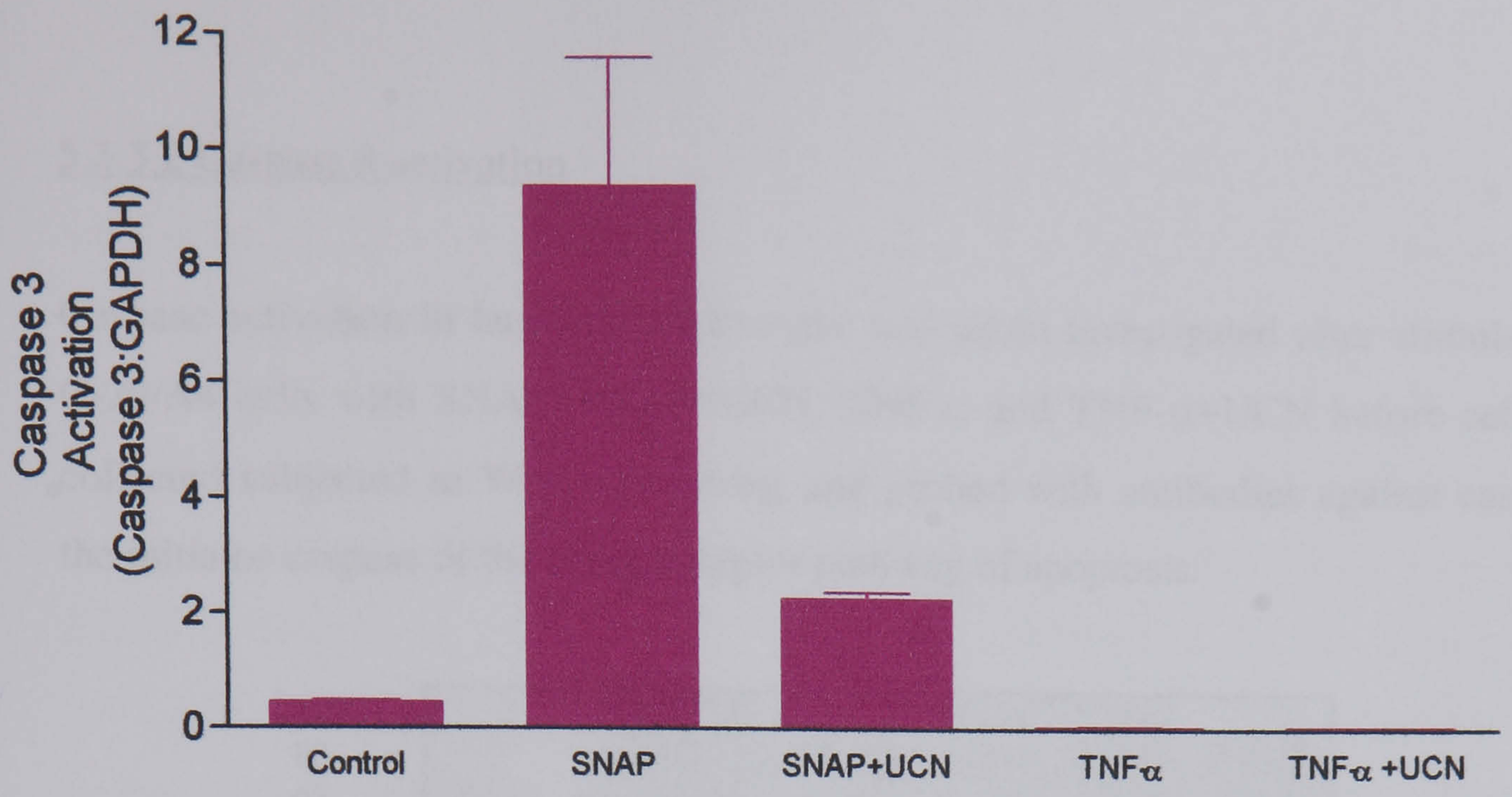

Figure 5.19: Caspase 3 activation following SNAP, TNF-α, and UCN co-treatment of C-20/A4 cells. Data are presented as the mean values (± standard deviations), of three independent experiments.

Figure 5.17 shows caspase 3 activation (P19 kDa) in the presence of various treatments of SNAP and TNF-α alone, and with the co-treatment of UCN with each stimuli. The membrane was stripped and re-probed with anti-GAPDH (Figure 5.18) to ensure consistent total protein loading. Figure 5.19 is a graphical representation of the ratio of densitometry values for activated caspase 3 against GAPDH for the various treatments. Clearly, SNAP treated cells showed a significant 9-fold increase compared to control ($P<0.001$). SNAP+UCN showed a significant decrease in caspase 3 activation as compared to SNAP alone ($P<0.001$). However, TNF-α and TNF-α+UCN failed to show activation of caspase 3.

5.3.3.2 Caspase 8 activation

Caspase activation in human chondrocytes was again investigated after stimulation of C-20/A4 cells with SNAP, SNAP+UCN, TNF-α and TNF-α+UCN before cells were collected subjected to Western blotting and probed with antibodies against caspase 8, the initiator caspase of the death receptor pathway of apoptosis.

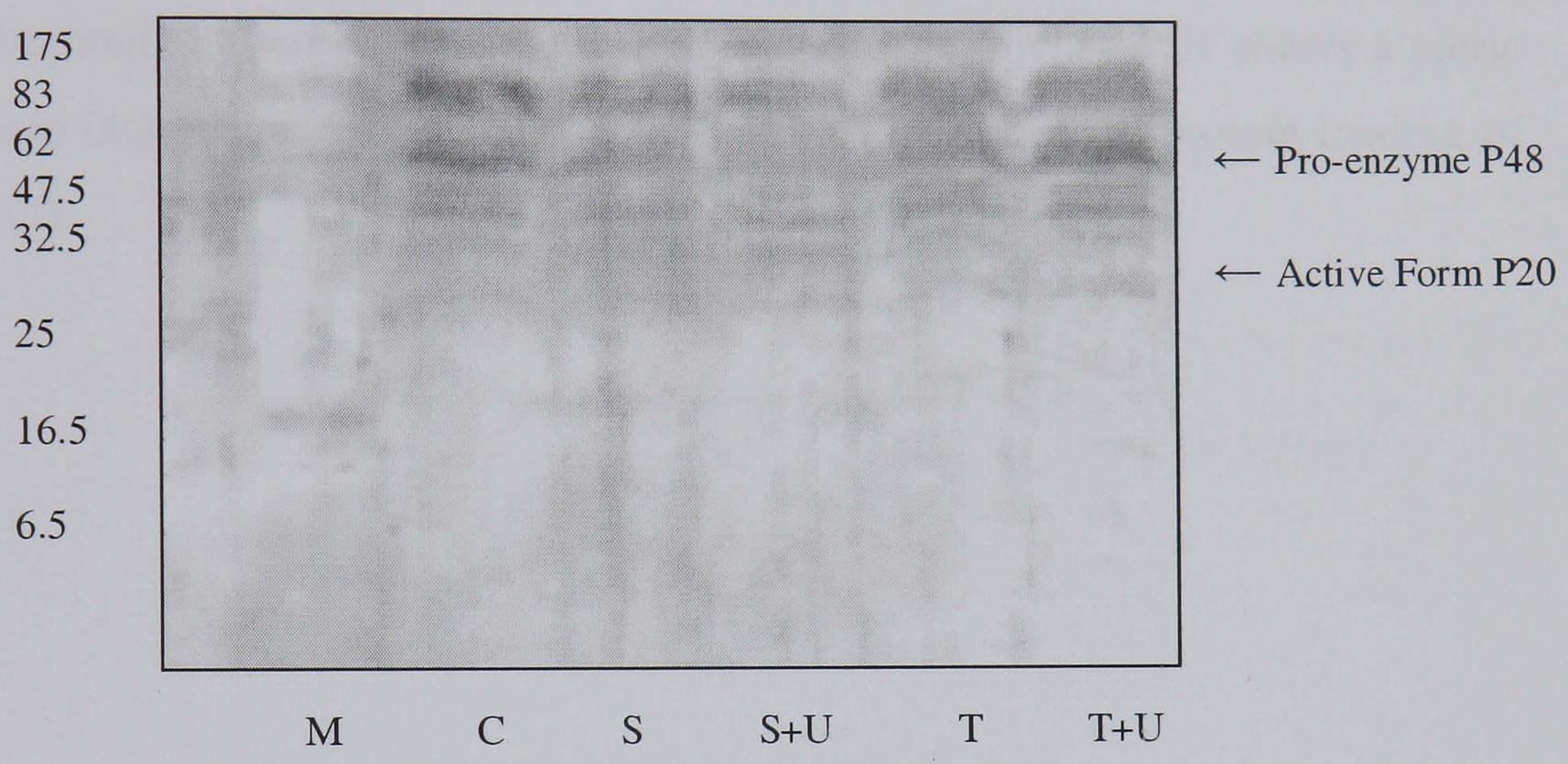

Figure 5.20: Activation of caspase 8 in C-20/A4 chondrocytes. Samples are probed with anti-caspase 8 antibody, which recognizes both the pro-enzyme and active form. From left to right, M-Pre-stained protein marker (Biolabs), C-control, S-SNAP, S+U-SNAP+UCN, T-TNF-α, T+U-TNF-α+UCN. Arrows denote the pro-enzyme and active form.

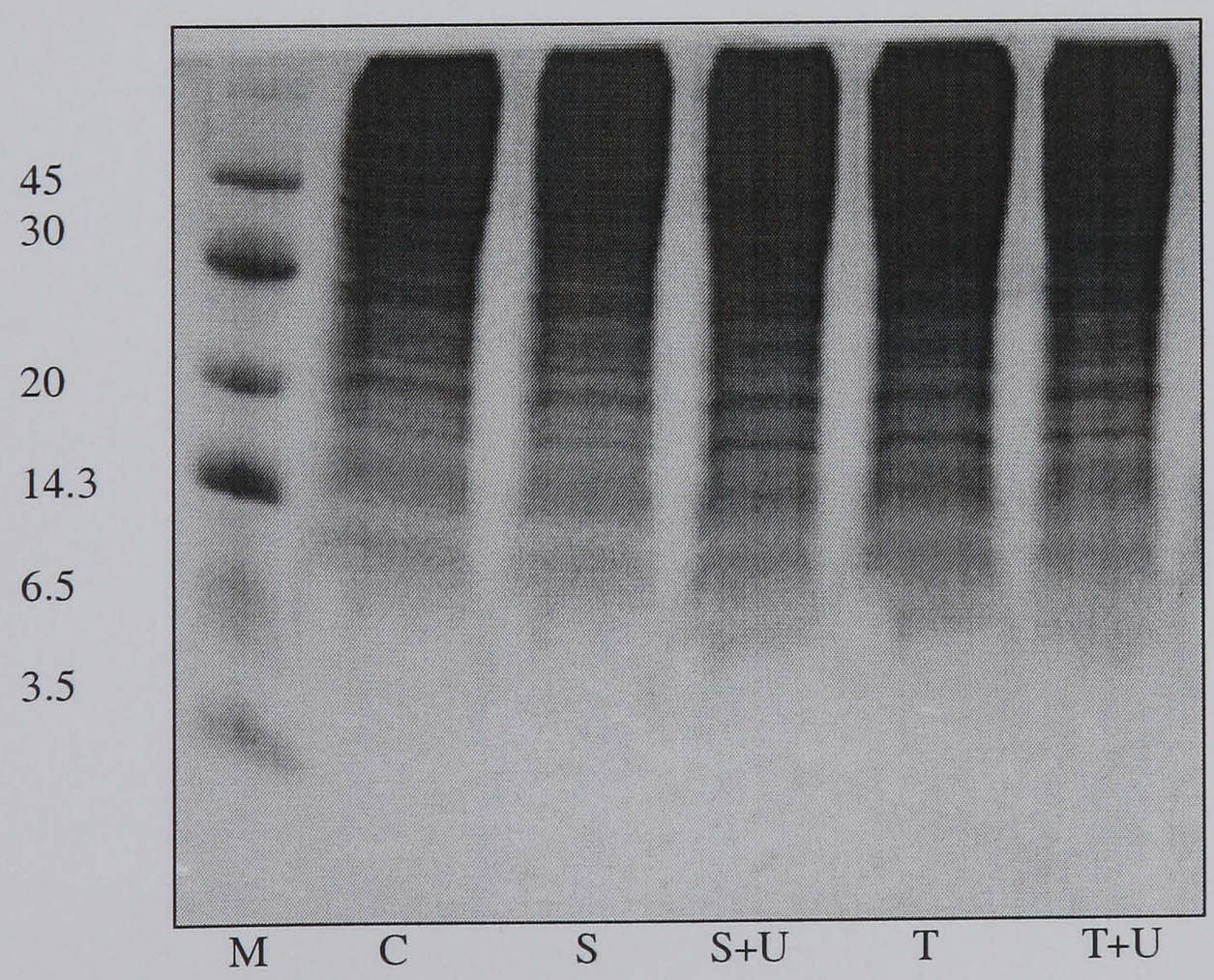

Figure 5.21: Picric acid coomassie blue staining of an SDS-PAGE gel revealing the loading of proteins for Figure 5.20. From left to right, M-Rainbow marker (Amersham), C-control, S-SNAP, S+U-SNAP+UCN, T-TNF-α, T+U-TNF-α+UCN.

Figure 5.20 shows a membrane probed with the anti-caspase 8 in the presence of various stimuli. Activation of caspase 8 occurs in two steps. The initial cleavage of the precursor gives rise to the P48 subunit, followed by the generation of the active P20 subunit. The pro-enzyme of caspase 8 (P48) is indicated by the arrow. Bands lower down indicate the expected active form (P20), which is unclear from this blot. These results, however, are unconfirmed as repeated experiments show inconsistencies in the results achieved. Treatments with various stimuli resulted in the appearance of undetectable amounts of active caspase 8 in C-20/A4 cells. Figure 5.21 shows a picric acid coomassie blue staining of an SDS PAGE gel, to indicate total protein loading of for Figure 5.20.

5.3.3.3 Caspase 9 activation

Caspase activation in human chondrocytes was again investigated after stimulation of C-20/A4 cells with SNAP, SNAP+UCN, TNF-α and TNF-α+UCN before cells were collected, subjected to Western blotting and probed with antibodies against caspase 9, which plays an important role in the mitochondrial pathway of apoptosis.

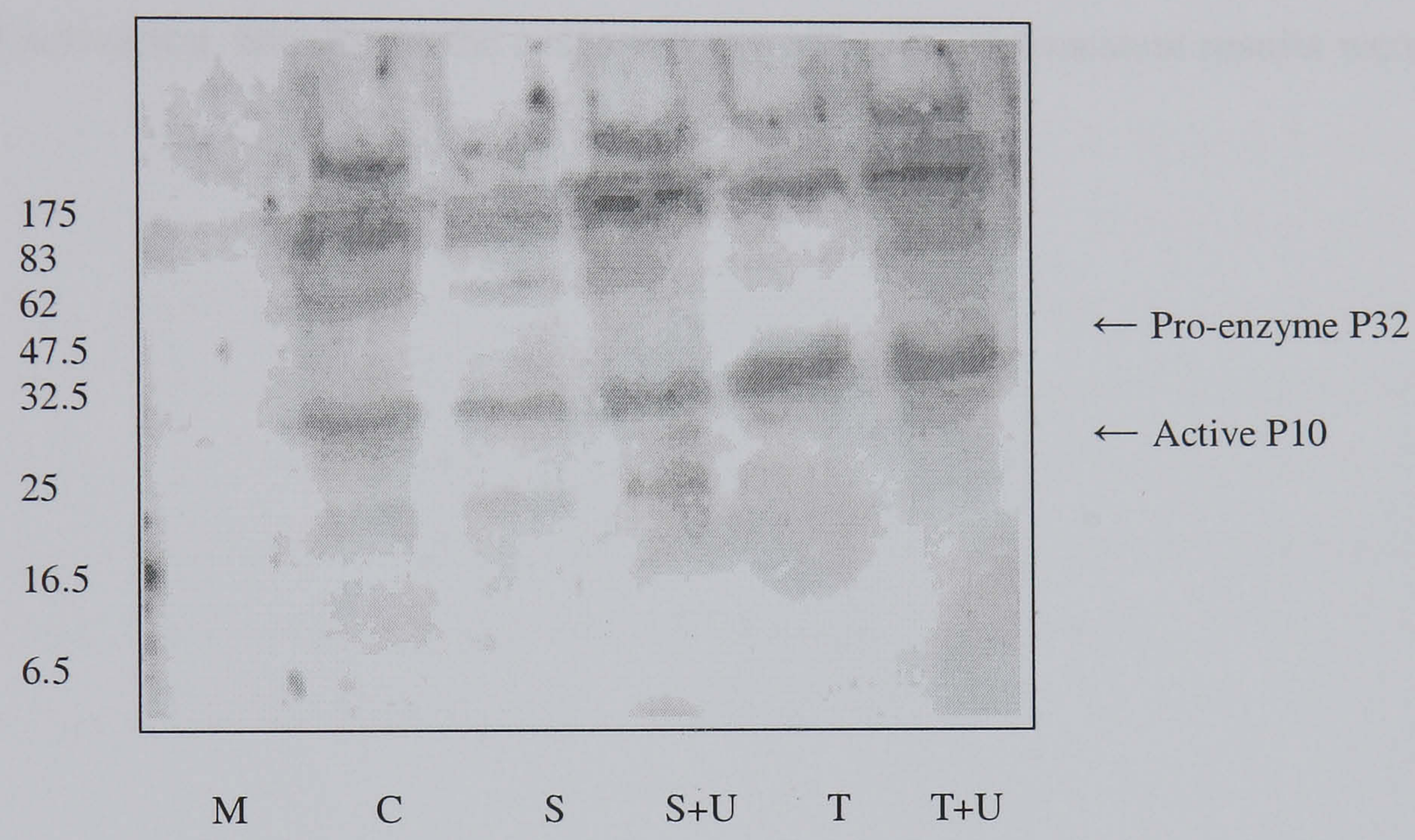

Figure 5.22: Activation of caspase 9 in C-20/A4 cells. Samples are probed with anti-caspase 9 antibody, which recognizes both the pro-enzyme and active form. From left to right, M-Pre-stained protein marker (Biolabs), C-control, S-SNAP, S+U-SNAP+UCN, T-TNF-α, T+U-TNF-α+UCN. Arrows denotes the pro-enzyme and active form

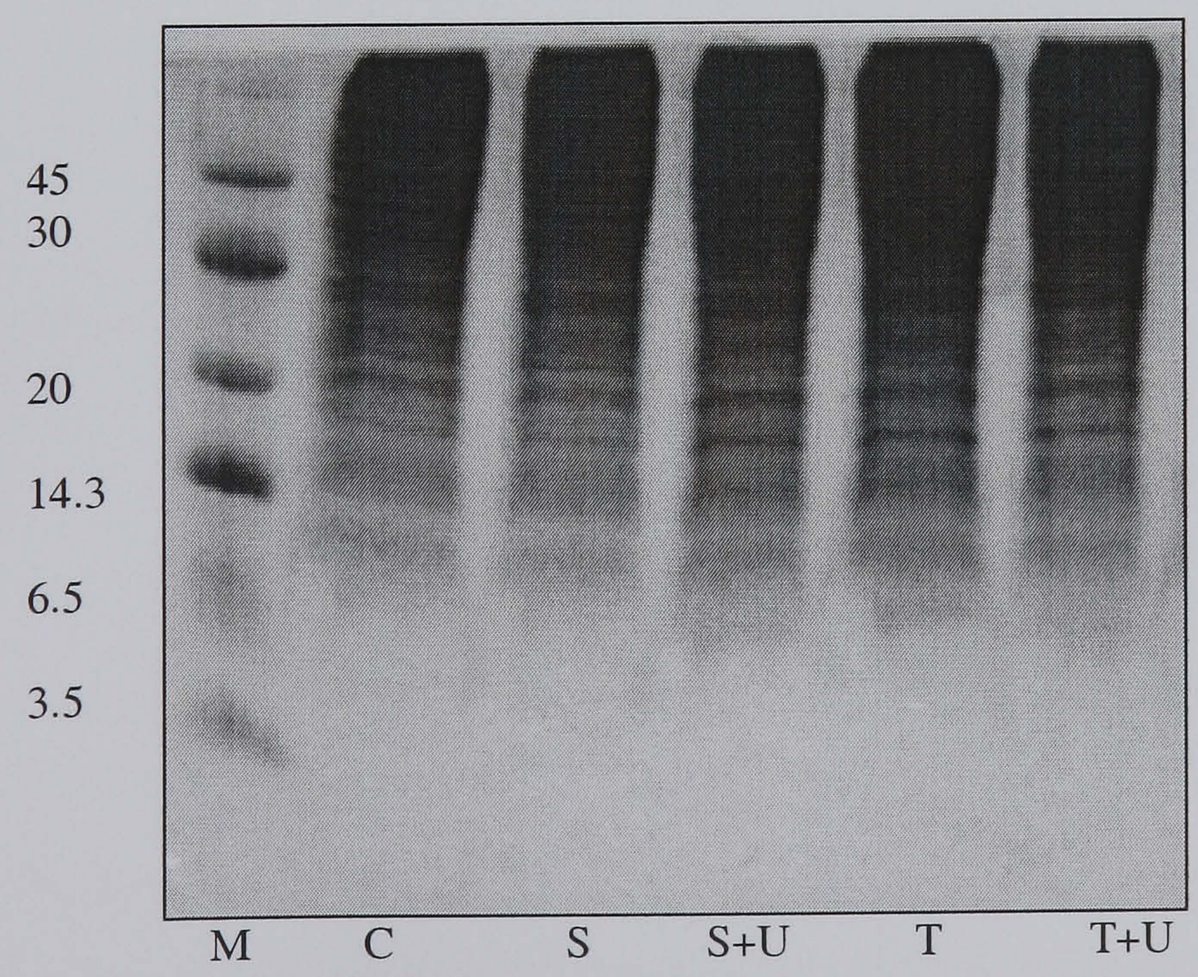

Figure 5.23: Picric acid coomassie blue staining of an SDS-PAGE gel revealing the loading of proteins for Figure 5.22. From left to right, M-Rainbow marker (Amersham), C-control, S-SNAP, S+U-SNAP+UCN, T-TNF-α, T+U-TNF-α+UCN.

Membranes were probed with anti-caspase 9 (Figure 5.22), in the presence of various stimuli. Figure 5.23 represents a picric acid coomassie blue staining of an SDS PAGE gel, to show consistant protein loading of all samples. It can be observed that chondrocytes treated with SNAP alone showed very little activation of caspase 9 similar to control cells. However, treatment of SNAP+UCN showed an increased level of caspase 9 activation than SNAP alone. Pro-enzyme (P32) is indicated by the arrow and the activated form (P10) is clearly labeled. TNF-α alone and TNF-α+UCN did not show any caspase 9 activation. Similar to the caspase 8 experiments, inconsistent results were obtained.

5.4 Discussion

As previously observed in this study, UCN protects chondrocytes against apoptotic death. Growth factors and cytokines control cellular functions by conveying their signals via specialized receptor-generated signal transduction pathways that may influence the cell survival or death decision. Consequently, signal transduction pathways which activate or prevent apoptosis are of major interest to this study. A range of extracellular signals have been shown to control various cell functions such as cell proliferation and differentiation via activation of mitogen activated protein kinases (MAPK) and phosphatidylinositol 3-kinase (PI3K) signal pathways. Recent studies by Brar *et al,* (2000; 2002) have shown that UCN protects cardiac cells via the P42/P44 MAPK, and the PI3 Kinase pathway and the experiments in this chapter were designed to investigate if the MAPK pathways (P38 MAPK, P42/44 MAPK) and the PI3K pathway are involved in UCN mediated 'chondroprotection'. The apoptotic pathways involved in chondrocyte death in response to SNAP and TNF-α treatment were also studied with regard to caspase activation.

To further investigate the intracellular signaling pathways activated by UCN, C-20/A4 chondrocytes were treated with cell signaling inhibitors, PI3K inhibitor LY294008 and the P38 and P42/P44 MAPK inhibitors SB202190 and PD98059 respectively.

Ligation of many growth factor receptors, cytokine receptors and G protein coupled receptors stimulate PI3K activity (Cantrell *et al*, 2001). In view of this, the involvement of the PI3K pathway was investigated in C-20/A4 protection as it has previously been shown that cardiac myocytes were protected by UCN acting via this pathway (Brar *et al*, 2002b).

Cells treated with SNAP+UCN+LY294002 (Figure 5.1) showed an increased level of apoptosis, which was significant compared to SNAP+UCN ($P<0.001$). These results indicate that PI3K is involved in the protection of C-20/A4 cells. This data is in agreement with Brar *et al,* (2002b) who showed that co-administration of LY294002 with UCN in cardiac myocytes exposed to hypoxia/reoxygenation had blocked the protective effect of UCN.

LY294002 was also used in conjunction with TNF-α (Figure 5.2). The degree of apoptosis induced with TNF-α+UCN+LY294002, was not significantly different as compared to TNF-α+UCN for Annexin V/PI staining ($P>0.05$), but a significantly increased apoptotic level was observed for TUNEL staining ($P<0.001$). This data is consistent with the data of Sandra *et al*, (2006) who showed that the apoptotic level in ameloblastoma cells as measured by flow cytometry DNA fragmentation increased by 14%, and when treated with LY294002 (25μM) in conjunction with TNF-α, above that induced by TNF-α alone. The two main differences in the present study and that of Sandra *et al*, are the cell type and the TNF-α concentration which at 100ng/ml was much higher than the one used in this study (70pg/ml).

The results obtained here clearly indicate that chondrocytes are protected by UCN in SNAP and TNF-α treated cells via the PI3K pathway. This data is consistent with the data of Chanalaris *et al*, (2003) who reported that the PI3K inhibitor LY294002 abolished the cardioprotective effects of UCN, UCN II and UCN III, suggesting that this peptide family were dependent on the activation of PI3K for their anti-apoptotic effects in cardiomyocytes. These authors showed that with the treatment of LY294002, apoptotic levels measured by the TUNEL assay increased by 22% as compared to basal cells, and co-treatment with UCN also resulted in high apoptotic levels. It has also been suggested that NF-κB survival signaling is regulated by the PI3K pathway (Sizemore *et al*, 2002). The present data however is not in agreement with Facci *et al*, (2003) who reported that UCN (30nM) prevented DNA fragmentation as well as LDH release from LY294002 (75μM) treated rat cerebellar granule neurons. Therefore the data from this study and that of Chanalaris *et al*, (2003) indicates that PI3K activity is important for UCN chondroprotection in C-20/A4 cells.

Figure 5.3 shows the co-treatment of SB202190+UCN+SNAP resulted in a significant increase in apoptotic death when compared to SNAP+UCN ($P<0.01$). Similarly, Figure 5.4 showed co-treatment with SB202190+UCN+TNF-α showed an increased level of Annexin V/PI and TUNEL staining in chondrocytes, in comparison to TNF-α+UCN, these levels were significantly different ($P<0.001$). These results suggest, along with the SNAP data that, P38 MAPK is involved in the protection of C-20/A4 cells. Therefore, it can be suggested that P38 MAPK may be a cellular stress response that is designed to protect cells from death. This was one reason why the effect of P38 MAPK inhibitor SB202190 on P38 activity in C-20/A4 cells were examined.

Taken together, Figures 5.3 and 5.4 show that with the addition of a P38 MAPK inhibitor SB202190 in SNAP and TNF-α treated cells apoptotic levels are increased clearly, indicating that P38 MAPK maybe involved in the mechanism of protection in C-20/A4 cells (more for TNF-α than SNAP). Zwerina *et al*, (2006) reported that P38 MAPK inhibition (by a P38 MAPK inhibitor) affected cartilage damage considerably. They reported that proteoglycan loss was significantly reduced, and P38 MAPK inhibition was similar to that observed in synovial inflammation. The protection of articular cartilage may not be a direct effect due to lower expression of proinflammatory cytokines. P38 MAPK plays a vital role in pro-inflammatory cytokine production by activating the transcription factor NF-κB which binds to the promoter regions of several pro-inflammatory cytokines, such as TNF-α via TNF-R1. However, P38 MAPK activation by NO may lead to the down regulation of Bcl-2 by interfering with gene transcription (probably due to caspases 9 activation and the release of cytochrome c). This is supported by Kim and Chun, (2003) who reported that P38 MAPK activates NF-κB, which is required for NO induced apoptosis in primary culture of rabbit articular chondrocytes. The data presented in this study, however, does not agree with the data of Chanalaris *et al*, (2003) who showed that a P38 MAPK inhibitor was unable to inhibit the cardioprotective effects of UCN and its homologues (UCN II and UCN III), suggesting that UCN along with its homologues were not dependent on the activation of P38 MAPK for their anti-apoptotic effects in cardiomyocytes. Whilst data obtained in this study appears to suggest that P38 MAPK inhibited the chondroprotective effects of UCN in C-20/A4 cells.

UCN has also previously shown to protect cardiac myocytes against hypoxia/reperfusion injury via activation of the P42/P44 MAPK pathway (Brar *et al*, 2000). Based on these findings, this pathway was investigated here to establish whether the observed UCN mediated protection of C-20/A4 chondrocyte cells also occurred via this pathway. In order to establish this, the P42/P44 MAPK inhibitor PD98059 was used which has been shown to act *in vivo* as a highly selective upstream inhibitor of MEK1 activation in the ERK1/2 pathways.

SNAP+UCN+PD98059 treatment (Figure 5.5), were observed to markedly enhance apoptosis and were significantly increased compared to SNAP+UCN ($P<0.001$). These results clearly indicate that UCN is again protecting C-20/A4 cells from apoptotic cell death, and when co-treated with PD98059, apoptotic levels increased suggesting that the

MAPK P42/P44 pathway is involved in the protection of C-20/A4 cells. This data agrees with the data of Kim *et al,* (2003) who shows that with the co-treatment of PD98059 (20μM) with an NO donor in rabbit chondrocytes, apoptotic levels are increased significantly (38%) as measured by TUNEL assay. Kim *et al,* (2002) also reported that in primary articular chondrocytes, NO caused apoptosis and dedifferentiation, which are mediated by MAPK subtypes ERK and P38 MAPK.

C-20/A4 cells subjected to TNF-α+UCN+PD98059 (Figure 5.6) showed an increased level of apoptosis and was significantly higher than TNF-α+UCN ($P<0.001$). PD98059+TNF-α+UCN treatment, clearly showed that TUNEL staining induced a significantly high level of apoptosis, as compared to the Annexin V/PI staining which resulted in a 2-fold increase against TNF-α+UCN, indicating protection by UCN via the P42/P44 MAPK pathway. This data agrees with the data of Chanalaris *et al*, (2003) who established that the P42/P44 MAPK inhibitor PD98059 completely abolished the anti-apoptotic effects of UCN, UCN II and UCN III, suggesting that all three peptides were dependent on the activation of P42/P44 MAPK for their effects in cardiomyocytes. The authors reported an increase in apoptosis in the presence of PD98059, measured by the TUNEL assay whilst co-treatment with UCN resulted in a further increase of 11% as compared to PD98059 alone, indicating that P42/P44 MAPK was involved in the cardioprotection of cardiomyocytes. The data of the present study does not agree with the data of Kim *et al,* (2002) who found that co-treatment of PD98059 and TNF-α (10ng/ml) did not result in any significant increase in human chondrocyte apoptosis. It is possible that TNF-α activation via P42/P44 MAPK may require low doses, as observed in this study, because the dose used by Kim and Song was substancial in comparison.

Figure 5.6 showed protective effect of UCN more on TNF-α than SNAP induced apoptosis as observed by TUNEL staining. The induction of apoptosis is generally restricted to receptors that contain 'death domains' as in TNF-α signaling. The TNF-R1 contains a death domain protein (TRADD), which is known to interact with TRAF-2 that is associated with TRADD and RIP-1 in the activation of nuclear factor kappa B (NF-κB). NF-κB inducing kinase is then activated, resulting in the activation of, the IκB kinase complexes, the phosphorylation of IκB, the degradation of IκB, and finally to the activation of NK-κB. It has been postulated that ERK signaling can be controlled by

NF-κB via autocrine mechanisms, such as TNF-α enhanced expression (Bhat-Natakshatri *et al*, 2002), suggesting one possible reason why increased level of late apoptosis may have been observed in C-20/A4 cells in the presence of the P42/P44 MAPK inhibitor.

Figure 5.7 shows the inhibitors treated alone in C-20/A4 cells. This was to observe if these inhibitors were exerting a toxic effect in chondrocytes. Treatment of LY294002, SB202190 and PD98059 were all significantly increased against the control respectively ($P<0.001$), and showed no toxic effect exerted on these cells.

The results obtained from the various inhibitor studies clearly showed that all three pathways are likely to be involved in the UCN mediated protection of C-20/A4 cells. UCN is believed to act in an autocrine/paracrine manner to protect chondrocytes by binding to an as yet unconfirmed receptor, which then activates these pathways. As inhibitor data alone cannot conclusively, determine that UCN is chondroprotective via these pathways (chemical inhibitors are not specific). Western blot analysis was used to investigate kinase activation by using specific antibodies for the various kinases. Due to time constraints, these studies were focused on the P42/P44 MAPK only, as UCN conferred protection was reversed mostly by PD98059 treatment compared to the other two inhibitors. This was observed after, the chondrocytes were treated with PD98059 in the presence and absence of SNAP and TNF-α, with or without UCN. The P38 MAPK inhibitor SB202190 was also used in the presence of UCN stimulation as a control. P42/P44 MAPK activation occurs via dual phosphorylation of threonine and tyrosine residues as specific antibodies for this phosphorylated form were used to quantify MAPK activation in C-20/A4 cells.

Figure 5.8 shows that the activation of P42/P44 MAPK was significantly blocked by PD98059 alone ($P<0.001$, PD98059 vs control). Significantly increased activation (2 fold) of P42/P44 MAPK was observed with UCN treated alone ($P<0.001$ UCN vs control), which was then blocked in the presence of PD98059. No significant difference in activation was observed with SB202190+UCN compared to UCN alone ($P>0.01$). This is to be expected as SB202190 is a P38 inhibitor and should not interfere with P42/P44 activation. Samples with PD98059+UCN showed some level of activation, but the inhibitor largely counters the UCN induced activation. This data along with the fact that chondroprotective effect was abolished by PD98059 (Figure 5.5 and 5.6), indicates

(that the chondroprotective mechanism of UCN involves the activation of P42/P44 MAPK. The apparent increase in signal for P42/P44 MAPK, especially in UCN treated cells, could however, be a result of the three factors:

i) an increase in the percentage of phosphorylated proteins in P42/P44 MAPK
ii) an increase in total expression of P42/P44 MAPK not including changes in the percentage of phosphorylation or
iii) combination of i and ii.

However, total P42/P44 MAPK levels were unchanged in all treatments (Figures 5.9, 5.12, 5.15) indicating, that the increased P42/P44 MAPK phosphorylation observed in UCN treated samples is genuine rather than a result of an increase in total expression levels of P42/P44 MAPK. The present data agrees with the data of Brar *et al*, (2002a) who showed that with the exogenous treatment of UCN (10^{-8}M), P42/P44 MAPK phosphorylation increased significantly in cardiac myocytes and when administered with PD98059, it had abolished the phosphorylation of P42/P44 MAPK by UCN.

Figure 5.11 clearly show that when PD98059 is added, P42/P44 MAPK activation is decreased as expected since it blocks the P42/P44 MAPK pathway. In SNAP treated cells, the increase in P42/P44 MAPK activation may be a result of endogenous UCN production stimulated by the applied NO insult. The presence of exogenous UCN in SNAP significantly activates P42/P44 MAPK ($P<0.001$ SNAP+UCN vs SNAP alone) as previously observed in this study. This data is in agreement with Kim *et al*, (2003) who showed NO donor treatment in articular chondrocytes activates the ERK 1/2 kinase, as established by Western blot analyses, although the specie was not identified in that report.

Figure 5.14 suggests that under TNF-α exposure, P42/P44 MAPK activation occurs significantly in C-20/A4 human chondrocytes ($P<0.001$ TNF-α vs control). The data shown in this study clearly showed that TNF-α does not induce endogenous UCN, so it may be possible that another mechanism is operating in these cells in the presence of TNF-α, most probably complex I. It has been reported that TNF-R1 ligation triggers activation of P42/P44 MAPK which can override the pro-apoptotic signaling pathway of this death receptor. Thus, P42/P44 MAPK may have a normally protective effect on death receptor-induced apoptosis that may be used under conditions when death

receptor reaction has to be switched off promptly i.e. causing the internalization of the receptor (TNF-R1) from the surface of the cell to the cytosol and inhibition of its cytotoxic ability (Zhang *et al*, 2003) which may be one possibility to why TNF-α alone induced the highest level of activation. However if this was the case, then TNF-α+UCN should have shown higher protection in C-20/A4 cells. This data however is consistent with the data of Sandra *et al*, (2005) who showed that when ameloblastoma cells were subjected to TNF-α (100ng/ml), it induced phosphorylation of P42/P44 MAPK, which may be involved in cell survival and/or proliferation in these cells.

Overall these findings clearly demonstrate that P42/P44 MAPK modulates cell survival in C-20/A4 cells and contributes to the cytoprotection effected by endogenous and exogenous UCN as this anti-apoptotic effect was correlated with the increased P42/P44 MAPK signaling activity. Activated P42/P44 MAPK (ERK1/ERK2) translocates into the nucleus and regulates the activities of numerous nuclear transcription factors (e.g. ELK-1) which in turn could activate transcription of the gene expression (Pearson *et al* as observed in the SNAP treatments, which was not observed because of UCN being a protective agent. At present there is no explanation as to why that could have occurred, 2001). Inhibition of ERK1/ERK2 prevents this translocation into the nucleus from the cytosol, potentially resulting in increased expression of genes which regulate pro-apoptotic proteins or decreased expression of genes which regulates anti-apoptotic proteins. Inhibiting ERK1/ERK2 may also prevent the inactivation of pro-apoptotic factors (Gebauer *et al*, 1999). P42/P44 MAPK are Ser/Thr kinases stimulated by G protein coupled receptors and protein tyrosine kinases via the initiation of Ras and Raf (Khokhlatchev *et al*, 1997). This tyrosine kinase is recognized to be intimately linked with focal adhesion complexes that are made when membrane spanning integrins work together with their extracellular ligands. It is possible that other tyrosine kinases functions as a link between mechanoreceptors, including integrins, and the P42/P44 MAPK pathway. The P42/P44 MAPK activation results obtained for both SNAP and TNF-α are consistent with the apoptosis observed in the PD98059 inhibitor studies, and provide further evidence that C-20/A4 cells are protected by UCN via the P42/P44 MAPK pathway. These results are in agreement with Brar *et al*, (2000) who showed that P42/P44 MAPK pathway mediate the cardioprotective effects of UCN (10^{-8}M) in neonatal rat cardiomyocytes. UCN has also been shown to activate and phosphorylate P42/P44 MAPK in cultured human pregnant myometrial cells (Light *et al*, 1996; Grammatopoulos *et al*, 2000). The finding of the present study is also consistent with

the studies of Liacini *et al,* (2003) who reported that TNF-α (20ng/ml) significantly stimulated the activation of ERK1/2 in human OA chondrocytes. However, due to limitations and nonspecificity of inhibitor studies, it is possible that other kinases may also be involved in C-20/A4 cells, such as P38 MAPK and PI3K which were not investigated and could be examined as future work. This data is also in agreement with Sandra *et al*, (2006) who reported that treatment of TNF-α (100ng/ml) in ameloblastoma cells caused an increased level of P42/P44 MAPK phosphorylation. These results indicate that TNF-α stimulated survival activity could no longer compensate the apoptosis signal, which also was induced by TNF-α. This could be due to TNF-α working through an anti-apoptotic pathway (Aizawa *et al*, 2001). The anti-apoptotic pathway regulated by NF-κB (complex I) controls the expression of several anti-apoptotic proteins and generally triggers cell survival signals (which have been discussed earlier in this study) (Micheau and Tschopp, 2003).

Due to caspases contributing to the overall apoptotic morphology by cleavage of various cellular substrates, and to verify the involvement of the caspase cascade in C-20/A4 chondrocyte death, caspase activation was examined. In order to establish which pathway of apoptosis may be operational in C-20/A4 cells, the activation of caspase 3, caspase 8 and caspase 9 was investigated. These caspases are located at important junctions in the apoptotic pathway. Caspase 8 and caspase 9 activate caspase 3 by proteolytic cleavage and caspase 3 then digests important cellular proteins (Hengartner, 2000).

Caspase 3 is one of the effector caspases that digests substrates crucial for cell death, and the amount of caspase 3 activity is thus a vital marker of the level of apoptosis. Caspase 3 is synthesized as a 32 kDa proenzyme (not shown due to antibody only recognizing cleaved form) that is cleaved during activation to yield a large catalytic subunit of 20 kDa (Mancini *et al*, 1998). This subunit (20kDa) was detected in C-20/A4 chondrocytes treated with SNAP (Figure 5.17), indicating a high level of activation, almost a 9-fold increase as compared to control cells which was significantly different ($P<0.001$). However, in the presence of SNAP+UCN, only a 7-fold increase was noted. This was shown to be significantly different when compared to SNAP treatment alone ($P<0.001$). Treatment with TNF-α and TNF-α+UCN failed to show any activation. These results show clearly that caspase 3 activation is enhanced by SNAP treatment but decreased in the presence of UCN indicating protection against apoptosis, in accordance

with previous results in this study. Other studies have shown TNF-α to activates caspase 3, but, why TNF-α failed to show any significant activation, in C-20/A4 chondrocytes is not known. One would have expected some activation of caspase 3 at least in the TNF-α only samples as caspase 3 is one of the main effectors of apoptosis and apoptotic C-20/A4 cell death does occur with TNF-α treatment. However, these experiments were repeated several times and the results were consistent. The present data is in agreement with Scarabelli *et al*, (2002) who showed that with the addition of exogenous UCN (10^{-8}M) in the isolated pulsed rat heart caspase 3 activation (using an enzymatic assay to measure caspase 3) is significantly reduced. The data presented here does not agree with that of Sandra *et al*, (2006) who showed that caspase 3 (using anti-caspase 3 antibody) was activated in ameloblastoma cells when treated with TNF-α, but does agree with that of Los *et al*, (2002) who showed that treatment of immortalized fibroblast cells with 40ng/ml of TNF-α does not induce caspase 3, activation until 8 hrs of treatment. These authors performed a time course of caspase activation on TNF-α mediated cell death, and established that after 8 hrs TNF-α only induced a weak, caspase activation. This may be one reason why TNF-α treatment did not result in caspase 3 activation in C-20/A4 cells, since caspase 3 activation was only assessed at 6 hours.

The SNAP data presented here is in agreement with Kim *et al*, (2003) who established that NO-induced apoptosis results in caspase 3 cleavage (using a ApoAlert CPP32 colorimetric assay kit) in rabbit chondrocytes. This data is also supported by Notoya *et al*, (2000) who showed that, in the presence of an NO donor, caspase 3 activity in human OA chondrocytes was increased as measured by a caspase assay kit. The present data is part supported by Maneiro *et al*, (2005) who showed that both an NO donor (0.5mM) and TNF-α (10ng/ml) induced an increase of caspase 3 mRNA in human chondrocytes, but the authors did not report if caspase 3 activation was observed. It is possible that if caspase expression is increased in cells due to insult, caspase 3 activation may not always occur.

Caspase 8 initiates cell disassembly due to extracellular apoptosis-inducing ligands and is stimulated in a complex linked with the cytoplasmic death domain of several cell surface receptors for the ligands (Chinnaiyan *et al*, 1995). The death receptor pathway was investigated with the same stimuli stated for caspase 3 (Figure 5.20). Figure 5.21

shows an SDS-PAGE picric acid gel of equal protein loading for caspase 8. Interpretation of the results, are complicated by the unexpected results obtained. One would have expected activation of caspase 8 in cells treated with TNF-α although, this was not observed. Activation for SNAP and SNAP+UCN was not detected either, but SNAP (NO) is known to work via the mitochondrial pathway (Zech *et al*, 2003). The pro-enzyme are shown by the arrows. Problems were experienced with the primary antibodies purchased from Santa Cruz Biotechnology for active caspase 8 and, despite these being replaced by Santa Cruz, inconsistencies in the data were still apparent. Another possibility could be low levels of caspases with short half lives, making detection harder (Mistry *et al*, 2004). Due to time restrictions, it was not possible to investigate these problems further although similar inconsistency problems were encountered with the original caspase 3 antibodies also purchased from Santa Cruz. This prompted a change of primary antibody to one purchased from Cell Signaling Technology which performed much better. If time allowed, the caspase 8 experiments would have been repeated using antibodies from Cell Signalling Technology in an attempt to improve consistency.

This data agrees in part with Kühn and Lotz, (2001) who detected no procaspase 8 processing by immunoblotting after stimulating human chondrocytes with CD-95 antibody, although the mRNA transcript of caspase 8 was detected. Caspase activation has also been reported by Spears *et al*, (2003) who showed that in rat temporomandibular joints, TNF-α (50ng/ml) caused a significant increase in caspase 3 and caspase 8 activation as compared to basal level by using the ApoAlert caspase colorimetric assay kit. The data of Spears *et al*, (2003) is supported by Mohamed *et al*, (2002) who reported by using Western blot analysis, caspase 3 and caspase 8 were activated after TNF-α (50ng/ml) treatment in Hela-TNFR2 cells.

Caspase 9 activates disassembly in response to insults that trigger the release of cytochrome c from mitochondria and is activated when complexed with APAF-1 and extramitochondrial cytochrome c. The mitochondrial pathway was also investigated with the same stimuli, as stated for caspase 3. Figure 5.22 shows the membrane probed with caspase 9 antibodies to establish if this initiator caspase, is activated in C-20/A4 chondrocytes subjected to the different stimuli. It can clearly be seen that there is a basal level of cleavage in control cells. Cells treated with SNAP alone showed almost the same level of cleavage shown at basal level. However, co-treatment with SNAP+UCN

showed an increase in cleavage of caspase 9. The reason for this at present is unknown. Due to UCN being a protective agent, based on previous data in this thesis, increased caspase 9 activation in the presence of UCN is unexpected. TNF-α and TNF-α+UCN failed to show any activation, which would be consistant with TNF-α acting through the death receptor pathway. This data thus, with activation of caspase 8 and 9 at present cannot be interpreted due to the inconsistencies observed.

The results presented in this chapter demonstrate that the cell survival/anti-apoptotic effect of UCN (which has been shown to protect C-20/A4 chondrocytes from SNAP and TNF-α stimulation) involves activation of the PI3K, P38 MAPK, and P42/P44 MAPK pathway. The activation of all these pathways may be involved in UCN mediated chondroprotection as blocking these pathways with the relevant inhibitors increases cell death even in the presence of exogenous UCN. Of all three however, the effect appears most pronounced with P42/P44 MAPK inhibition indicating that this may be the primary signaling pathway involved. This was further supported by Western blot analysis of P42/P44 MAPK activation by UCN. Due to time constraints, it was not possible to pursue the other two pathways, but these results clearly showed that UCN activates the P42/P44 MAPK signal cascade in C-20/A4 human chondrocytes. The involvement of the death receptor and mitochondrial apoptotic pathways, were also investigated for the two main proapoptotic stimuli used (NO and TNF-α) but due to inconsistent results it was not possible to draw conclusions from these studies and further work is necessary.

CHAPTER 6

FINAL DISCUSSION, CONCLUSIONS AND FUTURE WORK

Chondrocyte death by apoptosis has been implicated in the pathogenesis of osteoarthritis. The aims of this research were to study the potential inducers of chondrocyte death, determine the mechanism of that death and to investigate the role of the CRH-like peptide, Urocortin in 'chondroprotection', i.e. the prevention of chondrocyte death.

This study first sought to characterize the response of C-20/A4 chondrocytes to three pro-apoptotic stimuli implicated in the pathogenesis of OA, Nitric oxide (NO) TNF-α and IL-1β. NO regulates several cartilage functions including loss of chondrocyte phenotype, chondrocyte apoptosis, and extracellular matrix degradation. In keeping with this, the studies detailed in this thesis showed that SNAP (an NO donor) induces apoptosis in C-20/A4 cells. *In vitro* human articular cartilage can generate significant levels of NO that can be increased by pro-inflammatory cytokines such as TNF-α (Attur *et al*, 1997) and IL-1β which have also been shown to induce apoptosis in C-20/A4 cells

It was clearly observed in this study that apoptosis (as measured by TUNEL and Annexin V/PI assays) and not necrosis (as measured by LDH release) was the main cell death observed in C-20/A4 human chondrocytes treated with 1mM SNAP, 70pg/ml TNF-α and 8pg/ml IL-1β. SNAP treatment demonstrated a dose dependent increase in apoptosis, whilst TNF-α and IL-1β did not. TNF-α showed a dose dependent increase in cell death up to 80pg/ml after which a decreased cell death occurs. During this decrease in apoptosis from 80-100pg/ml, the complex I signal transduction cascade mediated by TNF-α could have activated a number of transcriptional factors including NF-κB and AP-1 (Ah-Kim *et al*, 2000). Since NF-κB activation is known to protect cells from the cytotoxic effects of TNF-α in a variety of cell lines, further work can be undertaken to elucidate the effects of C-20/A4 cells on degradation of its cytoplasmatic inhibitor IκB and NF-κB activation in TNF-α treated chondrocytes.

In 1998 Okosi *et al*, reported that the CRH family peptide UCN was produced by cardiac myocytes and that it was protective against hypoxia mediated apoptosis in these cells. It is therefore possible that UCN could play a comparable role in chondrocytes which may represent a mechanism to prevent chondrocyte death.

The endogenous production of UCN by chondrocytes was clearly shown in this study, the first time this has been demonstrated (Figure 4.11a). UCN is produced at a basal level consitutively in C-20/A4 cells but is also inducible by certain pro-apoptotic stimuli such as SNAP (NO) which increased C-20/A4 expression of UCN by approximately two fold whereas others such as TNF-α did not induce increased expression. This may indicate that UCN represents a protective mechanism against only certain types of stimuli, e.g. mitochondrial insults but not death receptor insults. The cytoprotective potential of UCN was further confirmed by CRH antagonist studies (4.3.2) where apoptotic levels increased significantly on the addition of α helical $CRH_{(9-41)}$, clearly indicating the existence of a CRH family peptide in C-20/A4 cells.

Following confirmation of the endogenous production of UCN by C-20/A4 cells, and the increase in apoptosis after α helical $CRH_{(9-41)}$ administration (section 4.3.2), it was suspected that UCN may represent endogenous cytoprotective and growth factor mechanism in chondrocytes. This was confirmed by the addition of a UCN specific antibody to C-20/A4 cultures which resulted in a high level of apoptosis whereas an isotype control, anti-albumin antibody did not. These experiments (section 4.3.3) confirm that UCN production is an endogenous 'chondroprotective' mechanism.

Brar *et al*, (1999) also reported that the addition of preconditioned media to cardiac myocytes protected these cells from necrotic and apoptotic cell death indicating the existence of a protective agent in the preconditioned media which was believed to be a member of the CRH family of peptides. The experiments performed in this study however failed to establish any chondrocyte protection from preconditioned media as shown in section 4.3.4. This may indicate that preconditioning is cell type specific or that the effects of protective elements in the media may be being masked by pro-apoptotic elements also present.

In assuming that UCN was a 'chondroprotective' agent, the next logical step was to treat chondrocyte cultures exposed to pro-apoptotic stimuli with exogenous UCN and observe the effects on the level of cell death. The addition of exogenous UCN at 10^{-8}M reduced chondrocyte death in cultures treated with SNAP and TNF-α but UCN appears to confer greater protection against SNAP (NO) initiated cell death than that caused by TNF-α (Figure 4.28 and Figure 4.29 respectively). This protection conferred by exogenous UCN was negated by the addition of α helical $CRH_{(9-41)}$.

Once it was confirmed that UCN was protecting chondrocytes from death, the next step was to establish the mechanism of chondrocyte protection by UCN. Since UCN activation of the PI3K, and P42/P44 MAPK, but not P38 MAPK survival pathways has been shown to suppress apoptosis in other cell systems (Chanalaris *et al*, 2003), the involvement of these signaling pathways in UCN mediated chondrocyte protection against SNAP and TNF-α induced apoptosis was studied. To gain further insights into the roles played by these signaling cascades, the PI3K, P38 MAPK and P42/P44 MAPK pathways were interrupted with the selective inhibitors LY294002, SB202190 and PD98059 respectively.

The data presented in chapter 5.3.1 indicates that all three pathways may be involved as the protective effects of UCN were reduced by all three of the inhibitors but the P42/P44 MAPK may be particularly significant as inhibition of this pathway resulted in the greatest reversal of UCN mediated protection. This was further confirmed by Western blot analysis using antibodies against phosphorylated (active) P42/P44 MAPK which clearly showed that UCN treatment of C-20/A4 chondrocytes results in an increased level of P42/P44 MAPK activation which was abolished by the selective inhibitor PD98059. The treatment of C-20/A4 cells with SNAP alone also shows some activation of P42/P44 MAPK, possibly as a result of endogenous UCN activity whilst co-treatment of cells with UCN and SNAP shows a greater level of activation than SNAP alone. These observations are in accordance with the data presented in section 4.3.5 of this thesis which showed that the co-treatment of C-20/A4 cells with UCN and SNAP resulted in a decreased level of apoptotic cell death than that observed with SNAP treatment. This seems to indicate a link between chondrocyte protection and P42/P44 MAPK activation in C-20/A4 cells.

Significant activation of the P42/P44 MAPK pathway was also observed in TNF-α treated C-20/A4 cells (at a much higher level than that observed for SNAP treatment) but the addition of UCN resulted in no significant change in P42/P44 MAPK activation with this stimulus. This too would support the data shown in section 4.3.5 where the degree of protection accorded by UCN co-treatment with TNF-α is minimal than SNAP co-treatment. It seems likely that P42/P44 MAPK activation in this instance is a direct result of TNF-α stimulation rather than UCN mediated P42/P44 MAPK activation. This phenomenon has been reported by others (Tselepis *et al*, 2002; Sandra *et al*, 2005). To assess this further, UCN makes a contribution to the P42/P44 MAPK activation in this

instance future experiments could be devised to include α helical $CRH_{(9-41)}$ with UCN/TNF-α co-treatment to observe if there is any decrease in the P42/P44 MAPK activation.

The role played by P38 MAPK in cells is quite controversial and remains a subject of debate (Dean *et al*, 1999; Manthey *et al*, 1998, Lee *et al*, 1994). This controversy could arise from many variables, including differences in the cell type or stress agent involved. Furthermore, because most studies have looked at a given pathway in isolation, the potential interactions between pathways have not been addressed. The P38, P42/P44 and PI3 kinase pathway all appear to be involved to some extent in the chondroprotective effect of UCN in C-20/A4 cells. Whether UCN phosphorylates and activates the P38 MAPK and PI3K pathway in C-20/A4 cells needs to be investigated further. But the possibility that different signaling pathways are used by chondrocytes to respond to different mechanical stimuli opens up more avenues for further study.

The final experiments detailed in this thesis were an attempt to establish the apoptotic pathway activated in C-20/A4 cells after treatment with SNAP or TNF-α. In section 5.3.3.1 activation of caspase 3, was increased in SNAP alone and decreased in SNAP+UCN treated cells. This data is consistent with previous data in this thesis (Figure 4.28), which showed that in the presence of SNAP alone, apoptotic levels had increased significantly, whilst in the presence of SNAP+UCN induction of apoptosis decreased significantly. There is however no explanation as to why caspase 3 activation was not observed in TNF-α treated cells at present, even though apoptotic levels were observed to significantly increase following TNF-α treatment throughout this study.

Whilst caspase 3 activation was shown with SNAP treatment and correlated with increased cell death, analysis of initiator caspase activation is less clear. Western blotting for activated caspase 9 (section 5.3.3.3) did show some cleavage in SNAP alone treated cells, but this increased with SNAP+UCN treatment which is not consistent with the cell death data documented in this thesis (Figure 4.28). However the results obtained from replicates of this experiment were not consistant so no real conclusions can be drawn from this data. Studies of Caspase 8 activation were similarly inconclusive due to similar inconsistency between repeat experiments. As a result of these inconsistancies, no meaningful conclusions can be drawn from this data and further work is required to

conclusively establish which of the initiator caspases is activated by the different stimuli.

The experiments and results documented in this thesis indicate that UCN is likely to represent an endogenous cyto-protective mechanism in human chondrocytes although, there is considerably more work that needs to be done to clarify how UCN may mediate its effects in chondrocytes. As UCN is believed to work in an autocrine/paracrine fashion, one of the most basic questions still to be answered is which cell surface molecule/receptor does UCN bind to in order to induce a response in the target cell. In other cell types, UCN has been shown to exert its effects through binding to either of the CRH receptors, CRH-R1 or CRH-R2. Whilst this is supported to a certain extent by the α helical $CRH_{(9\text{-}41)}$ experiments in this study, CRH-R expression has not yet been demonstrated on chondrocytes. It is equally possible that UCN may be exerting it's effects through calcium channel inhibition as reported by Tao *et al* (2004), in rat ventricular cells. An important area of future work would therefore be to determine chondrocyte expression of CRH-R and calcium channels and the subtypes thereof.

The other main area of future work that needs to be pursued is the mechanisms of action of UCN and how it effects cyto-protection against apoptosis. Due to the inconclusive nature of the capase activation experiments considered earlier, these certainly need to be repeated (with alternative reagents) to establish which apoptotic pathways the various pro-apoptotic stimuli induce in chondrocytes and then the pathways through which UCN mediated protection is achieved need to be further studied. As well as the possible mechanisms discussed earlier, a number of endogenous substances have been shown to be involved in cyto-protection in other tissues. Brar *et al*, (2002a) established that UCN induced the expression of the cytoprotective HSP90 heat shock protein. Heat shock protein production is enhanced by cell stress and they act as molecular chaperones contributing to cellular homeostasis by encouraging accurate folding of proteins, repairing denatured proteins or increasing their degradation (Benjamin and M^{c}millan, 1998). Increasing evidence also suggests that mitochondrial K_{ATP} channels may also be involved in UCN mediated cytoprotection. Lawrence *et al*, (2002) reported that UCN distinctively enhances gene expression of the $K_{ir}6.1$ subunit of the cardiac K^+ channel and that UCN mediated cardioprotection could be inhibited by mitochondrial K_{ATP} channel blockers. In support of this, Scarabelli *et al*, (2003) reported that live, UCN positive cells expressing the $K_{ir}6.1$ K_{ATP} channel that are surrounded by live, UCN

negative, but $K_{ir}6.1$ positive cells, indicatiing that autocrine and paracrine enhancement of K_{ATP} channel expression by endogenously released UCN also occurs. It would be interesting to see if these proteins and K_{ATP} channels are present in C-20/A4 chondrocytes and if UCN exerts similar effects on their levels in C-20/A4 cells.

The recent discovery of two new members of the CRH peptide family, UCN II and UCN III (Reyes *et al*, 2001; Lewis *et al*, 2001) also present further study opportunities. UCN II and UCN III show higher affinity for the CRH-R2 than CRH-R1, and it is possible that these peptides may therefore exhibit higher protective effects than UCN and/or produce these effects with higher specificity, since they bind only to CRH-R2. UCN III has already been shown to be more potent than UCN in protecting against apoptosis induced by hypoxia/reoxygenation injury in rat neonatal cardiomyocytes (Chanalaris *et al*, 2003). Thus comparing the protective potencies of UCN, UCN II and UCN III in chondrocytes is important in the development of CRH peptide-related therapies for the treatment of OA.

In conclusion, the data reported in this study indicate that the CRH-like peptide UCN is an endogenous chondroprotective agent which is induced in response to certain pro-apoptotic stimuli, in particular NO. These experiments also indicate that UCN mediated chondroprotection may occur via the PI3K, P38 MAPK and P42/P44 MAPK signaling pathways but the most significant is likely to be the P42/P44 MAPK. These experiments have also demonstrated that UCN is capable of reducing chondrocyte death when added exogenously which leads to the possibility that UCN, or an analogue of UCN, may have potential as a therapeutic agent for the prevention of chondrocyte death. This would represent a possible therapeutic avenue for the treatment/prevention of OA but it should be noted however that the potential for UCN activity outside the desired target tissue is high due to the distribution of the CRH receptors. This research has also identified other possible areas of intervention, such as the PI3K and MAPK pathways implicated in UCN activity which could be molecular targets for the prevention of chondrocyte apoptosis providing further possibilities for the treatment of OA. Additional investigation of the role of UCN and its homologues in human chondrocytes may help to guide researchers to a clear insight of the natural role of this unique peptide family and to its definitive therapeutic use in this degenerative disease and other conditions.

CHAPTER 7

REFERENCES

Abramson, S. B., A. R. Amin, R. M. Clancy and M. Attur **(2001)**. "The role of nitric oxide in tissue destruction." Best Pract Res Clin Rheumatol **15**(5): 831-45.

Abramson, S. B. and Y. Yazici **(2006)**. "Biologics in development for rheumatoid arthritis: relevance to osteoarthritis." Adv Drug Deliv Rev **58**(2): 212-25.

Adams, C. S. and W. E. Horton, Jr. **(1998)**. "Chondrocyte apoptosis increases with age in the articular cartilage of adult animals." Anat Rec **250**(4): 418-25.

Aggarwal, B. B. and K. Natarajan **(1996)**. "Tumor necrosis factors: developments during the last decade." Eur Cytokine Netw **7**(2): 93-124.

Agnello, D., R. Bertini, S. Sacco, C. Meazza, P. Villa and P. Ghezzi **(1998)**. "Corticosteroid-independent inhibition of tumor necrosis factor production by the neuropeptide urocortin." Am J Physiol **275**(5 Pt 1): E757-62.

Ah-Kim, H., X. Zhang, S. Islam, J. I. Sofi, Y. Glickberg, C. J. Malemud, R. W. Moskowitz and T. M. Haqqi **(2000)**. "Tumour necrosis factor alpha enhances the expression of hydroxyl lyase, cytoplasmic antiproteinase-2 and a dual specificity kinase TTK in human chondrocyte-like cells." Cytokine **12**(2): 142-50.

Aigner, T., L. McKenna, A. Zien, Z. Fan, P. M. Gebhard and R. Zimmer **(2005)**. "Gene expression profiling of serum- and interleukin-1 beta-stimulated primary human adult articular chondrocytes--a molecular analysis based on chondrocytes isolated from one donor." Cytokine **31**(3): 227-40.

Aizawa, T., S. Kokubun and Y. Tanaka **(1997)**. "Apoptosis and proliferation of growth plate chondrocytes in rabbits." J Bone Joint Surg Br **79**(3): 483-6.

Aizawa, T., T. Kon, T. A. Einhorn and L. C. Gerstenfeld **(2001)**. "Induction of apoptosis in chondrocytes by tumor necrosis factor-alpha." J Orthop Res **19**(5): 785-96.

Alsalameh, S., B. Manger, P. Kern and J. Kalden **(1998)**. "New onset of rheumatoid arthritis during interferon beta-1B treatment in a patient with multiple sclerosis: comment on the case report by Jabaily and Thompson." Arthritis Rheum **41**(4): 754.

Amin, A. R. **(1999)**. "Regulation of tumor necrosis factor-alpha and tumor necrosis factor converting enzyme in human osteoarthritis." Osteoarthritis Cartilage **7**(4): 392-4.

Amin, A. R. and S. B. Abramson **(1998)**. "The role of nitric oxide in articular cartilage breakdown in osteoarthritis." Curr Opin Rheumatol **10**(3): 263-8.

Amin, A. R., P. E. Di Cesare, P. Vyas, M. Attur, E. Tzeng, T. R. Billiar, S. A. Stuchin and S. B. Abramson **(1995)**. "The expression and regulation of nitric oxide synthase in human osteoarthritis-affected chondrocytes: evidence for up-regulated neuronal nitric oxide synthase." J Exp Med **182**(6): 2097-102.

Andree, H. A., C. P. Reutelingsperger, R. Hauptmann, H. C. Hemker, W. T. Hermens and G. M. Willems **(1990)**. "Binding of vascular anticoagulant alpha (VAC alpha) to planar phospholipid bilayers." J Biol Chem **265**(9): 4923-8.

Archer, C. W., H. Morrison and A. A. Pitsillides **(1994)**. "Cellular aspects of the development of diarthrodial joints and articular cartilage." J Anat **184 (Pt 3)**: 447-56.

Arden, N. and M. C. Nevitt **(2006)**. "Osteoarthritis: epidemiology." Best Pract Res Clin Rheumatol **20**(1): 3-25.

Attur, M. G., R. N. Patel, S. B. Abramson and A. R. Amin **(1997)**. "Interleukin-17 up-regulation of nitric oxide production in human osteoarthritis cartilage." Arthritis Rheum **40**(6): 1050-3.

Aydelotte, M. B., S. S. Mok, L. Michal and H. J. Hauselmann **(1996)**. "Effects of Misoprostol with Interleukin-1 on Proteoglycan Metabolism of Cultured Articular Chondrocytes." Am J Ther **3**(1): 3-8.

Babich, H. and E. Borenfreund **(1990)**. "Cytotoxic effects of food additives and pharmaceuticals on cells in culture as determined with the neutral red assay." J Pharm Sci **79**(7): 592-4.

Babich, H. and E. Borenfreund **(1991)**. "Cytotoxicity of T-2 toxin and its metabolites determined with the neutral red cell viability assay." Appl Environ Microbiol **57**(7): 2101-3.

Babich, H., E. Borenfreund and A. Stern **(1993)**. "Comparative cytotoxicities of selected minor dietary non-nutrients with chemopreventive properties." Cancer Lett **73**(2-3): 127-33.

Babich, H., C. Shopsis and E. Borenfreund **(1986)**. "In vitro cytotoxicity testing of aquatic pollutants (cadmium, copper, zinc, nickel) using established fish cell lines." Ecotoxicol Environ Saf **11**(1): 91-9.

Babich, H. and H. L. Zuckerbraun **(2001)**. "In vitro cytotoxicity of glyco-S-nitrosothiols. a novel class of nitric oxide donors." Toxicol In Vitro **15**(3): 181-90.

Bale, T. L. and W. W. Vale **(2004)**. "CRF and CRF receptors: role in stress responsivity and other behaviors." Annu Rev Pharmacol Toxicol **44**: 525-57.

Baliga, B. and S. Kumar **(2003)**. "Apaf-1/cytochrome c apoptosome: an essential initiator of caspase activation or just a sideshow?" Cell Death Differ **10**(1): 16-8.

Bancroft, C. C., Z. Chen, J. Yeh, J. B. Sunwoo, N. T. Yeh, S. Jackson, C. Jackson and C. Van Waes **(2002)**. "Effects of pharmacologic antagonists of epidermal growth factor receptor, PI3K and MEK signal kinases on NF-kappaB and AP-1 activation and IL-8 and VEGF expression in human head and neck squamous cell carcinoma lines." Int J Cancer **99**(4): 538-48.

Barchowsky, A., D. Frleta and M. P. Vincenti **(2000)**. "Integration of the NF-kappaB and mitogen-activated protein kinase/AP-1 pathways at the collagenase-1 promoter: divergence of IL-1 and TNF-dependent signal transduction in rabbit primary synovial fibroblasts." Cytokine **12**(10): 1469-79.

Bazan, J. F., J. C. Timans and R. A. Kastelein **(1996)**. "A newly defined interleukin-1?" Nature **379**(6566): 591.

Beckman, J. S. and W. H. Koppenol **(1996)**. "Nitric oxide, superoxide, and peroxynitrite: the good, the bad, and ugly." Am J Physiol **271**(5 Pt 1): C1424-37.

Behan, D. P., D. E. Grigoriadis, T. Lovenberg, D. Chalmers, S. Heinrichs, C. Liaw and E. B. De Souza **(1996)**. "Neurobiology of corticotropin releasing factor (CRF) receptors and CRF-binding protein: implications for the treatment of CNS disorders." Mol Psychiatry **1**(4): 265-77.

Bellometti, S., M. Cecchettin and L. Galzigna **(1997)**. "Mud pack therapy in osteoarthrosis. Changes in serum levels of chondrocyte markers." Clin Chim Acta **268**(1-2): 101-6.

Benjamin, I. J. and D. R. McMillan **(1998)**. "Stress (heat shock) proteins: molecular chaperones in cardiovascular biology and disease." Circ Res **83**(2): 117-32.

Bernassola, F., M. V. Catani, M. Corazzari, A. Rossi and G. Melino **(2001)**. "Inactivation of multiple targets by nitric oxide in CD95-triggered apoptosis." J Cell Biochem **82**(1): 123-33.

Beyaert, R., A. Cuenda, W. Vanden Berghe, S. Plaisance, J. C. Lee, G. Haegeman, P. Cohen and W. Fiers **(1996)**. "The p38/RK mitogen-activated protein kinase pathway regulates interleukin-6 synthesis response to tumor necrosis factor." Embo J **15**(8): 1914-23.

Bhat-Nakshatri, P., C. J. Sweeney and H. Nakshatri **(2002)**. "Identification of signal transduction pathways involved in constitutive NF-kappaB activation in breast cancer cells." Oncogene **21**(13): 2066-78.

Blanco, F. J., R. Guitian, J. Moreno, F. J. de Toro and F. Galdo **(1999)**. "Effect of antiinflammatory drugs on COX-1 and COX-2 activity in human articular chondrocytes." J Rheumatol **26**(6): 1366-73.

Blanco, F. J., R. Guitian, E. Vazquez-Martul, F. J. de Toro and F. Galdo **(1998)**. "Osteoarthritis chondrocytes die by apoptosis. A possible pathway for osteoarthritis pathology." Arthritis Rheum **41**(2): 284-9.

Blanco, F. J., M. J. Lopez-Armada and E. Maneiro **(2004)**. "Mitochondrial dysfunction in osteoarthritis." Mitochondrion **4**(5-6): 715-28.

Blanco, F. J., R. L. Ochs, H. Schwarz and M. Lotz **(1995)**. "Chondrocyte apoptosis induced by nitric oxide." Am J Pathol **146**(1): 75-85.

Boatright, K. M., M. Renatus, F. L. Scott, S. Sperandio, H. Shin, I. M. Pedersen, J. E. Ricci, W. A. Edris, D. P. Sutherlin, D. R. Green and G. S. Salvesen **(2003)**. "A unified model for apical caspase activation." Mol Cell **11**(2): 529-41.

Bonfanti, L., A. A. Mironov, Jr., J. A. Martinez-Menarguez, O. Martella, A. Fusella, M. Baldassarre, R. Buccione, H. J. Geuze, A. A. Mironov and A. Luini **(1998)**. "Procollagen traverses the Golgi stack without leaving the lumen of cisternae: evidence for cisternal maturation." Cell **95**(7): 993-1003.

Bonventure, J. V. **(1993)**. "Mechanisms of ischaemic acute renal failure." Kidney International **43**: 1160-1178.

Boorse, G. C. and R. J. Denver **(2006)**. "Widespread tissue distribution and diverse functions of corticotropin-releasing factor and related peptides." Gen Comp Endocrinol **146**(1): 9-18.

Borderie, D., P. Hilliquin, A. Hernvann, H. Lemarechal, C. J. Menkes and O. G. Ekindjian **(1999)**. "Apoptosis induced by nitric oxide is associated with nuclear p53 protein expression in cultured osteoarthritic synoviocytes." Osteoarthritis Cartilage **7**(2): 203-13.

Boulton, T. G. and M. H. Cobb **(1991)**. "Identification of multiple extracellular signal-regulated kinases (ERKs) with antipeptide antibodies." Cell Regul **2**(5): 357-71.

Bramono, D. S., J. C. Richmond, P. P. Weitzel, D. L. Kaplan and G. H. Altman **(2004)**. "Matrix metalloproteinases and their clinical applications in orthopaedics." Clin Orthop Relat Res(428): 272-85.

Brar, B. K., A. K. Jonassen, E. M. Egorina, A. Chen, A. Negro, M. H. Perrin, O. D. Mjos, D. S. Latchman, K. F. Lee and W. Vale **(2004)**. "Urocortin-II and urocortin-III are cardioprotective against ischemia reperfusion injury: an essential endogenous cardioprotective role for corticotropin releasing factor receptor type 2 in the murine heart." Endocrinology **145**(1): 24-35; discussion 21-3.

Brar, B. K., A. K. Jonassen, A. Stephanou, G. Santilli, J. Railson, R. A. Knight, D. M. Yellon and D. S. Latchman **(2000)**. "Urocortin protects against ischemic and reperfusion injury via a MAPK-dependent pathway." J Biol Chem **275**(12): 8508-14.

Brar, B. K., J. Railson, A. Stephanou, R. A. Knight and D. S. Latchman **(2002a)**. "Urocortin increases the expression of heat shock protein 90 in rat cardiac myocytes in a MEK1/2-dependent manner." J Endocrinol **172**(2): 283-93.

Brar, B. K., A. Stephanou, R. Knight and D. S. Latchman **(2002b)**. "Activation of protein kinase B/Akt by urocortin is essential for its ability to protect cardiac cells against hypoxia/reoxygenation-induced cell death." J Mol Cell Cardiol **34**(4): 483-92.

Brar, B. K., A. Stephanou, A. Okosi, K. M. Lawrence, R. A. Knight, M. S. Marber and D. S. Latchman **(1999)**. "CRH-like peptides protect cardiac myocytes from lethal ischaemic injury." Mol Cell Endocrinol **158**(1-2): 55-63.

Brauns, O., S. Brauns, B. Zimmermann, O. Jahn and J. Spiess **(2002)**. "Differential responsiveness of CRF receptor subtypes to N-terminal truncation of peptidic ligands." Peptides **23**(5): 881-8.

Bruijnzeel, A. W. and M. S. Gold **(2005)**. "The role of corticotropin-releasing factor-like peptides in cannabis, nicotine, and alcohol dependence." Brain Res Brain Res Rev **49**(3): 505-28.

Buckwalter, J. A., Mankin, H.J., **(1997)**. "Articular cartilage:tissue design and chondrocyte-matrix interactions." J Bobe Joint Surg. Am. **79A**: 600-632.
Buckwalter, J. A. and N. E. Lane **(1997)**. "Does participation in sports cause osteoarthritis?" Iowa Orthop J **17**: 80-9.

Buckwalter, J. A. and H. J. Mankin **(1998)**. "Articular cartilage: degeneration and osteoarthritis, repair, regeneration, and transplantation." Instr Course Lect **47**: 487-504.

Burnette, W. N. **(1981)**. ""Western blotting": electrophoretic transfer of proteins from sodium dodecyl sulfate--polyacrylamide gels to unmodified nitrocellulose and radiographic detection with antibody and radioiodinated protein A." Anal Biochem **112**(2): 195-203.

Burrage, P. S., K. S. Mix and C. E. Brinckerhoff **(2006)**. "Matrix metalloproteinases: role in arthritis." Front Biosci **11**: 529-43.

Bustin, S. A. **(2002)**. "Quantification of mRNA using real-time reverse transcription PCR (RT-PCR): trends and problems." J Mol Endocrinol **29**(1): 23-39.

Cameron-Donaldson, M., C. Holland, D. S. Hungerford and C. G. Frondoza **(2004)**. "Cartilage debris increases the expression of chondrodestructive tumor necrosis factor-alpha by articular chondrocytes." Arthroscopy **20**(10): 1040-3.

Cantrell, D. A. **(2001)**. "Phosphoinositide 3-kinase signalling pathways." J Cell Sci **114**(Pt 8): 1439-45.

Cao, M., A. Westerhausen-Larson, C. Niyibizi, K. Kavalkovich, H. I. Georgescu, C. F. Rizzo, P. A. Hebda, M. Stefanovic-Racic and C. H. Evans **(1997)**. "Nitric oxide inhibits the synthesis of type-II collagen without altering Col2A1 mRNA abundance: prolyl hydroxylase as a possible target." Biochem J **324 (Pt 1)**: 305-10.

Cardone, M. H., N. Roy, H. R. Stennicke, G. S. Salvesen, T. F. Franke, E. Stanbridge, S. Frisch and J. C. Reed **(1998)**. "Regulation of cell death protease caspase-9 by phosphorylation." Science **282**(5392): 1318-21.

Carswell, E. A., L. J. Old, R. L. Kassel, S. Green, N. Fiore and B. Williamson **(1975)**. "An endotoxin-induced serum factor that causes necrosis of tumors." Proc Natl Acad Sci U S A **72**(9): 3666-70.

Castro, R. R., F. Q. Cunha, F. S. Silva, Jr. and F. A. Rocha **(2006)**. "A quantitative approach to measure joint pain in experimental osteoarthritis-evidence of a role for nitric oxide." Osteoarthritis Cartilage **14**(8): 769-776.

Caswell, A. M., S. Y. Ali and R. G. Russell **(1987)**. "Nucleoside triphosphate pyrophosphatase of rabbit matrix vesicles, a mechanism for the generation of inorganic pyrophosphate in epiphyseal cartilage." Biochim Biophys Acta **924**(2): 276-83.

Chanalaris, A., K. M. Lawrence, A. Stephanou, R. D. Knight, S. Y. Hsu, A. J. Hsueh and D. S. Latchman **(2003)**. "Protective effects of the urocortin homologues stresscopin (SCP) and stresscopin-related peptide (SRP) against hypoxia/reoxygenation injury in rat neonatal cardiomyocytes." J Mol Cell Cardiol **35**(10): 1295-305.

Chanalaris, A., K. M. Lawrence, P. A. Townsend, S. Davidson, Y. Jamshidi, A. Stephanou, R. D. Knight, S. Y. Hsu, A. J. Hsueh and D. S. Latchman **(2005)**. "Hypertrophic effects of urocortin homologous peptides are mediated via activation of the Akt pathway." Biochem Biophys Res Commun **328**(2): 442-8.

Chang, L. and M. Karin **(2001)**. "Mammalian MAP kinase signalling cascades." Nature **410**(6824): 37-40.

Chang, T. J., C. C. Juan, P. H. Yin, C. W. Chi and H. J. Tsay **(1998)**. "Up-regulation of beta-actin, cyclophilin and GAPDH in N1S1 rat hepatoma." Oncol Rep **5**(2): 469-71.

Chao, D. T. and S. J. Korsmeyer **(1998)**. "BCL-2 family: regulators of cell death." Annu Rev Immunol **16**: 395-419.

Chatzaki, E., I. Charalampopoulos, C. Leontidis, I. A. Mouzas, M. Tzardi, C. Tsatsanis, A. N. Margioris and A. Gravanis **(2003)**. "Urocortin in human gastric mucosa: relationship to inflammatory activity." J Clin Endocrinol Metab **88**(1): 478-83.

Chen, C. Y., R. Gherzi, J. S. Andersen, G. Gaietta, K. Jurchott, H. D. Royer, M. Mann and M. Karin **(2000)**. "Nucleolin and YB-1 are required for JNK-mediated interleukin-2 mRNA stabilization during T-cell activation." Genes Dev **14**(10): 1236-48.

Chen, F., V. Castranova and X. Shi **(2001)**. "New insights into the role of nuclear factor-kappaB in cell growth regulation." Am J Pathol **159**(2): 387-97.

Chin, J. and M. J. Kostura **(1993)**. "Dissociation of IL-1 beta synthesis and secretion in human blood monocytes stimulated with bacterial cell wall products." J Immunol **151**(10): 5574-85.

Chinnaiyan, A. M., K. O'Rourke, M. Tewari and V. M. Dixit **(1995)**. "FADD, a novel death domain-containing protein, interacts with the death domain of Fas and initiates apoptosis." Cell **81**(4): 505-12.

Chomczynski, P. **(1993)**. "A reagent for the single-step simultaneous isolation of RNA, DNA and proteins from cell and tissue samples." Biotechniques **15**(3): 532-4, 536-7.

Conrad, P. W., R. T. Rust, J. Han, D. E. Millhorn and D. Beitner-Johnson **(1999)**. "Selective activation of p38alpha and p38gamma by hypoxia. Role in regulation of cyclin D1 by hypoxia in PC12 cells." J Biol Chem **274**(33): 23570-6.

Conti, A. A., D. Lippi and G. F. Gensini **(2005)**. "The historical evolution of the concept of apoptosis in rheumatic diseases." Reumatismo **57**(1): 57-61.

Cooray, S., L. Jin and J. M. Best **(2005)**. "The involvement of survival signaling pathways in rubella-virus induced apoptosis." Virol J **2**: 1.

Crane, B. R., A. S. Arvai, R. Gachhui, C. Wu, D. K. Ghosh, E. D. Getzoff, D. J. Stuehr and J. A. Tainer **(1997)**. "The structure of nitric oxide synthase oxygenase domain and inhibitor complexes." Science **278**(5337): 425-31.

Dachary-Prigent, J., J. M. Freyssinet, J. M. Pasquet, J. C. Carron and A. T. Nurden **(1993)**. "Annexin V as a probe of aminophospholipid exposure and platelet membrane vesiculation: a flow cytometry study showing a role for free sulfhydryl groups." Blood **81**(10): 2554-65.

Danial, N. N. and S. J. Korsmeyer **(2004)**. "Cell death: critical control points." Cell **116**(2): 205-19.

Datta, S. R., A. Brunet and M. E. Greenberg **(1999)**. "Cellular survival: a play in three Akts." Genes Dev **13**(22): 2905-27.

Dautzenberg, F. M., K. Dietrich, M. R. Palchaudhuri and J. Spiess **(1997)**. "Identification of two corticotropin-releasing factor receptors from Xenopus laevis with high ligand selectivity: unusual pharmacology of the type 1 receptor." J Neurochem **69**(4): 1640-9.

Dautzenberg, F. M. and R. L. Hauger **(2002)**. "The CRF peptide family and their receptors: yet more partners discovered." Trends Pharmacol Sci **23**(2): 71-7.

Davis, M. E., C. J. Pemberton, T. G. Yandle, J. G. Lainchbury, M. T. Rademaker, M. G. Nicholls, C. M. Frampton and A. M. Richards **(2004)**. "Urocortin-1 infusion in normal humans." J Clin Endocrinol Metab **89**(3): 1402-9.

Dean, J. L., M. Brook, A. R. Clark and J. Saklatvala **(1999)**. "p38 mitogen-activated protein kinase regulates cyclooxygenase-2 mRNA stability and transcription in lipopolysaccharide-treated human monocytes." J Biol Chem **274**(1): 264-9.

Decker, T. and M. L. Lohmann-Matthes **(1988)**. "A quick and simple method for the quantitation of lactate dehydrogenase release in measurements of cellular cytotoxicity and tumor necrosis factor (TNF) activity." J Immunol Methods **115**(1): 61-9.

Degli Esposti, M., G. Ferry, P. Masdehors, J. A. Boutin, J. A. Hickman and C. Dive **(2003)**. "Post-translational modification of Bid has differential effects on its susceptibility to cleavage by caspase 8 or caspase 3." J Biol Chem **278**(18): 15749-57.

Del Carlo, M., Jr. and R. F. Loeser **(2002)**. "Nitric oxide-mediated chondrocyte cell death requires the generation of additional reactive oxygen species." Arthritis Rheum **46**(2): 394-403.

Dent, P., A. Yacoub, P. B. Fisher, M. P. Hagan and S. Grant **(2003)**. "MAPK pathways in radiation responses." Oncogene **22**(37): 5885-96.

Dharmavaram, R. M., C. T. Baldwin, A. M. Reginato and S. A. Jimenez **(1993)**. "Amplification of cDNAs for human cartilage-specific types II, IX and XI collagens from chondrocytes and Epstein-Barr virus-transformed lymphocytes." Matrix **13**(2): 125-33.

Donaldson, C. J., S. W. Sutton, M. H. Perrin, A. Z. Corrigan, K. A. Lewis, J. E. Rivier, J. M. Vaughan and W. W. Vale **(1996)**. "Cloning and characterization of human urocortin." Endocrinology **137**(5): 2167-70.

Duan, H., A. M. Chinnaiyan, P. L. Hudson, J. P. Wing, W. W. He and V. M. Dixit **(1996)**. "ICE-LAP3, a novel mammalian homologue of the Caenorhabditis elegans cell death protein Ced-3 is activated during Fas- and tumor necrosis factor-induced apoptosis." J Biol Chem **271**(3): 1621-5.

Dudley, D. T., L. Pang, S. J. Decker, A. J. Bridges and A. R. Saltiel **(1995)**. "A synthetic inhibitor of the mitogen-activated protein kinase cascade." Proc Natl Acad Sci U S A **92**(17): 7686-9.

Eger, E. I., 2nd, P. Ionescu, M. J. Laster, D. Gong, T. Hudlicky, J. J. Kendig, R. A. Harris, J. R. Trudell and A. Pohorille **(1999)**. "Minimum alveolar anesthetic concentration of fluorinated alkanols in rats: relevance to theories of narcosis." Anesth Analg **88**(4): 867-76.

El-Kholy, W., P. E. Macdonald, J. H. Lin, J. Wang, J. M. Fox, P. E. Light, Q. Wang, R. G. Tsushima and M. B. Wheeler **(2003)**. "The phosphatidylinositol 3-kinase inhibitor LY294002 potently blocks K(V) currents via a direct mechanism." Faseb J **17**(6): 720-2.

Enari, M., H. Sakahira, H. Yokoyama, K. Okawa, A. Iwamatsu and S. Nagata **(1998)**. "A caspase-activated DNase that degrades DNA during apoptosis, and its inhibitor ICAD." Nature **391**(6662): 43-50.

Escobar, G. A., R. C. McIntyre, Jr., E. E. Moore, F. Gamboni-Robertson and A. Banerjee **(2006)**. "Clathrin heavy chain is required for TNF-induced inflammatory signaling." Surgery **140**(2): 268-72.

Facci, L., D. A. Stevens, M. Pangallo, D. Franceschini, S. D. Skaper and P. J. Strijbos **(2003)**. "Corticotropin-releasing factor (CRF) and related peptides confer neuroprotection via type 1 CRF receptors." Neuropharmacology **45**(5): 623-36.

Fadok, V. A., D. R. Voelker, P. A. Campbell, J. J. Cohen, D. L. Bratton and P. M. Henson **(1992)**. "Exposure of phosphatidylserine on the surface of apoptotic lymphocytes triggers specific recognition and removal by macrophages." J Immunol **148**(7): 2207-16.

Fan, Z., B. Bau, H. Yang, S. Soeder and T. Aigner **(2005)**. "Freshly isolated osteoarthritic chondrocytes are catabolically more active than normal chondrocytes, but less responsive to catabolic stimulation with interleukin-1beta." Arthritis Rheum **52**(1): 136-43.

Farrell, A. J., D. R. Blake, R. M. Palmer and S. Moncada **(1992)**. "Increased concentrations of nitrite in synovial fluid and serum samples suggest increased nitric oxide synthesis in rheumatic diseases." Ann Rheum Dis **51**(11): 1219-22.

Feelisch, M., F. Brands and M. Kelm **(1995)**. "Human endothelial cells bioactivate organic nitrates to nitric oxide: implications for the reinforcement of endothelial defence mechanisms." Eur J Clin Invest **25**(10): 737-45.

Fell, H. B. and R. W. Jubb **(1977)**. "The effect of synovial tissue on the breakdown of articular cartilage in organ culture." Arthritis Rheum **20**(7): 1359-71.

Feng, L., P. Precht, R. Balakir and W. E. Horton, Jr. **(1998)**. "Evidence of a direct role for Bcl-2 in the regulation of articular chondrocyte apoptosis under the conditions of serum withdrawal and retinoic acid treatment." J Cell Biochem **71**(2): 302-9.

Fernandes, J. C., J. Martel-Pelletier and J. P. Pelletier **(2002)**. "The role of cytokines in osteoarthritis pathophysiology." Biorheology **39**(1-2): 237-46.

Fiers, W., R. Beyaert, W. Declercq and P. Vandenabeele **(1999)**. "More than one way to die: apoptosis, necrosis and reactive oxygen damage." Oncogene **18**(54): 7719-30.

Finger, F., C. Schorle, S. Soder, A. Zien, M. B. Goldring and T. Aigner **(2004)**. "Phenotypic characterization of human chondrocyte cell line C-20/A4: a comparison between monolayer and alginate suspension culture." Cells Tissues Organs **178**(2): 65-77.

Fischer, B. A., S. Mundle and A. A. Cole **(2000)**. "Tumor necrosis factor-alpha induced DNA cleavage in human articular chondrocytes may involve multiple endonucleolytic activities during apoptosis." Microsc Res Tech **50**(3): 236-42.

Fischer, U., R. U. Janicke and K. Schulze-Osthoff **(2003)**. "Many cuts to ruin: a comprehensive update of caspase substrates." Cell Death Differ **10**(1): 76-100.

Fraser, A. and G. Evan **(1996)**. "A license to kill." Cell **85**(6): 781-4.
Freshney, I. (1987). Culture of Animal cells: A manual of basic techniques, Wiley-Liss,.

Fukai, T., M. R. Siegfried, M. Ushio-Fukai, Y. Cheng, G. Kojda and D. G. Harrison **(2000)**. "Regulation of the vascular extracellular superoxide dismutase by nitric oxide and exercise training." J Clin Invest **105**(11): 1631-9.

Galbraith, D. N. **(2004)**. "Regulatory and microbiological safety issues surrounding cell and tissue-engineering products." Biotechnol Appl Biochem **40**(Pt 1): 35-9.

Garg, A. and B. B. Aggarwal **(2002)**. "Nuclear transcription factor-kappaB as a target for cancer drug development." Leukemia **16**(6): 1053-68.

Gaur, U. and B. B. Aggarwal **(2003)**. "Regulation of proliferation, survival and apoptosis by members of the TNF superfamily." Biochem Pharmacol **66**(8): 1403-8.

Gavalda, N., E. Perez-Navarro, E. Gratacos, J. X. Comella and J. Alberch **(2004)**. "Differential involvement of phosphatidylinositol 3-kinase and p42/p44 mitogen activated protein kinase pathways in brain-derived neurotrophic factor-induced trophic effects on cultured striatal neurons." Mol Cell Neurosci **25**(3): 460-8.

Gebauer, G., A. T. Peter, D. Onesime and N. Dhanasekaran **(1999)**. "Apoptosis of ovarian granulosa cells: correlation with the reduced activity of ERK-signaling module." J Cell Biochem **75**(4): 547-54.

Geller, D. A., A. K. Nussler, M. Di Silvio, C. J. Lowenstein, R. A. Shapiro, S. C. Wang, R. L. Simmons and T. R. Billiar **(1993)**. "Cytokines, endotoxin, and glucocorticoids regulate the expression of inducible nitric oxide synthase in hepatocytes." Proc Natl Acad Sci U S A **90**(2): 522-6.

Ghafourifar, P. and C. Richter **(1999)**. "Mitochondrial nitric oxide synthase regulates mitochondrial matrix pH." Biol Chem **380**(7-8): 1025-8.

Giulivi, C., J. J. Poderoso and A. Boveris **(1998)**. "Production of nitric oxide by mitochondria." J Biol Chem **273**(18): 11038-43.

Goggs, R., S. D. Carter, G. Schulze-Tanzil, M. Shakibaei and A. Mobasheri **(2003)**. "Apoptosis and the loss of chondrocyte survival signals contribute to articular cartilage degradation in osteoarthritis." Vet J **166**(2): 140-58.

Goldring, M. B. **(2000)**. "The role of the chondrocyte in osteoarthritis." Arthritis Rheum **43**(9): 1916-26.

Goldring, M. B., J. Birkhead, L. J. Sandell, T. Kimura and S. M. Krane **(1988)**. "Interleukin 1 suppresses expression of cartilage-specific types II and IX collagens and increases types I and III collagens in human chondrocytes." J Clin Invest **82**(6): 2026-37.

Goldring, M. B., J. R. Birkhead, L. F. Suen, R. Yamin, S. Mizuno, J. Glowacki, J. L. Arbiser and J. F. Apperley **(1994)**. "Interleukin-1 beta-modulated gene expression in immortalized human chondrocytes." J Clin Invest **94**(6): 2307-16.

Goldring, S. R. and M. B. Goldring **(2004)**. "The role of cytokines in cartilage matrix degeneration in osteoarthritis." Clin Orthop Relat Res(427 Suppl): S27-36.

Grammatopoulos, D. K., H. S. Randeva, M. A. Levine, E. S. Katsanou and E. W. Hillhouse **(2000)**. "Urocortin, but not corticotropin-releasing hormone (CRH), activates the mitogen-activated protein kinase signal transduction pathway in human pregnant myometrium: an effect mediated via R1alpha and R2beta CRH receptor subtypes and stimulation of Gq-proteins." Mol Endocrinol **14**(12): 2076-91.

Graves, J. D., K. E. Draves, A. Craxton, E. G. Krebs and E. A. Clark **(1998)**. "A comparison of signaling requirements for apoptosis of human B lymphocytes induced by the B cell receptor and CD95/Fas." J Immunol **161**(1): 168-74.

Greisberg, J., M. Bliss and R. Terek **(2002)**. "The prevalence of nitric oxide in apoptotic chondrocytes of osteoarthritis." Osteoarthritis Cartilage **10**(3): 207-11.

Gross, A., J. M. McDonnell and S. J. Korsmeyer **(1999)**. "BCL-2 family members and the mitochondria in apoptosis." Genes Dev **13**(15): 1899-911.

Grutkoski, P. S., C. T. Graeber, A. Ayala and H. H. Simms **(2002)**. "Paracrine suppression of apoptosis by cytokine-stimulated neutrophils involves divergent regulation of NF-kappaB, Bcl-X(L), and Bak." Shock **17**(1): 47-54.

Guerne, P. A., F. Blanco, A. Kaelin, A. Desgeorges and M. Lotz **(1995)**. "Growth factor responsiveness of human articular chondrocytes in aging and development." Arthritis Rheum **38**(7): 960-8.

Guerne, P. A., A. Sublet and M. Lotz **(1994)**. "Growth factor responsiveness of human articular chondrocytes: distinct profiles in primary chondrocytes, subcultured chondrocytes, and fibroblasts." J Cell Physiol **158**(3): 476-84.

Han, J., J. D. Lee, L. Bibbs and R. J. Ulevitch **(1994)**. "A MAP kinase targeted by endotoxin and hyperosmolarity in mammalian cells." Science **265**(5173): 808-11.

Harrison, D. C., A. D. Medhurst, B. C. Bond, C. A. Campbell, R. P. Davis and K. L. Philpott **(2000)**. "The use of quantitative RT-PCR to measure mRNA expression in a rat model of focal ischemia--caspase-3 as a case study." Brain Res Mol Brain Res **75**(1): 143-9.

Hashimoto, S., R. L. Ochs, F. Rosen, J. Quach, G. McCabe, J. Solan, J. E. Seegmiller, R. Terkeltaub and M. Lotz **(1998a)**. "Chondrocyte-derived apoptotic bodies and calcification of articular cartilage." Proc Natl Acad Sci U S A **95**(6): 3094-9.

Hashimoto, S., M. Setareh, R. L. Ochs and M. Lotz **(1997)**. "Fas/Fas ligand expression and induction of apoptosis in chondrocytes." Arthritis Rheum **40**(10): 1749-55.

Hashimoto, S., K. Takahashi, D. Amiel, R. D. Coutts and M. Lotz **(1998b)**. "Chondrocyte apoptosis and nitric oxide production during experimentally induced osteoarthritis." Arthritis Rheum **41**(7): 1266-74.

Hauger, R. L., D. E. Grigoriadis, M. F. Dallman, P. M. Plotsky, W. W. Vale and F. M. Dautzenberg **(2003)**. "International Union of Pharmacology. XXXVI. Current status of the nomenclature for receptors for corticotropin-releasing factor and their ligands." Pharmacol Rev **55**(1): 21-6.

Hayashi, T., E. Abe, T. Yamate, Y. Taguchi and H. E. Jasin **(1997)**. "Nitric oxide production by superficial and deep articular chondrocytes." Arthritis Rheum **40**(2): 261-9.

Hazzalin, C. A., E. Cano, A. Cuenda, M. J. Barratt, P. Cohen and L. C. Mahadevan **(1996)**. "p38/RK is essential for stress-induced nuclear responses: JNK/SAPKs and c-Jun/ATF-2 phosphorylation are insufficient." Curr Biol **6**(8): 1028-31.

Heigold, S., C. Sers, W. Bechtel, B. Ivanovas, R. Schafer and G. Bauer **(2002)**. "Nitric oxide mediates apoptosis induction selectively in transformed fibroblasts compared to nontransformed fibroblasts." Carcinogenesis **23**(6): 929-41.

Hengartner, M. O. **(2000)**. "The biochemistry of apoptosis." Nature **407**(6805): 770-6.

Heraud, F., A. Heraud and M. F. Harmand **(2000)**. "Apoptosis in normal and osteoarthritic human articular cartilage." Ann Rheum Dis **59**(12): 959-65.

Hetts, S. W. **(1998)**. "To die or not to die: an overview of apoptosis and its role in disease." Jama **279**(4): 300-7.

Hill, M. M., C. Adrain and S. J. Martin **(2003)**. "Portrait of a killer: the mitochondrial apoptosome emerges from the shadows." Mol Interv **3**(1): 19-26.

Hillhouse, E. W., H. Randeva, G. Ladds and D. Grammatopoulos **(2002)**. "Corticotropin-releasing hormone receptors." Biochem Soc Trans **30**(4): 428-32.

Hilliquin, P., D. Borderie, A. Hernvann, C. J. Menkes and O. G. Ekindjian **(1997)**. "Nitric oxide as S-nitrosoproteins in rheumatoid arthritis." Arthritis Rheum **40**(8): 1512-7.

Hiran, T. S., P. J. Moulton and J. T. Hancock **(1997)**. "Detection of superoxide and NADPH oxidase in porcine articular chondrocytes." Free Radic Biol Med **23**(5): 736-43.

Hoare, S. R., S. K. Sullivan, J. Fan, K. Khongsaly and D. E. Grigoriadis **(2005)**. "Peptide ligand binding properties of the corticotropin-releasing factor (CRF) type 2 receptor: pharmacology of endogenously expressed receptors, G-protein-coupling sensitivity and determinants of CRF2 receptor selectivity." Peptides **26**(3): 457-70.

Hommes, D. W., M. P. Peppelenbosch and S. J. van Deventer **(2003)**. "Mitogen activated protein (MAP) kinase signal transduction pathways and novel anti-inflammatory targets." Gut **52**(1): 144-51.

Honjo, T., N. Inoue, R. Shiraki, S. Kobayashi, K. Otsui, M. Takahashi, K. Hirata, S. Kawashima, H. Yokozaki and M. Yokoyama **(2006)**. "Endothelial urocortin has potent antioxidative properties and is upregulated by inflammatory cytokines and pitavastatin." J Vasc Res **43**(2): 131-8.

Hortelano, S., B. Dallaporta, N. Zamzami, T. Hirsch, S. A. Susin, I. Marzo, L. Bosca and G. Kroemer **(1997)**. "Nitric oxide induces apoptosis via triggering mitochondrial permeability transition." FEBS Lett **410**(2-3): 373-7.

Horton, W. E., Jr., L. Feng and C. Adams **(1998)**. "Chondrocyte apoptosis in development, aging and disease." Matrix Biol **17**(2): 107-15.

Howard, O. M., K. A. Clouse, C. Smith, R. G. Goodwin and W. L. Farrar **(1993)**. "Soluble tumor necrosis factor receptor: inhibition of human immunodeficiency virus activation." Proc Natl Acad Sci U S A **90**(6): 2335-9.

Hsu, S. Y. and A. J. Hsueh **(2001)**. "Human stresscopin and stresscopin-related peptide are selective ligands for the type 2 corticotropin-releasing hormone receptor." Nat Med **7**(5): 605-11.

Huang, S., Y. Jiang, Z. Li, E. Nishida, P. Mathias, S. Lin, R. J. Ulevitch, G. R. Nemerow and J. Han **(1997)**. "Apoptosis signaling pathway in T cells is composed of ICE/Ced-3 family proteases and MAP kinase kinase 6b." Immunity **6**(6): 739-49.

Huang, Y., X. Q. Yao, C. W. Lau, Y. C. Chan, S. Y. Tsang and F. L. Chan **(2004)**. "Urocortin and cardiovascular protection." Acta Pharmacol Sin **25**(3): 257-65.

Hui, W., A. D. Rowan and T. Cawston **(2001)**. "Modulation of the expression of matrix metalloproteinase and tissue inhibitors of metalloproteinases by TGF-beta1 and IGF-1 in primary human articular and bovine nasal chondrocytes stimulated with TNF-alpha." Cytokine **16**(1): 31-5.

Hunter, D. J. and D. T. Felson **(2006)**. "Osteoarthritis." Bmj **332**(7542): 639-42.

Ikeda, K., K. Tojo, S. Sato, T. Ebisawa, G. Tokudome, T. Hosoya, M. Harada, O. Nakagawa and K. Nakao **(1998)**. "Urocortin, a newly identified corticotropin-releasing factor-related mammalian peptide, stimulates atrial natriuretic peptide and brain natriuretic peptide secretions from neonatal rat cardiomyocytes." Biochem Biophys Res Commun **250**(2): 298-304.

Inoue, K., G. R. Valdez, T. M. Reyes, L. E. Reinhardt, A. Tabarin, J. Rivier, W. W. Vale, P. E. Sawchenko, G. F. Koob and E. P. Zorrilla **(2003)**. "Human urocortin II, a selective agonist for the type 2 corticotropin-releasing factor receptor, decreases feeding and drinking in the rat." J Pharmacol Exp Ther **305**(1): 385-93.

Irmler, M., M. Thome, M. Hahne, P. Schneider, K. Hofmann, V. Steiner, J. L. Bodmer, M. Schroter, K. Burns, C. Mattmann, D. Rimoldi, L. E. French and J. Tschopp **(1997)**. "Inhibition of death receptor signals by cellular FLIP." Nature **388**(6638): 190-5.

Ishihara, S., Y. Yamamoto, K. Ifuku and F. Sato **(2005)**. "Functional analysis of four members of the PsbP family in photosystem II in Nicotiana tabacum using differential RNA interference." Plant Cell Physiol **46**(12): 1885-93.

Jackson, J. R., B. Bolognese, L. Hillegass, S. Kassis, J. Adams, D. E. Griswold and J. D. Winkler **(1998)**. "Pharmacological effects of SB 220025, a selective inhibitor of P38 mitogen-activated protein kinase, in angiogenesis and chronic inflammatory disease models." J Pharmacol Exp Ther **284**(2): 687-92.

Ji, Y., T. P. Akerboom, H. Sies and J. A. Thomas **(1999)**. "S-nitrosylation and S-glutathiolation of protein sulfhydryls by S-nitroso glutathione." Arch Biochem Biophys **362**(1): 67-78.

Jiang, X. and X. Wang **(2000)**. "Cytochrome c promotes caspase-9 activation by inducing nucleotide binding to Apaf-1." J Biol Chem **275**(40): 31199-203.

Jiang, Y., C. Chen, Z. Li, W. Guo, J. A. Gegner, S. Lin and J. Han **(1996)**. "Characterization of the structure and function of a new mitogen-activated protein kinase (p38beta)." J Biol Chem **271**(30): 17920-6.

Johnson, K., S. Hashimoto, M. Lotz, K. Pritzker, J. Goding and R. Terkeltaub **(2001)**. "Up-regulated expression of the phosphodiesterase nucleotide pyrophosphatase family member PC-1 is a marker and pathogenic factor for knee meniscal cartilage matrix calcification." Arthritis Rheum **44**(5): 1071-81.

Juretic, N., J. F. Santibanez, C. Hurtado and J. Martinez **(2001)**. "ERK 1,2 and p38 pathways are involved in the proliferative stimuli mediated by urokinase in osteoblastic SaOS-2 cell line." J Cell Biochem **83**(1): 92-8.

Kacena, M. A., G. A. Merrel, S. R. Konda, K. M. Wilson, Y. Xi and M. C. Horowitz **(2001)**. "Inflammation and bony changes at the temporomandibular joint." Cells Tissues Organs **169**(3): 257-64.

Kageyama, K., M. J. Bradbury, L. Zhao, A. L. Blount and W. W. Vale **(1999)**. "Urocortin messenger ribonucleic acid: tissue distribution in the rat and regulation in thymus by lipopolysaccharide and glucocorticoids." Endocrinology **140**(12): 5651-8.

Kageyama, K., K. Furukawa, I. Miki, K. Terui, S. Motomura and T. Suda **(2003)**. "Vasodilative effects of urocortin II via protein kinase A and a mitogen-activated protein kinase in rat thoracic aorta." J Cardiovasc Pharmacol **42**(4): 561-5.

Kahl, S. D., X. J. Liu, N. Ling, E. B. De Souza and D. R. Gehlert **(1998)**. "Characterization of [125I-Tyr0]-corticotropin releasing factor (CRF) binding to the CRF binding protein using a scintillation proximity assay." J Neurosci Methods **83**(2): 103-11.

Kemp, C. F., R. J. Woods and P. J. Lowry **(1998)**. "The corticotrophin-releasing factor-binding protein: an act of several parts." Peptides **19**(6): 1119-28.

Kerr, J. F., A. H. Wyllie and A. R. Currie **(1972)**. "Apoptosis: a basic biological phenomenon with wide-ranging implications in tissue kinetics." Br J Cancer **26**(4): 239-57.

Khokhlatchev, A., S. Xu, J. English, P. Wu, E. Schaefer and M. H. Cobb **(1997)**. "Reconstitution of mitogen-activated protein kinase phosphorylation cascades in bacteria. Efficient synthesis of active protein kinases." J Biol Chem **272**(17): 11057-62.

Khorana, H. G. **(1971)**. "Total synthesis of the gene for an alanine transfer ribonucleic acid from yeast." Pure Appl Chem **25**(1): 91-118.

Kim, H. A., Y. J. Lee, S. C. Seong, K. W. Choe and Y. W. Song **(2000)**. "Apoptotic chondrocyte death in human osteoarthritis." J Rheumatol **27**(2): 455-62.

Kim, J. S., Z. Y. Park, Y. J. Yoo, S. S. Yu and J. S. Chun **(2005)**. "p38 kinase mediates nitric oxide-induced apoptosis of chondrocytes through the inhibition of protein kinase C zeta by blocking autophosphorylation." Cell Death Differ **12**(3): 201-12.

Kim, S. J. and J. S. Chun **(2003)**. "Protein kinase C alpha and zeta regulate nitric oxide-induced NF-kappa B activation that mediates cyclooxygenase-2 expression and apoptosis but not dedifferentiation in articular chondrocytes." Biochem Biophys Res Commun **303**(1): 206-11.

Kim, S. J., J. W. Ju, C. D. Oh, Y. M. Yoon, W. K. Song, J. H. Kim, Y. J. Yoo, O. S. Bang, S. S. Kang and J. S. Chun **(2002)**. "ERK-1/2 and p38 kinase oppositely regulate nitric oxide-induced apoptosis of chondrocytes in association with p53, caspase-3, and differentiation status." J Biol Chem **277**(2): 1332-9.

Klose, J., K. Fechner, M. Beyermann, E. Krause, N. Wendt, M. Bienert, R. Rudolph and S. Rothemund **(2005)**. "Impact of N-terminal domains for corticotropin-releasing factor (CRF) receptor-ligand interactions." Biochemistry **44**(5): 1614-23.

Knott, I., M. Dieu, M. Burton, A. Houbion, J. Remacle and M. Raes **(1994)**. "Induction of cyclooxygenase by interleukin 1: comparative study between human synovial cells and chondrocytes." J Rheumatol **21**(3): 462-6.

Kobayashi, M., G. R. Squires, A. Mousa, M. Tanzer, D. J. Zukor, J. Antoniou, U. Feige and A. R. Poole **(2005)**. "Role of interleukin-1 and tumor necrosis factor alpha in matrix degradation of human osteoarthritic cartilage." Arthritis Rheum **52**(1): 128-35.

Kohno, M., Y. Kawahito, Y. Tsubouchi, A. Hashiramoto, R. Yamada, K. I. Inoue, Y. Kusaka, T. Kubo, I. J. Elenkov, G. P. Chrousos, M. Kondo and H. Sano **(2001)**. "Urocortin expression in synovium of patients with rheumatoid arthritis and osteoarthritis: relation to inflammatory activity." J Clin Endocrinol Metab **86**(9): 4344-52.

Konishi, S., Y. Kasagi, H. Katsumata, S. Minami and T. Imaki **(2003)**. "Regulation of corticotropin-releasing factor (CRF) type-1 receptor gene expression by CRF in the hypothalamus." Endocr J **50**(1): 21-36.

Koopman, G., C. P. Reutelingsperger, G. A. Kuijten, R. M. Keehnen, S. T. Pals and M. H. van Oers **(1994)**. "Annexin V for flow cytometric detection of phosphatidylserine expression on B cells undergoing apoptosis." Blood **84**(5): 1415-20.

Koppal, T., J. Drake, S. Yatin, B. Jordan, S. Varadarajan, L. Bettenhausen and D. A. Butterfield **(1999)**. "Peroxynitrite-induced alterations in synaptosomal membrane proteins: insight into oxidative stress in Alzheimer's disease." J Neurochem **72**(1): 310-7.

Korzeniewski, C. and D. M. Callewaert **(1983)**. "An enzyme-release assay for natural cytotoxicity." J Immunol Methods **64**(3): 313-20.

Kostich, W. A., A. Chen, K. Sperle and B. L. Largent **(1998)**. "Molecular identification and analysis of a novel human corticotropin-releasing factor (CRF) receptor: the CRF2gamma receptor." Mol Endocrinol **12**(8): 1077-85.

Kothny-Wilkes, G., D. Kulms, B. Poppelmann, T. A. Luger, M. Kubin and T. Schwarz **(1998)**. "Interleukin-1 protects transformed keratinocytes from tumor necrosis factor-related apoptosis-inducing ligand." J Biol Chem **273**(44): 29247-53.

Kouri, J. B., C. Arguello, M. Quintero, A. Chico and M. E. Ramos **(1996)**. "Variability in the cell phenotype of aggregates or "clones" of human osteoarthritic cartilage. A case report." Biocell **20**(3): 191-200.

Kozicz, T., H. Yanaihara and A. Arimura **(1998)**. "Distribution of urocortin-like immunoreactivity in the central nervous system of the rat." J Comp Neurol **391**(1): 1-10.

Kuhn, K., D. D. D'Lima, S. Hashimoto and M. Lotz **(2004)**. "Cell death in cartilage." Osteoarthritis Cartilage **12**(1): 1-16.

Kuhn, K. and M. Lotz **(2001)**. "Regulation of CD95 (Fas/APO-1)-induced apoptosis in human chondrocytes." Arthritis Rheum **44**(7): 1644-53.

Kuypers, F. A., R. A. Lewis, M. Hua, M. A. Schott, D. Discher, J. D. Ernst and B. H. Lubin **(1996)**. "Detection of altered membrane phospholipid asymmetry in subpopulations of human red blood cells using fluorescently labeled annexin V." Blood **87**(3): 1179-87.

Kyriakis, J. M. and J. Avruch **(2001)**. "Mammalian mitogen-activated protein kinase signal transduction pathways activated by stress and inflammation." Physiol Rev **81**(2): 807-69.

Laemmli, U. K. **(1970)**. "Cleavage of structural proteins during the assembly of the head of bacteriophage T4." Nature **227**(5259): 680-5.

Latchman, D. S. **(2001)**. "Urocortin protects against ischemic injury via a MAPK-dependent pathway." Trends Cardiovasc Med **11**(5): 167-9.

Latchman, D. S. **(2002)**. "Urocortin." Int J Biochem Cell Biol **34**(8): 907-10.

Lavoie, J. N., N. Rivard, G. L'Allemain and J. Pouyssegur **(1996)**. "A temporal and biochemical link between growth factor-activated MAP kinases, cyclin D1 induction and cell cycle entry." Prog Cell Cycle Res **2**: 49-58.

Lawen, A. **(2003)**. "Apoptosis-an introduction." Bioessays **25**(9): 888-96.

Lawlor, M. A. and D. R. Alessi **(2001)**. "PKB/Akt: a key mediator of cell proliferation, survival and insulin responses?" J Cell Sci **114**(Pt 16): 2903-10.

Lawrence, A. J., E. V. Krstew, F. M. Dautzenberg and A. Ruhmann **(2002)**. "The highly selective CRF(2) receptor antagonist K41498 binds to presynaptic CRF(2) receptors in rat brain." Br J Pharmacol **136**(6): 896-904.

Lawrence, K. M., A. Chanalaris, T. Scarabelli, M. Hubank, E. Pasini, P. A. Townsend, L. Comini, R. Ferrari, A. Tinker, A. Stephanou, R. A. Knight and D. S. Latchman **(2002)**. "K(ATP) channel gene expression is induced by urocortin and mediates its cardioprotective effect." Circulation **106**(12): 1556-62.

Lawrence, K. M., A. M. Kabir, M. Bellahcene, S. Davidson, X. B. Cao, J. McCormick, R. A. Mesquita, C. J. Carroll, A. Chanalaris, P. A. Townsend, M. Hubank, A. Stephanou, R. A. Knight, M. S. Marber and D. S. Latchman **(2005)**. "Cardioprotection mediated by urocortin is dependent on PKCepsilon activation." Faseb J **19**(7): 831-3.

Lawrence, K. M., T. M. Scarabelli, L. Turtle, A. Chanalaris, P. A. Townsend, C. J. Carroll, M. Hubank, A. Stephanou, R. A. Knight and D. S. Latchman **(2003)**. "Urocortin protects cardiac myocytes from ischemia/reperfusion injury by attenuating calcium-insensitive phospholipase A2 gene expression." Faseb J **17**(15): 2313-5.

Lawrence, K. M., P. A. Townsend, S. M. Davidson, C. J. Carroll, S. Eaton, M. Hubank, R. A. Knight, A. Stephanou and D. S. Latchman **(2004)**. "The cardioprotective effect of urocortin during ischaemia/reperfusion involves the prevention of mitochondrial damage." Biochem Biophys Res Commun **321**(2): 479-86.

Lecoeur, H., M. C. Prevost and M. L. Gougeon **(2001)**. "Oncosis is associated with exposure of phosphatidylserine residues on the outside layer of the plasma membrane: a reconsideration of the specificity of the annexin V/propidium iodide assay." Cytometry **44**(1): 65-72.

Lee, J. C., J. T. Laydon, P. C. McDonnell, T. F. Gallagher, S. Kumar, D. Green, D. McNulty, M. J. Blumenthal, J. R. Heys, S. W. Landvatter and et al. **(1994)**. "A protein kinase involved in the regulation of inflammatory cytokine biosynthesis." Nature **372**(6508): 739-46.

Lee, K. S., S. H. Hong and S. C. Bae **(2002)**. "Both the Smad and p38 MAPK pathways play a crucial role in Runx2 expression following induction by transforming growth factor-beta and bone morphogenetic protein." Oncogene **21**(47): 7156-63.

Legrand, C., J. M. Bour, C. Jacob, J. Capiaumont, A. Martial, A. Marc, M. Wudtke, G. Kretzmer, C. Demangel, D. Duval and et al. **(1992)**. "Lactate dehydrogenase (LDH) activity of the cultured eukaryotic cells as marker of the number of dead cells in the medium [corrected]." J Biotechnol **25**(3): 231-43.

Leibovich, S. J., P. J. Polverini, T. W. Fong, L. A. Harlow and A. E. Koch **(1994)**. "Production of angiogenic activity by human monocytes requires an L-arginine/nitric oxide-synthase-dependent effector mechanism." Proc Natl Acad Sci U S A **91**(10): 4190-4.

Lewis, K., C. Li, M. H. Perrin, A. Blount, K. Kunitake, C. Donaldson, J. Vaughan, T. M. Reyes, J. Gulyas, W. Fischer, L. Bilezikjian, J. Rivier, P. E. Sawchenko and W. W. Vale **(2001)**. "Identification of urocortin III, an additional member of the corticotropin-releasing factor (CRF) family with high affinity for the CRF2 receptor." Proc Natl Acad Sci U S A **98**(13): 7570-5.

Li, H., H. Zhu, C. J. Xu and J. Yuan **(1998)**. "Cleavage of BID by caspase 8 mediates the mitochondrial damage in the Fas pathway of apoptosis." Cell **94**(4): 491-501.

Li, J., C. A. Bombeck, S. Yang, Y. M. Kim and T. R. Billiar **(1999)**. "Nitric oxide suppresses apoptosis via interrupting caspase activation and mitochondrial dysfunction in cultured hepatocytes." J Biol Chem **274**(24): 17325-33.

Li, P., D. Nijhawan, I. Budihardjo, S. M. Srinivasula, M. Ahmad, E. S. Alnemri and X. Wang **(1997)**. "Cytochrome c and dATP-dependent formation of Apaf-1/caspase-9 complex initiates an apoptotic protease cascade." Cell **91**(4): 479-89.

Liacini, A., J. Sylvester, W. Q. Li, W. Huang, F. Dehnade, M. Ahmad and M. Zafarullah **(2003)**. "Induction of matrix metalloproteinase-13 gene expression by TNF-alpha is mediated by MAP kinases, AP-1, and NF-kappaB transcription factors in articular chondrocytes." Exp Cell Res **288**(1): 208-17.

Liang, Y., M. A. Eid, R. W. Lewis and M. V. Kumar **(2005)**. "Mitochondria from TRAIL-resistant prostate cancer cells are capable of responding to apoptotic stimuli." Cell Signal **17**(2): 243-51.

Lianxu, C., J. Hongti and Y. Changlong **(2006)**. "NF-kappaBp65-specific siRNA inhibits expression of genes of COX-2, NOS-2 and MMP-9 in rat IL-1beta-induced and TNF-alpha-induced chondrocytes." Osteoarthritis Cartilage **14**(4): 367-76.

Light, P. E., A. A. Sabir, B. G. Allen, M. P. Walsh and R. J. French **(1996)**. "Protein kinase C-induced changes in the stoichiometry of ATP binding activate cardiac ATP-sensitive K+ channels. A possible mechanistic link to ischemic preconditioning." Circ Res **79**(3): 399-406.

Lincoln, C. K. and M. G. Gabridge **(1998)**. "Cell culture contamination: sources, consequences, prevention, and elimination." Methods Cell Biol **57**: 49-65.

Lipton, S. A., Y. B. Choi, N. J. Sucher and H. S. Chen **(1998)**. "Neuroprotective versus neurodestructive effects of NO-related species." Biofactors **8**(1-2): 33-40.

Liu, X., H. Zou, C. Slaughter and X. Wang **(1997)**. "DFF, a heterodimeric protein that functions downstream of caspase-3 to trigger DNA fragmentation during apoptosis." Cell **89**(2): 175-84.

Loeser, R. F., C. S. Carlson, M. Del Carlo and A. Cole **(2002)**. "Detection of nitrotyrosine in aging and osteoarthritic cartilage: Correlation of oxidative damage with the presence of interleukin-1beta and with chondrocyte resistance to insulin-like growth factor 1." Arthritis Rheum **46**(9): 2349-57.

Loeser, R. F., S. Sadiev, L. Tan and M. B. Goldring **(2000)**. "Integrin expression by primary and immortalized human chondrocytes: evidence of a differential role for alpha1beta1 and alpha2beta1 integrins in mediating chondrocyte adhesion to types II and VI collagen." Osteoarthritis Cartilage **8**(2): 96-105.

Loeser, R. F. and N. Shakoor **(2003)**. "Aging or osteoarthritis: which is the problem?" Rheum Dis Clin North Am **29**(4): 653-73.

Lopez-Armada, M. J., B. Carames, M. Lires-Dean, B. Cillero-Pastor, C. Ruiz-Romero, F. Galdo and F. J. Blanco **(2006)**. "Cytokines, tumor necrosis factor-alpha and interleukin-1beta, differentially regulate apoptosis in osteoarthritis cultured human chondrocytes." Osteoarthritis Cartilage.

Lorenzo, H. K., S. A. Susin, J. Penninger and G. Kroemer **(1999)**. "Apoptosis inducing factor (AIF): a phylogenetically old, caspase-independent effector of cell death." Cell Death Differ **6**(6): 516-24.

Los, M., M. Mozoluk, D. Ferrari, A. Stepczynska, C. Stroh, A. Renz, Z. Herceg, Z. Q. Wang and K. Schulze-Osthoff **(2002)**. "Activation and caspase-mediated inhibition of PARP: a molecular switch between fibroblast necrosis and apoptosis in death receptor signaling." Mol Biol Cell **13**(3): 978-88.

Lotz, M. **(1995)**. "Interleukin-6: a comprehensive review." Cancer Treat Res **80**: 209-33.

Lotz, M., S. Hashimoto and K. Kuhn **(1999)**. "Mechanisms of chondrocyte apoptosis." Osteoarthritis Cartilage **7**(4): 389-91.

Lovejoy, D. A. and R. J. Balment **(1999)**. "Evolution and physiology of the corticotropin-releasing factor (CRF) family of neuropeptides in vertebrates." Gen Comp Endocrinol **115**(1): 1-22.

Lovenberg, T. W., D. T. Chalmers, C. Liu and E. B. De Souza **(1995)**. "CRF2 alpha and CRF2 beta receptor mRNAs are differentially distributed between the rat central nervous system and peripheral tissues." Endocrinology **136**(9): 4139-42.

Lubomirov, L., H. Gagov, P. Petkova-Kirova, D. Duridanova, V. U. Kalentchuk and R. Schubert **(2001)**. "Urocortin relaxes rat tail arteries by a PKA-mediated reduction of the sensitivity of the contractile apparatus for calcium." Br J Pharmacol **134**(7): 1564-70.

MacCannell, K. L., K. Lederis, P. L. Hamilton and J. Rivier **(1982)**. "Amunine (ovine CRF), urotensin I and sauvagine, three structurally-related peptides, produce selective dilation of the mesenteric circulation." Pharmacology **25**(2): 116-20.

MacFarlane, M. and A. C. Williams **(2004)**. "Apoptosis and disease: a life or death decision." EMBO Rep **5**(7): 674-8.

MacLeod, R. A., W. G. Dirks, Y. Matsuo, M. Kaufmann, H. Milch and H. G. Drexler **(1999)**. "Widespread intraspecies cross-contamination of human tumor cell lines arising at source." Int J Cancer **83**(4): 555-63.

Malfait, A. M., R. Q. Liu, K. Ijiri, S. Komiya and M. D. Tortorella **(2002)**. "Inhibition of ADAM-TS4 and ADAM-TS5 prevents aggrecan degradation in osteoarthritic cartilage." J Biol Chem **277**(25): 22201-8.

Mancini, M., D. W. Nicholson, S. Roy, N. A. Thornberry, E. P. Peterson, L. A. Casciola-Rosen and A. Rosen **(1998)**. "The caspase-3 precursor has a cytosolic and mitochondrial distribution: implications for apoptotic signaling." J Cell Biol **140**(6): 1485-95.

Maneiro, E., M. J. Lopez-Armada, M. C. de Andres, B. Carames, M. A. Martin, A. Bonilla, P. Del Hoyo, F. Galdo, J. Arenas and F. J. Blanco **(2005)**. "Effect of nitric oxide on mitochondrial respiratory activity of human articular chondrocytes." Ann Rheum Dis **64**(3): 388-95.

Manthey, C. L., S. W. Wang, S. D. Kinney and Z. Yao **(1998)**. "SB202190, a selective inhibitor of p38 mitogen-activated protein kinase, is a powerful regulator of LPS-induced mRNAs in monocytes." J Leukoc Biol **64**(3): 409-17.

Marks, P. H. and M. L. Donaldson **(2005)**. "Inflammatory cytokine profiles associated with chondral damage in the anterior cruciate ligament-deficient knee." Arthroscopy **21**(11): 1342-7.

Martel-Pelletier, J., R. McCollum, J. DiBattista, M. P. Faure, J. A. Chin, S. Fournier, M. Sarfati and J. P. Pelletier **(1992)**. "The interleukin-1 receptor in normal and osteoarthritic human articular chondrocytes. Identification as the type I receptor and analysis of binding kinetics and biologic function." Arthritis Rheum **35**(5): 530-40.

Martin, J. A. and J. A. Buckwalter **(2003)**. "The role of chondrocyte senescence in the pathogenesis of osteoarthritis and in limiting cartilage repair." J Bone Joint Surg Am **85-A Suppl 2**: 106-10.

Martinez, V., L. Wang, J. E. Rivier, W. Vale and Y. Tache **(2002)**. "Differential actions of peripheral corticotropin-releasing factor (CRF), urocortin II, and urocortin III on gastric emptying and colonic transit in mice: role of CRF receptor subtypes 1 and 2." J Pharmacol Exp Ther **301**(2): 611-7.

Matthews, J. R., C. H. Botting, M. Panico, H. R. Morris and R. T. Hay **(1996)**. "Inhibition of NF-kappaB DNA binding by nitric oxide." Nucleic Acids Res **24**(12): 2236-42.

Mayhan, W. G. **(1992)**. "Role of nitric oxide in modulating permeability of hamster cheek pouch in response to adenosine 5'-diphosphate and bradykinin." Inflammation **16**(4): 295-305.

Mc, M. J. **(1958)**. "Rudolf Virchow in 1858." Lab Invest **7**(6): 549-53.

McCarberg, B. H. and K. A. Herr **(2001)**. "Osteoarthritis. How to manage pain and improve patient function." Geriatrics **56**(10): 14-7, 20-2, 24.

McDonald, L. J. and F. Murad **(1995)**. "Nitric oxide and cGMP signaling." Adv Pharmacol **34**: 263-75.

McInnes, I. B., B. P. Leung, M. Field, X. Q. Wei, F. P. Huang, R. D. Sturrock, A. Kinninmonth, J. Weidner, R. Mumford and F. Y. Liew **(1996)**. "Production of nitric oxide in the synovial membrane of rheumatoid and osteoarthritis patients." J Exp Med **184**(4): 1519-24.

Melchiorri, C., R. Meliconi, L. Frizziero, T. Silvestri, L. Pulsatelli, I. Mazzetti, R. M. Borzi, M. Uguccioni and A. Facchini **(1998)**. "Enhanced and coordinated in vivo expression of inflammatory cytokines and nitric oxide synthase by chondrocytes from patients with osteoarthritis." Arthritis Rheum **41**(12): 2165-74.

Meldrum, D. R., B. D. Shames, X. Meng, D. A. Fullerton, R. C. McIntyre, Jr., F. L. Grover and A. H. Harken **(1998)**. "Nitric oxide downregulates lung macrophage inflammatory cytokine production." Ann Thorac Surg **66**(2): 313-7.

Melino, G., R. A. Knight and P. Nicotera **(2005)**. "How many ways to die? How many different models of cell death?" Cell Death Differ **12 Suppl 2**: 1457-62.

Micane, K. L., Huether, S.E., (1994). Pathophysiology: The biological basis for diseases in adults and children. , Hon Hoffman Press Inc.

Micheau, O. and J. Tschopp **(2003)**. "Induction of TNF receptor I-mediated apoptosis via two sequential signaling complexes." Cell **114**(2): 181-90.

Mistry, D., Y. Oue, M. G. Chambers, M. V. Kayser and R. M. Mason **(2004)**. "Chondrocyte death during murine osteoarthritis." Osteoarthritis Cartilage **12**(2): 131-41.

Mobasheri, A. **(1999)**. "Brefeldin A influences the cell surface abundance and intracellular pools of low and high ouabain affinity Na+, K(+)-ATPase alpha subunit isoforms in articular chondrocytes." Histol Histopathol **14**(2): 427-38.

Mobasheri, A., R. Mobasheri, M. J. Francis, E. Trujillo, D. Alvarez de la Rosa and P. Martin-Vasallo **(1998)**. "Ion transport in chondrocytes: membrane transporters involved in intracellular ion homeostasis and the regulation of cell volume, free [Ca2+] and pH." Histol Histopathol **13**(3): 893-910.

Mohamed, A. A., O. J. Jupp, H. M. Anderson, A. F. Littlejohn, P. Vandenabeele and D. J. MacEwan **(2002)**. "Tumour necrosis factor-induced activation of c-Jun N-terminal kinase is sensitive to caspase-dependent modulation while activation of mitogen-activated protein kinase (MAPK) or p38 MAPK is not." Biochem J **366**(Pt 1): 145-55.

Moncada, S., R. M. Palmer and E. A. Higgs **(1991)**. "Nitric oxide: physiology, pathophysiology, and pharmacology." Pharmacol Rev **43**(2): 109-42.

Moreau, J. L., G. Kilpatrick and F. Jenck **(1997)**. "Urocortin, a novel neuropeptide with anxiogenic-like properties." Neuroreport **8**(7): 1697-701.

Motyl, T. **(1999)**. "Regulation of apoptosis: involvement of Bcl-2-related proteins." Reprod Nutr Dev **39**(1): 49-59.

Moulton, P. J., T. S. Hiran, M. B. Goldring and J. T. Hancock **(1997)**. "Detection of protein and mRNA of various components of the NADPH oxidase complex in an immortalized human chondrocyte line." Br J Rheumatol **36**(5): 522-9.

Mukherjee, P., B. Wu, L. Mayton, S. H. Kim, P. D. Robbins and P. H. Wooley **(2003)**. "TNF receptor gene therapy results in suppression of IgG2a anticollagen antibody in collagen induced arthritis." Ann Rheum Dis **62**(8): 707-14.

Murakami, A., G. Gao, M. Omura, M. Yano, C. Ito, H. Furukawa, D. Takahashi, K. Koshimizu and H. Ohigashi **(2000)**. "1,1-Dimethylallylcoumarins potently suppress both lipopolysaccharide- and interferon-gamma-induced nitric oxide generation in mouse macrophage RAW 264.7 cells." Bioorg Med Chem Lett **10**(1): 59-62.

Muramatsu, Y., K. Fukushima, K. Iino, K. Totsune, K. Takahashi, T. Suzuki, G. Hirasawa, J. Takeyama, M. Ito, M. Nose, A. Tashiro, M. Hongo, Y. Oki, H. Nagura and H. Sasano **(2000)**. "Urocortin and corticotropin-releasing factor receptor expression in the human colonic mucosa." Peptides **21**(12): 1799-809.

Nakamura, H., M. Tanaka, K. Masuko-Hongo, K. Yudoh, T. Kato, M. Beppu and K. Nishioka **(2006)**. "Enhanced production of MMP-1, MMP-3, MMP-13, and RANTES by interaction of chondrocytes with autologous T cells." Rheumatol Int: 1-7.

Nguyen, T., D. Brunson, C. L. Crespi, B. W. Penman, J. S. Wishnok and S. R. Tannenbaum **(1992)**. "DNA damage and mutation in human cells exposed to nitric oxide in vitro." Proc Natl Acad Sci U S A **89**(7): 3030-4.

Nishida, Y., M. Sugahara-Kobayashi, Y. Takahashi, T. Nagata, K. Ishikawa and S. Asai **(2006)**. "Screening for control genes in mouse hippocampus after transient forebrain ischemia using high-density oligonucleotide array." J Pharmacol Sci **101**(1): 52-7.

Nishikimi, T., A. Miyata, T. Horio, F. Yoshihara, N. Nagaya, S. Takishita, C. Yutani, H. Matsuo, H. Matsuoka and K. Kangawa **(2000)**. "Urocortin, a member of the corticotropin-releasing factor family, in normal and diseased heart." Am J Physiol Heart Circ Physiol **279**(6): H3031-9.

Notoya, K., D. V. Jovanovic, P. Reboul, J. Martel-Pelletier, F. Mineau and J. P. Pelletier **(2000)**. "The induction of cell death in human osteoarthritis chondrocytes by nitric oxide is related to the production of prostaglandin E2 via the induction of cyclooxygenase-2." J Immunol **165**(6): 3402-10.

Ogura, N., M. Tobe, H. Sakamaki, H. Nagura, Y. Abiko and T. Kondoh **(2005)**. "Tumor necrosis factor-alpha increases chemokine gene expression and production in synovial fibroblasts from human temporomandibular joint." J Oral Pathol Med **34**(6): 357-63.

Oh, C. D. and J. S. Chun **(2003)**. "Signaling mechanisms leading to the regulation of differentiation and apoptosis of articular chondrocytes by insulin-like growth factor-1." J Biol Chem **278**(38): 36563-71.

Oki, Y., M. Iwabuchi, M. Masuzawa, F. Watanabe, M. Ozawa, K. Iino, T. Tominaga and T. Yoshimi **(1998)**. "Distribution and concentration of urocortin, and effect of adrenalectomy on its content in rat hypothalamus." Life Sci **62**(9): 807-12.

Oki, Y. and H. Sasano **(2004)**. "Localization and physiological roles of urocortin." Peptides **25**(10): 1745-9.

Okosi, A., B. K. Brar, M. Chan, L. D'Souza, E. Smith, A. Stephanou, D. S. Latchman, H. S. Chowdrey and R. A. Knight **(1998)**. "Expression and protective effects of urocortin in cardiac myocytes." Neuropeptides **32**(2): 167-71.

Oldham, R. K., J. R. Ortaldo, H. T. Holden and R. B. Herberman **(1977)**. "Direct comparison of three isotopic release microtoxicity assays as measures of cell-mediated immunity to Gross virus-induced lymphomas in rats." J Natl Cancer Inst **58**(4): 1061-7.

Oliver, B. L., C. G. Cronin, Y. Zhang-Benoit, M. B. Goldring and M. L. Tanzer **(2005)**. "Divergent stress responses to IL-1beta, nitric oxide, and tunicamycin by chondrocytes." J Cell Physiol **204**(1): 45-50.

Ornstein, L. **(1964)**. "Disc Electrophoresis. I. Background and Theory." Ann N Y Acad Sci **121**: 321-49.

Palmer, G., P. A. Guerne, F. Mezin, M. Maret, J. Guicheux, M. B. Goldring and C. Gabay **(2002)**. "Production of interleukin-1 receptor antagonist by human articular chondrocytes." Arthritis Res **4**(3): 226-31.

Pang, L., T. Sawada, S. J. Decker and A. R. Saltiel **(1995)**. "Inhibition of MAP kinase kinase blocks the differentiation of PC-12 cells induced by nerve growth factor." J Biol Chem **270**(23): 13585-8.

Parkes, D. G., J. Vaughan, J. Rivier, W. Vale and C. N. May **(1997)**. "Cardiac inotropic actions of urocortin in conscious sheep." Am J Physiol **272**(5 Pt 2): H2115-22.

Pearson, G., F. Robinson, T. Beers Gibson, B. E. Xu, M. Karandikar, K. Berman and M. H. Cobb **(2001)**. "Mitogen-activated protein (MAP) kinase pathways: regulation and physiological functions." Endocr Rev **22**(2): 153-83.

Pedersen, W. A., R. Wan, P. Zhang and M. P. Mattson **(2002)**. "Urocortin, but not urocortin II, protects cultured hippocampal neurons from oxidative and excitotoxic cell death via corticotropin-releasing hormone receptor type I." J Neurosci **22**(2): 404-12.

Pelletier, J., D. Jovanovic, J. C. Fernandes, P. Manning, J. R. Connor, M. G. Currie and J. Martel-Pelletier **(1999)**. "Reduction in the structural changes of experimental osteoarthritis by a nitric oxide inhibitor." Osteoarthritis Cartilage **7**(4): 416-8.

Penninger, J. M. and G. Kroemer **(2003)**. "Mitochondria, AIF and caspases--rivaling for cell death execution." Nat Cell Biol **5**(2): 97-9.

Perrin, M. H. and W. W. Vale **(1999)**. "Corticotropin releasing factor receptors and their ligand family." Ann N Y Acad Sci **885**: 312-28.

Peter, M. E. and P. H. Krammer **(2003)**. "The CD95(APO-1/Fas) DISC and beyond." Cell Death Differ **10**(1): 26-35.

Peters, I. R., C. R. Helps, E. J. Hall and M. J. Day **(2004)**. "Real-time RT-PCR: considerations for efficient and sensitive assay design." J Immunol Methods **286**(1-2): 203-17.

Petraglia, F., P. Florio, R. Gallo, T. Simoncini, M. Saviozzi, A. M. Di Blasio, J. Vaughan and W. Vale **(1996)**. "Human placenta and fetal membranes express human urocortin mRNA and peptide." J Clin Endocrinol Metab **81**(10): 3807-10.

Pettersen, I., Y. Figenschau, E. Olsen, W. Bakkelund, B. Smedsrod and B. Sveinbjornsson **(2002)**. "Tumor necrosis factor-related apoptosis-inducing ligand induces apoptosis in human articular chondrocytes in vitro." Biochem Biophys Res Commun **296**(3): 671-6.

Poiraudeau, S., F. Berenbaum and M. Corvol **(1996)**. "[Cartilage degradation and articular inflammation]." Rev Prat **46**(18): 2180-5.

Poliak, S., F. Mor, P. Conlon, T. Wong, N. Ling, J. Rivier, W. Vale and L. Steinman **(1997)**. "Stress and autoimmunity: the neuropeptides corticotropin-releasing factor and urocortin suppress encephalomyelitis via effects on both the hypothalamic-pituitary-adrenal axis and the immune system." J Immunol **158**(12): 5751-6.

Porcher, C., A. Peinnequin, S. Pellissier, J. Meregnani, V. Sinniger, F. Canini and B. Bonaz **(2006)**. "Endogenous expression and in vitro study of CRF-related peptides and CRF receptors in the rat gastric antrum." Peptides **27**(6): 1464-75.

Potter, E., D. P. Behan, W. H. Fischer, E. A. Linton, P. J. Lowry and W. W. Vale **(1991)**. "Cloning and characterization of the cDNAs for human and rat corticotropin releasing factor-binding proteins." Nature **349**(6308): 423-6.

Potter, E., S. Sutton, C. Donaldson, R. Chen, M. Perrin, K. Lewis, P. E. Sawchenko and W. Vale **(1994)**. "Distribution of corticotropin-releasing factor receptor mRNA expression in the rat brain and pituitary." Proc Natl Acad Sci U S A **91**(19): 8777-81.

Pulai, J. I., M. Del Carlo, Jr. and R. F. Loeser **(2002)**. "The alpha5beta1 integrin provides matrix survival signals for normal and osteoarthritic human articular chondrocytes in vitro." Arthritis Rheum **46**(6): 1528-35.

Rae, T. **(1977)**. "Tolerance of mouse macrophages in vitro to barium sulfate used in orthopedic bone cement." J Biomed Mater Res **11**(6): 839-46.

Raingeaud, J., A. J. Whitmarsh, T. Barrett, B. Derijard and R. J. Davis **(1996)**. "MKK3- and MKK6-regulated gene expression is mediated by the p38 mitogen-activated protein kinase signal transduction pathway." Mol Cell Biol **16**(3): 1247-55.

Raju, T. N. **(1999)**. "The Nobel chronicles. 1975: Renato Dulbecco (b 1914), David Baltimore (b 1938), and Howard Martin Temin (1934-94)." Lancet **354**(9186): 1308.

Rath, P. C. and B. B. Aggarwal **(1999)**. "TNF-induced signaling in apoptosis." J Clin Immunol **19**(6): 350-64.

Reddien, P. W. and H. R. Horvitz **(2004)**. "The engulfment process of programmed cell death in caenorhabditis elegans." Annu Rev Cell Dev Biol **20**: 193-221.

Reed, J. C. **(1997)**. "Double identity for proteins of the Bcl-2 family." Nature **387**(6635): 773-6.

Reed, J. C. **(2000)**. "Mechanisms of apoptosis." Am J Pathol **157**(5): 1415-30.

Renoux, M., P. Hilliquin, L. Galoppin, I. Florentin and C. J. Menkes **(1996)**. "Release of mast cell mediators and nitrites into knee joint fluid in osteoarthritis--comparison with articular chondrocalcinosis and rheumatoid arthritis." Osteoarthritis Cartilage **4**(3): 175-9.

Reyes, T. M., K. Lewis, M. H. Perrin, K. S. Kunitake, J. Vaughan, C. A. Arias, J. B. Hogenesch, J. Gulyas, J. Rivier, W. W. Vale and P. E. Sawchenko **(2001)**. "Urocortin II: a member of the corticotropin-releasing factor (CRF) neuropeptide family that is selectively bound by type 2 CRF receptors." Proc Natl Acad Sci U S A **98**(5): 2843-8.

Roach, H. I., T. Aigner and J. B. Kouri **(2004)**. "Chondroptosis: a variant of apoptotic cell death in chondrocytes?" Apoptosis **9**(3): 265-77.

Robbins, D. J., E. Zhen, H. Owaki, C. A. Vanderbilt, D. Ebert, T. D. Geppert and M. H. Cobb **(1993)**. "Regulation and properties of extracellular signal-regulated protein kinases 1 and 2 in vitro." J Biol Chem **268**(7): 5097-106.

Rosen, C. J. **(2000)**. "Pathophysiology of osteoporosis." Clin Lab Med **20**(3): 455-68.

Rucklidge, G. J., G. Milne and S. P. Robins **(1996)**. "Collagen type X: a component of the surface of normal human, pig, and rat articular cartilage." Biochem Biophys Res Commun **224**(2): 297-302.

Rudner, J., V. Jendrossek, K. Lauber, P. T. Daniel, S. Wesselborg and C. Belka **(2005)**. "Type I and type II reactions in TRAIL-induced apoptosis -- results from dose-response studies." Oncogene **24**(1): 130-40.

Ruf, A., J. Mennissier de Murcia, G. de Murcia and G. E. Schulz **(1996)**. "Structure of the catalytic fragment of poly(AD-ribose) polymerase from chicken." Proc Natl Acad Sci U S A **93**(15): 7481-5.

Sabatini, M., G. Rolland, S. Leonce, M. Thomas, C. Lesur, V. Perez, G. de Nanteuil and J. Bonnet **(2000)**. "Effects of ceramide on apoptosis, proteoglycan degradation, and matrix metalloproteinase expression in rabbit articular cartilage." Biochem Biophys Res Commun **267**(1): 438-44.

Saelens, X., N. Festjens, L. Vande Walle, M. van Gurp, G. van Loo and P. Vandenabeele **(2004)**. "Toxic proteins released from mitochondria in cell death." Oncogene **23**(16): 2861-74.

Saklatvala, J., L. M. Pilsworth, S. J. Sarsfield, J. Gavrilovic and J. K. Heath **(1984)**. "Pig catabolin is a form of interleukin 1. Cartilage and bone resorb, fibroblasts make prostaglandin and collagenase, and thymocyte proliferation is augmented in response to one protein." Biochem J **224**(2): 461-6.

Sakurai, H., H. Kohsaka, M. F. Liu, H. Higashiyama, Y. Hirata, K. Kanno, I. Saito and N. Miyasaka **(1995)**. "Nitric oxide production and inducible nitric oxide synthase expression in inflammatory arthritides." J Clin Invest **96**(5): 2357-63.

Salvesen, G. S. and V. M. Dixit **(1999)**. "Caspase activation: the induced-proximity model." Proc Natl Acad Sci U S A **96**(20): 10964-7.

Sandau, K., J. Pfeilschifter and B. Brune **(1997)**. "The balance between nitric oxide and superoxide determines apoptotic and necrotic death of rat mesangial cells." J Immunol **158**(10): 4938-46.

Sandau, K. B. and B. Brune **(2000)**. "Molecular actions of nitric oxide in mesangial cells." Histol Histopathol **15**(4): 1151-8.

Sandra, F., L. Hendarmin, Y. Nakao, N. Nakamura and S. Nakamura **(2005)**. "TRAIL cleaves caspase-8, -9 and -3 of AM-1 cells: a possible pathway for TRAIL to induce apoptosis in ameloblastoma." Tumour Biol **26**(5): 258-64.

Sandra, F., L. Hendarmin, Y. Nakao, N. Nakamura and S. Nakamura **(2006)**. "Inhibition of Akt and MAPK pathways elevated potential of TNFalpha in inducing apoptosis in ameloblastoma." Oral Oncol **42**(1): 39-45.

Scaffidi, C., S. Kirchhoff, P. H. Krammer and M. E. Peter **(1999)**. "Apoptosis signaling in lymphocytes." Curr Opin Immunol **11**(3): 277-85.

Scarabelli, T. M., E. Pasini, A. Stephanou, L. Comini, S. Curello, R. Raddino, R. Ferrari, R. Knight and D. S. Latchman **(2002)**. "Urocortin promotes hemodynamic and bioenergetic recovery and improves cell survival in the isolated rat heart exposed to ischemia/reperfusion." J Am Coll Cardiol **40**(1): 155-61.

Schimmer, A. D. **(2004)**. "Inhibitor of apoptosis proteins: translating basic knowledge into clinical practice." Cancer Res **64**(20): 7183-90.

Schmidt, M., H. G. Pauels, N. Lugering, A. Lugering, W. Domschke and T. Kucharzik **(1999)**. "Glucocorticoids induce apoptosis in human monocytes: potential role of IL-1 beta." J Immunol **163**(6): 3484-90.

Schuerwegh, A. J., J. F. Van Offel, W. J. Stevens, C. H. Bridts and L. S. De Clerck **(2003)**. "Influence of therapy with chimeric monoclonal tumour necrosis factor-alpha antibodies on intracellular cytokine profiles of T lymphocytes and monocytes in rheumatoid arthritis patients." Rheumatology (Oxford) **42**(4): 541-8.

Schulman, D., D. S. Latchman and D. M. Yellon **(2002)**. "Urocortin protects the heart from reperfusion injury via upregulation of p42/p44 MAPK signaling pathway." Am J Physiol Heart Circ Physiol **283**(4): H1481-8.

Seid, J. M., S. Rahman, R. Graveley, R. A. Bunning, R. Nordmann, W. Wishart and R. G. Russell **(1993)**. "The effect of interleukin-1 on cytokine gene expression in cultured human articular chondrocytes analyzed by messenger RNA phenotyping." Arthritis Rheum **36**(1): 35-43.

Seshagiri, S., W. T. Chang and L. K. Miller **(1998)**. "Mutational analysis of Caenorhabditis elegans CED-4." FEBS Lett **428**(1-2): 71-4.

Sgonc, R., M. S. Gruschwitz, H. Dietrich, H. Recheis, M. E. Gershwin and G. Wick **(1996)**. "Endothelial cell apoptosis is a primary pathogenetic event underlying skin lesions in avian and human scleroderma." J Clin Invest **98**(3): 785-92.

Shen, Y. H., X. L. Wang and D. E. Wilcken **(1998)**. "Nitric oxide induces and inhibits apoptosis through different pathways." FEBS Lett **433**(1-2): 125-31.

Shibasaki, T., E. Odagiri, K. Shizume and N. Ling **(1982)**. "Corticotropin-releasing factor-like activity in human placental extracts." J Clin Endocrinol Metab **55**(2): 384-6.

Siders, W. M., J. C. Klimovitz and S. B. Mizel **(1993)**. "Characterization of the structural requirements and cell type specificity of IL-1 alpha and IL-1 beta secretion." J Biol Chem **268**(29): 22170-4.

Simbulan-Rosenthal, C. M., D. S. Rosenthal, S. Iyer, H. Boulares and M. E. Smulson **(1999)**. "Involvement of PARP and poly(ADP-ribosyl)ation in the early stages of apoptosis and DNA replication." Mol Cell Biochem **193**(1-2): 137-48.

Singh, R., S. Ahmed, C. J. Malemud, V. M. Goldberg and T. M. Haqqi **(2003)**. "Epigallocatechin-3-gallate selectively inhibits interleukin-1beta-induced activation of mitogen activated protein kinase subgroup c-Jun N-terminal kinase in human osteoarthritis chondrocytes." J Orthop Res **21**(1): 102-9.

Sizemore, N., N. Lerner, N. Dombrowski, H. Sakurai and G. R. Stark **(2002)**. "Distinct roles of the Ikappa B kinase alpha and beta subunits in liberating nuclear factor kappa B (NF-kappa B) from Ikappa B and in phosphorylating the p65 subunit of NF-kappa B." J Biol Chem **277**(6): 3863-9.

Slack, J., C. J. McMahan, S. Waugh, K. Schooley, M. K. Spriggs, J. E. Sims and S. K. Dower **(1993)**. "Independent binding of interleukin-1 alpha and interleukin-1 beta to type I and type II interleukin-1 receptors." J Biol Chem **268**(4): 2513-24.

Slominski, A., B. Roloff, J. Curry, M. Dahiya, A. Szczesniewski and J. Wortsman **(2000)**. "The skin produces urocortin." J Clin Endocrinol Metab **85**(2): 815-23.

Smith, R. L. **(1999)**. "Degradative enzymes in osteoarthritis." Front Biosci **4**: D704-12.

Spears, R., R. Oakes, L. L. Bellinger and B. Hutchins **(2003)**. "Tumour necrosis factor-alpha and apoptosis in the rat temporomandibular joint." Arch Oral Biol **48**(12): 825-34.

Spina, M., E. Merlo-Pich, R. K. Chan, A. M. Basso, J. Rivier, W. Vale and G. F. Koob **(1996)**. "Appetite-suppressing effects of urocortin, a CRF-related neuropeptide." Science **273**(5281): 1561-4.

Stadler, J., M. Stefanovic-Racic, T. R. Billiar, R. D. Curran, L. A. McIntyre, H. I. Georgescu, R. L. Simmons and C. H. Evans **(1991)**. "Articular chondrocytes synthesize nitric oxide in response to cytokines and lipopolysaccharide." J Immunol **147**(11): 3915-20.

Stamler, J. S., D. J. Singel and J. Loscalzo **(1992)**. "Biochemistry of nitric oxide and its redox-activated forms." Science **258**(5090): 1898-902.

Stanton, L. A., S. Sabari, A. V. Sampaio, T. M. Underhill and F. Beier **(2004)**. "p38 MAP kinase signalling is required for hypertrophic chondrocyte differentiation." Biochem J **378**(Pt 1): 53-62.

Steer, S. A., K. C. Wirsig, M. H. Creer, D. A. Ford and J. McHowat **(2002)**. "Regulation of membrane-associated iPLA2 activity by a novel PKC isoform in ventricular myocytes." Am J Physiol Cell Physiol **283**(6): C1621-6.

Stefanovic-Racic, M., K. Meyers, C. Meschter, J. W. Coffey, R. A. Hoffman and C. H. Evans **(1994)**. "N-monomethyl arginine, an inhibitor of nitric oxide synthase, suppresses the development of adjuvant arthritis in rats." Arthritis Rheum **37**(7): 1062-9.

Stockwell, R. A. **(1991)**. "Morphometry of cytoplasmic components of mammalian articular chondrocytes and corneal keratocytes: species and zonal variations of mitochondria in relation to nutrition." J Anat **175**: 251-61.

Stoscheck, C. M. **(1990)**. "Increased uniformity in the response of the coomassie blue G protein assay to different proteins." Anal Biochem **184**(1): 111-6.

Sturgill, T. W. and L. B. Ray **(1986)**. "Muscle proteins related to microtubule associated protein-2 are substrates for an insulin-stimulatable kinase." Biochem Biophys Res Commun **134**(2): 565-71.

Sun, H., N. K. Tonks and D. Bar-Sagi **(1994)**. "Inhibition of Ras-induced DNA synthesis by expression of the phosphatase MKP-1." Science **266**(5183): 285-8.

Swanson, L. W., P. E. Sawchenko, J. Rivier and W. W. Vale **(1983)**. "Organization of ovine corticotropin-releasing factor immunoreactive cells and fibers in the rat brain: an immunohistochemical study." Neuroendocrinology **36**(3): 165-86.

Symons, J. A., W. L. Wong, M. A. Palladino and G. W. Duff **(1992)**. "Interleukin 8 in rheumatoid and osteoarthritis." Scand J Rheumatol **21**(2): 92-4.

Taher, M. M., C. M. Hershey, J. D. Oakley and K. Valerie **(2000)**. "Role of the p38 and MEK-1/2/p42/44 MAP kinase pathways in the differential activation of human immunodeficiency virus gene expression by ultraviolet and ionizing radiation." Photochem Photobiol **71**(4): 455-9.

Takacs, L., E. J. Kovacs, M. R. Smith, H. A. Young and S. K. Durum **(1988)**. "Detection of IL-1 alpha and IL-1 beta gene expression by in situ hybridization. Tissue localization of IL-1 mRNA in the normal C57BL/6 mouse." J Immunol **141**(9): 3081-95.

Takahashi, K., K. Totsune, M. Sone, O. Murakami, F. Satoh, Z. Arihara, H. Sasano, K. Iino and T. Mouri **(1998)**. "Regional distribution of urocortin-like immunoreactivity and expression of urocortin mRNA in the human brain." Peptides **19**(4): 643-7.

Tao, J., J. Chen, Y. Wu and S. Li **(2005)**. "Urocortin reduces the viability of adult rat vascular smooth muscle cells via inhibiting L-type calcium channels." Peptides **26**(11): 2239-45.

Tao, J., H. Xu, C. Yang, C. N. Liu and S. Li **(2004)**. "Effect of urocortin on L-type calcium currents in adult rat ventricular myocytes." Pharmacol Res **50**(5): 471-6.

Tartaglia, L. A. and D. V. Goeddel **(1992)**. "Two TNF receptors." Immunol Today **13**(5): 151-3.

Tartaglia, L. A., M. Rothe, Y. F. Hu and D. V. Goeddel **(1993)**. "Tumor necrosis factor's cytotoxic activity is signaled by the p55 TNF receptor." Cell **73**(2): 213-6.

Taskiran, D., M. Stefanovic-Racic, H. Georgescu and C. Evans **(1994)**. "Nitric oxide mediates suppression of cartilage proteoglycan synthesis by interleukin-1." Biochem Biophys Res Commun **200**(1): 142-8.

Tatsuta, T., J. Cheng and J. D. Mountz **(1996)**. "Intracellular IL-1beta is an inhibitor of Fas-mediated apoptosis." J Immunol **157**(9): 3949-57.

Tattersall, A. L., J. A. Browning and R. J. Wilkins **(2005)**. "Modulation of H+ transport mechanisms by interleukin-1 in isolated bovine articular chondrocytes." Cell Physiol Biochem **16**(1-3): 43-50.

Terui, K., A. Higashiyama, N. Horiba, K. I. Furukawa, S. Motomura and T. Suda **(2001)**. "Coronary vasodilation and positive inotropism by urocortin in the isolated rat heart." J Endocrinol **169**(1): 177-83.

Thiagarajan, P. and J. F. Tait **(1990)**. "Binding of annexin V/placental anticoagulant protein I to platelets. Evidence for phosphatidylserine exposure in the procoagulant response of activated platelets." J Biol Chem **265**(29): 17420-3.

Thompson, C. B. **(1995)**. "Apoptosis in the pathogenesis and treatment of disease." Science **267**(5203): 1456-62.

Thornberry, N. A. and Y. Lazebnik **(1998)**. "Caspases: enemies within." Science **281**(5381): 1312-6.

Todd Allen, R., C. M. Robertson, F. L. Harwood, T. Sasho, S. K. Williams, A. C. Pomerleau and D. Amiel **(2004)**. "Characterization of mature vs aged rabbit articular cartilage: analysis of cell density, apoptosis-related gene expression and mechanisms controlling chondrocyte apoptosis." Osteoarthritis Cartilage **12**(11): 917-23.

Todd, J. L., K. G. Tanner and J. M. Denu **(1999)**. "Extracellular regulated kinases (ERK) 1 and ERK2 are authentic substrates for the dual-specificity protein-tyrosine phosphatase VHR. A novel role in down-regulating the ERK pathway." J Biol Chem **274**(19): 13271-80.

Tortora, G. W., and Grabowski, S. R., (2000). Principles of Anatomy and Physiology, R R Donnelley and Sons Company.

Tortorella, M. D. and A. M. Malfait **(2003)**. "The usual suspects: verdict not guilty?" Arthritis Rheum **48**(12): 3304-7.

Tselepis, C., I. Perry, C. Dawson, R. Hardy, S. J. Darnton, C. McConkey, R. C. Stuart, N. Wright, R. Harrison and J. A. Jankowski **(2002)**. "Tumour necrosis factor-alpha in Barrett's oesophagus: a potential novel mechanism of action." Oncogene **21**(39): 6071-81.

Uehara, T., Y. Kikuchi and Y. Nomura **(1999)**. "Caspase activation accompanying cytochrome c release from mitochondria is possibly involved in nitric oxide-induced neuronal apoptosis in SH-SY5Y cells." J Neurochem **72**(1): 196-205.

Upholt., W. B., and Olsten., B. R., (1991). Molecular Aspects
Uzuki, M., H. Sasano, Y. Muramatsu, K. Totsune, K. Takahashi, Y. Oki, K. Iino and T. Sawai **(2001)**. "Urocortin in the synovial tissue of patients with rheumatoid arthritis." Clin Sci (Lond) **100**(6): 577-89.

Valdez, G. R., K. Inoue, G. F. Koob, J. Rivier, W. Vale and E. P. Zorrilla **(2002)**. "Human urocortin II: mild locomotor suppressive and delayed anxiolytic-like effects of a novel corticotropin-releasing factor related peptide." Brain Res **943**(1): 142-50.

van de Loo, F. A., O. J. Arntz, F. H. van Enckevort, P. L. van Lent and W. B. van den Berg **(1998)**. "Reduced cartilage proteoglycan loss during zymosan-induced gonarthritis in NOS2-deficient mice and in anti-interleukin-1-treated wild-type mice with unabated joint inflammation." Arthritis Rheum **41**(4): 634-46.

van der Kraan, P. M. and W. B. van den Berg **(2000)**. "Anabolic and destructive mediators in osteoarthritis." Curr Opin Clin Nutr Metab Care **3**(3): 205-11.

Vanhaesebroeck, B. and D. R. Alessi **(2000)**. "The PI3K-PDK1 connection: more than just a road to PKB." Biochem J **346 Pt 3**: 561-76.

Vanhaesebroeck, B., S. J. Leevers, K. Ahmadi, J. Timms, R. Katso, P. C. Driscoll, R. Woscholski, P. J. Parker and M. D. Waterfield **(2001)**. "Synthesis and function of 3-phosphorylated inositol lipids." Annu Rev Biochem **70**: 535-602.

Vaughan, J., C. Donaldson, J. Bittencourt, M. H. Perrin, K. Lewis, S. Sutton, R. Chan, A. V. Turnbull, D. Lovejoy, C. Rivier and et al. **(1995)**. "Urocortin, a mammalian neuropeptide related to fish urotensin I and to corticotropin-releasing factor." Nature **378**(6554): 287-92.

Vermes, I., C. Haanen and C. Reutelingsperger **(2000)**. "Flow cytometry of apoptotic cell death." J Immunol Methods **243**(1-2): 167-90.

Vermes, I., C. Haanen, H. Steffens-Nakken and C. Reutelingsperger **(1995)**. "A novel assay for apoptosis. Flow cytometric detection of phosphatidylserine expression on early apoptotic cells using fluorescein labelled Annexin V." J Immunol Methods **184**(1): 39-51.

Verschure, P. J., L. A. Joosten, P. M. van der Kraan and W. B. Van den Berg **(1994)**. "Responsiveness of articular cartilage from normal and inflamed mouse knee joints to various growth factors." Ann Rheum Dis **53**(7): 455-60.

Verschure, P. J. and C. J. Van Noorden **(1990)**. "The effects of interleukin-1 on articular cartilage destruction as observed in arthritic diseases, and its therapeutic control." Clin Exp Rheumatol **8**(3): 303-13.

Vignon, E., M. Arlot, L. M. Patricot and G. Vignon **(1976)**. "The cell density of human femoral head cartilage." Clin Orthop Relat Res(121): 303-8.

Vlahos, C. J., W. F. Matter, K. Y. Hui and R. F. Brown **(1994)**. "A specific inhibitor of phosphatidylinositol 3-kinase, 2-(4-morpholinyl)-8-phenyl-4H-1-benzopyran-4-one (LY294002)." J Biol Chem **269**(7): 5241-8.

Wang, L., K. F. Almqvist, C. Broddelez, E. M. Veys and G. Verbruggen **(2001)**. "Evaluation of chondrocyte cell-associated matrix metabolism by flow cytometry." Osteoarthritis Cartilage **9**(5): 454-62.

Wang, S. W., J. Pawlowski, S. T. Wathen, S. D. Kinney, H. S. Lichenstein and C. L. Manthey **(1999)**. "Cytokine mRNA decay is accelerated by an inhibitor of p38-mitogen-activated protein kinase." Inflamm Res **48**(10): 533-8.

Ward, L. S., M. E. Guariento, G. A. Fernandes and R. M. Maciel **(1999)**. "Serum cytokines in chronic Chagas' disease." Rev Soc Bras Med Trop **32**(3): 285-9.

Webb, G. R., C. I. Westacott and C. J. Elson **(1997)**. "Chondrocyte tumor necrosis factor receptors and focal loss of cartilage in osteoarthritis." Osteoarthritis Cartilage **5**(6): 427-37.

Webb, G. R., C. I. Westacott and C. J. Elson **(1998)**. "Osteoarthritic synovial fluid and synovium supernatants up-regulate tumor necrosis factor receptors on human articular chondrocytes." Osteoarthritis Cartilage **6**(3): 167-76.

Weber, K. and M. Osborn **(1969)**. "The reliability of molecular weight determinations by dodecyl sulfate-polyacrylamide gel electrophoresis." J Biol Chem **244**(16): 4406-12.

Webster, E. L., D. B. Lewis, D. J. Torpy, E. K. Zachman, K. C. Rice and G. P. Chrousos **(1996)**. "In vivo and in vitro characterization of antalarmin, a nonpeptide corticotropin-releasing hormone (CRH) receptor antagonist: suppression of pituitary ACTH release and peripheral inflammation." Endocrinology **137**(12): 5747-50.

Wei, L., X. J. Sun, Z. Wang and Q. Chen **(2006)**. "CD95-induced osteoarthritic chondrocyte apoptosis and necrosis: dependency on p38 mitogen-activated protein kinase." Arthritis Res Ther **8**(2): R37.

Weil, M. M., C. I. Amos, K. A. Mason and L. C. Stephens **(1996)**. "Genetic basis of strain variation in levels of radiation-induced apoptosis of thymocytes." Radiat Res **146**(6): 646-51.

Westacott, C. I. and M. Sharif **(1996)**. "Cytokines in osteoarthritis: mediators or markers of joint destruction?" Semin Arthritis Rheum **25**(4): 254-72.

Westacott, C. I., J. T. Whicher, I. C. Barnes, D. Thompson, A. J. Swan and P. A. Dieppe **(1990)**. "Synovial fluid concentration of five different cytokines in rheumatic diseases." Ann Rheum Dis **49**(9): 676-81.

Wiley, V., K. Carpenter, B. Bennetts and B. Wilcken **(2003)**. "Information overload--new technologies, can we store the data?" Southeast Asian J Trop Med Public Health **34 Suppl 3**: 59-62.

Wilson, K. P., P. G. McCaffrey, K. Hsiao, S. Pazhanisamy, V. Galullo, G. W. Bemis, M. J. Fitzgibbon, P. R. Caron, M. A. Murcko and M. S. Su **(1997)**. "The structural basis for the specificity of pyridinylimidazole inhibitors of p38 MAP kinase." Chem Biol **4**(6): 423-31.

Wink, D. A., I. Hanbauer, M. B. Grisham, F. Laval, R. W. Nims, J. Laval, J. Cook, R. Pacelli, J. Liebmann, M. Krishna, P. C. Ford and J. B. Mitchell **(1996)**. "Chemical biology of nitric oxide: regulation and protective and toxic mechanisms." Curr Top Cell Regul **34**: 159-87.

Woods, R. J., C. F. Kemp, J. David and P. J. Lowry **(1997)**. "Heterogeneity of the human corticotropin-releasing factor-binding protein." J Clin Endocrinol Metab **82**(5): 1566-71.

Woolley, D. E. and L. C. Tetlow **(2000)**. "Mast cell activation and its relation to proinflammatory cytokine production in the rheumatoid lesion." Arthritis Res **2**(1): 65-74.

Wyllie, A. H. **(1986)**. "What is apoptosis?" Histopathology **10**(9): 995-8.

Xia, Z., M. Dickens, J. Raingeaud, R. J. Davis and M. E. Greenberg **(1995)**. "Opposing effects of ERK and JNK-p38 MAP kinases on apoptosis." Science **270**(5240): 1326-31.

Xu, J., J. D. Hennebold and R. L. Stouffer **(2006)**. "Dynamic expression and regulation of the corticotropin-releasing hormone/urocortin-receptor-binding protein system in the primate ovary during the menstrual cycle." J Clin Endocrinol Metab **91**(4): 1544-53.

Yao, Z., S. L. Painter, W. C. Fanslow, D. Ulrich, B. M. Macduff, M. K. Spriggs and R. J. Armitage **(1995)**. "Human IL-17: a novel cytokine derived from T cells." J Immunol **155**(12): 5483-6.

Yaron, I., F. A. Meyer, J. M. Dayer, I. Bleiberg and M. Yaron **(1989)**. "Some recombinant human cytokines stimulate glycosaminoglycan synthesis in human synovial fibroblast cultures and inhibit it in human articular cartilage cultures." Arthritis Rheum **32**(2): 173-80.

Yasuhara, R., Y. Miyamoto, T. Akaike, T. Akuta, M. Nakamura, M. Takami, N. Morimura, K. Yasu and R. Kamijo **(2005)**. "Interleukin-1beta induces death in chondrocyte-like ATDC5 cells through mitochondrial dysfunction and energy depletion in a reactive nitrogen and oxygen species-dependent manner." Biochem J **389**(Pt 2): 315-23.

Yeh, P. Y., S. E. Chuang, K. H. Yeh, Y. C. Song, C. K. Ea and A. L. Cheng **(2002)**. "Increase of the resistance of human cervical carcinoma cells to cisplatin by inhibition of the MEK to ERK signaling pathway partly via enhancement of anticancer drug-induced NF kappa B activation." Biochem Pharmacol **63**(8): 1423-30.

Young, P., P. McDonnell, D. Dunnington, A. Hand, J. Laydon and J. Lee **(1993)**. "Pyridinyl imidazoles inhibit IL-1 and TNF production at the protein level." Agents Actions **39 Spec No**: C67-9.

Yuan, J., S. Shaham, S. Ledoux, H. M. Ellis and H. R. Horvitz **(1993)**. "The C. elegans cell death gene ced-3 encodes a protein similar to mammalian interleukin-1 beta-converting enzyme." Cell **75**(4): 641-52.

Zaniolo, K., A. Rufiange, S. Leclerc, S. Desnoyers and S. L. Guerin **(2005)**. "Regulation of the poly(ADP-ribose) polymerase-1 gene expression by the transcription factors Sp1 and Sp3 is under the influence of cell density in primary cultured cells." Biochem J **389**(Pt 2): 423-33.

Zech, B., R. Kohl, A. von Knethen and B. Brune **(2003)**. "Nitric oxide donors inhibit formation of the Apaf-1/caspase-9 apoptosome and activation of caspases." Biochem J **371**(Pt 3): 1055-64.

Zhang, B., J. Hirahashi, X. Cullere and T. N. Mayadas **(2003)**. "Elucidation of molecular events leading to neutrophil apoptosis following phagocytosis: cross-talk between caspase 8, reactive oxygen species, and MAPK/ERK activation." J Biol Chem **278**(31): 28443-54.

Zhang, J., F. Zhang, D. Ebert, M. H. Cobb and E. J. Goldsmith **(1995)**. "Activity of the MAP kinase ERK2 is controlled by a flexible surface loop." Structure **3**(3): 299-307.

Zhao, L., C. J. Donaldson, G. W. Smith and W. W. Vale **(1998)**. "The structures of the mouse and human urocortin genes (Ucn and UCN)." Genomics **50**(1): 23-33.

Zhen, X., L. Wei, Q. Wu, Y. Zhang and Q. Chen **(2001)**. "Mitogen-activated protein kinase p38 mediates regulation of chondrocyte differentiation by parathyroid hormone." J Biol Chem **276**(7): 4879-85.

Zwerina, J., S. Hayer, K. Redlich, K. Bobacz, G. Kollias, J. S. Smolen and G. Schett **(2006)**. "Activation of p38 MAPK is a key step in tumor necrosis factor-mediated inflammatory bone destruction." Arthritis Rheum **54**(2): 463-72.

CHAPTER 8

APPENDIX I: SEQUENCE DATA

Urocortin Gene Sequence

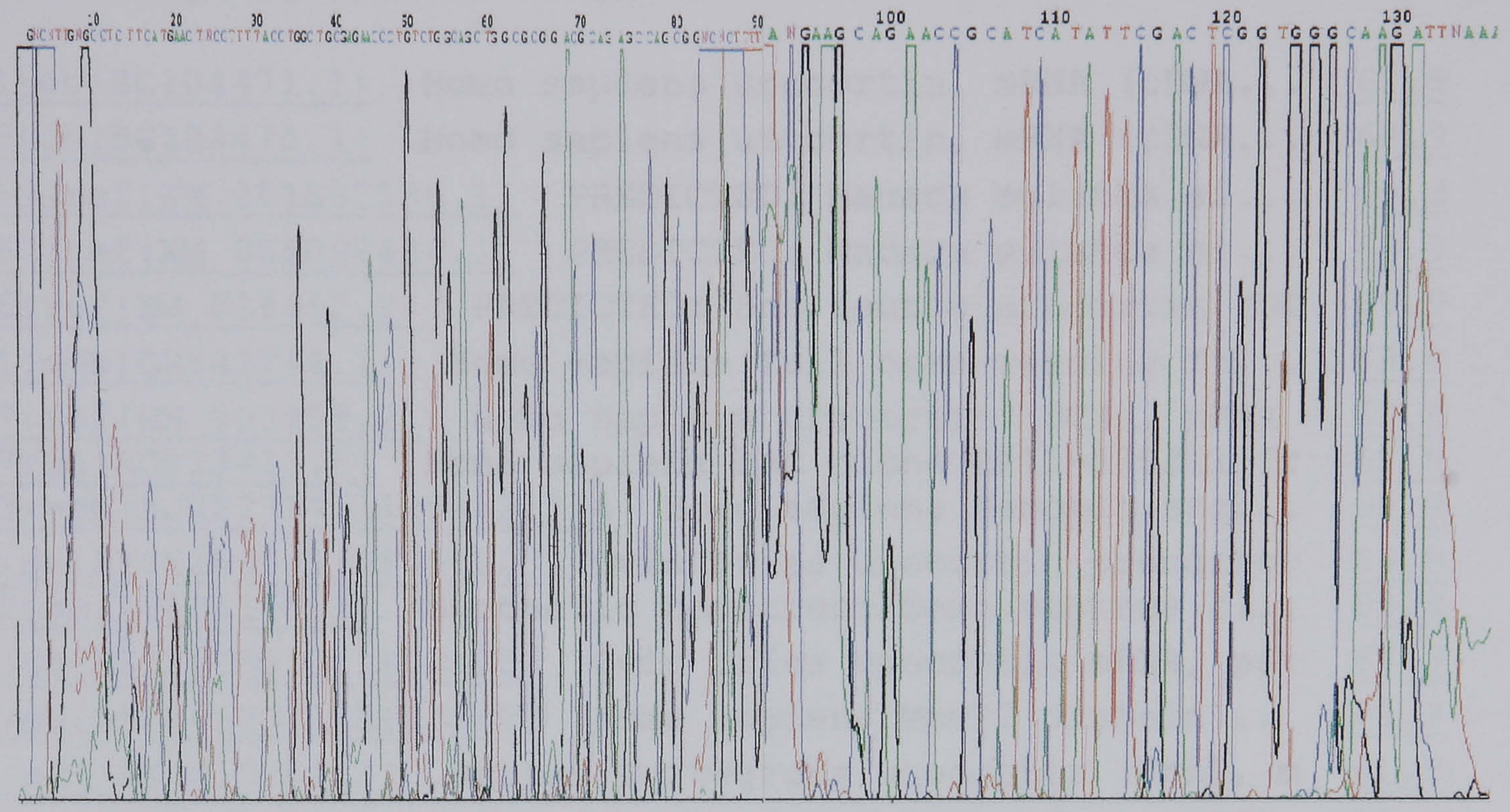

GNCNTTGNGCCTCTTCATGAACTNCCTTTTACCTGGCTGCGAGAACCCTGTCTGGCAGCTGGCGCGGACGCAGAGCCAGCGGNCNCTTTTTANGA
AGCAGAACCGCATCATATTCGACTCGGTGGGCAAGATTNAAAAANTNTNNNNNNTCNNGNTTTTNTTATTNTNNTTAAANTNAGAGNNANGAAN
NNNNNACTGNTATCNNNNTTAACCNCNCANGNTTTAANNTCNGCCNNNNGCACGTAANAAANGAGNNANNGAGNNNNCNNNTTACNCNAGTN
AANTATATNTNNTTTCTTGACTNGGACNNNTTTGTNNATANTNNNCAAAATTATATTTTGATTAGATCAANCNTANATTNACNNCAGNATNTNNN
NCNCANNTANGAACACCGAGTNCTGTAAGTNGTTTNAANNGNTGTNGGGGCNCNNCTANTCGANANANTAAAGTTTGTNCATTTCCTGGTTNGA
NNGAAANATANATTNTTGTNTTTTTTNNTNCTTGNANNCGGNTCTCGNNTTNCGGATGTANACNNCCTTGGTNTTGNAANCTNNGNNCCNTGNA
NNCTGNNAANTAAGANTCCGNTNCGAGATACTNTTNNTCTTCNTNTATNACTTANGCTGNAAANNNNNNNCNCCTGAAATANNATATTGGAATA
NGCCGTANNTANANNNANNCTTGTTNGAANCTAAAGANNCNNGNTTNTNGATNNCAGGTTNGAACGCANNANNGTTTANATANATCAATCTCT
TAGTNANNNCCNCGCCNNAAGNANTCNNTTATNGGAGCGNAAATTCGANNGNAGGCNTNNTANNNNGANCAAGNNNNANANACNNCAGNTNT
NNNCNNCAGTTTTNTNATGNGCTAGTNATNTNNAGTACTCGCANTCNNTNANAGNNTTTGNNNNTGNNTACNCANNGTGTGATNGATNTNTAN
NACAATNNNANATNGTGCNTNTNNTNNNTNGAANANTGNATCANNNNAGNATANNNNNNCNTTAGATTNCCTNNNTCNTTCNT

BLAST Data for the Urocortin Gene

Sequences producing significant alignments:	(Bits)	Value	
gi|74355441|gb|BC104471.1| Homo sapiens urocortin, mRNA (cDNA...	69.9	2e-08	U G
gi|74354435|gb|BC104470.1| Homo sapiens urocortin, mRNA (cDNA...	69.9	2e-08	U G
gi|109102369|ref|XM_001092536.1| PREDICTED: Macaca mulatta si...	69.9	2e-08	G
gi|109102367|ref|XM_001092424.1| PREDICTED: Macaca mulatta si...	69.9	2e-08	G
gi|76629936|ref|XM_618452.2| PREDICTED: Bos taurus urocortin (UC	69.9	2e-08	G
gi|49457481|emb|CR542244.1| Homo sapiens full open reading fr...	69.9	2e-08	U G
gi|12056477|ref|NM_003353.2| Homo sapiens urocortin (UCN), mRNA	69.9	2e-08	U G
gi|18158397|gb|AC013413.6| Homo sapiens BAC clone RP11-538J11 fr	69.9	2e-08	
gi|15867153|emb|AJ322774.1|HSA322774 Homo sapiens genomic seq...	69.9	2e-08	
gi|3335507|gb|AF051807.1|AF051807 Ovis aries urocortin precursor	69.9	2e-08	G
gi|60812522|gb|AY893178.1| Synthetic construct Homo sapiens c...	69.9	2e-08	
gi|3493655|gb|AF084258.1|AF084258 Ovis aries urocortin mRNA, par	69.9	2e-08	U G
gi|3252876|gb|AF038633.1|AF038633 Homo sapiens Mpv17 protein ...	69.9	2e-08	G
gi|9507228|ref|NM_019150.1| Rattus norvegicus urocortin (Ucn), m	61.9	4e-06	U G
gi|12025527|ref|NM_021290.1| Mus musculus urocortin (Ucn), mRNA	61.9	4e-06	U G
gi|66393194|gb|DQ019623.1| Rattus norvegicus antisense urocor...	61.9	4e-06	
gi|66393193|gb|DQ019622.1| Rattus norvegicus immature urocort...	61.9	4e-06	
gi|109733893|gb|BC116950.1| Mus musculus urocortin, mRNA (cDN...	61.9	4e-06	G
gi|109733563|gb|BC116948.1| Mus musculus urocortin, mRNA (cDN...	61.9	4e-06	G
gi|51241829|gb|AC114619.9| Mus musculus chromosome 5, clone RP24	61.9	4e-06	
gi|73980661|ref|XM_848667.1| PREDICTED: Canis familiaris simi...	61.9	4e-06	G
gi|73853459|ref|NM_001032301.1| Bos taurus urocortin (UCN), mRNA	61.9	4e-06	U G
gi|7527457|gb|AF093623.1|AF093623 Rattus norvegicus urocortin pr	61.9	4e-06	G
gi|71979892|dbj|AB201710.1| Bos taurus UCN mRNA for urocortin, c	61.9	4e-06	U G
gi|25046361|gb|AC109608.14| Mus musculus strain C57BL/6J chro...	61.9	4e-06	
gi|3252873|gb|AF038632.1|AF038632 Mus musculus Mpv17 protein ...	61.9	4e-06	G

β-actin Gene Sequence

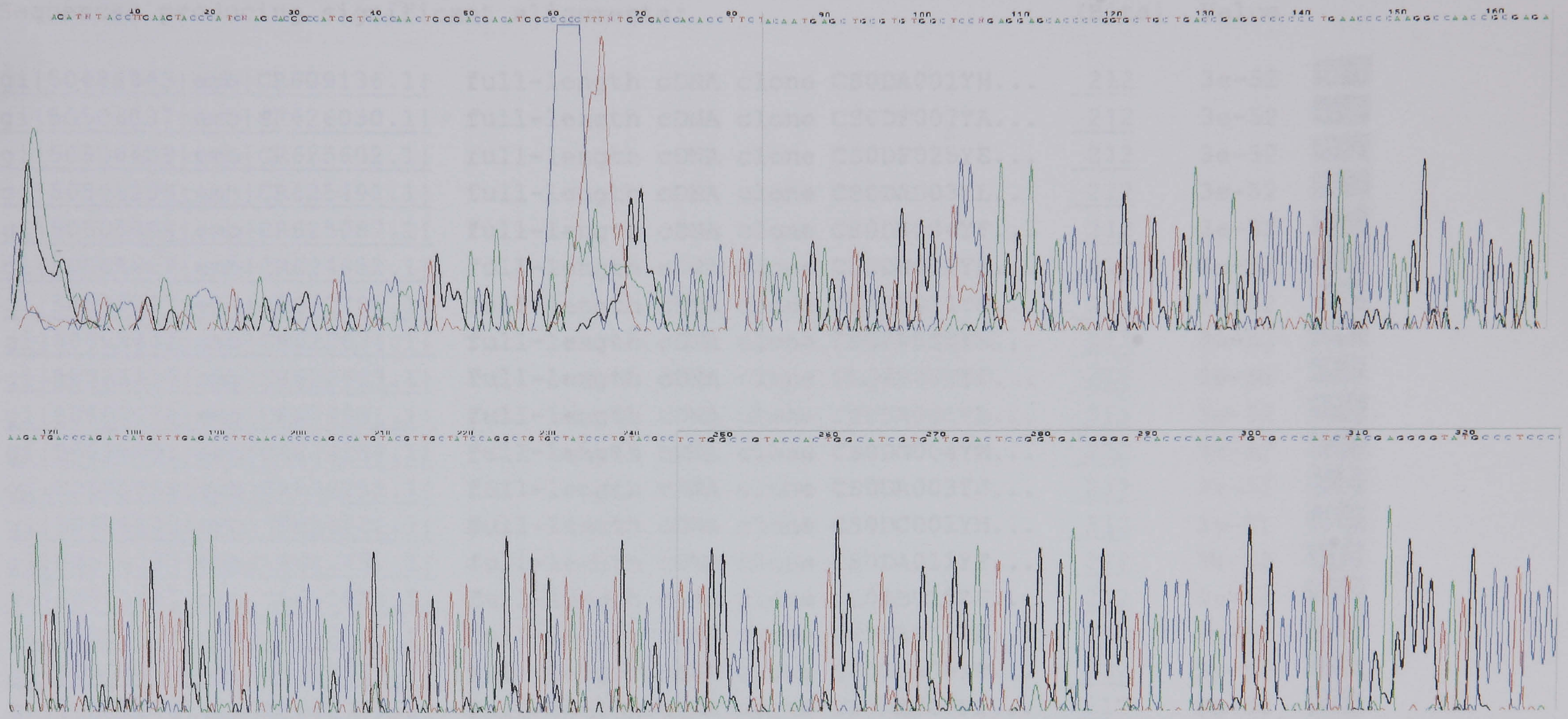

AGATNTACCTTGAAGTACCCATCNAGCACGGCCATCGTCACCAACTGGGACGACATGGCCCCCTTTNTGGGACCACACCTTCTACAATGAGCTGC
GTGTGGCTCCNGAGGAGCACCCCGGTGCTGCTGACCGAGGCCCCCCTGAACCCCAAGGCCAACCGCGAGAAGATGACCCAGATCATGTTTGAGA
CCTTCAACACCCCAGCCATGTACGTTGCTATCCAGGCTGTGCTATCCCTGTACGCCTCTGGCCGTACCACTGGCATCGTGATGGACTCCGGTGAC
GGGGTCACCCACACTGTGCCCATCTACGAGGGGTATGCCCTCCCCCATGCCATCCTGCGTCTGGACCTGGCTGGCCGGGACCTGACTGACTACCT
CATGAAGATCCTCACCGAGCGCGGCTACAGCTTCACCACCACGGCCGAGCGGGAAATCGTGCGTGACATTAAGGAGAAGCTGTGCTACGTCGCC
CTGGACTTCGAGCAAGAGATGGA

BLAST Data for the β-actin Gene

Sequences producing significant alignments:		Score (Bits)	E Value	
gi|50489943|emb|CR609136.1|	full-length cDNA clone CS0DA001YH...	212	3e-52	
gi|50506837|emb|CR626030.1|	full-length cDNA clone CS0DF007YA...	212	3e-52	
gi|50506409|emb|CR625602.1|	full-length cDNA clone CS0DF025YE...	212	3e-52	
gi|50506299|emb|CR625492.1|	full-length cDNA clone CS0DA003YL...	212	3e-52	
gi|50505894|emb|CR625087.1|	full-length cDNA clone CS0DN004YF...	212	3e-52	
gi|50505659|emb|CR624852.1|	full-length cDNA clone CS0DH002YK...	212	3e-52	
gi|50503507|emb|CR622700.1|	full-length cDNA clone CS0DE011YO...	212	3e-52	
gi|50503441|emb|CR622634.1|	full-length cDNA clone CS0DA010YH...	212	3e-52	
gi|50503410|emb|CR622603.1|	full-length cDNA clone CL0BB030ZG...	212	3e-52	
gi|50505158|emb|CR624351.1|	full-length cDNA clone CS0DA001YE...	212	3e-52	
gi|50505091|emb|CR624284.1|	full-length cDNA clone CS0DG004YM...	212	3e-52	
gi|50505058|emb|CR624251.1|	full-length cDNA clone CS0DA003YJ...	212	3e-52	
gi|50505009|emb|CR624202.1|	full-length cDNA clone CS0DC001YM...	212	3e-52	
gi|50504237|emb|CR623430.1|	full-length cDNA clone CS0DA011YF...	212	3e-52	
gi|50503641|emb|CR622834.1|	full-length cDNA clone CL0BB012ZF...	212	3e-52	
gi|50503309|emb|CR622502.1|	full-length cDNA clone CS0DA011YK...	212	3e-52	
gi|50503030|emb|CR622223.1|	full-length cDNA clone CS0DG005YD...	212	3e-52	
gi|50502896|emb|CR622089.1|	full-length cDNA clone CS0DM007YI...	212	3e-52	
gi|50502442|emb|CR621635.1|	full-length cDNA clone CS0DF007YA...	212	3e-52	
gi|50502432|emb|CR621625.1|	full-length cDNA clone CS0DF002YC...	212	3e-52	
gi|50502355|emb|CR621548.1|	full-length cDNA clone CS0DF032YG...	212	3e-52	
gi|50502209|emb|CR621402.1|	full-length cDNA clone CS0DH001YH...	212	3e-52	
gi|50501996|emb|CR621189.1|	full-length cDNA clone CS0DA009YN...	212	3e-52	
gi|50501990|emb|CR621183.1|	full-length cDNA clone CS0DF013YE...	212	3e-52	

gi|50501924|emb|CR621117.1|	full-length cDNA clone CS0DA009YP...	212	3e-52	U G
gi|50501919|emb|CR621112.1|	full-length cDNA clone CS0DA009YP...	212	3e-52	U G
gi|50501065|emb|CR620258.1|	full-length cDNA clone CS0DA008YK...	212	3e-52	U G
gi|50501004|emb|CR620197.1|	full-length cDNA clone CS0DN001YM...	212	3e-52	U G
gi|50500978|emb|CR620171.1|	full-length cDNA clone CS0DE007YM...	212	3e-52	U G
gi|50500777|emb|CR619970.1|	full-length cDNA clone CS0DF004YH...	212	3e-52	U G
gi|50500422|emb|CR619615.1|	full-length cDNA clone CS0DM007YG...	212	3e-52	U G
gi|50500414|emb|CR619607.1|	full-length cDNA clone CS0DF007YC...	212	3e-52	U G
gi|50500399|emb|CR619592.1|	full-length cDNA clone CS0DH007YM...	212	3e-52	U G
gi|50499747|emb|CR618940.1|	full-length cDNA clone CS0DF031YN...	212	3e-52	U G
gi|50499523|emb|CR618716.1|	full-length cDNA clone CS0DJ012YC...	212	3e-52	U G
gi|50498141|emb|CR617334.1|	full-length cDNA clone CS0DI032YL...	212	3e-52	U G
gi|50498066|emb|CR617259.1|	full-length cDNA clone CS0DF023YL...	212	3e-52	U G
gi|50495365|emb|CR614558.1|	full-length cDNA clone CS0DA009YI...	212	3e-52	U G
gi|50495312|emb|CR614505.1|	full-length cDNA clone CS0DA002YD...	212	3e-52	U G
gi|50497944|emb|CR617137.1|	full-length cDNA clone CS0DG006YK...	212	3e-52	U G
gi|50497793|emb|CR616986.1|	full-length cDNA clone CS0DH007YI...	212	3e-52	U G
gi|50497501|emb|CR616694.1|	full-length cDNA clone CS0DF017YD...	212	3e-52	U G
gi|50497488|emb|CR616681.1|	full-length cDNA clone CS0DM009YM...	212	3e-52	U G
gi|74316001|ref|NM_001033084.1|	Macaca mulatta actin, beta (ACTB	212	3e-52	U G
gi|62897670|dbj|AK223055.1|	Homo sapiens mRNA for beta actin var	212	3e-52	U G
gi|62897624|dbj|AK223032.1|	Homo sapiens mRNA for beta actin var	212	3e-52	U G
gi|62897408|dbj|AK222925.1|	Homo sapiens mRNA for beta actin var	212	3e-52	U G
gi|62421179|gb|AY970501.1|	Homo sapiens isolate 4T-18 actin-l...	212	3e-52	G
gi|62421173|gb|AY970498.1|	Homo sapiens isolate 4T-15 actin-l...	212	3e-52	G
gi|62421171|gb|AY970497.1|	Homo sapiens isolate 4T-14 actin-l...	212	3e-52	G
gi|62421167|gb|AY970495.1|	Homo sapiens isolate 4T-12 actin-l...	212	3e-52	G
gi|62421165|gb|AY970494.1|	Homo sapiens isolate 4T-11 actin-l...	212	3e-52	G

gi|62421163|gb|AY970493.1|	Homo sapiens isolate 4T-10 actin-l...	212	3e-52	G
gi|62421159|gb|AY970491.1|	Homo sapiens isolate 4T-8 actin-li...	212	3e-52	G
gi|62421155|gb|AY970489.1|	Homo sapiens isolate 4T-6 actin-li...	212	3e-52	G
gi|62421153|gb|AY970488.1|	Homo sapiens isolate 4T-5 actin-li...	212	3e-52	G
gi|62421151|gb|AY970487.1|	Homo sapiens isolate 4T-4 actin-li...	212	3e-52	G
gi|62421149|gb|AY970486.1|	Homo sapiens isolate 4T-3 actin-li...	212	3e-52	G
gi|62421135|gb|AY970479.1|	Homo sapiens isolate 4N-15 actin-l...	212	3e-52	G
gi|62421133|gb|AY970478.1|	Homo sapiens isolate 4N-14 actin-l...	212	3e-52	G
gi|62421131|gb|AY970477.1|	Homo sapiens isolate 4N-13 actin-l...	212	3e-52	G
gi|62421125|gb|AY970474.1|	Homo sapiens isolate 4N-10 actin-l...	212	3e-52	G
gi|62421123|gb|AY970473.1|	Homo sapiens isolate 4N-9 actin-li...	212	3e-52	G
gi|62421121|gb|AY970472.1|	Homo sapiens isolate 4N-8 actin-li...	212	3e-52	G
gi|62421119|gb|AY970471.1|	Homo sapiens isolate 4N-7 actin-li...	212	3e-52	G
gi|62421117|gb|AY970470.1|	Homo sapiens isolate 4N-6 actin-li...	212	3e-52	G
gi|62421115|gb|AY970469.1|	Homo sapiens isolate 4N-5 actin-li...	212	3e-52	G
gi|62421113|gb|AY970468.1|	Homo sapiens isolate 4N-4 actin-li...	212	3e-52	G
gi|62421066|gb|AY970443.1|	Homo sapiens isolate 3N-7 actin-li...	212	3e-52	G
gi|62421062|gb|AY970441.1|	Homo sapiens isolate 3N-5 actin-li...	212	3e-52	G
gi|62421020|gb|AY970420.1|	Homo sapiens isolate 2T-1 actin-li...	212	3e-52	G
gi|62421018|gb|AY970419.1|	Homo sapiens isolate 2N-12 actin-l...	212	3e-52	G
gi|62421016|gb|AY970418.1|	Homo sapiens isolate 2N-11 actin-l...	212	3e-52	G
gi|62421014|gb|AY970417.1|	Homo sapiens isolate 2N-10 actin-l...	212	3e-52	G
gi|62421012|gb|AY970416.1|	Homo sapiens isolate 2N-9 actin-li...	212	3e-52	G
gi|62421010|gb|AY970415.1|	Homo sapiens isolate 2N-8 actin-li...	212	3e-52	G
gi|62421008|gb|AY970414.1|	Homo sapiens isolate 2N-7 actin-li...	212	3e-52	G
gi|62421006|gb|AY970413.1|	Homo sapiens isolate 2N-6 actin-li...	212	3e-52	G
gi|62421000|gb|AY970410.1|	Homo sapiens isolate 2N-3 actin-li...	212	3e-52	G
gi|62420998|gb|AY970409.1|	Homo sapiens isolate 2N-2 actin-li...	212	3e-52	G

gi|62420996|gb|AY970408.1|	Homo sapiens isolate 2N-1 actin-li...	212	3e-52	G
gi|62420992|gb|AY970406.1|	Homo sapiens isolate 1T-23 actin-l...	212	3e-52	G
gi|62420990|gb|AY970405.1|	Homo sapiens isolate 1T-22 actin-l...	212	3e-52	G
gi|62420988|gb|AY970404.1|	Homo sapiens isolate 1T-21 actin-l...	212	3e-52	G
gi|62420986|gb|AY970403.1|	Homo sapiens isolate 1T-20 actin-l...	212	3e-52	G
gi|62420984|gb|AY970402.1|	Homo sapiens isolate 1T-19 actin-l...	212	3e-52	G
gi|62420934|gb|AY970377.1|	Homo sapiens isolate 1N-15 actin-l...	212	3e-52	G
gi|62420932|gb|AY970376.1|	Homo sapiens isolate 1N-14 actin-l...	212	3e-52	G
gi|62420930|gb|AY970375.1|	Homo sapiens isolate 1N-13 actin-l...	212	3e-52	G
gi|62420925|gb|AY970372.1|	Homo sapiens isolate 1N-10 actin-l...	212	3e-52	G
gi|62420923|gb|AY970371.1|	Homo sapiens isolate 1N-9 actin-li...	212	3e-52	G
gi|62420921|gb|AY970370.1|	Homo sapiens isolate 1N-8 actin-li...	212	3e-52	G
gi|62420917|gb|AY970368.1|	Homo sapiens isolate 1N-6 actin-li...	212	3e-52	G
gi|62420913|gb|AY970366.1|	Homo sapiens isolate 1N-4 actin-li...	212	3e-52	G
gi|62420909|gb|AY970364.1|	Homo sapiens isolate 1N-2 actin-li...	212	3e-52	G
gi|62420907|gb|AY970363.1|	Homo sapiens isolate 1N-1 actin-li...	212	3e-52	G
gi|60652764|gb|AY892160.1|	Synthetic construct Homo sapiens c...	212	3e-52	
gi|60655868|gb|AY889707.1|	Synthetic construct Homo sapiens c...	212	3e-52	
gi|61367074|gb|AY891016.1|	Synthetic construct Homo sapiens c...	212	3e-52	
gi|110623790|dbj|AK225414.1|	Homo sapiens mRNA for beta actin va	212	3e-52	

GAPDH Gene Sequence

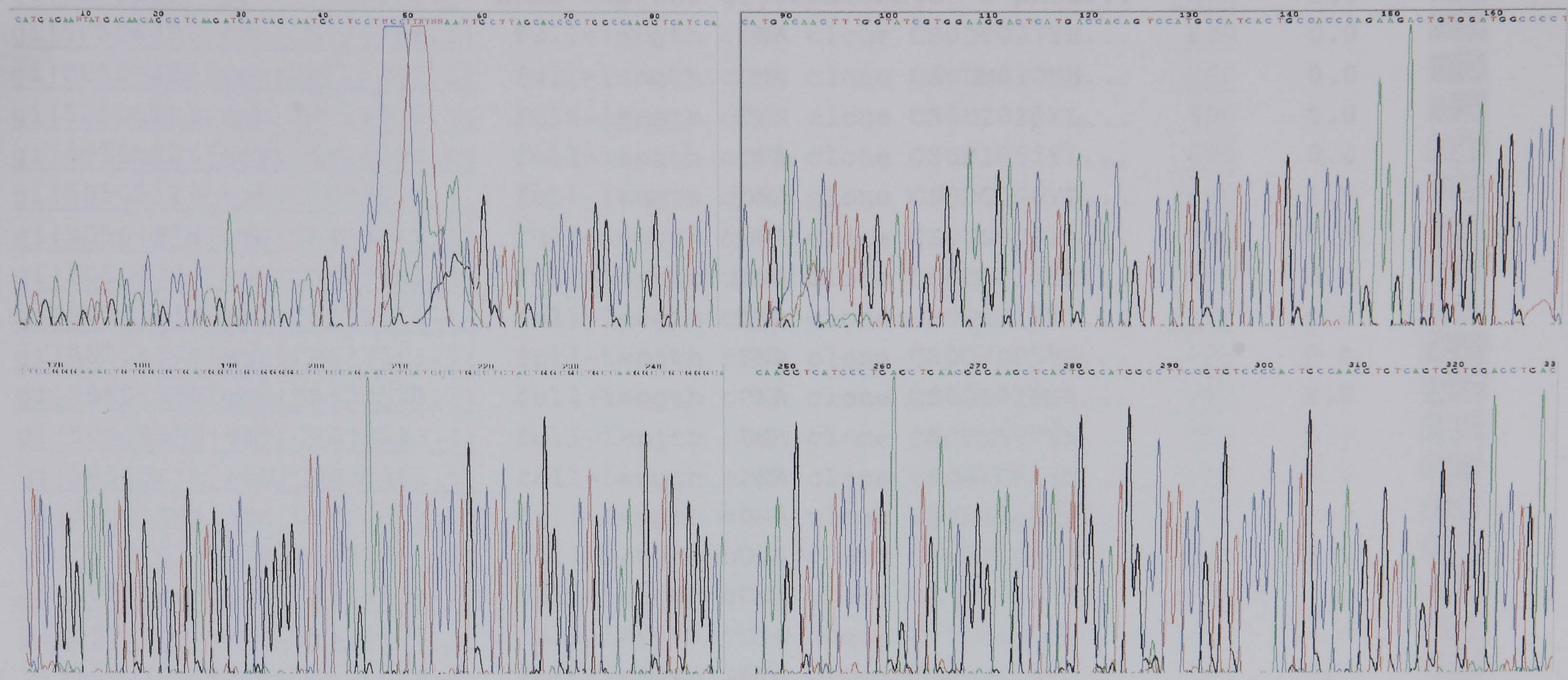

CATGAGAANTATGACAACAGCCTCAAGATCATCAGCAATGCCTCCTNCCTTNTNNAANTGCTTAGCACCCCTGGCCAAGGTCATCCATGACAAC
TTTGGTATCGTGGAAGGACTCATGACCACAGTCCATGCCATCACTGCCACCCAGAAGACTGTGGATGGCCCCTCCGGGAAACTGTGGCGTGATG
GCCGCGGGGCTCTCCAGAACATCATCCCTGCCTCTACTGGCGCTGCCAAGGCTGTGGGCAAGGTCATCCCTGAGCTGAACGGGAAGCTCACTGG
CATGGCCTTCCGTGTCCCCACTGCCAACGTGTCAGTGGTGGACCTGACCTGCCGTCTAGAAAAACCTGCCAAATATGATGACATCAAGAAGGTG
GTGAAGCAGGAGGNCTTNTTCTTTATAAATTGGGGNTNNNGTCNNACTTCNTNAGGANGACA

BLAST Data for GAPDH Gene

gi|53734501|gb|BC083511.1|	Homo sapiens glyceraldehyde-3-phos...	690	0.0	
gi|50506096|emb|CR625289.1|	full-length cDNA clone CS0DF027YB...	690	0.0	
gi|50503454|emb|CR622647.1|	full-length cDNA clone CS0DM010YH...	690	0.0	
gi|50505283|emb|CR624476.1|	full-length cDNA clone CS0DI025YL...	690	0.0	
gi|50505203|emb|CR624396.1|	full-length cDNA clone CS0DI051YL...	690	0.0	
gi|50505123|emb|CR624316.1|	full-length cDNA clone CS0DG006YL...	690	0.0	
gi|50504874|emb|CR624067.1|	full-length cDNA clone CS0DG007YL...	690	0.0	
gi|50504728|emb|CR623921.1|	full-length cDNA clone CS0DA011YM...	690	0.0	
gi|50504619|emb|CR623812.1|	full-length cDNA clone CS0DE010YL...	690	0.0	
gi|50504368|emb|CR623561.1|	full-length cDNA clone CS0DI005YG...	690	0.0	
gi|50504335|emb|CR623528.1|	full-length cDNA clone CS0DI018YA...	690	0.0	
gi|50504330|emb|CR623523.1|	full-length cDNA clone CS0DH007YB...	690	0.0	
gi|50503215|emb|CR622408.1|	full-length cDNA clone CS0DI084YM...	690	0.0	
gi|50503184|emb|CR622377.1|	full-length cDNA clone CS0DG004YL...	690	0.0	
gi|50502613|emb|CR621806.1|	full-length cDNA clone CS0DN004YF...	690	0.0	
gi|50502428|emb|CR621621.1|	full-length cDNA clone CL0BB006ZF...	690	0.0	
gi|50501141|emb|CR620334.1|	full-length cDNA clone CS0DH001YC...	690	0.0	
gi|50501051|emb|CR620244.1|	full-length cDNA clone CS0DA004YG...	690	0.0	
gi|50500953|emb|CR620146.1|	full-length cDNA clone CS0DF030YC...	690	0.0	
gi|50500549|emb|CR619742.1|	full-length cDNA clone CS0DF034YM...	690	0.0	
gi|50500545|emb|CR619738.1|	full-length cDNA clone CS0DA004YE...	690	0.0	
gi|50500204|emb|CR619397.1|	full-length cDNA clone CS0DI079YD...	690	0.0	
gi|50500109|emb|CR619302.1|	full-length cDNA clone CS0CAP001Y...	690	0.0	
gi|50499364|emb|CR618557.1|	full-length cDNA clone CS0DI058YF...	690	0.0	
gi|50498924|emb|CR618117.1|	full-length cDNA clone CS0DI076YE...	690	0.0	
gi|50498691|emb|CR617884.1|	full-length cDNA clone CS0DA006YK...	690	0.0	

gi|50498207|emb|CR617400.1|	full-length cDNA clone CS0DA006YE...	690	0.0	
gi|50498206|emb|CR617399.1|	full-length cDNA clone CS0DA006YE...	690	0.0	
gi|50497562|emb|CR616755.1|	full-length cDNA clone CS0DI022YH...	690	0.0	
gi|50497215|emb|CR616408.1|	full-length cDNA clone CS0DF021YB...	690	0.0	
gi|50497137|emb|CR616330.1|	full-length cDNA clone CS0DA001YO...	690	0.0	
gi|50497083|emb|CR616276.1|	full-length cDNA clone CS0DK007YD...	690	0.0	
gi|50497019|emb|CR616212.1|	full-length cDNA clone CS0DH005YG...	690	0.0	
gi|50496830|emb|CR616023.1|	full-length cDNA clone CS0DI065YL...	690	0.0	
gi|50496207|emb|CR615400.1|	full-length cDNA clone CS0DE011YB...	690	0.0	
gi|50496077|emb|CR615270.1|	full-length cDNA clone CS0DH005YB...	690	0.0	
gi|50495444|emb|CR614637.1|	full-length cDNA clone CS0DA003YC...	690	0.0	
gi|50494695|emb|CR613888.1|	full-length cDNA clone CS0DG005YB...	690	0.0	
gi|50494548|emb|CR613741.1|	full-length cDNA clone CS0DA003YD...	690	0.0	
gi|50494330|emb|CR613523.1|	full-length cDNA clone CS0DG001YA...	690	0.0	
gi|50494248|emb|CR613441.1|	full-length cDNA clone CS0DE005YH...	690	0.0	
gi|50494209|emb|CR613402.1|	full-length cDNA clone CS0DC026YK...	690	0.0	
gi|50493844|emb|CR613037.1|	full-length cDNA clone CS0DA011YK...	690	0.0	
gi|50493251|emb|CR612444.1|	full-length cDNA clone CS0DG004YF...	690	0.0	
gi|50492988|emb|CR612181.1|	full-length cDNA clone CS0DK009YG...	690	0.0	
gi|50492979|emb|CR612172.1|	full-length cDNA clone CS0DI006YD...	690	0.0	
gi|50492770|emb|CR611963.1|	full-length cDNA clone CS0DI082YN...	690	0.0	
gi|50492385|emb|CR611578.1|	full-length cDNA clone CS0DA011YG...	690	0.0	
gi|50492053|emb|CR611246.1|	full-length cDNA clone CS0DH005YB...	690	0.0	
gi|50491710|emb|CR610903.1|	full-length cDNA clone CS0DA003YA...	690	0.0	
gi|50491607|emb|CR610800.1|	full-length cDNA clone CS0DA012YA...	690	0.0	
gi|50491197|emb|CR610390.1|	full-length cDNA clone CS0CAP008Y...	690	0.0	
gi|50491049|emb|CR610242.1|	full-length cDNA clone CL0BB002ZH...	690	0.0	
gi|50490725|emb|CR609918.1|	full-length cDNA clone CS0DA009YO...	690	0.0	

gi|50490721|emb|CR609914.1|	full-length cDNA clone CS0DM008YM...	690	0.0	U G
gi|50490492|emb|CR609685.1|	full-length cDNA clone CS0DA002YD...	690	0.0	U G
gi|50490178|emb|CR609371.1|	full-length cDNA clone CS0DF002YL...	690	0.0	U G
gi|50489761|emb|CR608954.1|	full-length cDNA clone CS0DA008YJ...	690	0.0	U G
gi|50489287|emb|CR608480.1|	full-length cDNA clone CS0DJ002YH...	690	0.0	U G
gi|50489115|emb|CR608308.1|	full-length cDNA clone CS0DI011YO...	690	0.0	U G
gi|50489114|emb|CR608307.1|	full-length cDNA clone CS0DI037YB...	690	0.0	U G
gi|50488908|emb|CR608101.1|	full-length cDNA clone CS0DF031YH...	690	0.0	U G
gi|50487694|emb|CR606887.1|	full-length cDNA clone CS0DJ014YC...	690	0.0	U G
gi|50487152|emb|CR606345.1|	full-length cDNA clone CS0DG007YP...	690	0.0	U G
gi|50486914|emb|CR606107.1|	full-length cDNA clone CS0DI040YL...	690	0.0	U G
gi|50486239|emb|CR605432.1|	full-length cDNA clone CS0DA006YF...	690	0.0	U G
gi|50485164|emb|CR604357.1|	full-length cDNA clone CS0DI015YG...	690	0.0	U G
gi|50485040|emb|CR604233.1|	full-length cDNA clone CS0DF018YD...	690	0.0	U G
gi|50485026|emb|CR604219.1|	full-length cDNA clone CS0DF028YG...	690	0.0	U G
gi|50484981|emb|CR604174.1|	full-length cDNA clone CS0DG001YF...	690	0.0	U G
gi|50484976|emb|CR604169.1|	full-length cDNA clone CS0DI052YK...	690	0.0	U G
gi|50484664|emb|CR603857.1|	full-length cDNA clone CS0DI041YM...	690	0.0	U G
gi|50484577|emb|CR603770.1|	full-length cDNA clone CS0DH001YN...	690	0.0	U G
gi|50483992|emb|CR603185.1|	full-length cDNA clone CS0DA006YN...	690	0.0	U G
gi|50483289|emb|CR602482.1|	full-length cDNA clone CS0DJ008YG...	690	0.0	U G
gi|50483215|emb|CR602408.1|	full-length cDNA clone CS0DA011YE...	690	0.0	U G
gi|50483538|emb|CR602731.1|	full-length cDNA clone CS0DF033YN...	690	0.0	U G
gi|50483527|emb|CR602720.1|	full-length cDNA clone CS0DI082YE...	690	0.0	U G
gi|50483463|emb|CR602656.1|	full-length cDNA clone CS0DI081YL...	690	0.0	U G
gi|50482791|emb|CR601984.1|	full-length cDNA clone CS0DI040YD...	690	0.0	U G
gi|50482461|emb|CR601654.1|	full-length cDNA clone CS0DI072YH...	690	0.0	U G
gi|50482367|emb|CR601560.1|	full-length cDNA clone CS0DI001YP...	690	0.0	U G

gi|50481744|emb|CR600937.1|	full-length cDNA clone CS0DA008YI...	690	0.0	U G
gi|50481490|emb|CR600683.1|	full-length cDNA clone CS0CAP005Y...	690	0.0	U G
gi|50481419|emb|CR600612.1|	full-length cDNA clone CS0DA011YM...	690	0.0	U G
gi|50481401|emb|CR600594.1|	full-length cDNA clone CS0DA005YE...	690	0.0	U G
gi|50481313|emb|CR600506.1|	full-length cDNA clone CS0DE012YD...	690	0.0	U G
gi|50480938|emb|CR600131.1|	full-length cDNA clone CL0BB012ZH...	690	0.0	U G
gi|50480733|emb|CR599926.1|	full-length cDNA clone CS0DI027YI...	690	0.0	U G
gi|50480402|emb|CR599595.1|	full-length cDNA clone CS0DA008YB...	690	0.0	U G
gi|60654044|gb|AY892798.1|	Synthetic construct Homo sapiens c...	690	0.0	
gi|60654042|gb|AY892797.1|	Synthetic construct Homo sapiens c...	690	0.0	
gi|61362730|gb|AY890329.1|	Synthetic construct Homo sapiens c...	690	0.0	
gi|61362725|gb|AY890328.1|	Synthetic construct Homo sapiens c...	690	0.0	
gi|54303909|gb|AY633612.1|	Homo sapiens aging-associated gene 9	690	0.0	U G
gi|50489240|emb|CR608433.1|	full-length cDNA clone CS0DH003YJ...	686	0.0	U G
gi|50504305|emb|CR623498.1|	full-length cDNA clone CS0DA007YP...	680	0.0	U G
gi|50495582|emb|CR614775.1|	full-length cDNA clone CL0BA009ZC...	650	0.0	U G
gi|50487387|emb|CR606580.1|	full-length cDNA clone CS0DH004YC...	650	0.0	U G
gi|50481248|emb|CR600441.1|	full-length cDNA clone CS0DA008YG...	650	0.0	U G